microRNA expression profiling of pediatric acute myeloid leukemia patient samples and global identification of Argonaute protein-associated RNAs in respective cell line models

Inaugural-Dissertation

zur Erlangung des Doktorgrades
der Mathematisch-Naturwissenschaftlichen Fakultät
der Heinrich-Heine-Universität Düsseldorf

vorgelegt von

Svenja Daschkey
aus Oelde

Düsseldorf, April 2011

aus der Klinik für Kinder-Onkologie, -Hämatologie und Klinische Immunologie
des Universitätsklinikums Düsseldorf

Gedruckt mit der Genehmigung der
Mathematisch-Naturwissenschaftlichen Fakultät der
Heinrich-Heine-Universität Düsseldorf

Erstgutachter: Prof. Dr. Arndt Borkhardt
Zweitgutachter: Prof. Dr. Martin Lercher

Tag der mündlichen Prüfung: 30.05.2011

Table of Contents

Figure Directory

Table Directory

Summary

microRNAs (miRNAs) are small (21-24 nt), non-coding and highly conserved molecules, which are involved in several regulatory processes like cell growth, proliferation, differentiation, immune response and apoptosis, and play important roles in several diseases, including cancers like acute myeloid leukemia (AML). AML is a clinically and genetically heterogeneous disease characterized by rapid growth of abnormal white blood cells that accumulate in the bone marrow. In this doctoral thesis, the miRNA expression profiles of different AML subtypes were analyzed, in order to identify differentially expressed miRNAs, which may function as biomarkers for risk-group stratification of pediatric AML patients. Following, appropriate cell line models were used for global biochemical identification of miRNA targeting structures.

miRNA expression profiles of 102 pediatric AML patient samples were identified, using microarray technology, and analyzed by unsupervised hierarchical cluster analysis and statistical testing. AML subtypes with translocations t(8;21) and t(15;17) can be separated from each other, solely based on their miRNA expression profile, while other translocations involving mixed-lineage leukemia (MLL) rearrangements are interspersed and lack a characteristic miRNA signature. Only six and seven miRNAs are differentially expressed between AML samples with translocations t(8;21) and t(15;17), respectively, and all other AML subtypes. This is surprising, since patients of different AML subtypes, investigated in this study, differ greatly in their clinical presentation, emphasizing the suitability of miRNAs as future biomarkers. Differentially expressed miRNAs contain lineage specific miRNAs (miR-223), oncogenic miRNAs (miR-21) and more ubiquitously expressed miRNAs with no designated characteristics. Furthermore, they were not described as abundant in adult AML patients indicating that these miRNAs may function as pediatric-specific biomarkers in concordance with the clinical observation that adult and pediatric AML may be distinctive. miRNAs execute their function by guiding proteins of the Argonaute family (Ago proteins) to partially complementary sequences commonly located in the 3'-untranslated regions (3'-UTRs) of specific target-mRNAs leading to translational repression and/or mRNA destabilization. To gain further insights into the function of differentially expressed miRNAs, an Argonaute co-immunoprecipitation method termed PAR-CLIP-Array (Photo-activatable-Ribonucleoside-Enhanced Crosslinking-Immunoprecipitation and Microarray Hybridization) was established in this work, for global identification of Ago-associated miRNAs and miRNA targets. Argonaute-specific miRNAs and target-mRNAs were identified indicating separate binding preferences of the four human Argonaute proteins. Bioinformatical sequence analyses followed by pathway classification of Ago-associated target-mRNAs indicate a concerted action of the four human Argonaute proteins in AML-relevant pathways. The data denote that several Ago-associated miRNAs are able to repress the tumor suppressor TSC1 leading to activation of the mTOR pathway and increased cell growth in t(15;17)-positive AML. Moreover, the repression of the MAP kinase phosphatase DUSP6 by several Ago-associated miRNAs leads to activation of proliferative genes in the MAPK pathway of both, t(8;21)- and t(15;17)-positive AML.

In summary, miRNAs represent suitable biomarkers for differentiation of AML subtypes and possible risk-group stratification of pediatric AML patients. Furthermore, this thesis shows that the four human Argonaute proteins cooperate in the regulation of AML-relevant signaling pathways providing new insights into AML biology and may present the starting point for novel therapeutic interventions.

Zusammenfassung

microRNAs (miRNAs) sind kleine (21-24 nt), nicht-kodierende und hoch konservierte Moleküle, die an verschiedenen regulatorischen Prozessen wie Zellwachstum, Proliferation, Differenzierung, Immunreaktionen und Apoptose beteiligt sind und eine wichtige Rolle bei verschiedenen Erkrankungen und Krebsformen, wie der akuten myeloischen Leukämie (AML) spielen. AML ist eine klinisch und genetisch heterogene Erkrankung, die durch ein schnelles Wachstum von entarteten Leukozyten charakterisiert wird, die sich im Knochenmark anreichern. In dieser Arbeit wurden miRNA Expressionsprofile von unterschiedlichen AML Untergruppen analysiert, um differentiell exprimierte miRNAs zu identifizieren, die als potentielle Biomarker für die Einteilung von pädiatrischen AML Patienten in Risikogruppen dienen können. Für eine globale, biochemische Identifizierung von miRNA Zielstrukturen wurden entsprechende Zelllinienmodelle verwendet.

Mit Hilfe der Microarray-Technologie wurden die miRNA Expressionsprofile von 102 pädiatrischen AML Patientenproben identifiziert und mittels hierarchischer Clusteranalyse und statistischen Tests analysiert. Dabei konnte gezeigt werden, dass sich die AML Untergruppen mit den Translokationen t(8;21) und t(15;17) aufgrund ihrer miRNA Expressionsprofile komplett voneinander unterscheiden lassen, wohingegen Translokationen mit Beteiligung des *Mixed Lineage Leukemia*- (MLL-) Gens über das gesamte Cluster verteilt sind und kein charakteristisches miRNA Profil aufweisen. Nur sechs und sieben miRNAs konnten als differentiell exprimiert zwischen den Translokationen t(8;21) und t(15;17) und allen anderen AML Untergruppen identifiziert werden. Das ist überraschend, da die Patienten, die in dieser Arbeit untersucht wurden, stark in ihrem klinischen Erscheinungsbild variieren. Daher scheinen diese miRNAs als zukünftige Biomarker geeignet zu sein. Die differentiell exprimierten miRNAs beinhalten abstammungsspezifische miRNAs (miR-223), onkogene miRNAs (miR-21) und ubiquitär exprimierte miRNAs ohne bekannte spezifische Funktionen. Des Weiteren wurden diese miRNAs bisher nicht als signifikant in erwachsenen AML Patienten beschrieben. Daher scheinen diese miRNAs pädiatrisch-spezifische Biomarker zu sein.

miRNAs führen ihre Funktion mit Hilfe von sogenannten Argonaute-Proteinen (Ago-Proteine) durch, indem sie diese Proteine zu ihren spezifischen Ziel-mRNAs führen und komplementär an Sequenzen in deren 3'-untranslatierten Region (3'-UTR) binden, um die Ziel-mRNAs zu hemmen und/oder zu destabilisieren. Um mehr über mögliche Funktionen der differentiell exprimierten miRNAs zu erfahren, wurde in dieser Arbeit eine Methode zur co-Immunpräzipitation von Argonaute-Proteinen, genannt PAR-CLIP-Array (*Photoactivatable-Ribonucleoside-Enhanced Crosslinking-Immunoprecipitation and Microarray Hybridization*), etabliert, mit der global Ago-assoziierte miRNAs und Ziel-mRNAs identifiziert werden konnten. Dabei wurden Argonaute-spezifische miRNAs und deren Ziel-mRNAs identifiziert, die auf unterschiedliche Bindungsprioritäten der vier humanen Argonaute-Proteine hindeuten. Bioinformatische Sequenzanalysen und die Einordnung der Ago-assoziierten Ziel-mRNAs in Stoffwechselwege macht eine Kooperation der vier Argonaute-Proteine, hinsichtlich der Regulierung von AML-relevanten Stoffwechselwegen, deutlich. Anhand dieser Daten konnte zudem gezeigt werden, dass mehrere Ago-assoziierte miRNAs eine Bindungsstelle mit dem Tumor-suppressor TSC1 besitzen, um diesen reprimieren zu können, was zu einer Aktivierung des mTOR Signalwegs und einem erhöhten Zellwachstum in t(15;17)-positiver AML führen kann. Zudem kann die Inhibierung der MAP Kinase Phosphatase DUSP6 durch mehrere Ago-assoziierte miRNAs zu einer

Aktivierung von proliferativen Genen des MAPK Signalwegs in t(8;21)- und t(15;17)-positiver AML führen.

Zusammenfassend zeigen diese Daten, dass miRNAs geeignete Biomarker darstellen, um AML Untergruppen unterscheiden und pädiatrische AML-Patienten in Risikogruppen einteilen zu können. Des Weiteren zeigt diese Arbeit, dass die vier humanen Argonaute-Proteine bei der Regulierung von AML-relevanten Signalwegen kooperieren und dass die Entschlüsselung der Argonaute-miRNA-mRNA Komplexe neue Einblicke in die Biologie der AML liefern und den Startpunkt für neue therapeutische Eingriffe darstellen kann.

1 Introduction

1.1 Preface

The biology of gene regulation is a great area of research for several decades. A variety of gene inactivation mechanisms were discovered including gene mutation or deletion, repression of transcription, translational repression, destabilization of mRNAs and degradation of protein products. The inactivation of specific genes can be used for the investigation of gene functions in different cell types. Another mechanism, called RNAi (RNA interference), was characterized in detail by Andrew Fire and Craig Mello in 1998. They made a surprising observation that small-interfering RNAs (siRNA) are able to silence complementary genes in *Caenorhabditis elegans* (*C. elegans*) (Fire *et al.*, 1998). Various types of interfering RNAs exist which have specific functions, but use related mechanisms for gene-silencing (Zamore *et al.*, 2000). In human cells, one of the most abundant class of crucial regulators are microRNAs (miRNAs) and about 1000 different miRNAs control the activity of around 30% of the human genes (Kurreck, 2009). They regulate a variety of developmental and physiological processes, like cell differentiation, apoptosis and immune responses by post-transcriptional gene-silencing (Cao *et al.*, 2006; Plasterk, 2006; Shivdasani, 2006). Thus, gene regulation by miRNAs obtains very high significance. In addition, some recent studies have described a mechanistic role of individual miRNAs in several human malignancies, such as in the development of acute myeloid leukemia (AML) (Vasilatou *et al.*, 2010). The relationship between the expression of specific miRNAs and AML subtypes can have important implications for prognosis and treatment of adult and pediatric AML patients. The following introductory sections summarize the relationship between AML and miRNAs, together with the proteins that mediate the regulatory mechanisms of miRNAs.

1.2 Acute myeloid leukemia (AML)

1.2.1 Definition and prognosis of pediatric AML

AML is characterized by maturation arrest and proliferation of myeloid blasts in the bone marrow and in the blood. This leukemia arises by malignant mutations of immature myeloid cells, which are precursor cells of granulocytes, myeloblasts, or other myeloid cells like monocytes, erythrocytes or thrombocytes. The mutated precursor cells traverse several steps of development in the bone marrow and change their appearance and characteristics. If no treatment occurs, these cells extend and proliferate very fast affecting the whole body. They disrupt the normal hematopoiesis in the bone marrow, harm organs of the body and cause severe diseases leading to death within a few weeks or months (Creutzig and Reinhardt, 2006).

AML is the second most frequent leukemia in children and adolescent beside the acute lymphoblastic leukemia (ALL). AML accounts for 4.8% of all malignant diseases. According to the "*Deutsches Kinderkrebsregister in Mainz*" about 90 children and adolescents aged between 0 and 14 years are initially diagnosed with AML each year. The total number of patients to their 18th year of life counts about 110 each year. The prognosis of AML is less favorable compared to the prognosis of ALL. AML can appear in every age of life, but occurs most frequently in the higher adulthood. In infancy and adolescence, children are affected most frequently in the first two years of life. In addition, boys sicken slightly more often than girls (Creutzig and Reinhardt, 2006). Thus, the forecast of AML depends strongly upon the age and additional diseases of patients. Younger patients offer a better chance of healing, because in adult patients the AML proceeds more negatively due to attendant diseases and their common state of health (Creutzig and Reinhardt, 2006).

1.2.2 Cytogenetics of pediatric AML

AML is a clinically and genetically heterogeneous disease accounting for 15% to 20% of all childhood leukemias (Hall, 2001). Nowadays, the long term survival rate of pediatric AML patients has been increased from approximately 30% to more than 65% (Creutzig *et al*., 2005; Entz-Werle *et al*., 2005; Gibson *et al*., 2005; Perel *et al*., 2005). This progress was achieved by novel therapeutic drugs, intensification of doses, increased days of chemotherapy, improvement of bone marrow transplantation, and risk-group stratification mainly based on cytogenetics (Kaspers and Zwaan, 2007; Lange *et al*., 2008). Despite these improvements, nearly half of the pediatric patients relapse or die of the disease (Kaspers and Zwaan, 2007; Rubnitz *et al*., 2004). Therefore, a risk-group classification of childhood AML patients is needed, beside specific prognostic markers that can differentiate between patients with high and lower risk of relapse. This is important to allow treatment modifications and to minimize adverse side effects of treatment (Meshinchi *et al*., 2003). Such biomarkers can be patient characteristics like age, gender, ethnic background, body weight and physical limitations, or response to therapy, or disease characteristics such as white blood cell count (WBC), morphologic classification (French American British, FAB subtypes), and/or biological characteristics (Meshinchi and Arceci, 2007). The FAB classification divides AML patients into the following groups: M0 AML with minimal differentiation; M1 Myeloblastic leukemia without maturation; M2 Myeloblastic leukemia with

maturation; M3 Acute promyelocytic leukemia; M4 Acute myelomonocytic leukemia; M5 Acute monoblastic leukemia; M6 Acute erythroblastic leukemia and M7 Acute megakaryoblastic leukemia.

70% to 85% of chromosomal abnormalities were detected in childhood AML patients by cytogenetic analysis (Creutzig *et al.*, 2005; Entz-Werle *et al.*, 2005; Hall, 2001) and could be associated with distinct morphological subgroups. Based on chromosome rearrangements, like additional or absent chromosomes, translocations, deletions and inversions, it is possible to classify pediatric AML patients into different AML subtypes. Chromosomal abnormalities are often caused by rearrangement of parts between non homologous chromosomes. Unbalanced translocations occur frequently in AML, resulting in an exchange of chromosome material and the formation of extra genes called fusion genes, which could function as oncogenes and are involved in AML leukemogenesis. Specific chromosome aberrations vary between children and adults as well as within different pediatric age groups. 11q23 rearrangements appear, with highest frequency, during the first 3 years of life, and the frequency decreases strongly from around 50% to 8%, in children older than 24 months (Mrozek *et al.*, 2004). Other translocations, like t(1;22) and t(7;12), occur in general in young children and infants, whereas translocations, like t(8;21), t(15;17) and inv(16), are more common in older children.

1.2.3 Two of the most common translocations: t(8;21) and t(15;17)

The translocations t(8;21)(q22;q22) and t(15;17)(q22;q21) are two of the most common structural abnormalities in pediatric AML. t(8;21) interrupts the genes *AML1* (*RUNX1*) on chromosome 21q22 and *ETO* (*RUNX1T1*) on chromosome 8q22 resulting in the fusion gene *AML1-ETO*. It is reported that 7% to 16% of AML exhibits the translocation t(8;21), which is preferentially correlated with AML-M2 (Creutzig *et al.*, 2005). The combination of AML-M2 with t(8;21) can be differentiated clinically, morphologically and immunophenotypically from other M2 cases, as children are usually older, mostly male and have high remission rates. Although, pediatric patients with AML and t(8;21) are considered as having a good prognosis, approximately 50% of them relapse (Rubnitz *et al.*, 2002; Shimada *et al.*, 2006). Of all pediatric AML patients, between 3% and 10% possess the translocation t(15;17), although in Central and South America and in Italy the proportion was found to be much higher (Manola, 2009). Overall, this translocation is one of the most common morphologic aberrations, but it occurs infrequently in German pediatric AML patients. t(15;17) is a subtype of AML, called acute promyelocytic leukemia (APL or PML), and is correlated with AML-M3. This translocation fuses the *RARα* gene on chromosome 17q11-21 to the *PML* gene on chromosome 15q22. The chromosome 17 breakpoint occurs nearly always in intron 2 within the locus encoding for the retinoic acid receptor alpha gene (*RARα*). The chromosome 15 breakpoint falls within three different breakpoint cluster regions of the *PML* gene in intron 6 (*BCR1*, 70% of cases), intron 3 (*BCR3*, 20%) and exon 6 (*BCR2*, 10%). The fusion transcript of *PML* and *RARα* leads to maturation arrest in the promyelocyte stage. The arrest can be treated by doses of all-trans retinoic acid (ATRA) inducing differentiation of APL cells. ATRA targets *PML-RARα* and is used along with chemotherapy obtaining complete remission in more than 80% of patients. Chemotherapy after remission is also necessary, whereby long-term survival is reached in more than 70% of children. t(15;17) appears slightly more frequently in female and older children who offer low leukocyte count and often clotting abnormalities (Martinez-Climent, 1997).

1.3 microRNA and cancer

1.3.1 microRNA expression profiles classify human cancers

microRNAs (miRNAs) are small (~ 21 to 24 nt), non-coding, regulatory and highly conserved molecules encoded by humans, animals, plants and some viruses (Bartel, 2004; Ibanez-Ventoso *et al.*, 2008). It is estimated that 1% to 5% of animal genes encode for miRNAs (Bartel and Chen, 2004; Bentwich *et al.*, 2005; Berezikov *et al.*, 2005), which make them one of the most abundant class of regulators (Stark *et al.*, 2005). They regulate a variety of developmental and physiological processes like cell differentiation, apoptosis and immune responses (Cao *et al.*, 2006; Plasterk, 2006; Shivdasani, 2006). The miRNAs first discovered are lin-4 and let-7, identified in *C. elegans*. It was shown that they regulate the expression of potentially complementary mRNAs like lin-14 (Lee *et al.*, 1993; Moss *et al.*, 1997; Wightman *et al.*, 1993). Mammalian miRNAs are encoded throughout the whole genome, in intronic or exonic regions of protein-coding or non-coding genes. More than half of all human miRNAs are classified into genomic clusters, because they are transcribed as a single transcription unit (Landgraf *et al.*, 2007; Lee *et al.*, 2002; Winter *et al.*, 2009). Up to date, more than 1048 human miRNAs (miRBase release 16, sept. 2010) has been identified and registered in the miRBase database (Griffiths-Jones, 2004, 2006; Griffiths-Jones *et al.*, 2008). In the advent of deep-sequencing technologies the number of identified miRNAs is still growing.

Since 2002, the role of miRNAs in human cancers has gained more and more importance. The first detection of a deletion of miR-15a and miR-16 in chronic lymphocytic leukemia (CLL) suggested an association between these miRNAs and CLL (Calin *et al.*, 2002). Thereupon, a lot of miRNAs were found to be expressed in various types of cancer cell lines and clinical tumor samples. In animal models, an important role of miRNAs even in cancer development and progression was shown (Takamizawa *et al.*, 2004). Nowadays, it is known that miRNAs may function as tumor suppressors and are down-regulated in cancer cells, or as oncogenes inducing and promoting cancer development. It is also possible that miRNAs have an important role as tumor suppressor in the first case and an oncogenic role in a second case (Aguda *et al.*, 2008). Using microarray technology, Northern Blot or quantitative real time-reverse transcription-PCR (qrt-RT-PCR), differentially expressed miRNAs can be identified in clinical tumor specimens or cancer cell lines in comparison to healthy controls.

For instance, the miR-21 is highly expressed in glioblastoma cells, whereas the expression in normal brain tissues is relative low. Therefore, the miR-21 was established as potential biomarker for glioblastoma as well as miR-222 and miR-221. These miRNAs are markedly higher expressed in glioblastoma than in normal brain tissues, whereas miR-7 is down-regulated in human glioblastoma cells (Chan *et al.*, 2005; Gilliesand JK, 2007; Webster *et al.*, 2009). Due to the discovery of miRNA gene aberrations and certain expression profiles in almost all types of cancer, miRNAs have the ability to function as diagnostic or prognostic biomarker in risk-group stratification.

1.3.2 The role of miRNAs in acute myeloid leukemia

The role of miRNAs in adult AML was demonstrated several times by expression profiling, whereby AML could be differentiated from ALL (Mi *et al.*, 2007). By down-regulation of six miRNAs (miR-5, miR-128a, miR-128b, miR-130b, miR-151* and miR-210) and up-regulation of 21 miRNAs (for example, let-7a, -b, -c, -e, miR-21, miR-221, miR-222, miR-223 etc.), it is possible to distinguish AML patients from ALL patients. Among these miRNAs, let-7b, miR-128a, miR-128b and miR-223 are the most characteristic ones (Mi *et al.*, 2007). A reason could be a correlation between the location of miRNAs in the genome and cancer-associated regions. Often, miRNAs are located in fragile sites or common breakpoint regions in chromosome aberrations that involve oncogenes or tumor suppressor genes in cancer cells (Calin *et al.*, 2004). Thus, miRNAs were implicated as drivers of leukemogenesis. Studies of Starczynowski *et al.* demonstrated that, although around 70% of miRNAs are located in regions of leukemia-associated cytogenetic changes, a subset only (~ 20%) of these miRNAs are expressed and probably relevant myeloid malignancies (Starczynowski *et al.,* 2011). In this subset, the miRNAs, miR-143, miR-145, miR-146a, miR-155, miR-181, miR-221 and miR-222 are implicated in cellular processes relevant to AML (Baltimore *et al.,* 2008). Deletion of miR-145 and miR-146a results in a long-term myeloid disease in mice, and reintroduction of both miRNAs into AML cells significantly induced cell death and prevented growth *in vitro* (Starczynowski *et al.,* 2011). Overexpression of miR-155 leads to fatal and aggressive myeloproliferative disorder in mice (O'Connell *et al.*, 2008). Additionally, it was shown that expression profiles of miRNAs can not only be used for distinction of leukemias of different lineages, but also for differentiation of cytogenetic subtypes of adult AML. Three independent studies demonstrated that the cytogenetic subtypes t(8;21), t(15;17) and inv(16) offer unique miRNA expression profiles (Dixon-McIver *et al.,* 2008; Jongen-Lavrencic *et al.,* 2008; Li *et al.*, 2008). It was shown that miR-126 were highly overexpressed in t(8;21) and inv(16) and miR-224, miR-368 and miR-382 were exclusively overexpressed in t(15;17) in adult AML patients (Li *et al.*, 2008). The overexpression of miR-24 in patients carrying translocation t(8;21) leads to an inhibition of a mitogen-activated protein kinase (MAPK) phosphatase (MKP-7) and to an activation of downstream partners. Additionally, miR-24 blocks myeloid differentiation and speeds up cell proliferation (Garzon and Croce, 2008).

Moreover, recent reports suggested that miR-125b might act as oncogene as well as tumor suppressor, depending on the cellular context (Klusmann *et al.,* 2010). It has already been shown that this miRNA is involved in myeloid differentiation arrest in human cell lines, and that it is 6- to 90-fold overexpressed in AML patients carrying the translocation t(2;11) than in other AML subtypes or in healthy controls (Bousquet *et al.*, 2008). Overexpression of miR-125b was associated with the development of multiple types of leukemia, suggesting an effect of this miRNA on proliferation and inhibition of apoptosis because most miR-125b targets are involved in the p53 pathway. However, the exact role of miR-125b, as a second event in oncogenesis, has to be confirmed by further analyses (Bousquet *et al.,* 2010).

Furthermore, miR-223 is a known regulator of myelopoiesis with low expression in primary leukemia blasts. This expression is decreased by the interaction between the AML1-ETO fusion protein and the miRNA promoter region, which leads to miR-223 silencing (Fazi *et al.*, 2007). On this account, it was started to associate miRNAs with individual risk-groups of AML. For example, up-regulation of let-7b

and miR-9 was detected in patients with adverse cytogenetic risk-groups, and low expression of these miRNAs was detected in patients in the favorable risk-group (Dixon-McIver *et al.*, 2008). An overview of known miRNAs and their association with individual cytogenetic subtypes of AML are shown in Table 1.3.2.I below.

Table 1.3.2.I Overview of differentially expressed miRNAs identified in distinct cytogenetic AML subtypes. Listed are the up-regulated and down-regulated miRNAs in AML according to genetic alterations (Seca *et al.,* 2010). For more detailed information about each chromosomal translocation the corresponding references are also available in the right column.

Genetic alterations	Up-regulated miRNAs	Down-regulated miRNAs	References
t(8;21)	miR-126, miR-126*		Li *et al.*, 2008
	miR-146a	miR-133a	Dixon-McIver *et al.*, 2008
inv(16)	miR-126, miR-126*		Li *et al.*, 2008
	miR-99a, miR-100 and miR-224		Dixon-McIver *et al.*, 2008
t(15;17)	miR-127, miR-134, miR-323, miR-376a and miR-382		Jongen-Lavrencic *et al.*, 2008
	miR-127, miR-154, miR-154*, miR-299, miR-323, miR-368, miR-370		Dixon-McIver *et al.*, 2008
	miR-368, miR-382		Li *et al.*, 2008
MLL rearrangements		miR-10a, miR-331, miR-340	Dixon-McIver *et al.*, 2008
	miR-17-3p, miR-17-5p, miR-18a, miR-19a, miR-19b, miR-20a and miR-92		Li *et al.*, 2008
		let-7, miR-15a, miR-29a, miR-29b, miR-29c, miR-34b and miR-196a	Garzon and Croce, 2008
NPM1 mutation	miR-10a, miR-10b		Garzon and Croce, 2008
	miR-10a, miR-10b		Jongen-Lavrencic *et al.,* 2008
	miR-10a, miR-10b		Becker *et al.*, 2010
CEBPA mutation	miR-181a, miR-181a*, miR-181b, miR-181c and miR-181d		Marcucci *et al.*, 2008
High MN1	miR-126, miR-126*, miR-129-5p, miR-130b and miR-424	miR-16, miR-19a, miR-20a, miR-100 and miR-196a	Langer *et al.*, 2009
FLT3-ITD	miR-10a, miR-10b and miR-155		Garzon and Croce, 2008

1.3.3 miRNA biogenesis

Like all mRNAs, the majority of miRNA transcripts are polyadenylated and capped, so that the primary-miRNAs (pri-miRNAs) will be synthesized by Polymerase II (Pol II) (Lee *et al.*, 2004) (Figure 1.3.3.I a). The first step of miRNA biogenesis after transcription, is the nuclear cleavage of the pri-miRNA by RNase III endonuclease Drosha with co-factor DGCR8 (Figure 1.3.3.I b). Drosha cleaves 11 bp downstream from the hairpin stem to define the 5' end of the mature miRNA (Blaszczyk *et al.*, 2001) with a 2 nt overhang at the 3' end (Filippov *et al.*, 2000). The resulting precursor-miRNA (pre-miRNA) persists of a ~22 bp stem and a terminal loop (Basyuk *et al.*, 2003; Lee *et al.*, 2003). The pre-miRNA is exported from the nucleus into the cytoplasm by Exportin-5, a Ran-GTP-dependent dsRNA-binding domain (dsRBD) (Figure 1.3.3.I c) (Lund *et al.*, 2004; Yi *et al.*, 2003). Following, the RNA-induced silencing complex (RISC), Dicer and its dsRBD proteins, TRBP (Tar RNA-binding protein), and PACT (protein activator of PKR) accumulate and form the RISC-loading complex (RLC) (Figure 1.3.3.I d). After attachment of the core component (one of the four human Argonaute proteins (Ago proteins)) to this complex, the exported pre-miRNA enters the RLC (Gregory and Shiekhattar, 2005; Lee *et al.,*

2006; MacRae *et al.*, 2008; Maniataki and Mourelatos, 2005). In the RLC the 3' end of the pre-miRNA is processed by a second RNase III endonuclease, called Dicer, which cuts off the loop (Figure 1.3.3.I f) (Lee *et al.*, 2003). The generated miRNA duplex is separated into the functional guide strand and the subsequently degraded passenger strand (miRNA*) provoked by RLC dissociation (Gregory and Shiekhattar, 2005). It has been shown that the strand with the more stable base pair at the 5' end is typically degraded (Figure 1.3.3.I e), and the other one is incorporated into the RISC (Figure 1.3.3.I g) (Khvorova *et al.*, 2003; Schwarz *et al.*, 2003). The functional, mature miRNA is capable of silencing various mRNAs by cleavage, translational inhibition and mRNA decay (Eulalio *et al.,* 2008; Filipowicz *et al.*, 2008).
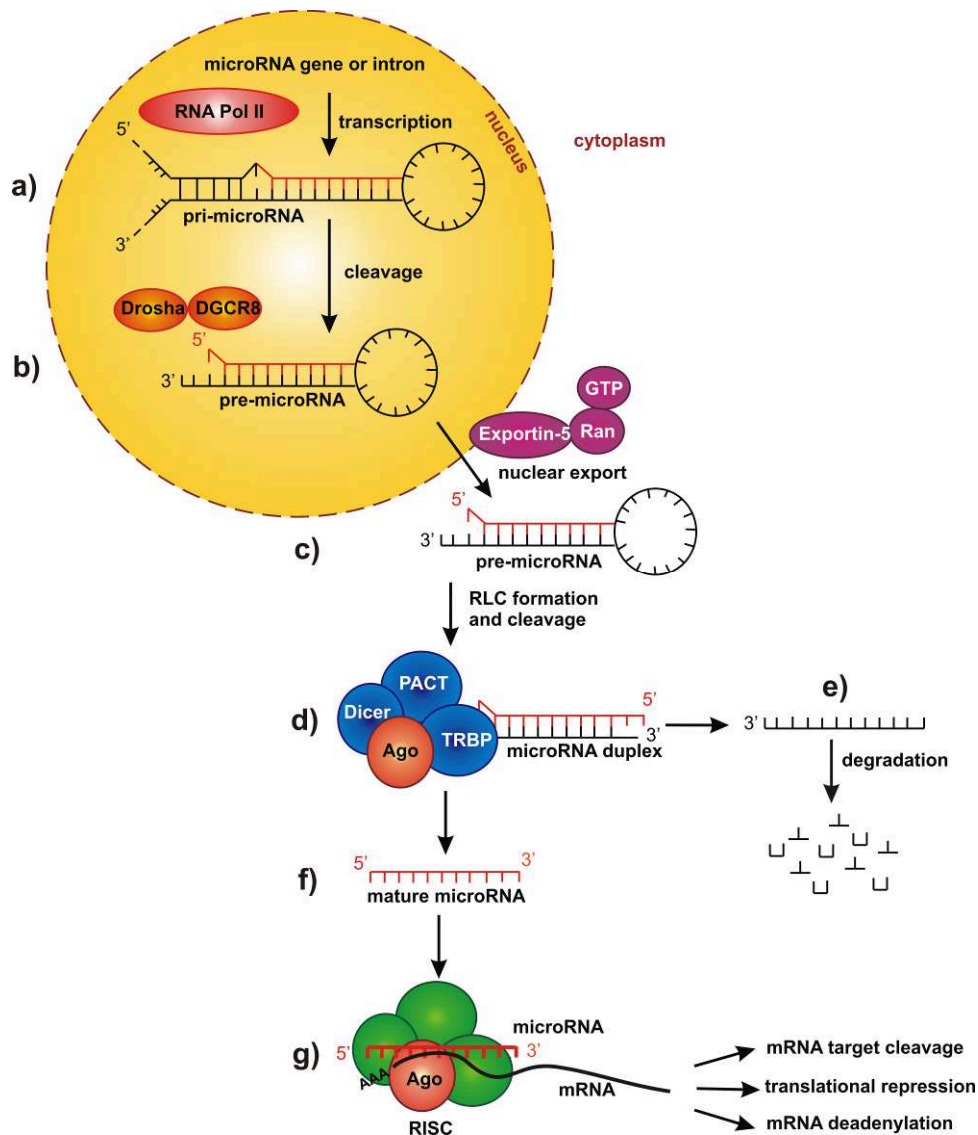
Figure 1.3.3.I Schematic depiction of miRNA biogenesis. **a)** Within the nucleus the pri-miRNA is produced by RNA polymerase II and **b)** cleaved by the microprocessor complex Drosha-DGCR8. **c)** The resulting precursor hairpin, the pre-miRNA, is exported into the cytoplasm by Exportin-5-Ran-GTP. **d)** In the cytoplasm, the RNase Dicer in complex with the double-stranded RNA binding protein TRBP and PACT cleaves the pre-miRNA hairpin to its mature length. **e)** The passenger strand will be degraded, whereas **f)** and **g)** the functional strand of the miRNA-duplex is loaded together with one of the four human Argonaute proteins into the RNA-induced silencing complex (RISC), where target-mRNAs are silenced by mRNA cleavage, translational repression or deadenylation (image modified according to Winter *et al.*, 2009).

1.4 Assembly and function of Argonaute protein complexes

1.4.1 Structure and function of Argonaute protein complexes

miRNAs perform their regulatory functions in cooperation with distinct proteins called Argonaute proteins (Ago, aliases: EIF2C1, EIF2C2, EIF2C3, EIF2C4), which cleave or repress the bound target-mRNA. In human, four Argonaute proteins are ubiquitously expressed, and share extensive structural and sequence homology. Members of the Ago protein family are crucial components of the RNA silencing effector complexes. They are the catalytic subunit of RISC that can inhibit or cleave target-mRNAs as directed by incorporated miRNAs (Martinez *et al.,* 2002). Eukaryotic Ago proteins are characterized by two domains, the PAZ domain, which is named according to three proteins that contain this domain: Piwi, Argonaute and Zwille, and the PIWI domain (Cerutti *et al.,* 2000).

PAZ domains are small, around 140 residue domains, which were identified in Ago proteins and Dicer enzymes, both involved in RNA interference (RNAi). The PAZ domain is composed of two subdomains with a cleft in between. In detail, the N-terminal, middle and PIWI domains form a crescent-shaped base, where the PAZ domain is located above, and held by a stalk-like linker region between the N-terminal and the PAZ domains (Figure 1.4.1.I). This architecture builds a large positively charged groove between the PAZ domain and the crescent base, and a smaller groove between the N-terminal and PIWI domain (Song and Joshua-Tor, 2006). The PAZ domain is responsible for binding the 3' end of small RNAs (Lingel *et al.*, 2003; Song *et al.*, 2003; Yan *et al.*, 2003), and the large positively charged groove represents the RNA-binding groove (Song *et al.,* 2004; Wang *et al.,* 2008). The 5' region of the mRNA lies between the PAZ and N-terminal domain. The PAZ domain binds preferentially RNA over DNA, whereas binding is sequence independent (Song *et al.*, 2003; Yan *et al.,* 2003). The MID domain is similar to the sugar binding domain of the Lac-repressor, which binds lactose between two such domains (Song and Joshua-Tor, 2006).
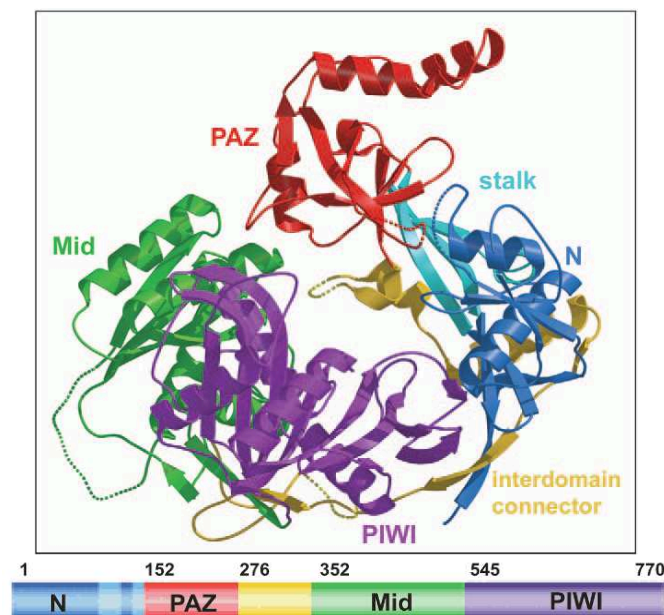
Figure 1.4.1.I The structure of *P. furiosus* Argonaute. Ribbon representation of Argonaute that shows the N-terminal domain (blue), the "stalk" (light blue), the PAZ domain (red), the MID domain (green), the PIWI domain (purple) and the interdomain connector (yellow) (3D structure according to Song and Joshua-Tor, 2006).

The PIWI domain is found only in Ago proteins (Song and Joshua-Tor, 2006), and it is structurally related to the RNase H family of ribonucleases (Song *et al.*, 2004). This domain is located at the C-terminus of Argonaute and contains three conserved catalytic residues, composed of two aspartates and one histidine, called the "DDH" motif, which is analogous to the "DDE" catalytic motif in RNase H fold enzymes (Yang and Steitz, 1995). A mutation in one residue of DDH eliminates "Slicer" activity of human Ago2 (Liu *et al.,* 2004; Rivas *et al.,* 2005).

Additionally, other Ago domains were identified which bind to the m^7G cap of mRNAs (Kiriakidou *et al.*, 2007) and two new Ago components called DExD box protein MOV10 (Moloney leukemia virus 10 homologue), and TNRC6B (trinucleotide repeat containing 6B) were detected. TNRC6B has a high sequence similarity to TNRC6A (GW182) (Eulalio *et al.*, 2007), which is a marker protein for cytoplasmatic processing bodies (P-bodies) preventing translation of mRNAs localized to P-bodies (Liu *et al.*, 2005). However, not all Argonautes are active as endonucleases. In human, only Ago2 possesses slicing activity because in Ago1, histidine is replaced by arginine, and in Ago4 the aspartates are missing and replaced by glycine (Rivas *et al.,* 2005). Interestingly, Ago3 exhibits all three residues and is still inactive for slicing (Liu *et al.*, 2004; Rivas *et al.*, 2005).

Recent studies demonstrated that expression of most miRNAs was reduced by more than 80% in Ago2-knockout or –knockdown mice leading to substantial dysregulation of thousands of genes (Liu *et al.,* 2004, Schmitter *et al.,* 2006, Kaneda *et al.*, 2009), and it was shown that *in vitro* knockout of all four human Argonaute proteins triggers apoptosis (Su *et al.*, 2009). The selective depletion of Ago1 or Ago3 impaired only up to 50% of mRNAs compared with Ago2, and the effect of Ago4 depletion was even smaller (Schmitter *et al.,* 2006). On this account, Grimm *et al.* suggest that at least Ago1, Ago3 and Ago4 are redundant which is supported by the fact that human wild-type Ago3 and Ago4 are located on the same chromosome suggesting that they are Ago1-pseudogenes (Grimm *et al.*, 2010). On the other hand, all four human Ago variants are expressed in a highly tissue- and developmental-specific manner indicating all Argonaute proteins as important for specific gene regulation (Cheloufi *et al.*, 2010, Gonzalez-Gonzalez *et al.*, 2008, Sasaki *et al.*, 2003). Moreover, some groups reported association of Ago2/Ago3 with specific miRNAs (Azuma-Mukai *et al.*, 2008), or of Ago1/Ago2 with unique mRNAs or proteins (Hock *et al.,* 2007, Beitzinger *et al.*, 2007, Landthaler *et al.,* 2008).

1.4.2 Regulation of mRNA translation and stability by RISC

The key component of the RISC is one of the four human Argonaute proteins, which interact with the 3' and the 5' ends of the miRNA as shown in Figure 1.4.2.I (Jinek and Doudna, 2009; Peters and Meister, 2007). Each of the four Ago proteins function in mRNA repression, but only Ago2 has an enzymatically active PIWI domain, which cleaves mRNA at the center of the miRNA-mRNA duplexes (Liu *et al.,* 2004).
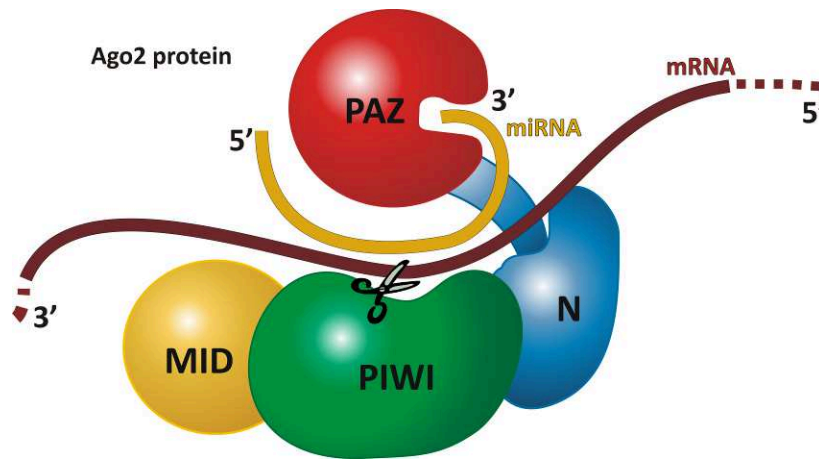
Figure 1.4.2.I Schematic depiction of interaction between Ago2, miRNA and mRNA. The miRNA is bound with its 3' end to the PAZ region of the Argonaute protein. The 5' region of the mRNA lies between the PAZ and N-terminal domain. Based on miRNA seed pairing, the mRNA is cleaved at a distinct site by Ago2. Alignment of the complementary base pairing produces an Ago-mRNA footprint. Analysis of this restricted sequence region allows prediction and validation of miRNA binding sites and target-mRNAs (www.cshl.edu).

The repression of mRNA translation is mediated by miRNAs, which are bound to the Ago proteins and guide them to specific mRNAs. Thus, miRNAs either inhibit translation of target-mRNAs (Figure 1.4.2.II) or facilitate their deadenylation and subsequent degradation (Figure 1.4.2.III).

miRNAs inhibit translation of distinct mRNAs during translation initiation, after translation initiation or by direct destabilization of mRNAs with subsequent degradation. First, it was demonstrated that miRNAs block translation initiation by repression of the ribosome composition (Figure 1.4.2.III a). In *Drosophila melanogaster* (*D. melanogaster*), miRNAs repress the assembly of the 40S subunit of the ribosome, whereby the 60S ribosomal subunit will not be joined to the 40S subunit to form the ribosome complex (Chendrimada *et al.*, 2007). Secondly, the RISC requires the presence of cap structure to repress formation of the translational initiation complex (Humphreys *et al.*, 2005; Pillai *et al.*, 2005). Some studies showed that, instead of the eIF4F complex, which includes the m^7G cap-binding translation initiation factor eIF4E (Mathonnet *et al.*, 2007), the Ago2 can bind the m^7G cap of mRNAs through its MID domain (Kiriakidou *et al.*, 2007). Hence, Ago2 competes with the translation machine for the m^7G cap binding and represses formation of the translation initiation complex, whereas overexpression of eIF4F could reverse miRNA-mediated translation inhibition (Mathonnet *et al.,* 2007). The third way of translational inhibition can be the blocking of the Poly(A) Binding Protein (PABP) binding on mRNAs by miRNAs, which induce deadenylation of the mRNA and shorten their poly(A)-tail. Thereby, PABP is no longer able to bind to the poly(A)-tail of the mRNA, which could affect the translation initiation (Wakiyama *et al.*, 2007).

The inhibition of mRNA translation by miRNAs is also possible after translational initiation (Figure 1.4.2.II b). It was demonstrated that miRNAs inhibit mRNA translation, while polysomes are active (Nottrott *et al.*, 2006). Moreover, cap-independent translation initiated by internal ribosome entry site (IRES) was also repressed by miRNAs, indicating that repression occurred after the initiation step (Petersen *et al.*, 2006). The co-translational degradation of the nascent polypeptide chain, encoded by the target-mRNA, could result from this post-initiation inhibition. This leads to high rate of ribosome drop-off and increased immature termination during elongation. The results are incomplete protein products that would be rapidly degraded (Petersen *et al.*, 2006).
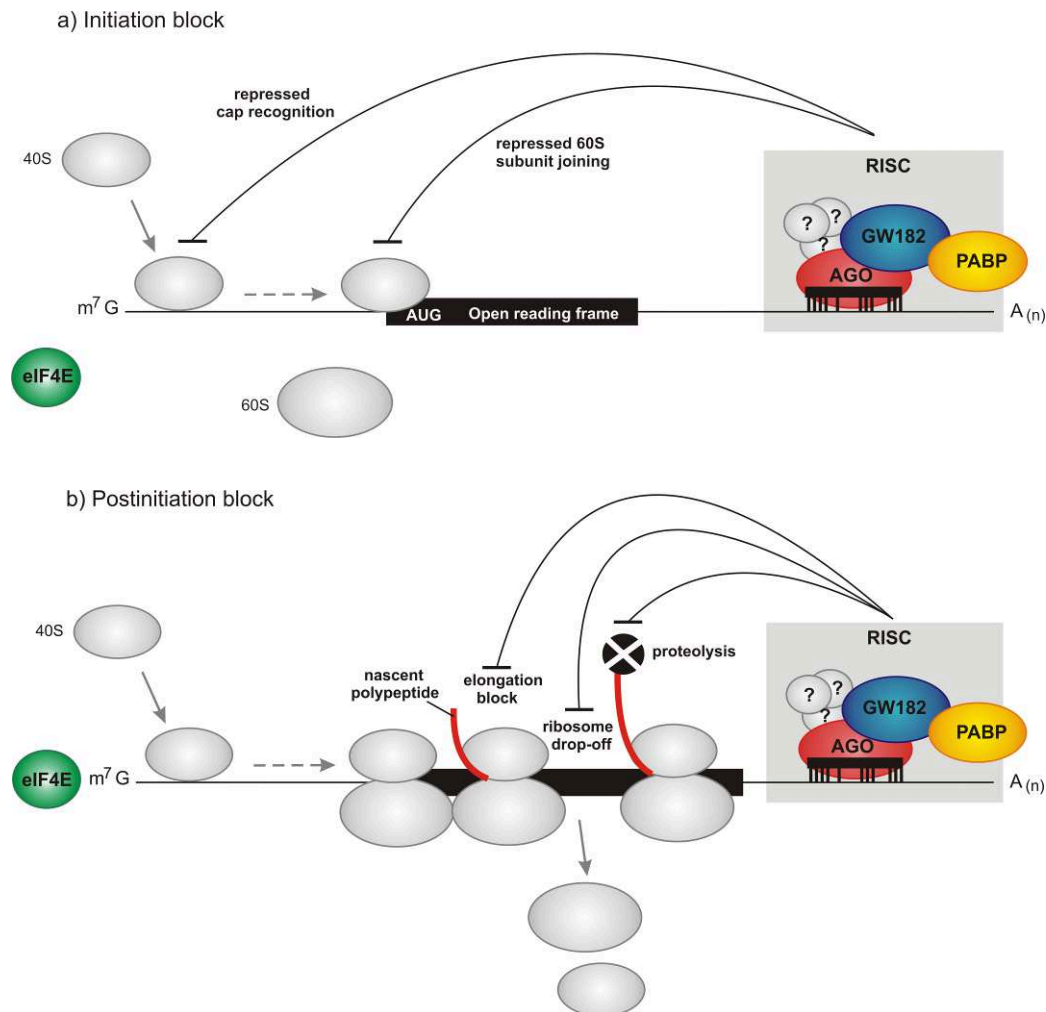
Figure 1.4.2.II Schematic diagram of miRNA-mediated translational repression. **a)** Initiation block: The RISC inhibits translation initiation by interfering with eIF4F-cap recognition and 40S small ribosomal subunit recruitment or by antagonizing 60S subunit joining and preventing 80S ribosomal complex formation. The interaction of the GW182 with the poly(A)-binding protein (PABP) might interfere with the closed-loop formation mediated by the eIF4G-PABP interaction and thus contribute to the repression of translation initiation. **b)** Postinitiation block: The miRISC might inhibit translation at postinitiation steps by inhibiting ribosome elongation, including ribosome drop-off, or facilitating proteolysis of nascent polypeptides. There is no mechanistic insight to any of these proposed "postinitiation" models. The 40S and 60S ribosomal subunits are represented by small and large gray spheres, respectively. Ovals with question marks represent potential additional uncharacterized RISC proteins that might facilitate translational inhibition (picture was taken from Fabian *et al.*, 2010).

The degradation of mRNAs often starts with the removal of the poly(A)-tail by 3'-5' exoribonucleases, which include the CCR4 (carbon catabolite repression 4) –NOT1 (negative on TATA-less) complex and other proteins like CAF1 (CCR4-associated factor) deadenylase (RNase D family deadenylase) (Figure 1.4.2.III). Subsequently, the mRNA is degraded in 3'-5' direction. Another possibility is a removal of the 5'-terminal cap by the decapping DCP1-DCP2 enzyme complex and a degradation of the body by Xrn1, a 3'-5' exonuclease (Coller and Parker, 2004). For deadenylation subsequent decapping and degradation of mRNAs, Ago proteins and GW182 components of miRISC are required (Behm-Ansmant *et al.,* 2006). Ago proteins act as scaffolds to recruit GW182 to the mRNA. On the other hand, GW182 recruits the CCR4-NOT1 complex to induce deadenylation of miRNA-targeted mRNAs (Behm-Ansmant *et al.,* 2006).
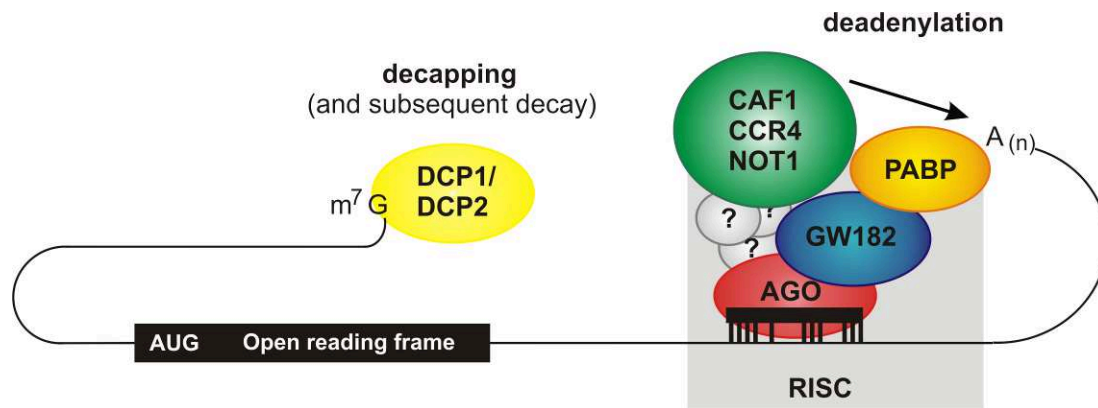
Figure 1.4.2.III Schematic diagram of miRNA-mediated mRNA decay. The miRISC interacts with the CCR4-NOT1 deadenlyases complex to facilitate deadenylation of the poly(A)-tail. Deadenylation requires the direct interaction of the GE182 protein with the poly(A)-binding protein (PABP). Following deadenylation the 5'-terminal cap (m^{7}G) is removed by the decapping DP1-DCP2 complex. The open reading frame is denoted by a black rectangle (picture taken from Fabian *et al.*, 2010).

In specific situations, miRNAs are also able to activate protein biosynthesis (Henke *et al.*, 2008; Orom *et al.,* 2008; Vasudevan *et al.*, 2007). They repress translation in proliferating cells, but activate translation in resting cells arrested in G0/G1. For instance, it was shown that Ago2-miR-369-3 complex, which bound to the 3'-UTR of TNFα, mRNA recruited FXR1 (fragile X-related protein 1) and stimulate mRNA translation (Vasudevan *et al.,* 2007). FXR1 may regulate intracellular transport and local translation of certain mRNAs, but broad translation activation by miRNAs and Ago2 is rather unexpected, because it is probably not a general mechanism in quiescent cells (Lee *et al.*, 2004).

1.5 Methods for identification of Ago-miRNA-mRNA interactions

1.5.1 Different methods used for identification of Argonaute protein associated nucleic acids

For experimental identification of miRNAs and their target-mRNAs associated with Argonaute proteins, different methods have been developed. One of the first methods generated so far was the immunoprecipitation (IP) of RNA-binding proteins (RBPs) with subsequent microarray profiling called RIP-Chip (Keene *et al.*, 2006; Tenenbaum et al., 2000). This method allows a global identification of multiple RNA targets of RBPs of crosslinked or non-crosslinked cells (Keene *et al.,* 2006). After immunoprecipitation, the bead bound RBPs were washed extensively and digested using proteinase K, to release the ribonucleo protein (RNP) components. The extracted RNA was purified and detected by microarray profiling or high-throughput sequencing (Keene *et al.*, 2006). It is possible that free RNAs present in all cells, could interact with RBPs, after cell lysis leading to a high background of false-positive RNAs and artifacts (Mili and Steitz, 2004; Penalva *et al.*, 2004; Yang *et al.*, 2005). The extensive washing steps of the RIP-Chip protocol minimize such inappropriate interactions (Penalva *et al.*, 2004; Tenenbaum *et al.,* 2003; Tenenbaum *et al.*, 2000), indeed loosing many true interactions as well. To minimize this problem, *in vivo* crosslinking using ultraviolet light (Greenberg, 1979; Wagenmakers *et al.*, 1980) and immunoprecipitation were combined (Dreyfuss *et al.,* 1984; Mayrand *et al.*, 1981), in order to recover more RBP target site information. This method, combined with a subsequent isolation of crosslinked RNA fragments and cDNA sequencing, called CLIP (Ule *et al.*,

2003), was used to identify targets of different splicing regulators, as well as Ago2 protein binding sites (Chi *et al.*, 2009). The CLIP method uses UV light at a wavelength of 254 nm to covalently crosslink RNA-protein complexes. After immunoprecipitation, the RNA was partially digested, to get small RNA fragments remaining attached to the protein. After protein digestion, the isolated intact RNA was competent for RNA linker ligation, reverse transcriptase polymerase chain reaction (RT-PCR) amplification and sequencing (Jensen and Darnell, 2008).

A slightly different approach for identification of miRNA-mRNA interactions within Argonaute proteins, was termed high-throughput sequencing of RNAs isolated by crosslinking immunoprecipitation (HITS-CLIP) (Chi *et al.,* 2009). After UV irradiation and immunoprecipitation of Ago-RNA complexes, the RNA was partially digested as well, radiolabeled and purified by SDS-PAGE and nitrocellulose transfer. Subsequently, the RNA was finally analyzed by RT-PCR and sequenced by high-throughput methods (Licatalosi *et al.*, 2008). Additionally, an immunoprecipitation of normal IgG as negative control was analyzed by Western Blot to show the specificity of Ago-antibody.

A further improved method for isolation of segments of RNA bound by RBPs is called PAR-CLIP (Photoactivatable-Ribonucleoside-Enhanced Crosslinking and Immunoprecipitation) (Hafner *et al.*, 2010a). For this approach, 4-thiouridine (s^{4}U), which incorporates into transcripts, was added to cultured cells to facilitate UV-crosslinking. In this way, RBP binding sites could be identified precisely by scoring for thymidine (T) to cytidine (C) transitions in the sequenced cDNA (Hafner *et al.*, 2010a). Compared to conventional UV 254 nm crosslinking, 4-thiouridine improved RNA recovery 100- to 1000-fold. With this method tens of thousands of binding sites for various RBPs were discovered, which shows the complexity of posttranscriptional regulation of cellular systems (Hafner *et al.*, 2010a).

1.5.2 miRNA – target interactions

In order to investigate miRNA functionality in AML, target-mRNAs, which underlie post-transcriptional gene-silencing carried out by miRNAs, have to be analyzed experimentally and bioinformatically. For computational prediction of miRNA targets, the different binding possibilities between miRNA and mRNA have to be investigated, because a unique miRNA offers the potential to target and regulate hundreds of mRNAs in different ways (Brennecke *et al.*, 2005; Grun *et al.*, 2005; Krek *et al.*, 2005; Lewis *et al.*, 2005; Xie *et al.*, 2005). Therefore, different experimental and computational approaches were implemented to find miRNA-mRNA interactions.

An early study demonstrated that regions of the 5' end of metazoan miRNAs are more conserved than the 3' end, suggesting that these parts are crucial for interactions between miRNAs and mRNAs (Lim *et al.,* 2003). These conserved 5' regions of miRNAs are around 2 to 8 nt in length, called "seed sequence". By seed pairing with a distinct region of the 3'-UTR, the target-mRNA will be destabilized or repressed. If the seed sequence is disrupted by a mutation, the miRNA-guided repression of the mRNA will be reduced (Brennecke *et al.*, 2005; Doench and Sharp, 2004; Kloosterman *et al.*, 2004). In human, miRNA seed matches are highly conserved (Lewis *et al.*, 2005), showing a significantly lower single nucleotide polymorphism (SNP) frequency than other conserved 3'-UTR elements. This indicates that miRNA seed pairing is under negative selective pressure and that SNPs are destructive in many miRNA seed binding sites (Chen and Rajewsky, 2006). Today, the vast amount of data indicates that miRNA seed pairing is the most crucial determinant of miRNA-mRNA interactions.

However, mismatches or mutations in the seed sequence of a miRNA can be compensated by high complementarity of the 3' end of the miRNA sequence. Thus, miRNA seed pairing is important, but not always required for repression (Brennecke *et al.,* 2005). There are more components, influencing the efficiency of miRNA-mRNA pairing. Statistically, in long 3'-UTRs of mRNAs the binding efficiency is higher if the miRNA binding site is located at the beginning or at the end of the 3'-UTR (Grimson *et al.,* 2007). A detailed analysis revealed that genes with more miRNAs sites have, on average, longer 3'-UTRs, but also significantly more sites per kb of 3'-UTR sequence (Stark *et al.,* 2005). Moreover, the ability of miRNA binding is enhanced in AU-rich 3'-UTRs, because such regions are more accessible (Grimson *et al.*, 2007; Kertesz *et al.*, 2007). Cell type specific factors appear to have another influence on miRNA binding ability. These factors are RNA binding proteins that either favor or avoid silencing of specific target-mRNAs (Didiano and Hobert, 2006). It was demonstrated, that a miRNA repressing an mRNA in a particular cell type, can fail to suppress the same target in a different cell type (Kedde *et al.,* 2007). Moreover, it was demonstrated that miRNPs can repress the translation of ribosomal proteins by binding to the 5'-UTRs of ribosomal mRNAs (Orom *et al.*, 2008). However, more studies are needed, to investigate if miRNA binding to 5'-UTRs is a frequent event or limited to a small set of target-mRNAs.

1.5.3 miRNA target prediction algorithms and their experimental validation

For a global analysis of sequence complementarity between miRNAs and mRNAs, a lot of prediction methods were developed, which are different in approach and performance (Baek *et al.*, 2008; Selbach *et al.*, 2008). Knowledge about the miRNA seed reduces the appearance of false-positive predictions markedly, because perfect seed pairing improves prediction and recognition of miRNA targets (Lewis *et al.,* 2003). As mentioned above, the 5' region of miRNAs is the most conserved part (Lim *et al.,* 2003). Therefore, it is possible to calculate a target prediction by simply searching for a 7 nt miRNA seed at the 5' end, which is complementary to 3'-UTR of mammalian mRNAs. Searching for an 8 nt seed match increases the specificity of the prediction, whereas a 6 nt seed match provides increased sensitivity and less specificity. However, it became evident that most targets have only a 7 nt match to the miRNA seed (Lewis *et al.*, 2005). Hence, it can be concluded that members of the same miRNA family, offering the same seed sequence share the same mRNA targets (Gaidatzis *et al.*, 2007).

Moreover, only 5% of all predicted targets contain more than one conserved site for any single miRNA, indicating that stringent regulation by a single miRNA is rare (Stark *et al.*, 2005). About 50% of target 3'-UTRs have sites for two or more 5' unique miRNAs, and some have sites for up to 12. After subtraction of sites conserved by chance, a high number of predicted targets remain, because highly conserved miRNA are able to target a high number of mRNAs. Around 300 conserved targets will be predicted for only one miRNA using different searching algorithms. That means, almost half of the human protein-coding genes were regulated by miRNAs (Friedman *et al.*, 2009). Experimental studies strengthen the findings of computational analysis. By introducing exogenous miRNA into HELA cells, which these cells do not express normally, microarray analysis exposed a changed expression of hundreds of mRNAs (Lim *et al.,* 2005).

There are several prediction tools available like: TargetScan (Friedman *et al.*, 2009; Grimson *et al.*, 2007; Lewis *et al.*, 2005), PicTar (Chen and Rajewsky, 2006; Grun *et al.,* 2005; Krek *et al.*, 2005; Lall *et al.,* 2006) or EMBL (Brennecke *et al.,* 2005; Stark *et al.*, 2005; Stark *et al.*, 2003), which have a high grade of overlap, but do not lead to 100% identical results. These tools are based on Watson-Crick seed pairing, providing better results than tools that do not (Lewis *et al.*, 2005). For example, the database MovingTargets (Burgler and Macdonald, 2005) has the highest specificity, as it predicts the smallest number of non-functional targets (2%), but has a low sensitivity of only 11% (Stark *et al.,* 2005). The database PicTar (Grun *et al.*, 2005) requires extensive site conservation, but has otherwise relaxed criteria. Therefore, the specificity lies in the same range (3%), but with a much higher sensitivity of 48% (Stark *et al.*, 2005). In contrast, the database miRanda (Betel *et al.*, 2010; Betel *et al.,* 2008; Enright *et al.*, 2003; John B, 2005) has an accuracy value of around 70% only, whereas PicTar is in the 90% range of trustworthiness. As the predictions of miRanda were based on empirical rules derived from very few examples, the accuracy is not that high (Stark *et al.*, 2005). Targets predicted by miRanda have small intersections with targets predicted by PicTar, EMBL or TagetScan. PicTar predictions are very similar to predictions by EMBL and have by far the highest overlap. Consequently, the poor overlap of predictions by methods other than PicTar and MovingTargets could reflect that these methods miss a substantial part of valid targets, whereas other methods, like miRanda, substantially overpredict non-functional sites (Stark *et al.*, 2005).

1.6 Aims of the PhD thesis

The previous introductory sections illustrate the crucial regulatory roles of miRNAs in various diseases and cancers, particularly AML. Thus, miRNAs gain more and more importance in leukemogenesis, due to their abnormal expression in distinct AML subtypes leading to activation or inhibition of essential pathways. Since the functionality of miRNAs in AML is not fully understood yet, the elucidation of specific regulatory mechanisms of these molecules is necessary for the development of novel therapeutic strategies. The present thesis will support the understanding of AML pathogenesis by miRNA expression profiling and miRNA target identification in patient samples carrying different chromosomal aberrations.

It is known that in adult AML patients, miRNAs may function as biomarker for risk-group stratification, but this is still unclear for pediatric AML patients.

- Therefore, the first aim of this PhD thesis is the miRNA expression profiling and analysis of about 100 pediatric AML patient samples, in order to investigate if miRNAs could function as biomarker in pediatric AML patients as well, and which miRNAs are responsible for the differentiation of AML subtypes.

- In order to get more insights into miRNA functionality in AML, the second aim is the improvement and optimization of a CLIP method for the rapid identification of miRNAs and their target-mRNAs, associated with the four human Argonaute proteins in appropriate AML cell line models.

- Following, the third aim is the identification of miRNA-mRNA interactions in AML via different prediction algorithms.

- Finally, the fourth aim is the classification of Ago-associated transcripts into gene ontology groups and pathway networks together with the identified, regulatory miRNAs, to find putative interactions between these components and the development of AML pathogenesis.

2 Materials

2.1 Patients

The patient material was provided by the Children's University Hospital in Giessen under the direction of Prof. Dr. Jochen Harbott. The agreement for the molecular characterization of this material was obtained in the scope of previous therapy protocols. All patient samples were obtained following informed written consent from legal guardians of the children. The samples were obtained in approved clinical studies of the German pediatric oncology and hematology society (GPOH) that were reviewed in appropriate ethical commissions. All personal data were encoded and obscured for privacy reasons. In order to determine miRNA expression profiles, the following 102 pediatric AML patient samples carrying different chromosomal abnormalities were analyzed by microarray technology (details see Supplement Table V.1).

Table 4.1.1.I Characteristics of pediatric AML patient samples, Abbreviation: eo - eosinophilia

Characteristic	pediatric AML cohort (n = 102)	
Age, y		
Median	10.3	
Range	0.5 - 17.9	
Sex, no. (%)		
Female	51 (50)	
Male	51 (50)	
White cell count, x 10^3/µl		
Median	92.3	
Range	15.5 - 290.7	
Bone marrow blasts, %		
Median	80	
Range	20 - 100	
Cytogenetic abnormalities, no. (% of patient cohort)		French-American-British classification
t(4;11)	1 (0.98)	-
t(6;11)	2 (1.96)	M5
t(9;11)	16 (15.69)	M5
t(10;11)	6 (5.88)	M4, M5
t(11;19)	5 (4.90)	M2, M4, M5
t(11q23)	3 (2.94)	-
t(15;17)	14 (13.73)	M3
inv(16)	13 (12.75)	M2, M4, M4eo
t(8;21)	24 (23.53)	M0, M1, M2, M4eo
normal	4 (3.92)	M2, M4, M5, M6
other	14 (13.73)	M2, M4, M5, M6

2.2 Human, adherent cell lines

Cell line: SNB19

Cell type: human astrocytoma (derivative of U-251 MG)

DSMZ No: ACC 325 (*Deutsche Sammlung für Mikroorganismen und Zellkulturen, Braunschweig*)

Origin: Established from the surgical resection of a left parieto-occipital glioblastoma from a 47-year-old man in 1980. Cells were described to secrete plasminogen activator, to be clonogenic in soft agar and to be tumorigenic in nude mice. DNA fingerprinting showed unequivocally that SNB19 is a subclone of the astrocytoma cell line U-251 MG.

References: (Gross *et al.*, 1988) Cancer Res 48: 291-296, PubMed ID 3121170

Cell line: HELA

Cell type: human cervix carcinoma

DSMZ No: ACC 57 (*Deutsche Sammlung für Mikroorganismen und Zellkulturen, Braunschweig*)

Origin: Established from the epitheloid cervix carcinoma of a 31-year-old black woman in 1951. Later diagnosis changed to adenocarcinoma. First aneuploid continuously cultured human cell line.

References: (Scherer *et al.*, 1953) J Exp Med 97: 695-710, PubMed ID 13052828

2.3 Human, suspension cell lines

Cell line: KASUMI-1

Cell type: human acute myeloid leukemia

DSMZ No: ACC 220 (*Deutsche Sammlung für Mikroorganismen und Zellkulturen, Braunschweig*)

Origin: Established from the peripheral blood of a 7-year-old Japanese boy with acute myeloid leukemia (AML FAB M2) (in 2nd relapse after bone marrow transplantation) in 1989. Cells carry the t(8;21) *AML1-ETO* fusion gene.

Reference: (Asou *et al.*, 1991) Blood 77: 2031-2036, PubMed ID 2018839
review: (Drexler *et al.*, 1995a) Leukemia 9: 480-500, PubMed ID 7885046

Cell line: NB4

Cell type: human acute promyelocytic leukemia

DSMZ No: ACC 207 (*Deutsche Sammlung für Mikroorganismen und Zellkulturen, Braunschweig*)

Origin: Established from the bone marrow of a 23-year-old woman with acute promyelocytic leukemia (APL = AML FAB M3) in second relapse in 1989. Patented cell line. Cells carry the t(15;17) *PML-RARα* fusion gene.

References: (Lanotte *et al.*, 1991) Blood 77: 1080-1086, PubMed ID 1995093
(Duprez *et al.*, 1992) Leukemia 6: 1281-1287, PubMed ID 1453773
review: (Drexler *et al.,* 1995b) Leuk Res 19: 681-691, PubMed ID 7500643

2.4 Chemicals

2.4.1 General chemicals

Identifier	Company	Ordernumber
1,4.dithio-DL-threitol (DTT)	Roth, Karlsruhe, Germany	6908.2
2-Propanol for Analysis	Merck, Darmstadt, Germany	67-63-0
Bis-Acrylamide 30% (19:1)	Bio-Rad, München, Germany	161-0154
Agarose	Biozym, Hessisch Odendorf, Germany	840004
Ammonium Persulfate	Sigma-Aldrich, St. Louis, MO, USA	A-3678
Bromphenolblue	Sigma-Aldrich, St. Louis, MO, USA	115-39-9
BSA 10 mg/ml	NEB, Frankfurt a. M., Germany	B90015
Chloroform 99.4%	Merck, Darmstadt, Germany	67-66-3
DMSO (Dimethylsulfoxide)	Sigma-Aldrich, St. Louis, MO, USA	D2650
EDTA (Ethylenediamine-tetraacetic acid)	Sigma-Aldrich, St. Louis, MO, USA	60-00-4
Ethanol	Merck, Darmstadt, Germany	1.00983.2511
Ethidiumbromide Solution	Sigma-Aldrich, St. Louis, MO, USA	E1510-10ML
Glycerine	Merck, Darmstadt, Germany	1.04094.2500
Glycine	Merck, Darmstadt, Germany	1.04201.1000
H_3BO_3 (Boric acid)	Merck, Darmstadt, Germany	1.00165.
HCl (Hydrochloric acid)	Merck, Darmstadt, Germany	1.09911.0001
KCl (Potassium chloride)	Merck, Darmstadt, Germany	1.04938.
KOH (Potassium hydroxide)	Merck, Darmstadt, Germany	105012
Magnesium (Mg_2)	Merck, Darmstadt, Germany	105815
Methanol	Merck, Darmstadt, Germany	1.06007.2500
Mg_2Cl	Merck, Darmstadt, Germany	1.05833.0250
Milk Powder	Roth, Karlsruhe, Germany	T145.2
Na_2EDTA	Sigma-Aldrich, St. Louis, MO, USA	E5134-500G
Na_2HPO_4 (di-Sodiumhydrogen-phosphat-Dihydrat)	Merck, Darmstadt, Germany	6580
NaCl (Sodium chloride)	Merck, Darmstadt, Germany	1.06404.1000
NaF (Sodium fluoride)	AppliChem, Darmstadt, Germany	A3904.0500
NaH_2PO_4 (Sodiumhydrogenphosphat Monohydrat	Merck, Darmstadt, Germany	6346.1000
NaOH (Sodiumhydroxide)	Merck, Darmstadt, Germany	1.06498.100
Nonidet P40 Substitute	Fluka Biochemica	74385
Ponceau S Solution	Sigma-Aldrich, St. Louis, MO, USA	P-7170
SDS 20%	Ambion, Huntingdon, UK	AM9820
50 x TAE (Tris/Acetic Acid/EDTA) Buffer	Bio-Rad, München, Germany	161-0743
TEMED (Tetramethylethylendiamin)	Merck, Darmstadt, Germany	1.10732.0100
Tris	Roth, Karlsruhe, Germany	5429.3
Tween 20	Merck, Darmstadt, Germany	8.22184.2500
Urea	Merck, Darmstadt, Germany	66612
β-Mercaptoethanol	Merck, Darmstadt, Germany	15433.0100

Abbreviations: NEB - New England Biolabs, a.M. - am Main,

2.4.2 Specific chemicals

Identifier	Company	Ordernumber
[γ-P32] Adenosine 5'-triphosphate (ATP)	Hartmann Analytic, Braunschweig, Germany	FP-301
4-Thioruidine 25 mg	Sigma-Aldrich, St. Louis, MO, USA	T4509
50 x Denhardt Solution	AppliChem, Darmstadt, Germany	A3792.0050
AccuPrime SuperMix I	Invitrogen, Carlsbad, CA, USA	12342-028
Complete, EDTA-free Protease Inhibitor Cocktail Tablets	Roche Diagnostics, Mannheim, Germany	11244800
Cyanine Dye (Cy3, Cy5)	New York Rockefeller University (T. Tuschl lab)	-
GlycoBlue 300 µl (15 mg/ml)	Ambion, Huntingdon, Cambridgeshire, UK	AM9515
Isoamylalcohol	Merck, Darmstadt, Germany	100979
Phenol	Merck, Darmstadt, Germany	100206
Phenol acid	Sigma-Aldrich, St. Louis, MO, USA	P4682-400ML
Quick Start Bradford Dye Reagent	Bio-Rad, München, Germany	500-0205
Salmon Sperm DNA 1 ml (10 mg/ml)	Invitrogen, Carlsbad, CA, USA	15632-011
SuperSignal West Femto Maximum Sensitivity Substrate	Thermo Scientific, Braunschweig, Germany	34095
SuperSignal West Pico Chemiluminescent Substrate	Thermo Scientific, Braunschweig, Germany	34080
SYBR Green PCR Master Mix	ABI, Carlsbad, CA, USA	4309155
TaqMan Uni. PCR Master Mix, No Amperase UNG	ABI, Carlsbad, CA, USA	4324018
TRIzol Reagent	Invitrogen, Carlsbad, CA, USA	15596-018

Abbreviation: ABI – Applied Biosystems

2.5 Nucleic acids

2.5.1 Oligonucleotides

Description	Company	Length	Sequence (5' ⟶ 3')
AGO1 e3/e4 forward	MWG, Ebersberg, Germany	21 nt	GCACTGCCCATTGGCAACGAA
AGO1 e3/e4 reverse	MWG, Ebersberg, Germany	22 nt	CATTCGCCAGCTCACAATGGCT
AGO2 e5/e6 forward	MWG, Ebersberg, Germany	20 nt	CGCGTCCGAAGGCTGCTCTA
AGO2 e5/e6 reverse	MWG, Ebersberg, Germany	22 nt	TGGCTGTGCCTTGTAAAACGCT
AGO3 e4/e5 forward	MWG, Ebersberg, Germany	23 nt	GGAATTAGACAAGCCAATCAGCA
AGO3 e4/e5 reverse	MWG, Ebersberg, Germany	22 nt	AGGGTGGTCATATCCTTCTGGA
AGO4 e6/e7 forward	MWG, Ebersberg, Germany	22 nt	CTAACAGACTCCCAGCGTGTCA
AGO4 e6/e7 reverse	MWG, Ebersberg, Germany	21 nt	GACTGGCTGGCCGTCTAGTCA
ARL2 forward	MWG, Ebersberg, Germany	20 nt	CTGCCCGCTGCTGCTCTGTG
ARL2 reverse	MWG, Ebersberg, Germany	20 nt	ATGAGGCCCACAGCCTCGGT
ATOX1 forward	MWG, Ebersberg, Germany	21 nt	GCACAGCATGGACACTCTGCT
ATOX1 reverse	MWG, Ebersberg, Germany	21 nt	ACCATCACCCGGCATGACTGC
FoxG1 forward	MWG, Ebersberg, Germany	18 nt	CCAGATTTCCATGTGCAG

2.5.1 Oligonucleotides (continued)

FoxG1 forward for qRT-PCR	MWG, Ebersberg, Germany	21 nt	CATTCGTAGTAAAGGTGCCCA
FoxG1 reverse	MWG, Ebersberg, Germany	20 nt	TTGCGCAACACAGGTTACAT
FoxG1 reverse for qRT-PCR	MWG, Ebersberg, Germany	20 nt	GCAGTGTTGCCAACTGAAAC
HMGA2 forward	MWG, Ebersberg, Germany	20 nt	GACCAAGGTGCTTTTCTTCG
HMGA2 forward for qRT-PCR	MWG, Ebersberg, Germany	22 nt	AGCCTGCTCAGGAGGAAACTGA
HMGA2 reverse	MWG, Ebersberg, Germany	22 nt	CCTAGGAGCGACTTGGTTAAAA
HMGA2 reverse for qRT-PCR	MWG, Ebersberg, Germany	23 nt	ACCCCACCCCAGATGAAAGTGGA
hsa-miR-16 for Northern Blot	MWG, Ebersberg, Germany	21 nt	GCCAATATTTACGTGCTGCTA
hsa-miR-21 for Northern Blot	MWG, Ebersberg, Germany	22 nt	TCAACATCAGTCTGATAAGCTA
hsa-miR-9 for Northern Blot	MWG, Ebersberg, Germany	23 nt	TCATACAGCTAGATAACCAAAGA
hsa-let7a for Northern Blot	MWG, Ebersberg, Germany	22 nt	AACTATACAACCTACTACCTCA
PDCD4 forward	MWG, Ebersberg, Germany	20 nt	CGAGGGGGCAAGGAGGGACA
PDCD4 reverse	MWG, Ebersberg, Germany	21 nt	ACAGCAGCAGCCAACATGGGG
ATP6V0E1 forward	MWG, Ebersberg, Germany	22 nt	AGATGGCTCCTGCCTTCTCACG
ATP6V0E1 reverse	MWG, Ebersberg, Germany	23 nt	TGGCTCTTCCCTCTGAACGTGCT
PRTN3 forward	MWG, Ebersberg, Germany	20 nt	CACTTTCGTCCCTCGCCGCA
PRTN3 reverse	MWG, Ebersberg, Germany	20 nt	GGGAAAAGGCGGGTGGCACA

Abbreviation: MWG – Eurofins MWG Operon

2.5.2 TaqMan microRNA assays

Identifier	Company	Ordernumber	Assay ID	Description
hsa-miR-16	ABI, Carlsbad, CA, USA	4427975	000391	TaqMan Micro RNA Assay
hsa-miR-9	ABI, Carlsbad, CA, USA	4427975	000583	TaqMan Micro RNA Assay
hsa-let-7a	ABI, Carlsbad, CA, USA	4427975	000377	TaqMan Micro RNA Assay
hsa-miR-223	ABI, Carlsbad, CA, USA	4427975	002295	TaqMan Micro RNA Assay
hsa-miR-125b	ABI, Carlsbad, CA, USA	4427975	000449	TaqMan Micro RNA Assay
hsa-miR-181a	ABI, Carlsbad, CA, USA	4427975	000480	TaqMan Micro RNA Assay
hsa-miR-335	ABI, Carlsbad, CA, USA	4427975	000546	TaqMan Micro RNA Assay
hsa-miR-146a	ABI, Carlsbad, CA, USA	4427975	000468	TaqMan Micro RNA Assay
hsa-let-7c	ABI, Carlsbad, CA, USA	4427975	000379	TaqMan Micro RNA Assay
hsa-miR-100	ABI, Carlsbad, CA, USA	4427975	000437	TaqMan Micro RNA Assay
hsa-let-7b	ABI, Carlsbad, CA, USA	4427975	002619	TaqMan Micro RNA Assay
hsa-miR-126	ABI, Carlsbad, CA, USA	4427975	002228	TaqMan Micro RNA Assay
hsa-miR-106b	ABI, Carlsbad, CA, USA	4427975	000442	TaqMan Micro RNA Assay
hsa-miR-191	ABI, Carlsbad, CA, USA	4427975	002299	TaqMan Micro RNA Assay
hsa-miR-106a	ABI, Carlsbad, CA, USA	4427975	002169	TaqMan Micro RNA Assay
hsa-miR-181b	ABI, Carlsbad, CA, USA	4427975	-	TaqMan Micro RNA Assay

Abbreviation: ABI – Applied Biosystems

2.5.3 Other nucleic acids and nucleotides

Identifier	Company	Ordernumber
Universal Reference (miRBase 8.2)	MACS Miltenyi Biotec, Bergisch Gladbach, Germany	130-094-407
Oligo dT Primers 100 µl (0.4 µg/µl)	Qiagen, Hilden, Germany	79237
Hexanucleotide Primers H0268-1UN	Sigma-Aldrich, St. Louis, MO, USA	067K6109
dATP, PCR Grade 100mM	Qiagen, Hilden, Germany	1039397
dCTP, PCR Grade 100mM	Qiagen, Hilden, Germany	1039396
dGTP, PCR Grade 100mM	Qiagen, Hilden, Germany	1039395
dTTP, PCR Grade 100mM	Qiagen, Hilden, Germany	1039394

2.6 Proteins

2.6.1 Enzymes

Identifier	Company	Ordernumber
T4 Polynucleotide Kinase (10 U/µl)	NEB, Frankfurt a. M., Germany	M0236L
RNA Ligase 2 (Rnl2 (1-249) K227Q) 1 µg/µl	New York Rockefeller University (Thomas Tuschl lab)	-
SuperScriptIII Reverse Transcriptase 10,000 U (200 U/µl)	Invitrogen, Carlsbad, CA, USA	18080-044

Abbreviations: NEB - New England Biolabs, a.M. - am Main

2.7 Antibodies

2.7.1 Primary antibodies

Identifier	Usage	Company	Reference/ Ordernumber
Ago1 4B8	IP, WB 1:50	MPI Biochemistry Martinsried (Gunter Meister lab)	Beitzinger *et al.*, 2007
Ago2 11A9	IP, WB 1:50	MPI Biochemistry Martinsried (Gunter Meister lab)	Beitzinger *et al.*, 2007
Ago3 5A3	IP, WB 1:50	MPI Biochemistry Martinsried (Gunter Meister lab)	-
Ago4 6C10	IP, WB 1:50	MPI Biochemistry Martinsried (Gunter Meister lab)	-
Purified Mouse Antibody Mono HA.11	WB 1:1,000	Covance, Princeton, NJ, USA	MMS-101P
Rat IgG2a, kappa monoclonal [aRTK 2758]	IP	Abcam, Cambridge, MA, USA	ab18450

2.7.2 Secondary antibodies

Identifier	Usage	Company	Ordernumber
Goat anti Rat IgG HRP	WB 1:10,000	Jackson Immuno Research, Suffolk, UK	112-035-003
Goat anti Mouse IgG polyclonal HRP	WB 1:4,000	Abcam, MA, USA	ab97090

2.8 Culture media, buffers and dilutions

2.8.1 Media, dilutions and additives for cell cultivation

Identifier	Company	Ordernumber
Dulbecco' s Modified Eagle Medium 1x (DMEM)	Gibco, Invitrogen, Carlsbad, CA, USA	21969-035
RPMI 1640	Gibco, Invitrogen, Carlsbad, CA, USA	32404-014
Penicillin 10,000 U/ml	Gibco, Invitrogen, Carlsbad, CA, USA	15140-122
Streptomycin 10,000 µg/ml	Gibco, Invitrogen, Carlsbad, CA, USA	15140-122
L-Glutamine 100 x	Gibco, Invitrogen, Carlsbad, CA, USA	25030-024
Trypsin-EDTA 1 x	PAA, Pasching, Austria	L11-004
Dulbecco's PBS without Ca & Mg 1 x	PAA, Pasching, Austria	H15-002
Fetal Bovine Serum (FBS) heat inactivated	PAA, Pasching, Austria	A15-104
Geneticin G418	Gibco, Invitrogen, Carlsbad, CA, USA	10131035

Cultivation of SNB19   1 x DMEM 500 ml, 1% (v/v) Penicillin 10,000 U/ml, 1% (v/v) Streptomycin 10,000 µg/ml, 1% 200 mM L-Glutamine, 10% FBS heat inactivated

Cultivation of KASUMI-1 and NB4   1 x RPMI 500 ml, 1% (v/v) Penicillin 10,000 U/ml, 1% (v/v) Streptomycin 10,000 µg/ml, 1% 200 mM L-Glutamine, 10% FBS heat inactivated

Freezing medium for cryopreservation: 90% culture medium and 10% DMSO

2.8.2 Buffers for immunoprecipitation

NP40 Lysis Buffer   20 mM Tris-HCl (pH 7.5), 150 mM KCl, 2 mM EDTA, 1 mM NaF, 0.5% NP40
add fresh before use: 0.5 mM DTT, 1 x complete EDTA-free protease inhibitor cocktail (Roche Diagnostics)

300 mM, 500 mM, 750 mM and 1000 mM Wash Buffer   20 mM Tris-HCl (pH 7.5), 300 mM (500 mM, 750 mM, 1000 mM) KCl, 0.05% NP40, 5 mM $MgCl_2$,
add fresh before use: 1 x complete EDTA-free protease inhibitor cocktail (Roche Diagnostics)

4 x SDS Sample-Buffer   250 mM Tris-HCl pH (6.8), 8% SDS, 40% Glycerin, 20% β-Mercaptoethanol, a pinch of Bromphenol blue

2.8.3 Buffers for Western Blot

Separation gel	8% Acrylamide (30% Acryl-Bisacrylamide mix 19:1), 375 mM Tris-HCl (pH 8.8), 0.1% SDS, 0.06% TEMED and 0.1% APS
Stacking gel	5% Acrylamide (30% Acryl-Bisacrylamide mix 19:1), 189 mM Tris-HCl (pH 6.8), 0.1% SDS, 0.1% TEMED and 0.1% APS
10 x SDS Running Buffer	25 mM Tris, 192 mM Glycine, 0.1% SDS
10 x Transfer Buffer	20 mM Tris, 150 mM Glycine, 0.038% SDS
1 x Transfer Buffer	10% 10 x Transfer Buffer, 20% Methanol
10 x TBST Blocking and Washing Buffer	1 M Tris-HCl, 1.5 M NaCl, 1% Tween 20

2.8.4 Buffers for Northern Blot

SequaGel 15%	10% Buffer, 3.33% Diluent, 1.66% Concentrate, 0.1% TEMED, 4% APS
20 x SSC	3 M NaCl and 300 mM NaCitrate (pH 7.0)
10 x TBE Buffer (Tris-borate-EDTA)	890 mM Tris and 890 mM Boric acid, 20 mM Na_2EDTA (pH 8)
2 x Bromphenolblue-Sample Buffer	8 M Urea, 50 mM EDTA, a pinch of Bromphenolblue
Hybridization Solution	5 x SSC, 20 mM Na_2HPO_4 (pH 7.2), 1 % SDS, 5 x Denhardt Solution add before hybridization: 1% Salmon Sperm DNA (10 mg/ml)
Labeling reaction of DNA probes	22 nt Oligonucleotide (20 µM), γ-32P-ATP (150 to 3000 Ci/mmol), 1 x T4 Polynucleotide kinase (PNK) buffer, 2 U/µl T4 PNK
Washing Buffer I	5 x SSC and 1% SDS
Washing Buffer II	1 x SSC and 1% SDS

2.8.5 Buffers for RNA labeling and microarray hybridization

10 x RNase Dilution Buffer   50 mM Tris-HCl (pH 7.6), 250 mM NaCl, 50% Glycerine, 0.05% TritonX-100, 1 mM DTT

10 x RNA Ligation Buffer   500 mM Tris-HCl (pH 7.5), 100 mM Mg_2Cl, 100 mM β-Mercaptoethanol, 1 mg/ml acetylated BSA, 1 mg/ml Rnl2 (1-249) K227Q

2.8.6 Kits, size markers and other materials

Kit Identifier	Company	Ordernumber
GeneChip 3' IVT Express Kit	Affymetrix, Santa Clara, CA, USA	901228
TaqMan MicroRNA Reverse Transcription Kit	ABI, Carlsbad, CA, USA	4366596
miRXplore Microarray Kit (8)	MACS Miltenyi Biotec, Bergisch Gladbach, Germany	130-093-272
QuickStart Bovine Serum Albumin (BSA) Standard Set	Bio-Rad, München, Germany	500-0207
SequaGel Sequencing System Kit (National diagnostics)	Biozym, Hessisch Odendorf, Germany	900000 (EC-833)

Identifier	Company	Ordernumber
1kb Plus DNA Ladder 250 µg (1 µg/µl)	Invitrogen, Carlsbad, CA, USA	10787-018
Amersham Hybond-N+ Positively Charged Nylon Transfer Membrane	GE Healthcare, Freiburg, Germany	RPN203B
Amersham Hybond-P PVDF Transfer Membrane	GE Healthcare, Freiburg, Germany	RPN303F
Anti-FLAG Beads M2 Agarose from mouse	Sigma-Aldrich, St. Louis, MO, USA	A2220 (068K60031)
Cryo freezing container 500 ml	Nalgene, NY, USA	5100-0001
Culture Dish 150 x 25 mm	Corning, Amsterdam, Netherlands	430597
Dynabeads Protein G 30 mg/ml	Invitrogen, Carlsbad, CA, USA	100-03D
Extra Thick Blot Paper	Bio-Rad, München, Germany	170-3965
GeneChip Human Genome U133 A 2.0	Affymetrix, Santa Clara, CA, USA	900471
illustra MicroSpin G-25 Columns	GE Healthcare, Freiburg, Germany	27-5325-01
Microcentrifuge Tube 1.7ml prelubricated RNase/DNase free	Corning, Amsterdam, Netherlands	3207
Page Ruler Prestained Protein Ladder	Fermentas, St. Leon-Rot, Germany	SM0671
PCR Stripes	Eppendorf, Hamburg, Germany	14.11.2008
Protein G Sepharose 4 Fast Flow	GE Healthcare, Freiburg, Germany	17-0618-01
Quick Load 100bp DNA Ladder	NEB, Frankfurt a. M., Germany	N0467L
Quick Load Low Molecular Weight DNA Ladder	NEB, Frankfurt a. M., Germany	N0474S

Abbreviations: NEB - New England Biolabs, a.M. - am Main

2.9 Software and hardware

2.9.1 Software and databases

Software and Databases	Available at	Reference
GenePix Pro 6	MD, Sunnyvale, CA, USA	Fielden *et al.*, 2002
Acuity 4.0	MD, Sunnyvale, CA, USA	-
R 2.11.1	http://www.r-project.org/	Ihaka and Gentleman, 1996
EGAN 1.4	http://akt.ucsf.edu/EGAN/	Paquette and Tokuyasu, 2010
RMAExpress 1.0.4	http://rmaexpress.bmbolstad.com/	Bolstad *et al.*, 2003
KEGG Release 56.0	http://www.genome.jp/kegg/	Kanehisa, 1996
miRanda Release August 2010	http://www.microrna.org/	Betel *et al.,* 2010; Betel *et al.*, 2008; Enright *et al.*, 2003; John B, 2005
miRBase Release 15.0	http://www.mirbase.org/	Griffiths-Jones, 2004, 2006; Griffiths-Jones *et al.*, 2008
TargetScan Release 5.1	http://www.targetscan.org/	Friedman *et al.*, 2009; Grimson *et al.*, 2007; Lewis *et al.,* 2005
PicTar March 26, 2007	http://pictar.mdc-berlin.de/	Chen and Rajewsky, 2006; Grun *et al.,* 2005; Krek *et al.*, 2005; Lall *et al.*, 2006
SAM (Significance Analysis of Microarrays) Release 3.0	http://www-stat.stanford.edu/~tibs/SAM/	Tusher *et al.*, 2001

Abbreviation: MD – Molecular Devices

2.9.2 Hardware

Hardware	Company
7900 HT Fast Real-Time PCR System	ABI, Carlsbad, CA, USA
Agilent 2100 Bioanalyzer Serial No. DE72905088	Agilent Technologies, Böblingen, Germany
a-Hyb Hybridization Station	MACS Miltenyi Biotec, Bergisch Gladbach, Germany
Centrifuge 5403	Eppendorf, Hamburg, Germany
Centrifuge 5417R	Eppendorf, Hamburg, Germany
FLA-7000 Phosphor Imager	Fujifilm, Düsseldorf, Germany
Gene Amp PCR System 2700	ABI, Carlsbad, CA, USA
GenePix Professional 4200 A Microarray Scanner	MD, Sunnyvale, CA, USA
HeroLab UVT 2035 UV lamp	HeroLab, Wiesloch, Germany
Hybaid Hybridization Oven	Biometra, Göttingen, Germany
LAS-3000 mini 2UV Transilluminator	Fujifilm, Düsseldorf, Germany
Mastercycler gradient	Eppendorf, Hamburg, Germany
Milli-Q Integral 15 Serial No. FODA 15851D	Millipore, Billerica, MA, USA
NanoDrop Spectrophotometer ND-1000	PeqLab, Erlangen, Germany
Thermomixer Comfort	Eppendorf, Hamburg, Germany
Transfer Blot SD Semi-Dry Transfer Cell	Bio-Rad, München, Germany
Vortex2 Genie	Scientific Industries, NY, USA

Abbreviations: ABI - Applied Biosystems, MD - Molecular Devices

3 Methods

3.1 Cell cultivation

The handling with human cell lines was performed under sterile conditions. The rules for working with "Genetically Modified Organisms" (GMO) were followed as prescribed. Biological waste and cell contaminated working equipment were autoclaved.

3.1.1 Cultivation of human, adherent cells

SNB19 and HELA cells were grown in DMEM (1 x Dulbecco's Modified Eagle Medium, Gibco Invitrogen) with 10% (v/v) FBS (PAA), 1% 200 mM L-Glutamine (100 x, Gibco, Invitrogen) and 1% (v/v) 10,000 U/ml Penicillin, 10,000 µg/ml Streptomycin (Gibco, Invitrogen) until they reached a confluence of 80%-90%. They were cultivated at a temperature of 37°C in humid, saturated atmosphere with 5% CO_2. Already transfected cells were kept under selective conditions by addition of 1% Geneticin G418 to the culturing medium. Cells were split 1:2 three times a week (SNB19) or 1:4 every three to five days (HELA), using Trypsin-EDTA. The determination of cell numbers was performed using a "*Neubauer*" counting chamber, and 5×10^7 cells were used for further experimental analyses.

3.1.2 Cultivation of human, suspension cells

KASUMI-1 and NB4 cells were grown in RPMI 1640 (Gibco, Invitrogen) with 10% (v/v) FBS (PAA), 1% 200 mM L-Glutamine (100 x, Gibco, Invitrogen) and 1% (v/v) 10,000 U/ml Penicillin, 10,000 µg/ml Streptomycin (Gibco, Invitrogen). They were also cultivated at a temperature of 37°C in humid, saturated atmosphere with 5% CO_2. Cells were split every three days in a ratio 1:2. The number of cells was counted using a "*Neubauer*" counting chamber. Between 5 x 10^7 and 3 x 10^8 cells were used for subsequent experimental analyses.

3.1.3 Cryopreservation of human cells

For long time storage of living retain-samples, human cells were removed from the culture flask and pelletized for 5 minutes at 500 x g. The cells were washed with PBS, and 1 x 10^6 cells/ml were resuspended in 1 ml freezing medium and transferred into cryotubes. The cryotubes were placed into a cryobox filled with isopropanol and frozen at -80°C for at least 24 hours. Subsequently, the cryotubes were placed into the gas phase of liquid nitrogen. For recultivation of the cells, an aliquot was thawed in a water bath at 37°C. The freezing medium was removed by pelletizing the cells at 500 x g for 5 minutes, removing the supernatant and resuspending the cells into fresh medium.

3.2 4-thiouridine incubation and UV-crosslinking of human cells

Cells of four 162 cm^2 culture flasks (~ 5 x 10^7 cells) were removed, using 2 ml of 1 x Trypsin-EDTA, and transferred into a 150 mm x 25 mm culture dish (Corning) containing 20 ml DMEM with 100 µM 4-thiouridine. Cells were cultured in DMEM/4-thiouridine for 14 hours at 37°C.

For UV-crosslinking, adherent cells were washed once with ice-cold PBS, while still attached to the plates. Suspension cells were first pelletized and washed in 1 ml ice-cold PBS and transferred to a 150 mm x 25 mm culture dish again. PBS was removed completely, and cells were irradiated on ice with 366 nm UV light (150 mJ/cm^2). Afterwards, the cells were scraped off using a cell scraper (Nunc), washed off with PBS, collected by centrifugation at 500 x g for 5 minutes, frozen in liquid nitrogen and stored at -80°C.

3.3 Methods for protein analysis

3.3.1 Determination of protein concentration according to Bradford

In order to measure the protein concentration, a standard curve was first established. The linear range of these assays for BSA is 125 to 1000 µg/ml. For the standard and the protein samples, 250 µl of Quick Start Bradford Dye Reagent was mixed with 5 µl standard or protein sample. Protein binds to the coomassie dye in the acidic environment of the reagent, which results in a spectral shift from the reddish/brown form of the dye (absorbance maximum at 465 nm) to the blue form of the dye (absorbance maximum at 610 nm). The difference between the two forms of the dye is greatest at 595 nm. The protein solutions were assayed in triplicates using the NanoDrop spectrophotometer.

3.3.2 Preparation of antibody-bead binding

40 µl of Sepharose Protein G beads (GE Healthcare) per 1 ml cell lysate of ~ 5 x 10^7 cell/ml were washed twice with 1 ml NP40 lysis buffer. Beads were collected by centrifugation at 3,000 x g for 1 minute at 4°C. About 850 µg of Argonaute protein hybridoma supernatant, and separately 15 µg rat IgG2a antibody (isotype control) together with NP40 lysis buffer, were added to washed beads to a final volume of 1 ml. The antibody-bead mix was incubated in a rotating wheel at 4°C over night. The next day, antibody coupled beads were washed twice with 1 ml NP40 lysis buffer. Between the washing steps, the tubes were inverted 20 times.

3.3.3 Preparation of cell lysates

Cell pellets were lyzed manually and resuspended in 3 cell pellet volumes with NP40 lysis buffer (~ 1ml), and incubated on ice for 10 minutes. The cell lysate was cleared by centrifugation at 13,000 x g at 4°C for 10 min and transferred to prepared antibody bound beads.

3.3.4 Immunoprecipitation (IP) of proteins

About 1 ml cell lysate was added to 40 µl antibody-conjugated sepharose beads and incubated in a rotating wheel at 4°C for 4 hours. The beads were collected by centrifugation at 3,000 x g for 1 minute at 4°C, washed twice with 1 ml 300 mM wash buffer, twice with 1 ml 500 mM wash buffer, once with 1 ml PBS, and resuspended in 100 µl PBS. Between the washing steps, the beads were rotated at 4°C for 10 minutes. 2 x SDS-Sample Buffer was added to 20% of the IP approach (antibody-conjugated beads), resuspended in PBS and heated to 95°C for at least 2 minutes. Afterwards, the sample mix was loaded to an 8% SDS-polyacrylamide gelelectrophoresis (PAGE) for Western Blot analysis. 1 ml TRIzol Reagent (Invitrogen) was added to the remaining 80% of the IP approach. The mix was transferred to RNase- and DNase-free, prelubricated, 1.7 ml tubes (Corning) together with 5 µg of yeast-tRNA to facilitate RNA precipitation and stored at -80°C for subsequent RNA isolation.

3.4 Gelelectrophoretic separation and detection of proteins

3.4.1 SDS-PAGE separation of proteins

The separation of proteins, using discontinuous SDS-PAGE, was performed according to Laemmli (Laemmli, 1970). The 8% separation gel at the bottom was covered with a 5% stacking gel. Before protein samples were loaded to the SDS-PAGE, they were mixed with 1 x SDS-Sample Buffer and denatured at 95°C for at least 2 minutes. The gelelectrophoresis was started in 1x SDS Running buffer in a Mini-Cell gel chamber (Bio-Rad) with 20 mA per gel. Subsequently, the gels were analyzed via Western Blot.

3.4.2 Western Blot analysis of proteins

After running the SDS-PAGE, the gel was blotted to a Hybond P membrane (GE Healthcare) with 80 mA per blot for 2 hours with 1 x Transfer Buffer, using a Semidry Transfer Cell (Applied Biosystems). Subsequently, the membrane was blocked in 1 x TBST buffer with 5% powdered skim milk for 1 hour. The membrane was incubated over night with one of the four primary monoclonal

Argonaute-antibodies (Beitzinger *et al.*, 2007), diluted 1:50 in 1 x TBST buffer. The next day, the membrane was washed three times for 5 minutes with 1 x TBST and incubated with secondary polyclonal goat anti rat antibody (Jackson Immuno Research) diluted 1:10,000 in 1 x TBST, for 1 hour. Afterwards, the membrane was washed again three times for 10 minutes with 1 x TBST buffer, and the proteins were detected by incubation with SuperSignal West Pico Chemiluminescent Substrate or SuperSignal West Femto Maximum Sensitivity Substrate for 5 minutes, using the LAS 3000 UV mini system (Fujifilm) for visualization of protein bands.

3.5 Methods of molecular biology

3.5.1 Agarose gel electrophoresis of nucleic acids

For analytical and preparative separation of nucleic acids, 0.8% to 3% agarose gels were prepared in 1 x TAE buffer. The agarose gels were stained with 0.5 µg/ml ethidiumbromide (EtBr), which intercalates into nucleic acids. Due to the fluorescence emission of EtBr, the nucleic acids could be detected by stimulation of EtBr with a wavelength of 302 nm, using a UV transilluminator.

3.5.2 Polyacrylamide gel electrophoresis of RNA

10 µg of total RNA was mixed with 2 x bromphenolblue sample buffer and loaded to a 15 x 17 cm, 15% polyacrylamide gel, together with a molecular weight scale consisting of 5 µg yeast-tRNA and 1 fmol, 2 fmol, 10 fmol and 20 fmol of synthetic hsa-miR-16. The gel was started with 10 W for 10 minutes and 30 W for 1 hour in 1 x TBE buffer. Subsequently, the gel was stained with EtBr, and the RNA bands were detected using the FLA 7000 system (Fujifilm).

3.5.3 General TRIzol Reagent extraction of RNA for microarray hybridization

1 ml of TRIzol Reagent was added to 1×10^7 cells, which were resuspended by pipetting up and down. After this, 200 µl of chloroform were added to the mix that was vortexed for 20 seconds and incubated for 2 to 3 minutes at room temperature. Following, the mix was centrifuged for 15 minutes at 4 °C and 12,000 x g. The upper phase was mixed with P:C:I (phenol:chloroform:isoamylalcohol), vortexed and centrifuged again. 3 to 4 volumes of ethanol were added to the upper phase, both were vortexed and incubated at -20 °C for at least 2 hours. The RNA was pelletized by centrifugation for 15 minutes at 4 °C and 12,000 x g. The ethanol supernatant was removed, and the RNA was air dried. Finally, the RNA was resuspended in 25 µl nuclease free water.

3.5.4 TRIzol Reagent extraction of RNA from Argonaute proteins

200 µl of chloroform was added to the remaining 80% IP approach (Argonaute-antibody-conjugated beads) resuspended in 1 ml TRIzol Reagent. The mix was vortexed for 20 seconds and centrifuged at 12,000 x g for 15 minutes at 4 °C. The aqueous phase was transferred to a new RNase- and DNase-free, prelubricated, 1.7 ml tube, and three volumes of 100% ethanol were added relative to aqueous phase. The mix was vortexed for 20 seconds once more and incubated for 3 hours until over night at -20 °C. Following, the RNA was pelletized by centrifugation at 12,000 x g for 15 minutes at 4 °C. The supernatant was removed, and the RNA pellet was dried and resuspended in 25 µl nuclease free water.

3.5.5 Concentration and purity determination of nucleic acids

The concentration of nucleic acids was determined using the NanoDrop spectrophotometer by absorption at 260 nm. The ratio E_{260}/E_{280} served as estimation for the purity of nucleic acids. For pure solutions a value above 1.8 was expected.

3.5.6 Northern Blot analysis of miRNAs

After gelelectrophoresis, the separated RNA was transferred with 0.5 x TBE buffer to a Hybond N^+ membrane, using a Transfer Blot SD Semi-Dry Transfer Cell (Bio-Rad). The blotting was performed with 255 mA for two hours. Afterwards, the membrane was dried and UV crosslinked at a wavelength of 366 nm for a few seconds.

During blotting, the DNA probes were labeled with ATP γ - ^{32}P. The labeling mix was incubated for 15 minutes at 37°C. Thereafter, 30 µl of 30 mM EDTA (pH 8.0) was added to the mix to stop the reaction. The labeled DNA probe was purified using an equilibrated, dried MicroSpin G-25 Column. The remaining PNK (polynucleotide kinase) was inactivated by incubation at 95°C for 1 minute, before adding the DNA probe to the hybridization solution.

For prehybridization and hybridization, salmon sperm DNA was denatured at 100°C for 5 minutes before adding to the hybridization solution. The hybridization solution was prewarmed to 40 to 50°C (hybridization temperature) in a rotator. For prehybridization, 15 ml of hybridization solution was added to the dried, UV crosslinked membrane, and incubated at 40 to 50°C for 2 hours under permanent rotation. Subsequently, the hybridization solution was replaced by 15 ml fresh hybridization solution, containing the labeled DNA probe followed by incubation at 40 to 50°C over night under permanent rotation.

The next day, the hybridization solution was removed, and the membrane was washed twice for 10 minutes with 100 ml washing buffer I, and once for 10 minutes with 100 ml washing buffer II at hybridization temperature. The membrane was wrapped into transparency film and placed into a developer cassette with a white screen onto the membrane for 4 and 24 hours. Following, a picture was taken of the exposed screen using the FLA 7000 system (Fujifilm).

For stripping the DNA probes off the membrane, the membrane was washed for 5 minutes in boiling water containing 1% SDS. Finally, the membrane was exposed on the screen for 3 hours again, to check if the DNA probes disappeared.

3.5.7 cDNA synthesis of total RNA and RNA isolated from Argonaute proteins

1 µg total RNA or 4.2 µl of Argonaute isolated RNA (25 µl in total) was denatured at 90°C for 30 seconds. After this, the cDNA synthesis master mix (10 mM DTT, 1 x SuperScript buffer, dNTPs 2 mM each, 0.33 µM Oligo dT primer, 0.33 µM hexamer primer) was added to the denatured RNA, and the mix was cooled to 50°C for 3 minutes. 0.7 µl SuperScript III Reverse Transcriptase (Invitrogen) was added to each RNA sample, and incubated for 45 minutes at 50°C. Following, 20 µl of 150 mM KOH-20 mM Tris was added to the mix, and incubated for 10 minutes at 90°C, to degrade the RNA. After addition of 19 µl of 150 mM HCl, the mix was neutralized (pH 7-8) and cooled on ice.

3.6 Polymerase chain reaction (PCR)

3.6.1 Standard PCR

After cDNA synthesis, the PCR was used to amplify certain gene regions, using specific PCR primers or as much gene regions as possible using random hexamer primers. The standard PCR was used only as control PCR for first detection of Argonaute-associated genes. For these PCRs, the AccuPrime Super Mix I was used. The mixture contains anti-*Taq* DNA polymerase antibodies, thermostable AccuPrime protein, Mg_2^{++}, deoxyribonucleotide triphosphates (dNTPs), and recombinant *Taq* DNA polymerase at concentrations sufficient to allow amplification during PCR. The PCR reaction was performed in 25 µl containing ~ 10% of cDNA mix (5 µl), 1 x AccuPrime Super Mix I, 0.25 µM of each PCR primer and H_2O. The annealing temperature for gene specific primer was 55 to 58 °C. For PCR, 0.33 µM random hexamer primers were applied and an annealing temperature of 20 °C. A standard PCR looked like this: 94 °C for 5 minutes, 94 °C for 40 seconds, 55 °C for 40 seconds, 68 °C for 40 seconds, repeating steps 2 to 4 for 29 times, and 68 °C for 7 minutes. A standard PCR with hexamer primers looked like this: 94 °C for 5 minutes, 94 °C for 1 minute, 20 °C for 1 minute and 25 seconds, 68 °C for 1 minute, repeating steps 2 to 4 for 29 times, and 68 °C for 7 minutes (Gene Amp PCR System 2700, Applied Biosystems).

3.6.2 Quantitative reverse transcription-real time-PCR (qrt-RT-PCR)

For quantitative reverse transcription-real time-PCR, the SYBR Green PCR Master Mix (Applied Biosystems) was used. The reaction was performed in 20 µl containing ~ 10% of cDNA mix (5 µl), 1 x SYBR Green PCR Master Mix, 0.25 µM of each PCR primer and H_2O. A reaction looked like this: 94 °C for 5 minutes, 94 °C for 40 seconds, 55 °C for 40 seconds, 68 °C for 40 seconds, repeating steps 2 to 4 for 29 times, and 68 °C for 7 minutes. At the end, a dissociation curve was performed (95 °C for 15 seconds, 60 °C for 15 seconds, and 95 °C for 15 seconds). For the performance of the qrt-RT-PCR, the 7900 HT Fast Real-Time PCR System (Applied Biosystems) was used.

3.6.3 TaqMan miRNA assay

The TaqMan miRNA Assays (Applied Biosystems) were used for detection of individual miRNAs, using qrt-RT-PCR, and performed according to the manufacturers' instructions (see TaqMan® MicroRNA Assays Protocol; Applied Biosystems). The reverse transcription of miRNAs was modified and differs from the manufacturers' instructions. 1 to 10 ng of total RNA and 1.66 µl of Argonaute isolated RNA was needed. The master mix for the cDNA synthesis contained 1 mM dNTPs, 3.3 U/µl MultiScribe Reverse Transcriptase, 1 x Reverse Transcription buffer, 0.252 U/µl RNase Inhibitor and 20% TaqMan miRNA Primer. The next steps were performed corresponding to the TaqMan® MicroRNA assay protocol (Applied Biosystems).

3.7 Microarray hybridization

3.7.1 Labeling of miRNA using cyanine dyes

For the microarray hybridization, a two-color or two-channel miRNA microarray, called miRXplore Microarray (Miltenyi Biotec), was used. "Two-color" means, the RNA sample was labeled with Cy5, and the universal reference (UR; pool of 493 synthetic human miRNA oligonucleotides) was labeled with Cy3. For the labeling of one RNA sample, 9.6 µl of a labeling mix was prepared with the following components and final concentrations: 1 x RNA Ligation Buffer, 15% DMSO, 1 µl of miRC1 (Position control Oligos, miRXplore Kit 8) and 0.6 µl of miRC3 (Calibration Oligos, miRXplore Kit 8). The labeling mix was added to 200 µM Cy5 with 3 µg of RNA sample and to 200 µM Cy3 with the universal reference (1 fmol each oligo). The RNA was denatured at 95°C for 30 seconds and cooled directly on ice for 1 minute. 1 µg/µl Rnl2 (1-249) K227Q was added to the labeling mix and incubated on ice over night in a cooling room. The next day, the reaction was stopped at 65°C for 15 minutes.

3.7.2 MACS Miltenyi Biotec microarray hybridization of miRNAs

The microarray hybridization was done using miRXplore™ Microarrays and the a-Hyb Hybridization Station of Miltenyi Biotec. The miRNA sequences of human, mouse, rat as well as viral sequences are combined on the miRXplore™ Microarray with the up-to-date miRNA content as published in the latest miRBase database (http://www.mirbase.org) release. In this thesis, microarrays, containing miRNA sequences according to miRBase 13 and 14, were used.

The hybridization procedure was started by pre-warming of the 2 x Hybridization Solution (miRXplore Microarray Kit 8) up to 42°C, and the Prehybridization Solution was heated to 98°C for 2 minutes, centrifuged briefly, and cooled to 42°C. After this preparation, 20 µl of labeled UR was mixed with 20 µl of labeled RNA sample. The mix was adjusted to a volume of 100 µl with nuclease free water. 100 µl of 2 x Hybridization Solution was added to the mix and incubated at 70°C for 3 minutes. 200 µl of the RNA sample/UR mix was transferred into the reservoir of the a-Hyb™ Hybridization Station, and hybridized to the complementary RNA oligonucleotides on the microarray surface at 42°C for 16 hours. After hybridization, the microarrays were dipped quickly five times into nuclease free water, dried with compressed, dry air and stored in a dust free hybridization cassette. After the drying step, the microarrays were ready for miRNA detection using the GenePix Professional 4200 A Microarray scanner.

3.7.3 Affymetrix-chip hybridization of mRNAs

The labeling and preparation of Argonaute protein-associated mRNAs were executed according to the GeneChip 3' IVT Express Kit User Manual (Affymetrix). The RNA was hybridized to GeneChip Human Genome U133A 2.0 Arrays of Affymetrix by the core facility BMFZ (*Biologisch-Medizinisches Forschungszentrum*). The Human Genome U133A 2.0 Array is a single array representing 14,500 well characterized human genes and more than 22,000 probe sets. The probe sets were selected from sequences in GenBank, dbEST and RefSeq. The sequence clusters were created from the UniGene database.

3.8 Bioinformatics

3.8.1 Evaluation of miRNA microarray data using different software

After miRNA detection via GenePix Professional 4200A Microarray scanner, the quality control of microarray hybridization was performed, using GenePix Pro 6 (Axon Instruments). The image analysis software produces a large number of raw data points, describing the spot fluorescence (Cy3 and Cy5) intensity, background intensities and a variety of other spot quality measurements. First, the raw spot intensity values of the first fluorescence were corrected for background signal, and then compared to the corrected spot intensity value of the other fluorescence to generate ratios (Fielden *et al.*, 2002). The ratios represent the relative difference between the RNA sample labeled with Cy5 and the universal reference labeled with Cy3 co-hybridized to the microarray. Additionally, synthetic spike-in control oligonucleotides were used as positive, negative and calibration controls, and for sample-independent normalization. Once the microarray images were analyzed in GenePix Pro, and the GenePix results were imported into Acuity 4.0 (Axon Instruments) database, the normalization was performed using the miRC3 calibration oligonucleotides. Afterwards, the software was used for data filtering. Spots, which possess background-corrected signal intensities over 100 light units (LU) in both colors and 50% of feature pixels with intensities more than two standard deviations above the background pixel intensity were flagged as "good" and applied for further analysis.

3.8.2 Calculation of differentially expressed miRNAs using SAM

SAM (Significance Analysis of Microarrays) is a statistical method for finding significant genes or miRNAs in a set of microarray experiments (Tusher *et al.*, 2001). SAM computes a statistic d_i for each gene i, measuring the strength of the relationship between gene expression and the response variable. It uses repeated permutations of the data to determine if the expression of any gene is significantly related to the response. The cutoff for significance is determined by a tuning parameter Δ, chosen by the user, based on the false-positive rate. One can also choose a fold change parameter, to ensure that called genes change at least a pre-specified amount. The SAM analysis was used to get another significance criterion for differentially expressed miRNAs, identified within the chromosomal abnormalities of the 102 pediatric AML patient samples.

3.8.3 Evaluation of mRNA microarray data using RMA algorithm

The analysis of mRNA expression data was executed using the Robust Multichip Average algorithm (RMA), implemented in RMAExpress (Bolstad *et al.*, 2003). The RMA algorithm consists of three steps: background adjustment for separation of noise from probe signal intensities, quantile normalization for adjustment of signal distribution of two or more arrays, and finally probe signal intensity summarization in order to get one signal value for each gene. For the analysis, the CEL and CDF files were merged into a CDFRME file, in which every spotted probe got a value for the position on the chip. After this, the probe expression values were background corrected, normalized and summarized into probe sets, which were exported as text file in natural or log scale. mRNAs offering signal intensities < 30 LU were considered as background signals and replaced by not available (NA) in the heatmap calculations.

3.8.4 Cluster analysis and statistical testing using R

For cluster analysis, heatmap calculations and statistical testing, the ratio values sustained from two-color miRNA microarrays were $\log_2$ transformed. The ratio values consist of miRNA signal intensity of the sample, divided by corresponding miRNA signal intensity of the universal reference (UR) comprising 493 synthesized, human miRNAs according to miRBase 8.2. The miRNA microarrays used, include miRNAs according to miRBase 13 and 14. Signal intensities of miRNAs identified in the sample, for which no corresponding miRNA of the UR is available, were divided by the average signal intensity of all miRNAs identified in the UR. For detection of differentially expressed miRNAs between AML subtypes, a fold change (FC) between Φ $\log_2$ miRNA signal intensities between different AML subtypes and a Mann-Whitney-U test (MWU) were calculated. For identification of miRNAs with highest probability to be associated with an Argonaute protein, a FC (Φ $\log_2$ miRNA signal intensities between the Ago experiments and the isotype control experiments) and a two-sample, two-tailed Welch-test for unequal variances were calculated, using the packages foldchange and t.test implemented in R 2.11.1 (R Project for Statistical Computing (Ihaka and Gentleman, 1996)). The FC and p-value calculations of data, obtained from one-color mRNA microarrays, were performed in natural scale, because the data are nearly normally distributed. With regard to the Argonaute experiments, three replicates of each isotype control experiment were pooled and hybridized to one microarray and at least three isotype control replicates were used for statistical testing. miRNAs or mRNAs offering signal intensities in at least two replicates, a FC > 1.8 and a p-value < 0.05 were considered as highly significant and were applied for further analyses. Though, with regard to the Argonaute experiment, it has to be taken into account that the FC is the more important criteria for considering RNAs as Ago-associated, due to the possible high variance of signal intensities of RNAs randomly attached to the isotype controls, resulting in worse p-values. All miRNAs identified in the total RNA were used for further analysis, whereas mRNAs with signal intensities < 30 LU were discarded, because such low signal intensities were considered as background noise.

The agglomorative, unsupervised hierarchical clustering was implemented for both miRNA and mRNA microarray data, using R. The package heatmap.2 was used for computation of enhanced heatmaps, visualizing a false-color image with high signal intensities shown in red and low signal intensities shown in green. The dendrograms on the left side and/or on the top were produced by an agglomerative algorithm, which begins with each element as a separate cluster and merge them into successively larger clusters. The similarity of two elements was calculated by Euclidean distance d,

$$d(p,q) = \sqrt{\sum_{i=1}^{n}(p_i - q_i)^2}$$

where p and q are the signal intensities of two miRNAs or mRNAs. In order to merge two clusters, developed by Euclidian distance, the complete linkage D was used,

$$D(X,Y) = \max_{x \in X,\ y \in Y} d(x,y)$$

where d(x,y) is the distance between the cluster x and y, and X and Y are two sets of clusters.

3.8.5 miRNA target prediction using R

The miRNA target prediction was also implemented in R 2.11.1 under BioConductor 2.6, using the package RmiR and the function read.mir(). The package is useful to merge miRNAs and respective targets using different databases. In order to use this package, a list of significant miRNAs and a list of significant genes were imported to investigate the correlation between miRNAs and their targets. For the target prediction of Argonaute protein-associated miRNAs, the databases TargetScan (http://www.targetscan.org/), PicTar (http://pictar.mdc-berlin.de/) and miRanda (http://www.microrna.org) were used. Only those miRNA target predictions that were found in at least two databases were accepted as confident.

3.8.6 GO term analysis using GOEAST

Gene Ontology (GO) analysis was used for functional analysis of the large-scale genomic data. For this purpose, the Gene Ontology Enrichment Analysis Software Toolkit (GOEAST), an easy-to-use web-based toolkit, was used for identification of statistically overrepresented GO terms within the given gene sets, using the hypergeometric distribution. This distribution describes the probability of obtaining by chance a number of annotated genes (mRNAs) of a given GO term among the Ago-associated mRNAs, with respect to the total number of all gene members belonging to this GO term. The p-value obtained denotes the probability if the enrichment of the corresponding GO term was calculated by chance. GOEAST displays enriched GO terms in graphical format, according to their relationships in the hierarchical tree of each GO category (biological process, molecular function and cellular component). Therefore, it provides better understanding of the correlations among enriched GO terms.

3.8.7 KEGG pathway analysis using EGAN

EGAN (Exploratory Gene Association Network) is a software tool for visualization and interpretation of miRNA and mRNA expression data in an interactive hypergraph. The tool provides direct links to web resources and literature like NCBI Entrez Gene, PubMed, KEGG (Kyoto Encyclopedia of Genes and Genomes), Gene Ontology etc. (Paquette and Tokuyasu, 2010). By the aid of EGAN, the detected and most significant miRNAs and mRNAs were visualized in a graph, where the nodes depict the Argonaute protein-associated genes. The edges labeled in blue show the connection of these genes to one or more KEGG pathways (http://www.genome.jp/kegg), and the edges labeled in green show the connection between genes and one or more miRNAs which are predicted (by TargetScan, PicTar and miRanda algorithms) to offer binding site complementarity with the detected mRNAs. The pathway enrichment was also calculated using the hypergeometric distribution.

4 Results

4.1 miRNA expression profiling differentiates cytogenetic AML subtypes

4.1.1 Global miRNA expression analysis by miRNA microarray hybridization

The role of miRNAs in adolescent AML patients, and the differentiation between cytogenetic subtypes of AML, was demonstrated several times by expression profiling. Three independent studies showed that the cytogenetic subtypes t(8;21), t(15;17) and inv(16) offer unique miRNA expression profiles (Dixon-McIver *et al.*, 2008; Jongen-Lavrencic *et al.*, 2008; Li *et al.*, 2008). In order to confirm these findings in pediatric AML patients, miRNA expression profiles of 102 pediatric AML patient samples were analyzed and miRNAs discriminating different AML subtypes were identified, using microarray technology. AML patient samples carrying the following chromosomal aberrations were analyzed in detail:

Table 4.1.1.I Characteristics of pediatric AML patient samples, Abbreviation: eo – eosinophilia

Cytogenetic abnormalities, no. (% of patient cohort)	pediatric AML cohort (n = 102)	French-American-British classification
t(4;11)	1 (0.98)	-
t(6;11)	2 (1.96)	M5
t(9;11)	16 (15.69)	M5
t(10;11)	6 (5.88)	M4, M5
t(11;19)	5 (4.90)	M2, M4, M5
t(11q23)	3 (2.94)	-
t(15;17)	14 (13.73)	M3
inv(16)	13 (12.75)	M2, M4, M4eo
t(8;21)	24 (23.53)	M0, M1, M2, M4eo
normal	4 (3.92)	M2, M4, M5, M6
other	14 (13.73)	M2, M4, M5, M6

Figure 4.1.1.I Unsupervised hierarchical clustering of miRNA expression profiles of 102 pediatric AML patient samples. The dendrograms were calculated using Euclidian distance and complete linkage algorithm (R 2.11.1). The clustering at the top and the left side represent the distance/similarity between miRNA expression profiles of the patient samples and between individual miRNAs, respectively. Yellow and red boxes show a division of the cluster analysis into two major groups, Cluster 1 and Cluster 2. In addition, the chromosomal translocations of AML patient samples were color-coded according to the color legend on the left side. Beneath the dendrogram at the top, the corresponding heatmap shows high expressed miRNAs in red and low expressed miRNAs in green. Undetected miRNAs were labeled in dark grey. The signal intensities were corrected for each miRNA using 1 fmol of a universal reference (UR) consisting of synthetic ribooligonucleotides corresponding to 493 known human miRNAs.

The large-scale miRNA expression profiles of pediatric AML patient samples are represented as unsupervised, hierarchical cluster, together with the corresponding heatmap (Figure 4.1.1.I; Supplement Table V.2). Overall, 259 different miRNAs of all leukemia samples and on average 64 miRNAs of a single sample, could be identified with confidently detectable expression values. Remarkably, the miRNA expression patterns divide into two major clusters separating AML subtypes with translocation t(15;17) labeled in yellow (Cluster 1), and t(8;21) labeled in red (Cluster 2), while other AML subtypes are interspersed between the two clusters. A great part of t(8;21)-positive and t(15;17)-positive samples, respectively, group together within the two superior clusters, in spite of the great heterogeneity of all leukemia samples, indicating that this difference is based on the different miRNA expression signatures. Moreover, 55% and 24% of patient samples with mixed-lineage leukemia (MLL) rearrangements like translocations t(9;11), t(10;11) and t(11;19) group into several small clusters distributed over the whole dendrogram. The heatmap represents filtered data consisting of 114 different miRNAs. miRNAs detected in less than three samples were joined together into the

group termed "all others", because it is very improbable for these single miRNAs to reach a definite significance level.

4.1.2 Statistical tests reveal differentially expressed miRNAs between AML subtypes

Due to the clear separation of AML samples harboring the translocations t(8;21) and t(15;17), differentially expressed miRNAs of these samples and all other samples were identified by statistical testing, to determine the most distinguishing miRNAs (Supplement Table V.2). The Expression of individual miRNAs was analyzed by fold change (FC), two-sample, two-tailed Mann-Whitney-U test, false discovery rate (FDR) corrected p-value and Significance Analysis of Microarrays (SAM) q-value calculations. The Mann-Whitney-U test and SAM, together with permutation tests were used to identify differentially expressed miRNAs with a "t(8;21) - vs. - all of the others and t(15;17) - vs. - all of the others" approach. Furthermore, the average signal intensity and the number of the corresponding miRNA of t(8;21)-positive and t(15;17)-positive samples, respectively, and all other samples were calculated in order to demonstrate the abundance of differentially expressed miRNAs. Table 4.1.2.I and Table 4.1.2.II below list the most significant miRNAs identified in the translocations t(8;21) and t(15;17).

Table 4.1.2.I Most significant miRNAs of 24 samples with translocation t(8;21). Up-regulated miRNAs are framed in red and down-regulated miRNAs are framed in green. Abbreviations: SI – miRNA signal intensity (sample/UR); UR – universal reference, FDR – false discovery rate, No. – number, MWU – Mann-Whitney-U-test

miRNA Name	Φ SI t(8;21)	Φ SI all other	No. miRNAs t(8;21)	No. miRNAs all other	FC	MWU (p-value)	FDR corrected p-value	SAM q-value
miR-126	2.11	0.29	18	51	7.12	0.000004	0.00006	0
miR-146a	0.39	0.21	18	65	1.85	0.044931	0.436	54.5
let-7b	0.39	0.70	20	73	0.56	0.022812	0.419	0
miR-335	0.17	0.31	10	20	0.55	0.020925	0.363	0
let-7c	0.14	0.24	19	74	0.58	0.038245	0.823	10.35
miR-21	2.00	3.64	14	51	0.55	0.041917	0.121	62

Table 4.1.2.II Most significant miRNAs of 14 samples with translocation t(15;17). Up-regulated miRNAs are framed in red and down-regulated miRNAs are framed in green. Abbreviations: SI – miRNA signal intensity (sample/UR); UR – universal reference, FDR – false discovery rate, No. – number, MWU – Mann-Whitney-U-test

miRNA Name	Φ SI t(15;17)	Φ SI all other	No. miRNAs t(15;17)	No. miRNAs all other	FC	MWU (p-value)	FDR corrected p-value	SAM q-value
miR-100	0.65	0.05	14	15	13.43	0.000079	0.00286	1.46
miR-125b	0.67	0.09	13	28	7.80	0.000052	0.00754	1.46
miR-181a	3.30	0.68	14	88	4.86	0.000013	0.00121	0
miR-181b	1.07	0.30	14	79	3.59	0.000035	0.00131	0
miR-126	0.09	0.73	12	57	0.12	0.0000033	0.000004	0
miR-494	0.04	0.21	9	3	0.20	0.004545	1.0	0
miR-223	2.00	6.50	14	86	0.31	0.000007	0.000093	0

Table 4.1.2.I lists the most significant miRNAs, discriminating the samples with translocation t(8;21) from all other samples with a FC > 1.8 and a p-value < 0.05. The q-value exceeds the standard false-positive rate of 5% in three cases (miR-146a, let-7c and miR-21). Though, miR-126 and miR-146a belong to the most up-regulated miRNAs in t(8;21)-positive pediatric patients, whereas the miRNAs let-7b, miR-335, let-7c and miR-21 are down-regulated. The miRNAs miR-100, miR-125b, miR-181a and miR-181b are the most up-regulated miRNAs observed in the translocation t(15;17) vs. all other chromosomal abnormalities offering a FC > 3, a p-value < 0.005 and a q-value < 2 (see Table 4.1.2.II). Of notice, miR-126, up-regulated in patient samples harboring translocation t(8;21), is the most down-regulated miRNA in patient samples with translocation t(15;17) distinguishing these two AML subtypes. miR-494 and miR-223 are also down-regulated in t(15;17) with high significance. Surprisingly, only six and seven miRNAs are differentially expressed in t(8;21) and t(15;17), respectively, in which miR-126 is the most discriminating miRNA between both translocations.

4.1.3 qrt-RT-PCR confirmes the most discriminatory miRNAs

The qrt-RT-PCR was used for validation of microarray results by selection of six differentially expressed miRNAs, most discriminating the AML subtypes with translocations t(8;21) and t(15;17) and all other aberrations (Figure 4.1.3.I).
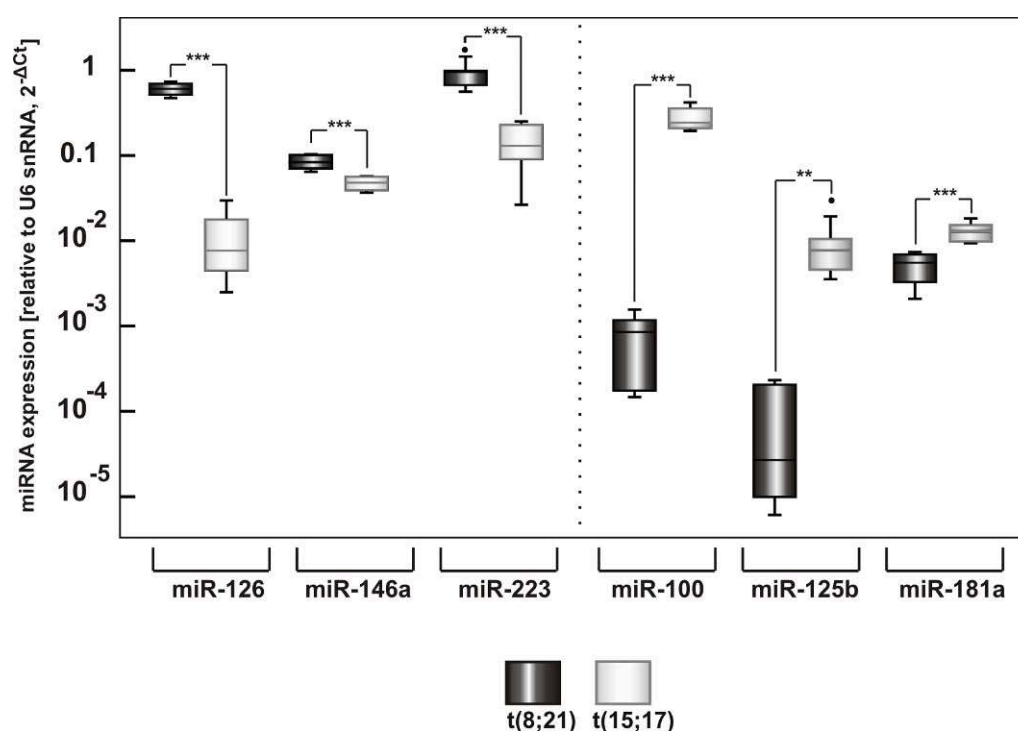
Figure 4.1.3.I Validation of microarray results of six selected miRNAs by qrt-RT-PCR. Samples with chromosomal translocation t(8;21) were marked in red and those harboring the translocation t(15;17) were labeled in yellow. The significance of differential expression between translocations t(15;17) and t(8;21) is denoted by one or three stars above the boxplots (* = p-value < 0.05; *** = p-value < 0.001).

The miRNAs, miR-126, miR-146a and miR-223 show differential expression with high significance (p-value < 0.001) between the chromosomal translocations t(8;21) and t(15;17) (Figure 4.1.3.I). These miRNAs offer expressions up to 3 fold higher in t(8;21) than in t(15;17). The miRNAs, miR-100 and miR-181a, differentiate significantly between t(15;17) and t(8;21) with a p-value < 0.001, whereas the

miR-125b offers a p-value < 0.05 in comparison with these two chromosomal translocations. Furthermore, these miRNAs are up to 3.6 fold higher expressed in t(15;17) than in t(8;21). Hence, miRNAs identified as differentially expressed and most significantly discriminatory between these tested chromosomal aberrations by microarray technology and statistical testing, could be confirmed by qrt-RT-PCR results with higher sensitivity.

4.1.4 Removing differentially expressed miRNAs as second proof

To test the robustness of the hierachrical cluster analysis and its dependence on the differentially expressed miRNAs for separating translocation t(8;21) and t(15;17), the identified miRNAs were removed. The second verification of the differentially expressed miRNAs as most characteristic ones of the translocations t(8;21) and t(15;17) is depicted in Figure 4.1.4.I.
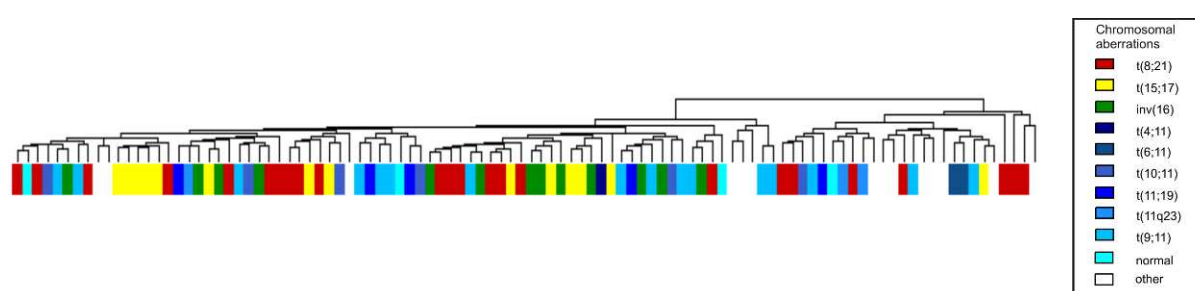
Figure 4.1.4.I Hierarchical cluster analysis of data lacking the most differentially expressed miRNAs identified in the translocations t(8;21) (red) and t(15;17) (yellow) shows a disorder of the two major clusters, which previously separated these two translocations from each other. The chromosomal aberrations are color-coded according to the legend on the right side.

The removal of differentially expressed miRNAs leads to a breaking-up of the two superior clusters previously shown in Figure 4.1.1.I. The t(8;21)- and t(15;17)-positive leukemia patient samples are distributed through the complete dendrogram due to their current miRNA expression signatures. The two smaller clusters, exclusively consisting of samples harboring the translocations t(8;21) and t(15;17), are largely disrupted, suggesting that the removed miRNAs are in fact the most important ones for the characterization of t(8;21) and t(15;17)-positive patient samples.

Taken together, these findings indicate that miRNAs are suitable as biomarkers in pediatric AML patients. For further investigations of these miRNAs and their functionality, a biochemical target complex isolation method was established, and appropriate AML cell line systems were chosen.

4.2 Single steps of „PAR-CLIP-Array" improvement

miRNAs execute their regulatory function in a ribonucleoprotein complex containing one of the four human Argonaute proteins as core component. They guide these proteins to the 3'-UTR of target-mRNAs to enforce post-transcriptional gene regulation. For investigation of miRNA functionality executed by Argonaute-miRNA-mRNA interactions, an improved co-immunoprecipitation method convenient for Argonaute-RNA complex isolation called PAR-CLIP-Array (Photoactivatable-Ribonucleoside-enhanced Crosslinking-Immunoprecipitation and microarray hybridization) was established stepwise.

4.2.1 Improvement of immunoprecipitation and crosslinking procedures

4.2.1.1 The first step: improvement of antibody-bead coupling

Two stable transfected cell lines (SNB19 overexpressing Ago1 and Ago3 and HELA overexpressing Ago2) were used for the first steps of the PAR-CLIP-Array establishment. A cell line overexpressing Ago4 was not available.

For antibody-bead binding optimization different binding buffers, volumes and incubation times were tested, using SNB19 and HELA cells transfected with one of the three Argonaute proteins anchored with FLAG and HA sequences. In order to find the optimal conditions for the antibody-bead binding, (i) 1% BSA in PBS and 30 mM Na_2HPO_4/NaH_2PO_4 (pH = 7.0) as binding buffers, (ii) 425 µg, 850 µg and 8500 µg Argonaute-antibody (hybridoma supernatant) per 40 µl bead volume, (iii) an incubation time of 2 hours and 16 hours, as well as (iv) lysate to bead volume in the ratios 10:1 and 100:1 were tested. In the first approach, a combination of 1% BSA in PBS as binding buffer, 850 µg Argonaute-antibody per 40 µl bead volumes, antibody-bead binding time of 2 hours and a lysate to bead volume in the ratio 10:1, were used as "standard" conditions. In the second and third approaches, the amount of Argonaute-antibody was changed resulting in less or equal precipitation of Argonaute protein. Exchange of the PBS buffering system with Na_2HPO_4/NaH_2PO_4 buffering system resulted in less efficient Ago precipitation with detection of an equal amount of Argonaute protein in the lysate fraction. In the fifth approach, an extended antibody-bead binding over night yielded more Ago precipitate than the standard condition. The last approach was used to test a lysate to bead volume in a ratio 100:1, which resulted in no detectable Argonaute precipitate.
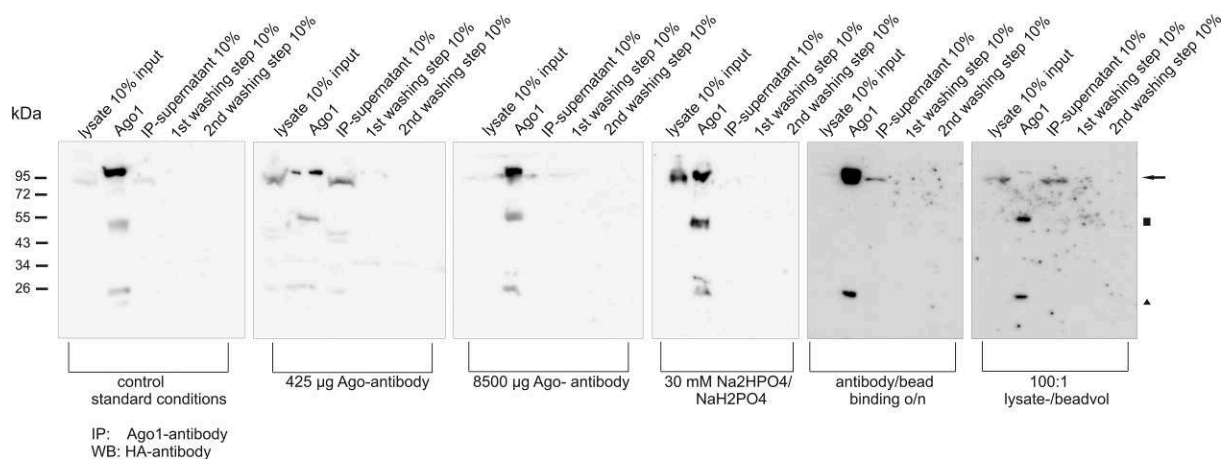
Figure 4.2.1.1.I Six Western Blots showing different Ago1 protein amounts (~ 97 kDa) due to the different antibody-bead binding conditions prior to immunoprecipitation. Different binding buffers, varying volumes of Argonaute-antibody, two different incubation times for antibody-bead binding as well as the ratio of 10:1 and 100:1 between lysate and bead volume were tested as indicated and compared to the standard conditions (left blot). ⊸ immunoprecipitated Ago protein; ■ heavy chain of Ago-antibody; ▲ light chain of Ago-antibody

In summary, the conditions of approach five (1% BSA in PBS, 850 µg Argonaute-antibody per 40 µl bead volume, antibody-bead binding over night, and lysis volume to bead volume 10:1) were considered as the most efficient.

To simplify the antibody-bead binding procedure, it was tested if Ago-antibody coupled beads could be stored without losing their bound antibody. The approaches one and five of section 4.2.1.1 were executed again as positive controls (Figure 4.2.1.2.I first Western Blot). In this process, the first approach was performed, using SNB19 cells expressing exogenous FLAG-HA tagged Argonaute protein. In the third approach, beads prepared three days in advance were tested for functionality. In addition, a third binding and lysis buffer, called NP40 buffer, was applied for antibody-bead binding and cell lysis. SNB19 cells, overexpressing FLAG-HA tagged Ago proteins, pre-coupled FLAG-beads, and HA antibody for Western Blot analysis, were used for performance and detection of a secondary positive control.
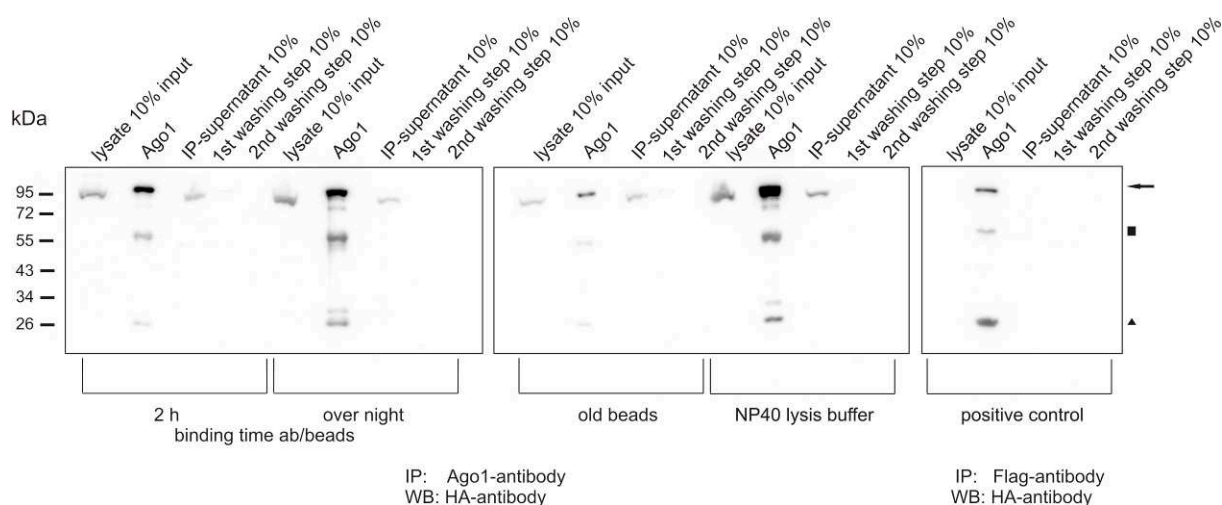
Figure 4.2.1.1.II Detection of different Ago1 protein amounts by Western Blot analysis due to further antibody-bead binding improvements. Though, a third lysis and binding buffer, antibody bound beads prepared in advance were tested in a separate approach. Abbreviation: ab - antibody; ← immunoprecipitated Ago protein; ■ heavy chain of Ago-antibody; ▲ light chain of Ago-antibody

The Western Blots depicted in Figure 4.2.1.1.II show that the conditions of the first and second approaches provide a high amount of Ago1 protein as already shown in Figure 4.2.1.1.I, whereas the use of NP40 buffer for binding and lysis leads to a three fold higher content of this protein. Therefore, this buffer was used for all following IPs. Only a very small amount of Ago1 protein could be immunoprecipitated with the use of antibody-coupled beads, prepared a few days in advance. Hence, the antibody-bead binding has to be prepared fresh at least one day before starting IP.

4.2.1.2 Optimization of cell lysis prior to immunoprecipitation

Different amounts of NP40 lysis buffer in relation to the pellet volume were analyzed for IP improvement. For this examination, SNB19 cells stable transfected with FLAG-HA tagged Ago1 were used once more. Three approaches were performed, using NP40 buffer as antibody-bead binding and lysis buffer, 850 µg of Argonaute-antibody (hybridoma supernatant) per 40 µl beads, antibody-bead binding time over night, pellet volume to bead volume in the ratio 10:1 and lysis buffer volume to pellet volume in the ratio 3:1 and 1:1. The positive control was executed using ready for use FLAG-beads and HA antibody for Western Blot analysis.
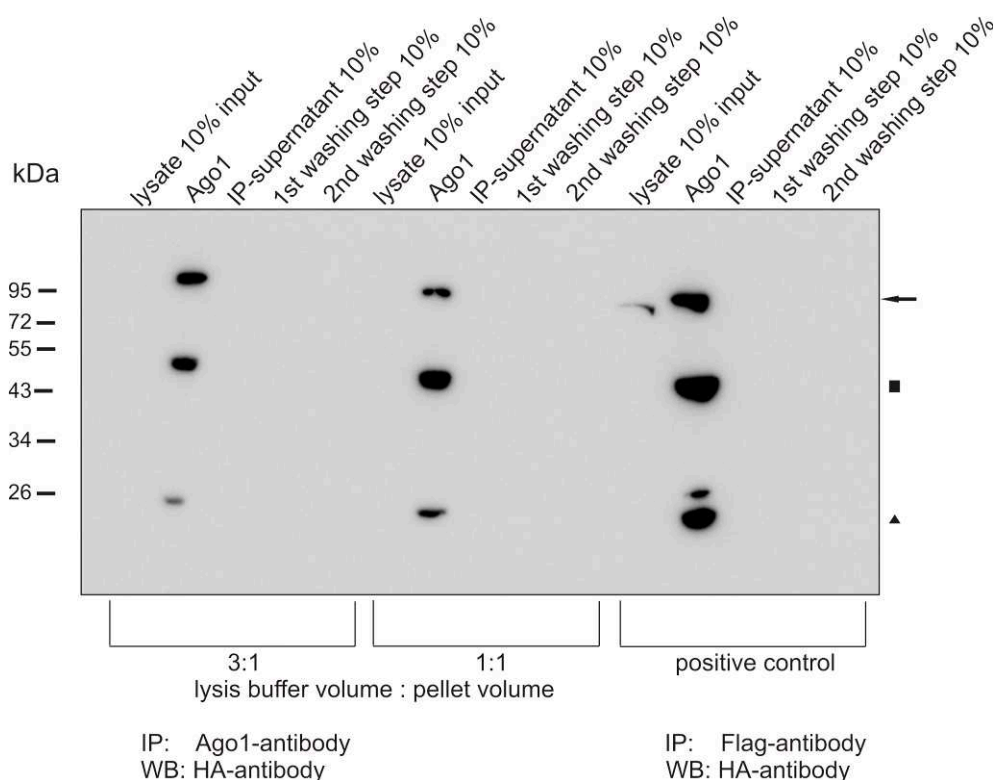
Figure 4.2.1.2.I Western Blot analysis presents the amount of Ago1 protein after testing different lysis buffer amounts. The three fold volume of lysis buffer in relationship to the pellet volume provides a higher amount of Ago1 protein than a lysis - to pellet volume in a ratio 1:1. ⟵ immunoprecipitated Ago protein; ■ heavy chain of Ago-antibody; ▲ light chain of Ago-antibody

The use of one volume only of lysis buffer per pellet volume provides a small amount of Ago1 as pictured in Figure 4.2.1.2.I. The three-fold volume of NP40 buffer in respect to the pellet volume leads to better disruption of the cells and a higher Argonaute protein amount could be immunoprecipitated. Thus, for following experiments, the NP40 buffer volume will be applied in the ration 3:1 with regard to the pellet volume. Up to now, the detection of Argonaute proteins via Western Blot was executed using HA-antibody. Due to the fact that only one specific antibody is available for each Argonaute protein and the detection of endogenous Ago protein is not possible using HA-antibody, these antibodies have to be used and optimized for both, IP and Western Blot analysis.

4.2.1.3 Adjustment of antibody concentration for Western Blot analysis

In this part of the thesis, it was tested if Argonaute-antibodies could be used for Western Blot analysis as well. Two different antibody dilutions were prepared in the ratios 1:50 and 1:500. Additionally, positive and negative controls using Ago1 stable transfected SNB19 cells were executed as well.
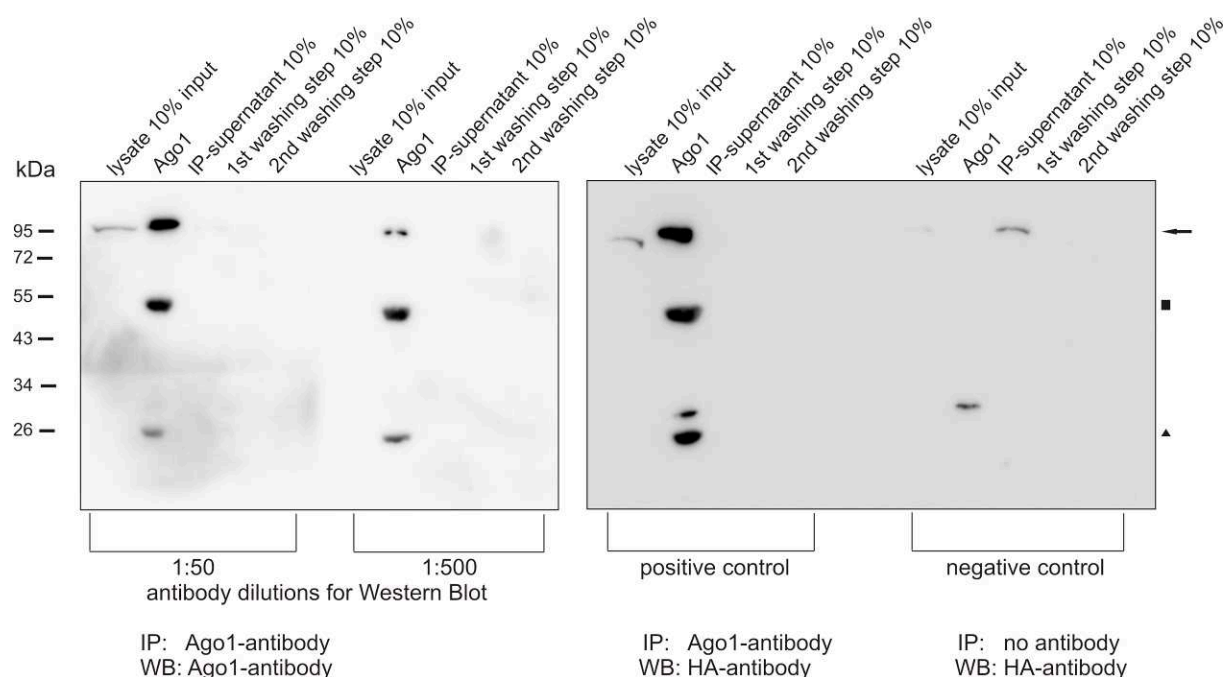
Figure 4.2.1.3.I Improvement of Argonaute protein detection using Ago1-antibody for Western Blot. A dilution of Ago-antibody in a ratio 1:50 provides a detection of much more Ago1 protein than a dilution 1:500. ← immunoprecipitated Ago protein; ■ heavy chain of Ago-antibody; ▲ light chain of Ago-antibody

As expected, the Western Blot displayed in Figure 4.2.1.3.I on the left side shows a significant improvement of Ago1 protein detection by using a 1:50 dilution in comparison to a 1:500 dilution of the Argonaute-antibody. Hence, the antibody dilution should be at most 1:50 for detection of a high amount of immunoprecipitated Argonaute protein separated by SDS page electrophoresis followed by Western blotting.

4.2.1.4 Testing antibody specificity

For all experiments, performed by using one of the Argonaute-antibodies, it is important to prove the binding specificity of each antibody, before analyzing the Argonaute-miRNA complexes in detail. On this account, the Argonaute-antibody specificity was tested for IP since Ago-IP specificity is most important and fundamental. Thus, three different IPs were performed using the three cell lines overexpressing FLAG-HA tagged Ago1, 2 and 3, respectively. Each cell line was used for Ago1-, Ago2- and Ago3-IP. The Ago proteins were detected by Western Blot using HA-antibody.
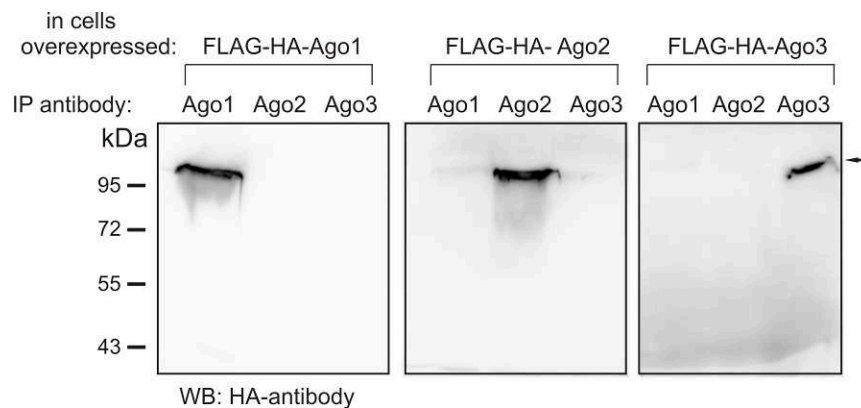
Figure 4.2.1.4.I Verification of Argonaute-antibody specificity during immunoprecipitation. Three different IPs were performed using the three cell lines overexpressing FLAG-HA tagged Argonaute1, 2 and 3. Each cell line was used for Ago1-, Ago2- and Ago3-IP. The Ago proteins were detected by Western blotting using HA-antibody. ⟵ immunoprecipitated Ago protein

To test for specific detection on Western Blot membrane by monoclonal Argonaute-antibodies, IPs of cell lines, overexpressing FLAG-HA tagged Ago1-3, were used in addition to native SNB19 cells. Figure 4.2.1.4.I shows that the respective Argonaute protein only was immunoprecipitated without co-immunoprecipitation of the other Argonaute proteins.

For the second specificity test, four different IPs were performed, using all four human Argonaute-antibodies and cell lines, overexpressing Ago1-3, together with native SNB19 cells. The different Ago-IPs were loaded in parallel onto the SDS-PAGE. The Western Blots were incubated with each Argonaute-antibody separately. For the loading control the four Argonaute-antibodies were applied to the Western Blot at the same time for detection of all Ago-IPs.
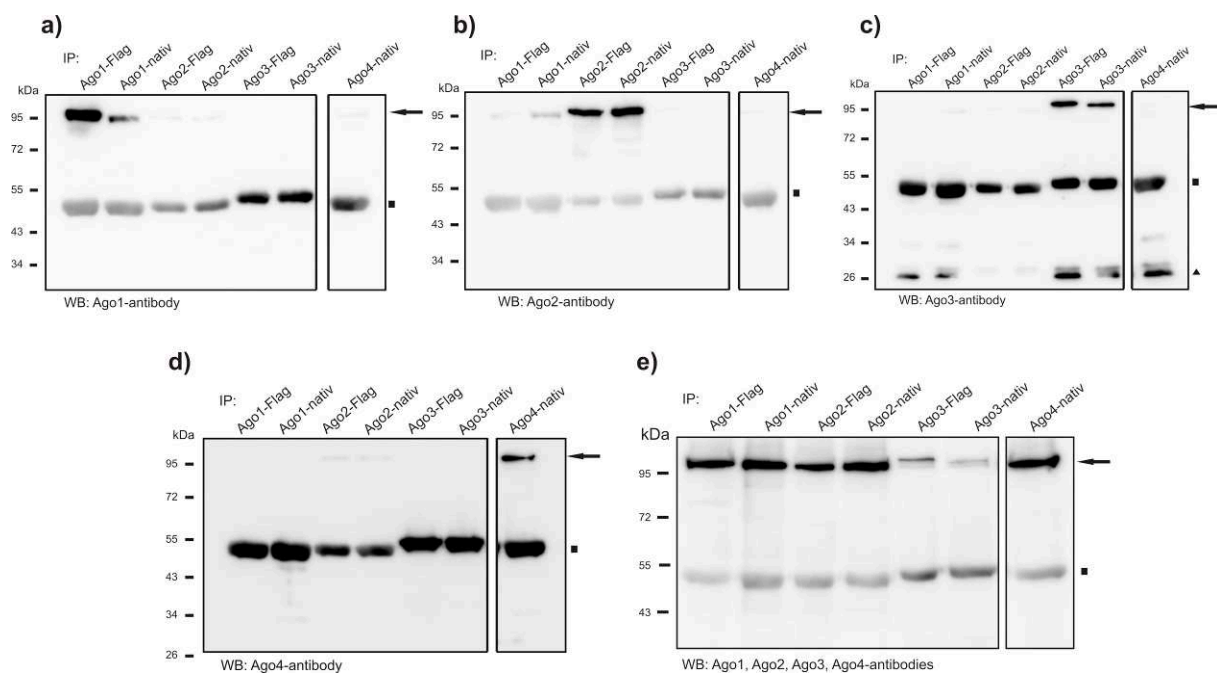
Figure 4.2.1.4.II Validation of Argonaute-antibody specificity on Western Blot. Four different IPs using antibodies for all four human Argonaute proteins were performed and loaded onto one SDS-PAGE. The Western Blots were incubated with **a)** Ago1-antibody, **b)** Ago2-antibody, **c)** Ago3-antibody, **d)** Ago4-antibody and **e)** all four antibodies representing the loading control. The Argonaute-antibodies are highly specific except of Ago2-antibody, which detects a very small amount of Ago1 as well. ⟵ immunoprecipitated Ago protein; ■ heavy chain of Ago-antibody; ▲ light chain of Ago-antibody

The antibodies are also specific with regard to the Western Blots shown in Figure 4.2.1.4.II, because most antibodies detect only their corresponding protein with one exception. The Ago2-antibody binds a small amount of Ago1 on the Western Blot as well (Figure 4.2.1.4.II b), but this is a rather minor detection problem, since IPs are highly specific (Figure 4.2.1.4.I).

4.2.1.5 Improvement of 4-thiouridine concentrations and duration of UV-crosslinking

Based on the results of previous optimization steps, specific Argonaute protein complexes can be immunoprecipitated from native cells, using the conditions, tested so far. For identification of Argonaute-associated RNAs, the RNA molecules were fixed to distinct sites of the Argonaute protein via 4-thiouridine (s^4U) incubation and irradiation using ultraviolet (UV) light at a wavelength of 366 nm. This photo-activated UV cross-linking strategy was performed prior to cell lysis and immunoprecipitation to avoid reassociation of RNA with Argonaute proteins after cell lysis as well. s^4U incorporates into transcripts and facilitates crosslinking between RNA and protein. To get the RNAs binding to Argonaute proteins with very high efficiency, different s^4U concentrations and different UV crosslinking times were tested. SNB19 native cells were incubated for 14 hours with 50 µM, 100 µM and 500 µM s^4U and irradiated with 150 mJ/cm^2, 450 mJ/cm^2 and 1700 mJ/cm^2 UV light. In addition, two approaches were performed using 100 and 500 µM s^4U, but without UV crosslinking and one approach with UV irradiated (150 mJ/cm^2), but without prior 4-thiouridine incubation (Figure 4.2.1.5.I).
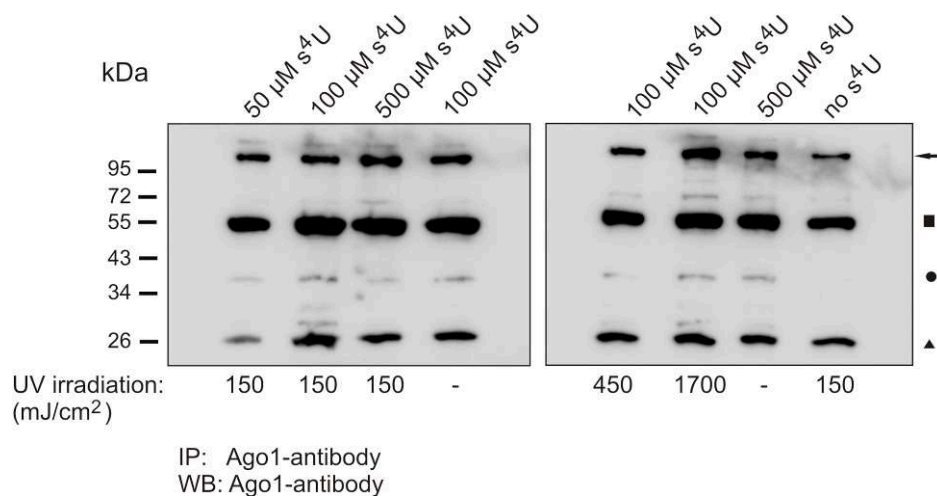
Figure 4.2.1.5.I Western Blot detection of Ago1 protein amounts after treatment of cells with different s^4U concentrations and UV-crosslinking times. These conditions have no effect on the precipitated Ago protein amount. ➤ immunoprecipitated Ago protein; ■ heavy chain of Ago-antibody; ● unspecific or degraded protein; ▲ light chain of Ago-antibody

In order to verify the quality and quantity of the Ago-IPs, Western Blot analyses were performed showing that s^4U incubation and UV irradiation have no influence on the amount of immunoprecipitated Argonaute protein (Figure 4.2.1.5.I). Only slight differences could be detected as expected since crosslinking should not interfere with immunoprecipitation of the Argonaute protein itself. Following, Ago-associated RNAs were analyzed, to find out, which conditions provide the most efficient co-immunoprecipitation of complexed RNA. For this reason, the RNA was separated from the Argonaute complex using TRIzol Reagent (Invitrogen), reverse transcribed into cDNA, and amplified,

using different gene specific primers. *HMGA2* was shown to be regulated by hsa-let-7 miRNA family (Motoyama *et al.*, 2008) and *FoxG1* regulated by hsa-miR-9 (Shibata *et al.*, 2008), whereas no miRNA binding site was detected on *GAPDH*.
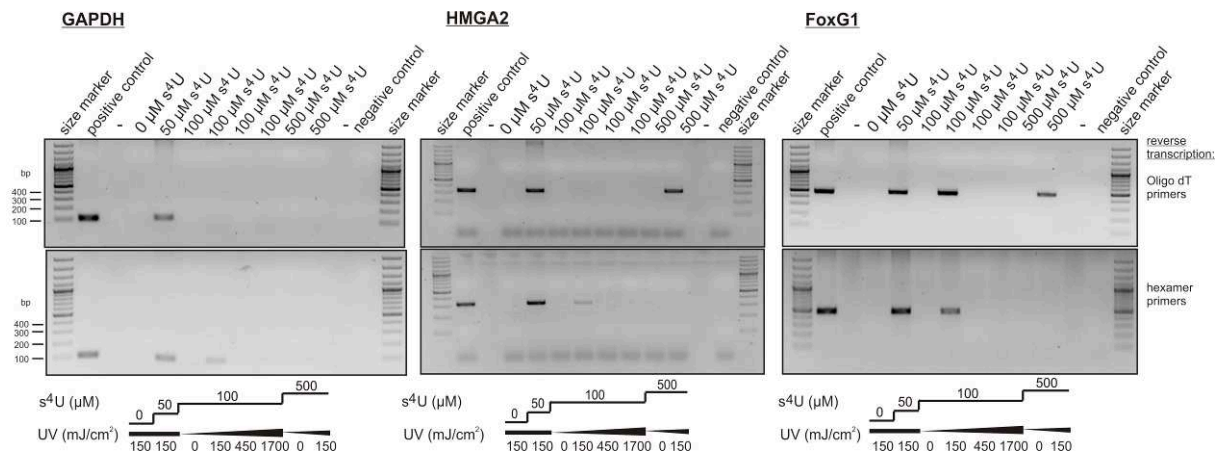
Figure 4.2.1.5.II Detection of Argonaute-RNA-association influenced by s^{4}U and UV-crosslinking. The agarose gel images show PCR products for the mRNAs *GAPDH, HMGA2* and *FoxG1,* reverse transcribed into cDNA using Oligo-dT (upper images) and Oligo-dT and random hexamer primers (lower images) and amplified, using gene-specific primers. The chart below the gel images describes the used conditions for each lane. Expected band sizes: *GAPDH* 100 bp, *HMGA2* 322 bp and *FoxG1* 483 bp

The approaches with 150 mJ/cm^2 UV irradiation or without UV irradiation provide overall no amplification products of analyzed genes (Figure 4.2.1.5.II). cDNA synthesis was performed, using Oligo dT primers or random hexamer primers for reverse transcription with subsequent PCR amplification. With regard to *GAPDH,* the use of Oligo-dT primers, together with random hexamer primers, shows unspecific crosslinking of this RNA and the Ago proteins (conditions: 50 µM 4SU, 150 mJ/cm^2 and 100 µM 4SU, 150 mJ/cm^2), because *GAPDH* could be amplified in both approaches, which was not expected. Thus, the use of 50 µM 4SU is not stringent enough for identification of Ago-specific RNAs. These unspecifically bound RNAs will get lost, using simply Oligo-dT primers (upper images, lane 5; 100 µM 4SU, 150 mJ/cm^2), since no *GAPDH* could be amplified, but the highest amount of *FoxG1,* indicating these conditions as appropriate for following investigations. However, *HMGA2* could not be amplified under these conditions, indicating that *HMGA2* seems to be not associated with Ago1 in SNB19 cells. The results obtained indicate that an increase of crosslinking time and reagent decreases the amount of detected mRNAs.

4.2.1.6 Testing different thiouridine incubation times

The incubation time of cells with s^{4}U was optimized by testing 4, 14 and 48 hours s^{4}U incubation, 100 µM s^{4}U and 150 mJ/cm^2 UV irradiation. In addition, one approach without s^{4}U and one approach without UV irradiation were executed as negative controls (Figure 4.2.1.6.I).
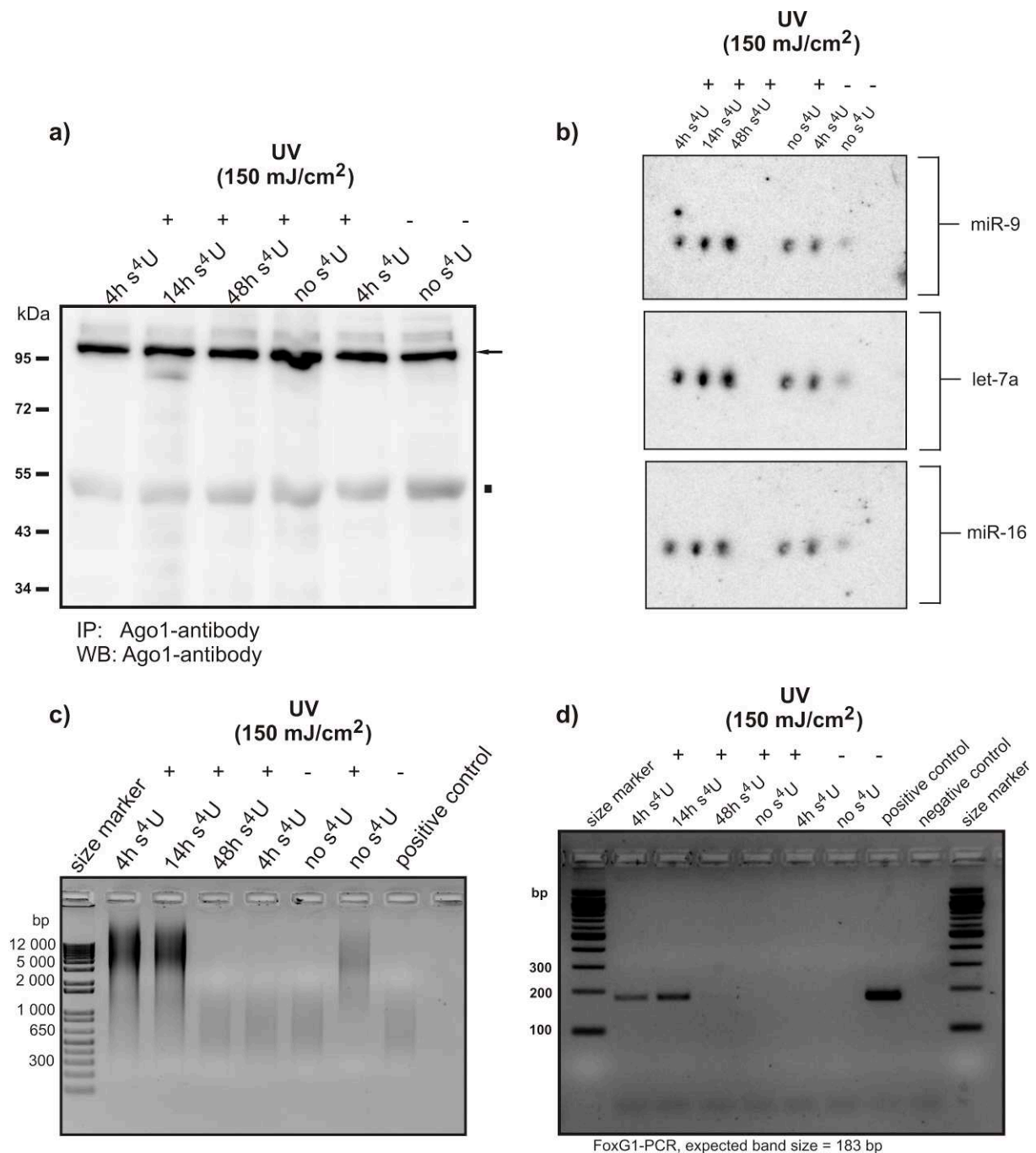
Figure 4.2.1.6.I Optimization of s⁴U incubation time. SNB19 native cells were incubated with 100 µM s⁴U for 4, 14 and 48 hours. For comparison reasons, three negative controls, one lacking s⁴U, one lacking UV irradiation and one lacking both, were analyzed in parallel. Equal cell counts were used and the protein amounts were analyzed using **a)** Western Blot, Ago-associated miRNAs by **b)** Northern Blot and Ago-associated mRNAs by **c)** PCR amplification of all mRNAs, and **d)** PCR amplification of *FoxG1*. The s⁴U incubation time has no effect to the Ago1 protein amount depicted by Western Blot. The Northern Blot and PCR amplifications show that the highest amount of Ago bound miRNAs and mRNAs were yield by s⁴U incubation for 14 hours. → immunoprecipitated Ago protein; ■ heavy chain of Ago-antibody

Figure 4.2.1.6.I a) represents the Western Blot of the Ago1-IPs performed under improved conditions tested so far. It is important that each IP shows similar amount of Ago1 protein for a precise comparison of the subsequent isolated RNA amounts. The miRNAs, miR-9, let-7a and miR-16 were verified via Northern Blot (Figure 4.2.1.6.I b). The amount of detected miRNAs was measured for each single band, background corrected and used for calculation of the miRNA fraction in comparison to the

whole amount of detected miRNAs. 26.8% of let-7a could be isolated from Ago1 precipitated from cells incubated for 14 hours with s⁴U, whereas the other approaches reveal between 3.6% and 26.0% of this miRNA. 23.4% of miR-16 could be isolated from Ago1 precipitated from cells incubated for 14 and 48 hours with s⁴U. For the other approaches, an amount between 4.2% and 18.4% of miR-16 could be measured. A very high amount of miR-9 could be detected in these approaches as well. However, with incubation time of 14 hours, 22.8% of miR-9 could be measured, whereas 31.0% of miR-9 could be detected after 48 hours s⁴U incubation. Additionally, the mRNA was reverse transcribed into cDNA and amplified using random hexamer and *FoxG1* primers. With the random hexamer primers, the whole Ago protein-associated RNAs could be detected. Figure 4.2.1.6.I c) depicts clearly that an incubation time of 4 and 14 hours with s⁴U provides the highest amount of Ago-associated mRNAs. The same could be shown, using gene specific primers. The *FoxG1* gene could be detected among the Ago1 bound mRNAs of cells, incubated for 4 and 14 hours with s⁴U (Figure 4.2.1.6.I d), whereat the RNA isolated from Ago1 precipitated from cells incubated for 14 hours with s⁴U offers a higher amount of PCR product *FoxG1* (total RNA = 100%, 4h = 29.45%, 14h = 47.44%). For all other approaches, no *FoxG1* fragment could be amplified. Therefore, a s⁴U incubation time for 14 hours is the best compromise for obtaining a high amount of specific Ago-associated miRNAs and mRNAs and a very low amount of false-positive RNAs. On this account, cells were incubated for 14 hours with s⁴U in subsequent experiments.

4.2.1.7 Optimizing specificity of IP procedure

For further improvement of the purity and specifity of the Ago-IP, isotype controls and empty beads were analyzed in the same way as the Argonaute complexes. Both, the isotype control and the empty beads, function as negative controls. For the isotype control, beads were coupled with rat IgG2a antibody, which has no affinity to human proteins. The empty beads were not coupled with an antibody, but treated in the same way as all other approaches. For this step of improvement, the Ago2-antibody was used, providing a higher amount of Argonaute protein in general. Four different approaches were performed to decrease detection of false-positive RNAs: (i) the number of washing steps was increased from three to five (Figure 4.2.1.7.I), (ii) beads were blocked and precleared (Figure 4.2.1.7.I), (iii) the stringency of washing was tested by using different salt amounts (Figure 4.2.1.7.II) and (iv) additionally magnatic beads were tested against sepharose beads (Figure 4.2.1.7.III). First, the IP was washed twice with a washing buffer, containing 500 mM KCl and once with PBS (~ 170 mM salt). A second IP was washed twice with a washing buffer, containing 300 mM KCl and twice with a washing buffer, containing 500 mM KCl and once with PBS. In addition, the antibody-coupled beads of approach three were blocked with 0.5% BSA in NP40 buffer, before starting IP, and the lysate of approach four was precleared, using empty beads. Theoretically, these empty beads catch excessive proteins of the lysate, which was subsequently transferred to Ago-antibody-coupled beads to perform IP.
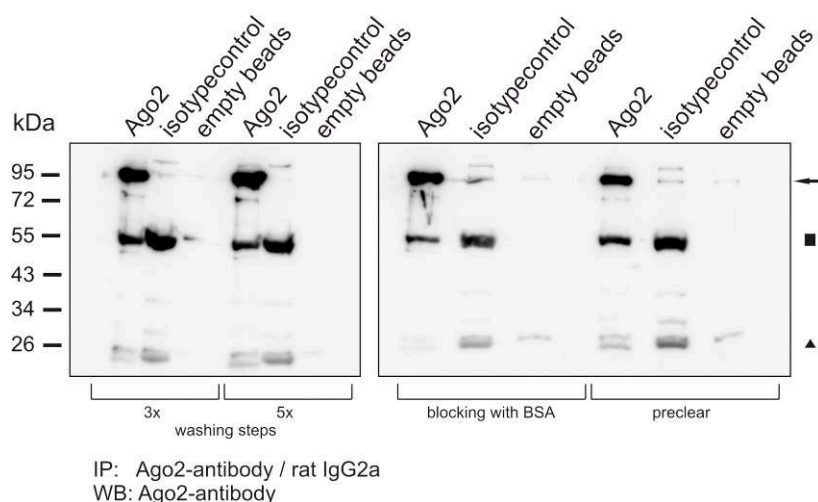
Figure 4.2.1.7.I Testing specificity of immunoprecipitation using different washing steps and blocking methods. Extensive washing is the only possibility to get a very high purity of the IP, because bead blocking with BSA or preclear of the lysate show unspecific bound Ago2 protein in the isotype control and empty beads. ← immunoprecipitated Ago protein; ■ heavy chain of Ago-antibody; ▲ light chain of Ago-antibody

As shown in Figure 4.2.1.7.I, the condition using five washing steps shows highest amount of immunoprecipitated Ago protein and no Argonaute protein in the isotype control and empty beads. The blocking of beads with BSA and the preclear of the lysate provide a decreased amount of Ago protein and moreover unspecific bound Ago protein could be detected in both negative controls as well. In addition, three washing steps are not stringent enough to achieve the purity and specificity of IP as desired and needed. Therefore, at least two washing steps using 300 mM and 500 mM KCl washing buffers, respectively, and one washing step with ice cold PBS are needed for elimination of unspecific bound Argonaute protein complexes. In order to verify these conditions for optimality, four different washing buffers containing different salt concentrations were tested.
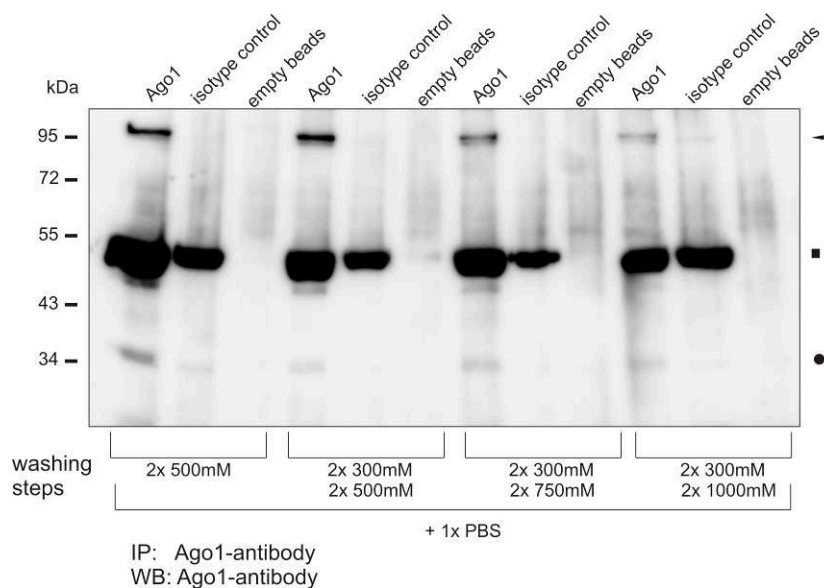
Figure 4.2.1.7.II Testing washing buffers with different salt concentrations. The Western Blot shows, the higher the salt concentration of the washing buffer, the more Ago1 protein will be removed after IP. ← immunoprecipitated Ago protein; ■ heavy chain of Ago-antibody; ● unspecific or degraded protein or antibody chain

The first three washing conditions show no unspecific bound Ago1 protein in the isotype control and the empty beads. However, the use of washing buffers with increasing salt concentrations leads to decrease of immunoprecipitated Ago1 amount as seen in Figure 4.2.1.7.II. The measurement of the four Ago protein bands (= 100%) reveals an Ago protein amount of 38.5%, using washing buffers with 300 mM and 500 mM KCl, whereas the other conditions provide 33.8% (2 x 500 mM KCl), 21.2% (2 x 300 mM and 2 x 750 mM KCl) and 6.6% only (2 x 300 mM and 2 x 1 M KCl) of the complete Ago protein amount in comparison to each other. To ensure the optimal conditions, miRNAs and mRNAs associated with Ago1, isotype control and empty beads were validated using qrt-RT-PCR.
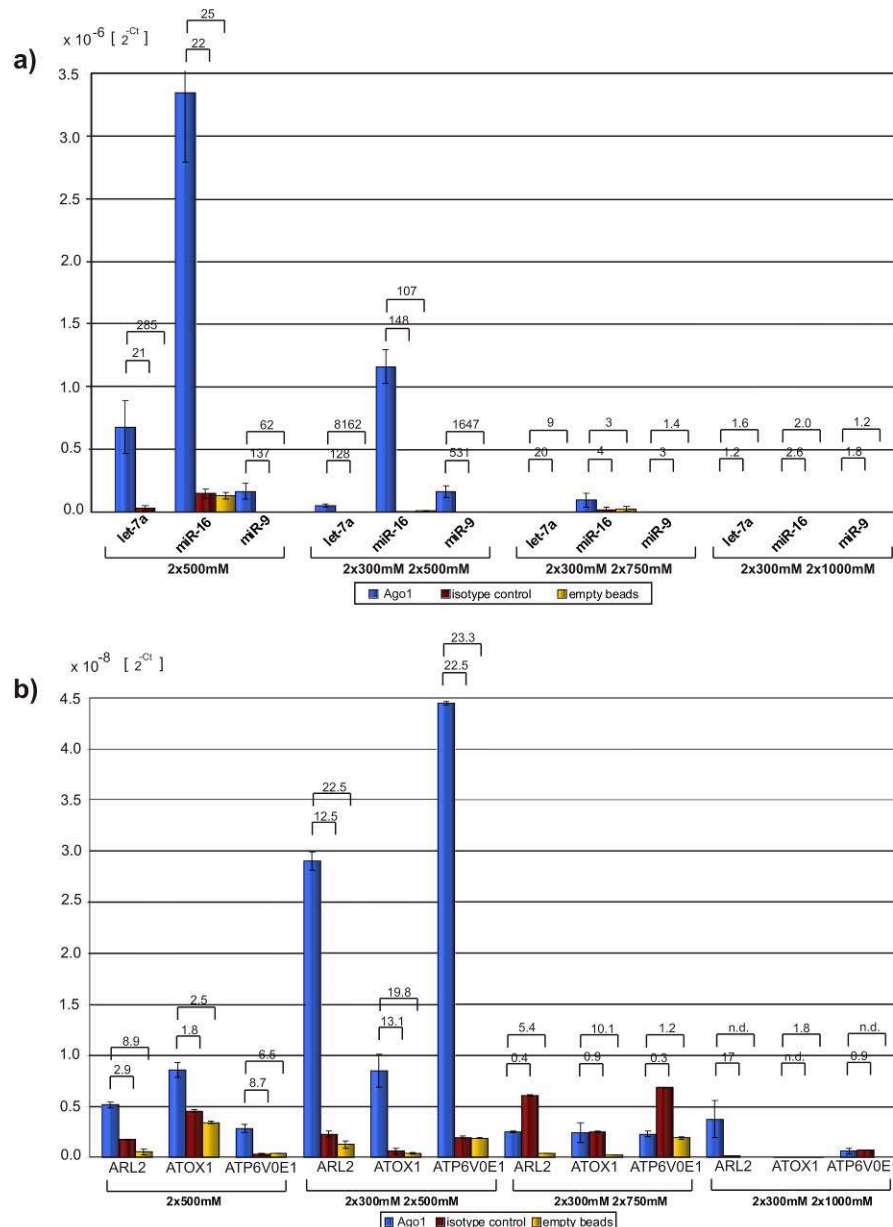
Figure 4.2.1.7.III Verification of distinct RNAs using qrt-RT-PCR. The diagrams show Ago1-associated **a)** miRNAs and **b)** mRNAs. The use of washing buffer with salt concentrations of 300 and 500 mM KCl after IP do not provide the highest miRNA amount, but the most purified, whereat the same approach provides the highest mRNA amount in Ago1 (blue bar) and the lowest mRNA amount in the isotype control (red bar) and the empty beads (yellow bar). The numer above the blue and red bars denotes the fold change between Ago-associated RNAs and unspecific RNAs detected in the isotype control and the number above the blue and the yellow bars presents the fold change between Ago-associated RNAs and unspecific RNAs detected on empty beads.

The analysis of the miRNAs, hsa-let-7a, hsa-miR-16 and hsa-miR-9, using qrt-RT-PCR, indicates that the use of a washing buffer with 500 mM salt concentration only, is not stringent enough to eliminate unspecific bound miRNAs from the Ago1 protein complex as shown in Figure 4.2.1.7.III a). Moreover, the use of 750 mM and 1 M salt concentration shows a high reduction of Ago1 protein amount and accordingly a high loss of specific miRNAs. Using 300 mM and 500 mM KCl washing buffers is optimal for obtaining a high amount of pure and specific Argonaute bound miRNAs. The same could be demonstrated with regard to the detected mRNAs, *ARL2, ATOX1* and *ATP6V0E1* (Figure 4.2.1.7.III b). The washing steps, using salt concentrations of 300 and 500 mM in the washing buffers, provide the highest mRNA amount in association with Ago1, and the lowest mRNA amount in the negative control approaches. So, these conditions were considered optimal for identification of high confident Ago-associated RNAs.

Another alternative could be the use of Protein G Dynabeads instead of Protein G Sepharose beads because the handling with dynabeads is much faster due to the magnatic separation methodology. Beside the test of these two kinds of beads, both IPs were washed twice with 300 mM and twice with 500 mM KCl washing buffers, and alternatively three times with 300 mM and three times with 500 mM KCl washing buffers. After these washing steps, the IPs were washed once with ice cold PBS.
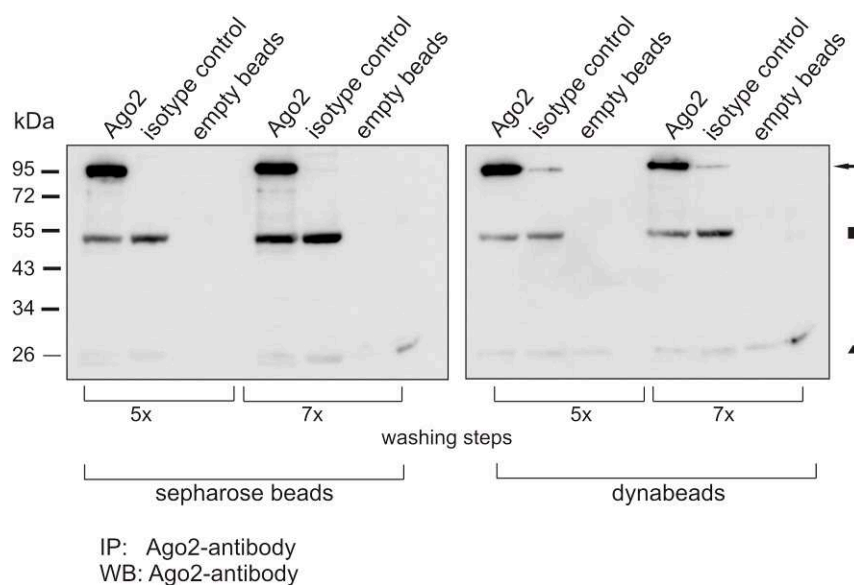
Figure 4.2.1.7.IV Western Blot visualizing Ago2-IP performed with different beads. The IPs shown on the left Western Blot were performed using sepharose beads and on the right Western Blot using dynabeads. The use of dynabeads reveals unspecific bound Ago protein in the isotype control, whereas the use of sepharose beads provides Ago-IPs with high purity. ◄— immunoprecipitated Ago protein; ■ heavy chain of Ago-antibody; ▲ light chain of Ago-antibody

The Western Blots of Figure 4.2.1.7.IV illustrate no loss of Ago2 protein amount by performing 5 or 7 washing steps, but there is a great difference in IP purity using sepharose- or magnatic beads. A small amount of unspecific bound Argonaute protein was detected after IP of the isotype control (right Western Blot) by application of dynabeads. Consequently, the handling with Protein G Dynabeads is much faster, but the purity and specificity of the Ago-IP, achieved up to now, will get lost. Finally, after all these different optimization steps, the PAR-CLIP-Array method could be applied easily to other cell line systems.

4.2.2 Improved RNA labeling and microarray hybridization

For rapid detection of a vast amount of Ago-associated miRNAs and mRNAs, microarray hybridization was used after co-immunoprecipitation and isolation of complexed RNA. Compared with mRNAs, for miRNAs a much higher dynamic range of melting temperatures is observed, and it is not possible to adjust hybridization probes or PCR primers for each miRNA. Each miRNA/probe pair exhibits its specific physicochemical properties and hybridization efficiencies. Furthermore, true miRNA "housekeeper", to which miRNA signal intensities could be normalized, hardly exist (Bissels *et al.*, 2009). Therefore, a microarray platform (miRXplore) that enabled a semiquantitative description of differential miRNA expression was used for the analysis of miRNA expression patterns of 102 pediatric AML patient samples (section 4.1.1 as well as for the detection of Argonaute-associated miRNAs. A universal reference consisting of 493 synthetic human miRNA oligonucleotides according to miRBase 8.2 was used for quantification of any single miRNA detected on a microarray. The signal intensity of a sample miRNA could be directly compared with the signal intensity of the same miRNA sequence, present in the universal reference. Thus, the bias related to sequence, labeling, hybridization or signal detection of signal intensities could be adjusted by using the universal reference. Synthetic miRNAs of the universal reference and the miRNAs of the sample were labeled enzymatically with cyanine dyes Cy3 and Cy5, respectively, together with 18 spike in controls (miRControl 3 calibration - and miRControl 1 position oligonucleotides), using a mutated and truncated RNA-ligase 2 (Rnl2 (1-249) K227Q). This ligase reduces the effect of self-circularization of miRNAs, whereby sequence bias will be compensated. After hybridization, the arrays were scanned, and each spot was analyzed by normalization against the median of the miRControl 3. Thereafter, a false-color image was generated giving a first rough overview of detected miRNAs and their signal intensities.
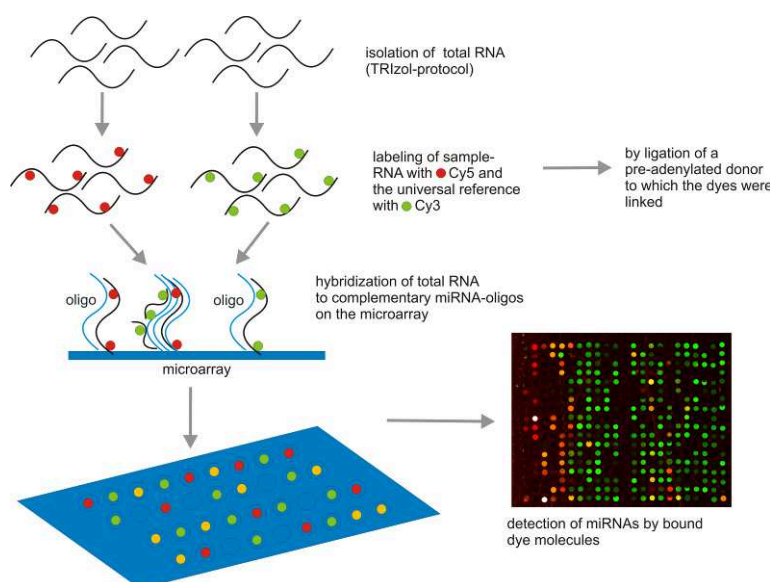
Figure 4.2.2.I Schematic overview of microarray hybridization. After RNA isolation, the samples were labeled enzymatically with Cy5 and the universal reference with Cy3. For the labeling procedure the Rnl2 (1-249) K227Q was used. The labeled RNA fractions were co-hybridized to a microarray. After hybridization the microarray was scanned and the signal intensities were measured and illustrated by a false-color image.

4.3 KASUMI-1 and NB4 cell lines act as t(8;21) and t(15;17) models for AML

Two human AML and APL cell lines, called KASUMI-1 and NB4, were chosen for further investigations of miRNA functionality, especially miRNAs identified as differentially expressed in pediatric AML patients. These cell lines are characterized cytogenetically by the chromosomal translocations t(8;21) and t(15;17).

4.3.1 Comparison of miRNA expression patterns between AML patients and AML cell lines

The miRNA expression patterns of both cell lines were compared with the signatures of differentially expressed miRNAs, identified among subtypes of pediatric AML patients, showing that the cell lines are suitable models for further analyses of the chromosomal transloccations t(8;21) and t(15;17). Therefore, the miRNA expression profiles of AML patients carrying translocation t(8;21) was compared with the miRNA expression profile of KASUMI-1 cells, and the miRNA expression signature of AML patients harboring translocation t(15;17) was compared with the one of NB4 cells, as listed in Table 4.3.1.I and Table 4.3.1.II.

Table 4.3.1.I Comparison of miRNA signal intensities and molecule counts of AML patients with t(8;21) and KASUMI-1 cells. <u>Abbreviations</u>: SI – signal intensity (sample/UR); UR – universal reference

miRNA Name	Φ miRNA SI of AML patients with t(8;21)	Molecules per cell (t(8;21))	miRNA SI of KASUMI-1	Molecules per cell (KASUMI-1)
hsa-miR-126-3p	2,11	~ 637	0,79	~ 1175
hsa-miR-146a	0,39	~ 117	0,18	~ 268
hsa-let-7b	0,39	~ 117	-	-
hsa-miR-335	0,17	~ 51	0,33	~ 491
hsa-let-7c	0,14	~ 42	0,27	~ 401
hsa-miR-21	2,23	~ 673	0,63	~ 935

Table 4.3.1.II Comparison of miRNA signal intensities and molecule counts of AML patients with t(15;17) and NB4 cells <u>Abbreviations</u>: SI – signal intensity (sample/UR); UR – universal reference

miRNA Name	Φ miRNA SI of AML patients with t(15;17)	Molecules per cell (t(15;17))	miRNA SI of NB4	Molecules per cell (NB4)
hsa-miR-100	0,64	~ 193	-	-
hsa-miR-125b	0,66	~ 199	-	-
hsa-miR-181a	3,34	~ 1006	1,21	~ 2257
hsa-miR-181b	1,05	~ 316	0,87	~ 1618
hsa-miR-126	0,09	~ 27	-	-
hsa-miR-223	2,00	~ 602	2,85	~ 5294
hsa-miR-494	0,04	~ 12	-	-

Most miRNAs, identified as differentially expressed with high significance in pediatric AML patient samples with chromosomal translocations t(8;21) and t(15;17), could also be detected in the total RNA of KASUMI-1 and NB4 cells, as listed in Table 4.3.1.I and Table 4.3.1.II. Hence, both cell line systems are suitable models for the examination of functional aspects of distinct miRNAs detected in both, AML patient samples and respective cell lines.

4.3.2 Quantification of Argonaute protein complexes in AML cell lines

The quantification of *Argonaute* gene expression on transcriptional level in KASUMI-1 and NB4 cells, was the first step of analysis on transcriptional and translational level (Figure 4.3.2.I and Figure 4.3.2.II). On this account, RNA was isolated from KASUMI-1 and NB4 cells, reverse transcribed into cDNA and amplified using qrt-RT-PCR. For transcriptional analysis, the qrt-RT-PCR was performed, using Ago1-4 specific primers located in exon/exon intersections.
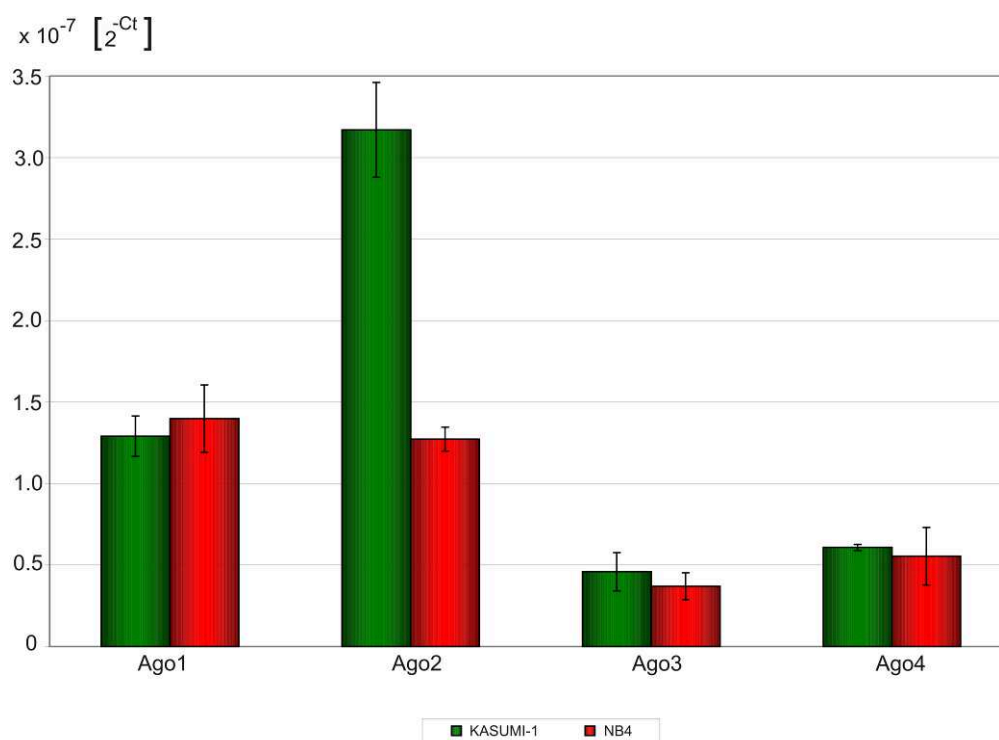
Figure 4.3.2.I The amount of Ago1-4 expressed in KASUMI-1 (green bars) and NB4 (red bars) cells on transcriptional level was verified using qrt-RT-PCR. This picture illustrates that the expressions of Ago1 and Ago2 are relatively higher than of Ago3 and Ago4.

It is not correct to compare the absolute quantities of the amplified transcripts of the Argonaute proteins among each other directly, because different primers own different binding efficiencies. Nevertheless, Figure 4.3.2.I shows that the four *Argonaute* mRNAs could be verified in KASUMI-1 - and NB4 cells. In addition, there is a bias showing a higher amount of *Ago1* and *Ago2* transcripts in contrast to *Ago3* and *Ago4* transcripts. Interestingly, the amount of *Ago2* transcript is more than 2 fold higher in KASUMI-1 cells than in NB4 cells, which should be taken into account for further investigations. Taken together, the *Argonaute* gene expression could be verified on transcriptional level in both cell lines. Following, the validation of Argonaute protein amount by Western Blot analysis, and the identification of Argonaute-associated RNAs, using the improved PAR-CLIP-Array method, characterize the next steps of miRNA functionality analysis. The four human Argonaute protein complexes were immunoprecipitated from the two AML cell lines, KASUMI-1 and NB4. For IP and Western Blot analysis, the monoclonal Argonaute-antibodies Ago1-4 were used, as well as rat IgG2a isotype control antibody. Though, the Western Blot analysis serves as first purity control for all immunoprecipitations.
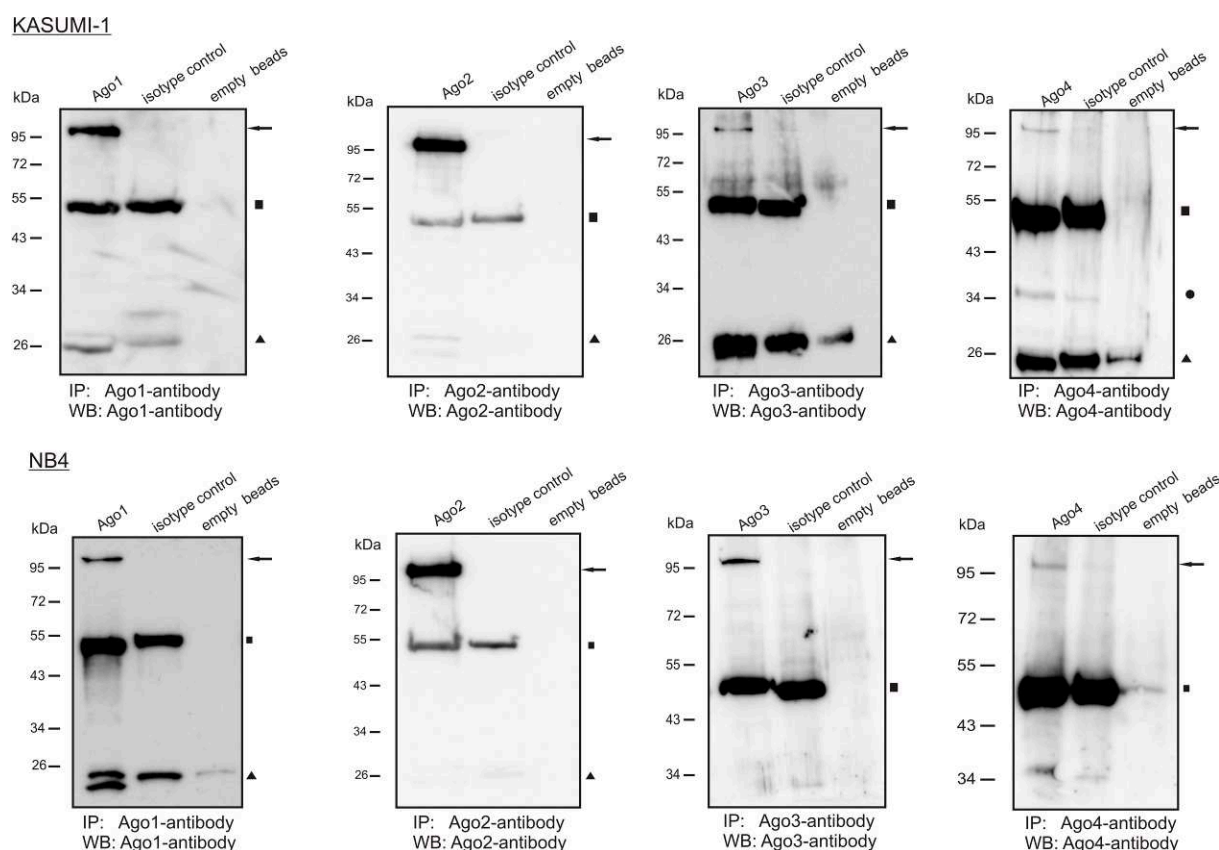
Figure 4.3.2.II Western Blot analysis of human Ago1-4 of AML cell lines, KASUMI-1 and NB4. In the first lane, a distinct band of approximately 97 kDa represents the Argonaute protein present in all Western Blots. The second lane displays the IP performed with isotype control antibody (rat IgG2a), showing no unspecific bound Argonaute protein. The third lane describes the second negative control, consisting of empty beads, showing no unspecific bound Argonaute protein as well. These IPs were performed in triplicates. ⟶ immunoprecipitated Ago protein; ■ heavy chain of Ago-antibody; ● unspecific or degraded protein; ▲ light chain of Ago-antibody

As shown in Figure 4.3.2.II, all Ago proteins could be immunoprecipitated with a high purity, since the negative controls show no unspecific bound Argonaute protein. Based on the qrt-RT-PCR of Ago1-4 (Figure 4.3.2.I), it was expected that a high amount of Ago1 and Ago2 could be extracted compared to the amount of Ago3 and Ago4 consistent with transcription analysis. Although, a 3 to 6 fold higher amount of cells was applied for Ago3- and Ago4-IPs, respectively, the immunoprecipitated amount of these Argonaute proteins was very low, but sufficient for following RNA analyses.

4.4 The four human Argonaute proteins show different miRNA association signatures in AML cell lines

To learn more about miRNA functionality, all miRNAs identified in the different Argonaute protein complexes of KASUMI-1 and NB4 cells, were analyzed, using unsupervised hierarchical clustering (Supplement Table V.3 and Table V.4). As demonstrated in Figure 4.4.I, the three replicates of each Argonaute protein complex group together, since their associating miRNA expression signatures reveal high similarity, whereas the different Ago proteins cluster into separate groups, due to their different miRNA expression profiles.

The heatmap below represents the whole miRNA data sets and gives an overview of highly expressed miRNAs shown in red (> 1 fmol), and low expressed miRNAs shown in green (< 1 fmol) with $\log_2$ signal intensity ranging between approximately -6 and 6 (between 0.02 and 64 fmol per 1 x 10^8 cells and < 1 and 385 molecules per cell).
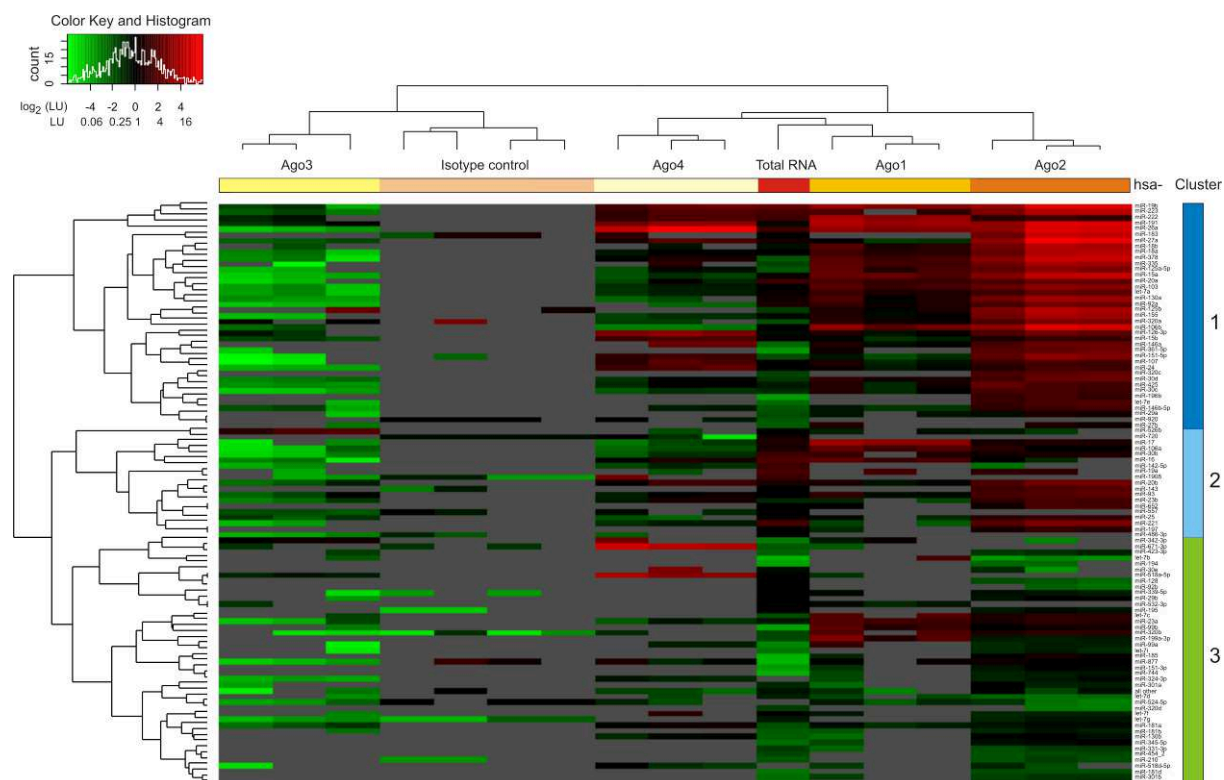
Figure 4.4.I Detection of Argonaute protein-associated miRNAs isolated from KASUMI-1 cells. Unsupervised hierarchical cluster analysis and heatmap calculations show separation of detected miRNAs, associated with Ago1, Ago2, Ago3 and Ago4. The signal intensity of each miRNA was corrected using 1 fmol of a universal reference consisting of synthetic ribooligonucleotides corresponding to 493 known human miRNAs. In the expression heatmap, miRNAs with a concentration below 1 fmol appear green and miRNAs with a concentration over 1 fmol appear red, according to the color key above. Overall, 42, 92, 43 and 40 miRNAs were detected on average for Ago1, Ago2, Ago3 and Ago4, respectively. For the isotype controls 15 miRNAs were identified on average.

Moreover, the dendrogram on the left was divided into three major clusters. Most of the miRNAs with very high expression levels were identified in association with Ago2 (97; average of three replicates), most of them being members of Cluster 1 (vertical, right). The miRNAs associated with Ago3 (59; average of three replicates) reveal mostly lower expressions, whereas the miRNAs associated with Ago1 (51; average of three replicates) and Ago4 (55; average of three replicates) offer signal intensities in the whole range presented by the color key top left. A few miRNAs (15 on average) could be identified in the isotype controls as well, although there was no Argonaute protein visible in the negative control lanes on the Western Blot. Therefore, unspecific bound miRNAs are still detectable, despite the intensive washing steps under stringent conditions after IP. Most of these detected miRNAs possess very low expression levels (between $\log_2$ -1 to -4; 0.06 to 0.5 fmol/1 x 10^8 cells or ~ 3 molecules per cell). In order to increase the likelihood, to apply only the most significant miRNAs to subsequent analyses, they have to pass the standard criteria (figured out for AML patient samples; section 4.1.2) by comparison of miRNA signal intensities detected in the Argonaute proteins and in the

isotype controls. miRNAs, which were detected in association with at least one Argonaute protein, but not in the isotype control, were considered highly significant. If the signal intensities of the miRNAs are at least 1.8 fold lower in the isotype control than in the Argonaute experiment with a p-value < 0.05, they will be applied for further analysis. Otherwise, these miRNAs were considered as unspecific and were removed from the data set. For comparison reasons, the expression profile of the total RNA was also included into the cluster analysis. Further calculations reveal that on average 23, 35 and 14 miRNAs associated with Ago1, Ago2 and Ago4, respectively are more than 1.8 fold enriched in the Argonaute proteins compared to the total RNA, whereas all Ago3 associated miRNAs show no enrichment concerning the total RNA.

The same cluster analysis was performed for miRNAs associated with the four human Argonaute protein complexes, immunoprecipitated from NB4 cells shown in Figure 4.4.II.
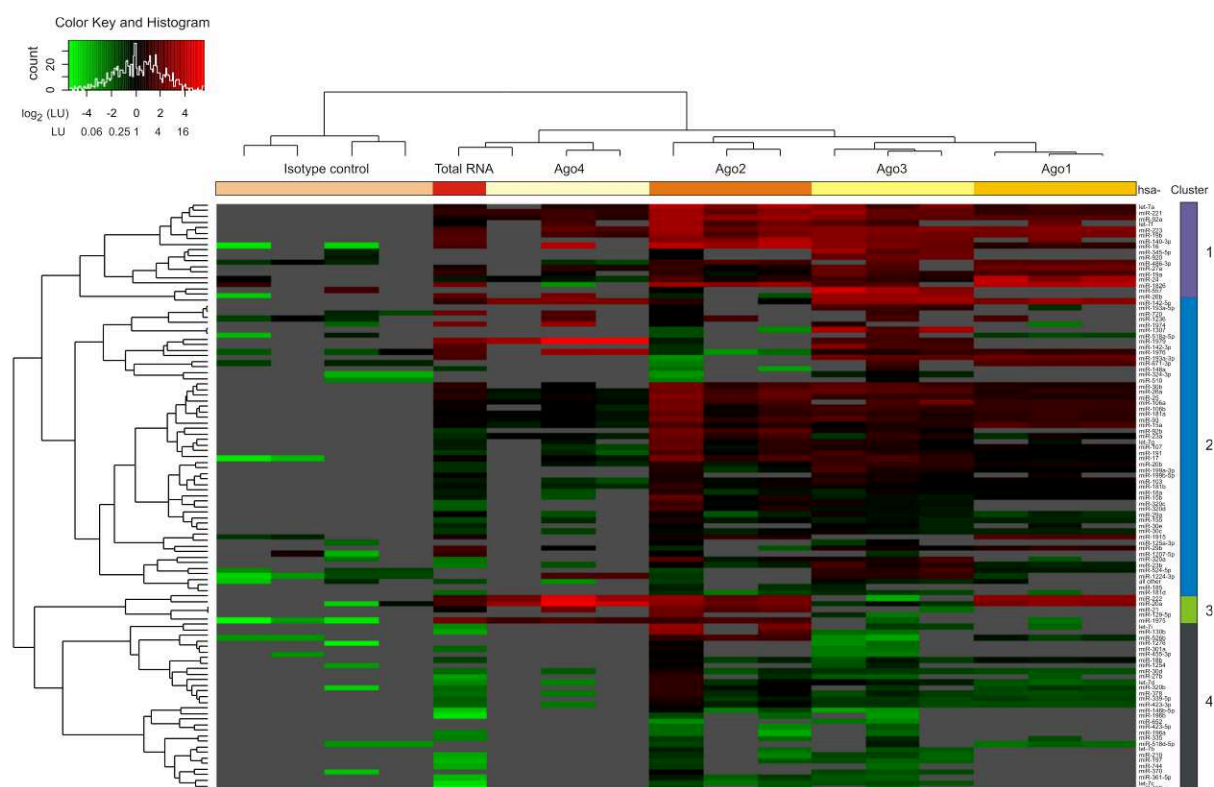
Figure 4.4.II Detection of Argonaute protein-associated miRNAs isolated from NB4 cells. As shown for KASUMI-1 the hierarchical cluster analysis and corresponding heatmap represent separation of detected miRNAs associated with Ago1, Ago2, Ago3 and Ago4. Again, the signal intensities were normalized for each miRNA using 1 fmol of a universal reference. In the expression heatmap, miRNAs with a concentration below 1 fmol appear green and miRNAs with a concentration over 1 fmol appear red according to the color key above. Overall, 53, 76, 83 and 30 miRNAs were detected on average for Ago1, Ago2, Ago3 and Ago4, respectively. For the isotype controls 15 miRNAs have been identified on average.

The cluster analysis and corresponding heatmap demonstrate many agreements with the result of KASUMI-1 Argonaute protein-associated miRNAs, but there are slight differences as well.

The triplicate miRNA expression profiles of each Argonaute protein also group together, whereas the miRNA expression patterns of the different Argonaute proteins group separate from each other. There are miRNAs, which are common in all Argonaute proteins and miRNAs, which are associated with one Argonaute protein only. The heatmap depicts the expression level of each miRNA in the range of $\log_2$

-6 and 6 (between 0.02 and 64 fmol per 1 x 10^8 cells and < 1 and 385 molecules per cell). In contrast to the miRNAs, associated with Ago3 in KASUMI-1 cells, the miRNAs associated with Ago3 in NB4 cells offer very high expression levels (up to 64 fmol). In addition, the most miRNAs associate with Ago3 (83; average of three replicates), whereby 53, 76 and 30 miRNAs could be associated with Ago1, Ago2 and Ago4, respectively, offering signal intensities in the logarithmic range from -6 to 6 as well. On average, 15 miRNAs were identified in the isotype controls possessing signal intensities more than 1.8 fold lower than measured for Ago-associated miRNAs and a p-value < 0.05. That means, none of the identified miRNAs has to be filtered out according to these criteria. In comparison to the total RNA, on average 13, 17, 30 and 16 miRNAs associated with Ago1, Ago2, Ago3 and Ago4, respectively, revealed an amount of 1.8 fold higher compared to the total RNA. Interestingly, among 83 Ago3-associated miRNAs identified in NB4 cells, 30 miRNAs are enriched with regard to total RNA, whereby only 43 Ago3-associated miRNAs were identified in KASUMI-1 cells, none of which was identified to be enriched.

Summing up, the cluster analyses revealed a difference in miRNA expression patterns between the four human Argonaute protein complexes, indicating that in both, AML and APL cell lines, common and Argonaute-specific miRNAs could be identified.

4.5 Identification of common and Argonaute-specific miRNAs

Intersection analyses were performed, after removing Ago-associated miRNAs with signal intensities < 1.8 fold and a p-value > 0.05 in comparison to the signal intensities of the corresponding miRNAs identified in the isotype controls. Thereby, common and Argonaute-specific RNAs were visualized by Venn-diagrams displayed in Figure 4.5.I a) for KASUMI-1 and Figure 4.5.I b) for NB4.
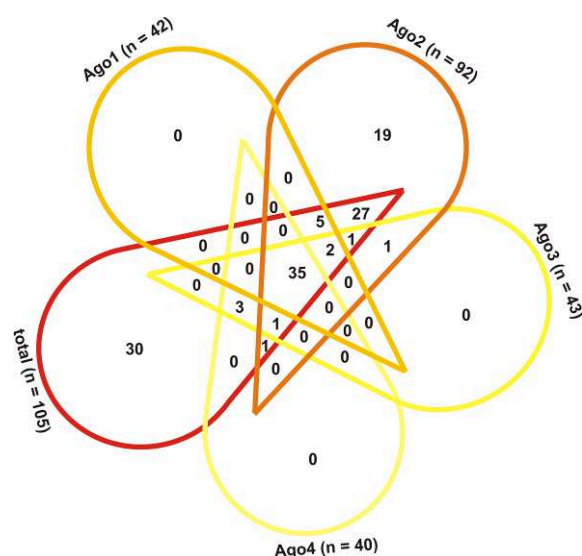
a) Ago-associated miRNAs of KASUMI-1   **b) Ago-associated miRNAs of NB4**
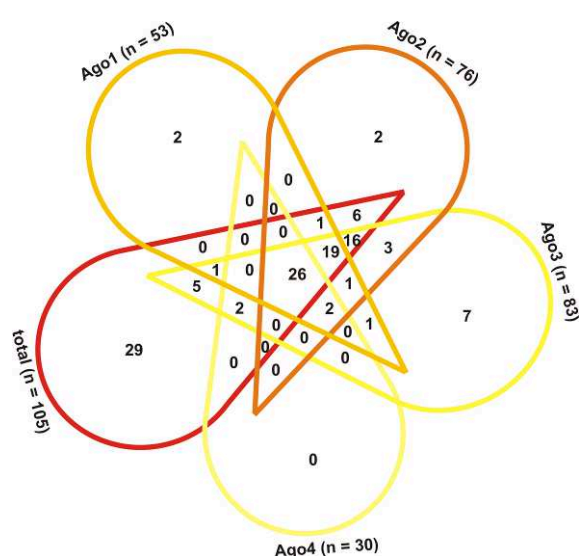
Figure 4.5.I Intersection analysis showing the relationship between significant Ago-associated miRNAs and the total RNA isolated directly from KASUMI-1 and NB4 cells. **a)** Displayed are common and Ago-specific miRNAs of KASUMI-1 and **b)** NB4. The total number of RNAs is given at the outer border of each set (n = x).

As shown in Figure 4.5.I, 19 miRNAs were associated with Ago2 and could not be identified in the total RNA of KASUMI-1 cells. 17 of these miRNAs reveal low expression levels < 1 fmol per 1 x 10^8 cells, and two miRNAs offer expression sizes of 1.2 and 1.3 fmol per 1 x 10^8 cells (~ 8 miRNA molecules per cell). These miRNAs could be identified in the Argonaute protein due to the protein enrichment during IP, but those low abundant miRNAs are in attomolar concentration in the total RNA, and might thus be under the detection threshold of the array method (Bissels *et al.,* 2009). 30 miRNAs were identified in the total RNA only, whereof 9 miRNAs exhibit very high expression up to 5.88 fmol (but 35 miRNA molecules per cell only). Between 33.3% and 87.5% of miRNAs were associated with all four Argonaute proteins and the total RNA, whereas about 50% of Ago2-associated miRNAs seem to be specific for this protein, as these miRNAs were only detected in Ago2 and the total RNA. In NB4 cells, miRNAs were found in association with only one Argonaute protein, but could not be identified as well in total RNA. There are 2, 2 and 7 miRNAs associated with Ago1, Ago2 and Ago3, respectively, offering very low expression values < 1 fmol per 1 x 10^8 cells, with one exception possessing an expression of 2.5 fmol per 1 x 10^8 cells (15 miRNA molecules per cell). Due to the marginal low expression of these miRNAs in attomolar range, their detection in the total RNA was not possible using these miRNA microarrays. 29 miRNAs were detected in the total RNA only. The most abundant 3 miRNAs own expression levels of around 3 fmol per 1 x 10^8 cells. Between 24.8% and 86.7% of miRNAs could be associated with all four human Argonaute proteins and were identified in the total RNA. In contrast to KASUMI-1 cells, in NB4 cells only 10.5% of the Ago2-associated miRNAs seem to be Ago2 specific, whereas Ago3 offers just about 14.5% specific miRNAs. To get more protein- and species-specific information, the identified miRNAs were compared between both cell lines. Identified miRNAs of the total RNA of both cell lines even accord for 72.1%. By comparison of Ago-associated miRNAs of KASUMI-1 and NB4 cells, 50.8% of Ago1-, 60% of Ago2-, 43.2% of Ago3- and 59.1% of Ago4-associated miRNAs coincide, respectively. As expected for different cell types, there are differences in Argonaute-miRNA binding, indicating that miRNAs possess Argonaute specificity changing in different cell types.

Sum together, the intersection analyses indicate the number of miRNAs, identified in all human Argonaute proteins, and the number of miRNAs exclusively identified in one Argonaute protein more precisely. Additionally, the number of common and Argonaute-specific miRNAs differs between both cell lines suggesting that there species-specific Argonaute-miRNA interactions may exist.

4.6 Differentially expressed miRNAs of pediatric AML associate with distinct Argonaute proteins

In order to identify the relationship between differentially expressed miRNAs of pediatric t(8;21)- and t(15;17)-positive AML patients and the four human Argonaute proteins, these miRNAs were filtered out of the whole spectrum of Ago-associated miRNAs identified by microarray technology, and were validated by qrt-RT-PCR. miR-16 was included as positive control, due to the fact that this miRNA is ubiquitous expressed in nearly all cells.

4.6.1 Validation of t(8;21)-relevant miRNAs in KASUMI-1 cells

miR-126 and miR-146a have been identified as up-regulated and let-7b, let-7c and miR-335 have been identified as down-regulated miRNAs in pediatric t(8;21)-positive AML patient samples, with highest significance in contrast to the corresponding miRNAs of all other AML patient samples. Additionally, these miRNAs could be verified also in association with one or multiple Argonaute proteins shown in Table 4.6.1.I.

Table 4.6.1.I Listing of median signal intensities (SI) (sample/UR) of six miRNAs, detected via microarray hybridization in KASUMI-1, n.d. = not detected; n.a. = not available

Microarray results: SI (sample/UR) Median of 3 replicates	miR-126	miR-16	miR-146a	let-7b	let-7c	miR-335
Ago1	0.84	8.58	0.64	n.d.	n.d.	2.26
isotype control	n.d.	1.05	n.d.	n.d.	n.d.	n.d.
FC: Ago1/control	n.a.	8.78	n.a.	n.a.	n.a.	n.a.
Ago2	5.07	23.70	2.30	0.45	0.61	1.53
isotype control	n.d.	1.16	n.d.	n.d.	n.d.	n.d.
FC: Ago2/control	n.a.	16.08	n.a.	n.a.	n.a.	n.a.
Ago3	0.06	0.29	n.d.	n.d.	n.d.	n.d.
isotype control	n.d.	n.d.	n.d.	n.d.	n.d.	n.d.
FC: Ago3/control	n.a.	n.a.	n.a.	n.a.	n.a.	n.a.
Ago4	0.76	3.42	n.d.	n.d.	n.d.	n.d.
isotype control	n.d.	n.d.	n.d.	n.d.	n.d.	n.d.
FC: Ago4/control	n.a.	n.a.	n.a.	n.a.	n.a.	n.a.

Interestingly, miR-126, which passes all three significance criteria (FC > 1.8, p-value < 0.05 and q-value < 5) in AML patients carrying translocation t(8;21) in comparison to all other patients expressing this miRNA, is highly abundant in Ago2, and it is the only miRNA showing association with all human Argonaute proteins as well (except of miR-16). miR-146a, which also belongs to the up-regulated miRNAs in translocation t(8;21) was identified in connection with Ago1 and Ago2, as well as miR-335, which is down-regulated in t(8;21)-positive pediatric AML patients. The miRNAs, let-7b and let-7c, were detected with low signal intensity in association with Ago2 only. As none of these miRNAs could be detected in the isotype controls, the results are considered as valid. For verification of the microarray hybridization results, these miRNAs were confirmed, using miRNA specific TaqMan probes in the qrt-RT-PCR.
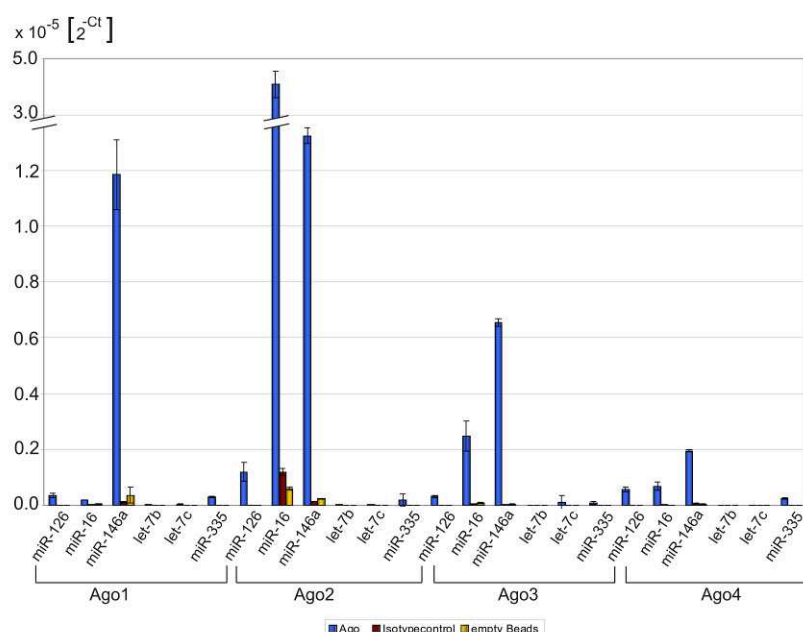
Figure 4.6.1.I Verification of distinct Ago-associated miRNAs using quantitative reverse transcriptase real time PCR. Shown are the measured expression levels of six selected miRNAs of the four Argonaute protein complexes.

In Figure 4.6.1.I, the amplification sizes of the six miRNAs, differentially expressed in AML patients, were depicted as bar chart. Thereby, Ago2 shows the highest enrichment of the miRNAs, miR-126, miR-16 and miR-146a, which shows a great abundance in Ago1, Ago2 and Ago3, whereas the miRNAs, let-7b, let-7c and miR-335, could be detected with a very small amount in each Argonaute protein.

The qrt-RT-PCR results show a similar expression pattern of miRNAs as shown for the AML patients, indicating that an appropriate cell line system was chosen. For completion of qrt-RT-PCR analysis, the fold change calculations between miRNA expression levels, identified in the Argonaute complexes in comparison to the expression levels of these miRNAs, detected in the isotype controls and the empty beads, were listed in Table 4.6.1.II.

Table 4.6.1.II Listing of median fold change (FC) of six selected miRNAs detected via qrt-RT-PCR in KASUMI-1

qrt-RT-PCR results: FC (Median of 3 replicates)	miR-126	miR-16	miR-146a	let-7b	let-7c	miR-335
Ago1/isotype control	43.8	123	99	30	302	131
Ago1/empty beads	14055	88	32	20	57	108
Ago2/isotype control	164	340	87	32	1386	11581
Ago2/empty beads	47557	680	53	25	38	63
Ago3/isotype control	206	66	156	0.008	569	597
Ago3/empty beads	128	27	265	0.017	969	302
Ago4/isotype control	517	29	26	0.009	14	1532
Ago4/empty beads	350	88	46	0.003	41	2998

4.6.2 Validation of t(15;17)-relevant miRNAs in NB4 cells

The miRNAs, miR-181a and miR-181b were identified as highly up-regulated in AML patients, harboring translocation t(15;17) together with miR-126 and miR-223, which were detected as down-regulated in t(15;17) with high significance in comparison to all other patients. Most of these miRNAs could be associated with the four human Argonaute proteins in NB4 cells (Table 4.6.2.I). miR-181a, miR-181b and miR-223 could be linked to each of the four Argonaute proteins with highest abundance in Ago1 and Ago2. The miRNA offers very high signal intensities visible for Ago1-4, in spite of the down-regulation of miR-223 in t(15;17)-positive AML patients, indicating this miRNA as important for several regulatory processes regulated in cooperation with Ago1-4. The second down-regulated miRNA, miR-126, which was not identified within the total RNA of NB4 cells, could not be detected in association with any of the Argonaute proteins as well. In this validation analysis, the miR-16 was included as positive control once more.

Table 4.6.2.I Listing of median signal intensities (SI) of five selected
miRNAs detected via microarray hybridization in NB4, n.d. = not detected; n.a. = not available

Microarray SI (median of 3 replicates)	miR-181a	miR-181b	miR-16	miR-126	miR-223
Ago1	1.67	1.21	5.92	n.d.	8.43
isotype control	n.d.	n.d.	0.026	n.d.	n.d.
FC: Ago1/control	n.a.	n.a.	228	n.a.	n.a.
Ago2	1.90	1.36	11.36	n.d.	7.6
isotype control	n.d.	n.d.	n.d.	n.d.	n.d.
FC: Ago2/control	n.a.	n.a.	n.a.	n.a.	n.a.
Ago3	1.85	0.87	6.09	n.d.	6.57
isotype control	n.d.	n.d.	0.028	n.d.	n.d.
FC: Ago3/control	n.a.	n.a.	242	n.a.	n.a.
Ago4	0.85	0.40	2.87	n.d.	2.68
isotype control	n.d.	n.d.	n.d.	n.d.	n.d.
FC: Ago4/control	n.a.	n.a.	n.a.	n.a.	n.a.

These findings, using microarray technology, were also validated by specific TaqMan miRNA probes and qrt-RT-PCR. The expression levels of each miRNA, detected in the Argonaute protein, isotype control or empty beads, are depicted in Figure 4.6.2.I and the corresponding FCs are listed in Table 4.6.2.II.

$x\ 10^{-5}\ \left[2^{-Ct}\right]$
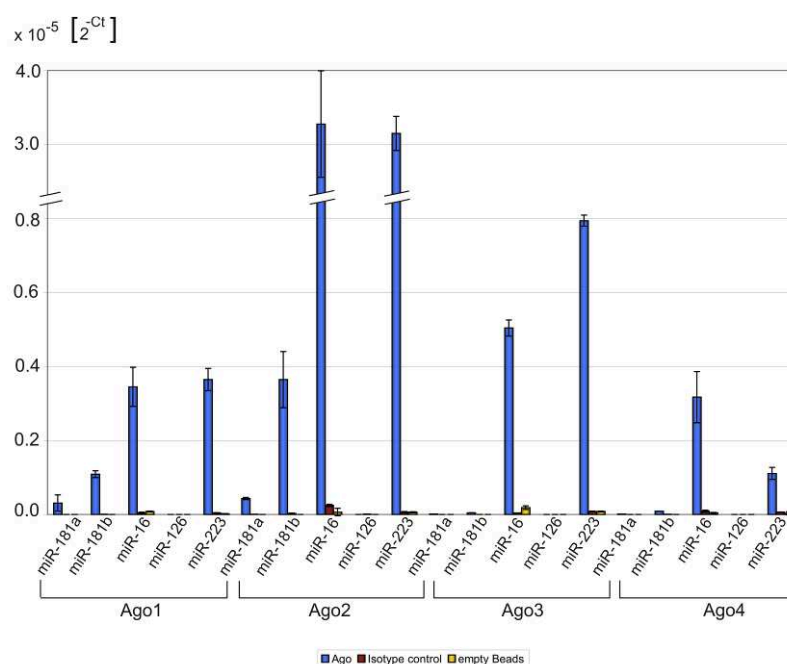
Figure 4.6.2.I Verification of distinct Ago-associated miRNAs using quantitative reverse transcriptase real time PCR. Shown are the measured expression levels of five selected miRNAs of the four Argonaute protein complexes.

As illustrated in the bar chart of Figure 4.6.2.I, the miRNAs, miR-181b, miR-16 and miR-223, were identified with highest expression. Although, miR-223 was identified as down-regulated in t(15;17)-positive pediatric AML patients, this miRNA possesses very high expression sizes in Ago1, Ago2 and Ago3. The miRNA, miR-181a detected as up-regulated in t(15;17)-positive AML patients, presents relative low amplification in all Argonaute proteins in contrast to the miR-223, indicating that the expression of miR-181a is lower, and the expression of miR-223 is higher in other AML cell types. Moreover, the miR-126 is down-regulated in t(15;17)-positive pediatric AML patients and was also margianal amplified using qrt-RT-PCR.

Altogether, the highest amount of all tested miRNAs could be detected in Ago2, with regard to both, the microarray as well as qrt-RT-PCR results. The fold changes between the miRNA expression size of the Argonaute proteins in contrast to the expression of the corresponding miRNA detected in the isotype controls and the empty beads were listed in Table 4.6.2.II.

Table 4.6.2.II Listing of median fold change (FC) of five selected miRNAs detected via qrt-RT-PCR in NB4

RT-PCR FC (median of 3 replicates)	miR-181a	miR-181b	miR-16	miR-126	miR-223
Ago1/isotype control	215	325	78	26	90
Ago1/empty beads	25350	1725	43	7	200
Ago2/isotype control	115	140	144	0.3	514
Ago2/empty beads	171	5292	554	77	549
Ago3/isotype control	16	18	123	28	97
Ago3/empty beads	n.a.	3868	27	29	100
Ago4/isotype control	4.4	25	36	11	18
Ago4/empty beads	1460	1497	76	21	39

In summary, the use of two different experimental methods for identification and validation of distinct miRNAs, reveals associations between the analyzed miRNAs and the four different Argonaute proteins and uncover miRNAs, which preferentially associate with only one or two Argonaute proteins.

4.7 Different mRNAs associate with different Argonaute proteins in AML cell lines

In order to discover the function of miRNAs in the cell environment, their regulatory targets have to be identified as well. Therefore, besides the identification of Argonaute protein-associated miRNAs, the analysis of Argonaute-associated mRNAs, potentially regulated by these miRNAs, is also essential. Bioinformatical studies indicate that a single miRNA possesses the ability to target and regulate hundreds of mRNAs (Brennecke et al., 2005; Grun et al., 2005; Krek et al., 2005; Lewis et al., 2005; Xie et al., 2005). Thus, the whole spectrum of identified Ago-associated mRNAs of KASUMI-1 and NB4 cells was investigated by using hierarchical cluster analysis, too (Figure 4.7.I and Figure 4.7.II; Supplement Table V.5 and Table V.6).

For KASUMI-1, the dendrogram at the top of Figure 4.7.I displays the classification of each sample on the basis of the complete data. It can be seen that the triplicate mRNA expression profiles of each Argonaute protein group together, whereas the mRNA expression signatures of different Argonaute proteins cluster separately. The heatmap below represents the signal intensities of significant mRNAs, offering a FC > 1.8 and a p-value < 0.05 in all three replicates, and in comparison to the isotype controls. On average 382, 460, 340 and 256 significant mRNAs could be linked to Ago1, Ago2, Ago3 and Ago4, respectively, with signal intensities between approximately 60 and 14,000 light units (LU). In the isotype controls, hundreds of unspecific bound mRNAs were identified with signal intensities more than 1.8 fold higher than the signal intensities of the corresponding Argonaute-associated mRNAs. However, less than a handful mRNAs in the isotype controls execute signal intensities with a FC > 1.8 together with a p-value < 0.05 in comparison to the signal intensities of Argonaute-associated mRNAs. Consequently, a mass of randomly bound mRNAs reside still attached on the isotype controls and within the Ago-isolated RNAs, despite stringent washing conditions after IP. Therefore, it is mandatory to remove mRNAs whose signal intensities are not statistically significant by comparison of Ago-associated mRNAs with mRNAs identified in the isotype controls.
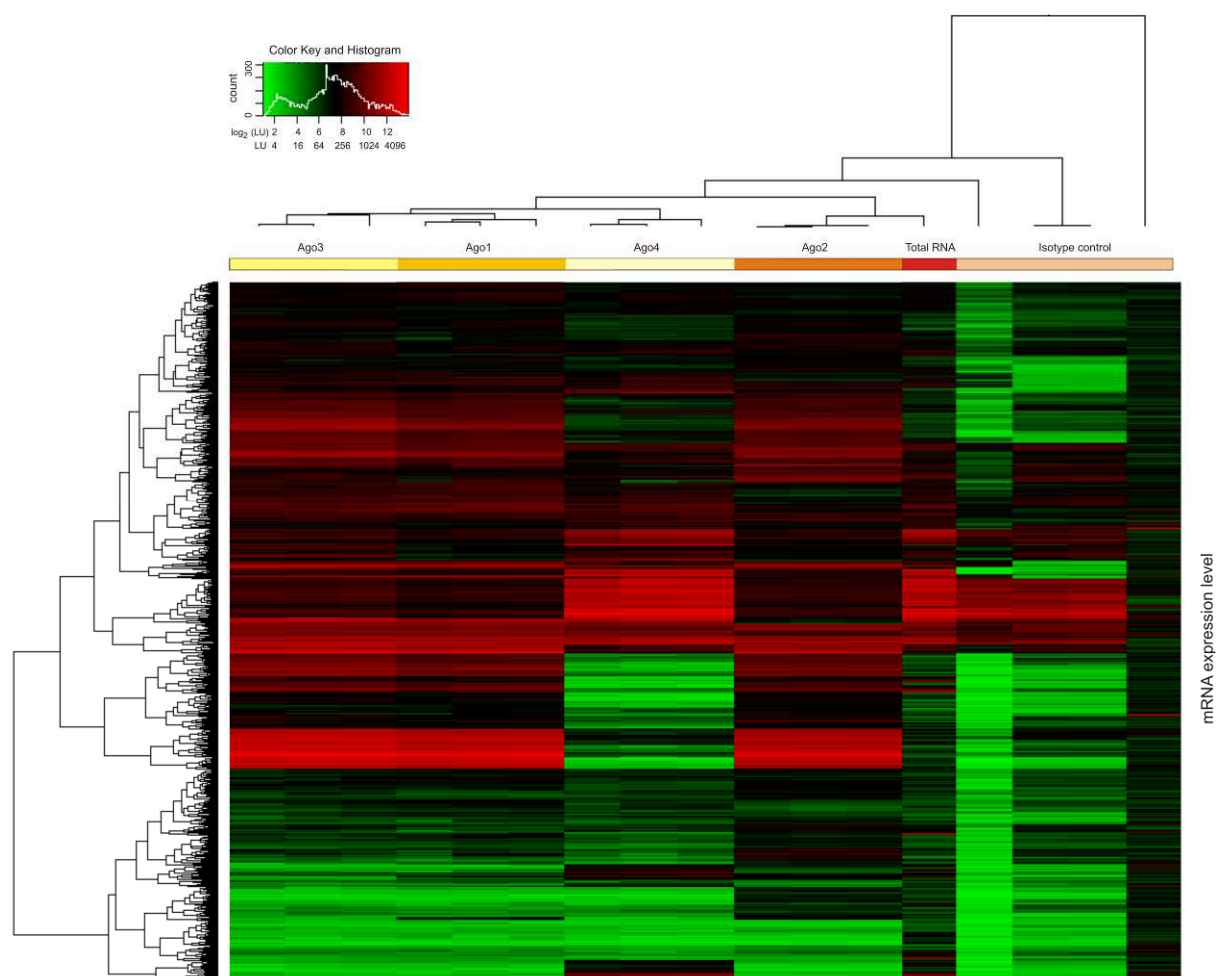
Figure 4.7.I Detection of Argonaute protein-associated mRNAs of KASUMI-1 cells. Hierarchical cluster analysis was computed, using the complete mRNA expression data of the triplicates of each Argonaute protein in comparison to the isotype controls (shown at the top). The heatmap was drawn for all significant mRNAs, identified on the basis of the hierarchical clustering of all mRNAs. Significant mRNAs offer a fold change > 1.8 and a p-value < 0.05 in all replicates of the Argonaute experiments in comparison to the isotype controls.

The composition of the clustering and the heatmap calculated for Argonaute-associated mRNAs of KASUMI-1 cells was computed in the same way for Ago-associated mRNAs of NB4 cells (Figure 4.7.II). The complete mRNA data were used for hierarchical cluster analysis, showing a separation of the different Argonaute proteins, due to their mRNA expression patterns. The heatmap shows the signal intensities of all significant mRNAs in the range of approximately 60 to 8,400 LU. The highest peak of the histogram, in the color key top left, clarifies that about 3 fold more significant Ago-associated mRNAs with less signal intensities were detected in NB4 cells than in KASUMI-1 cells. Overall, on average 281, 1399, 1338 and 1204 significant mRNAs associate with Ago1, Ago2, Ago3 and Ago4, respectively. Conversely, on average 26 mRNAs were found in the isotype controls with signal intensities 1.8 fold higher and a p-value < 0.05 in contrast to the signal intensities of Argonaute-associated mRNAs, indicating that a vanishing little number of unspecific bound mRNAs were solely identified in the isotype controls. Those unspecific bound mRNAs and mRNAs not satisfying the selection criteria were obviated from following analysis.
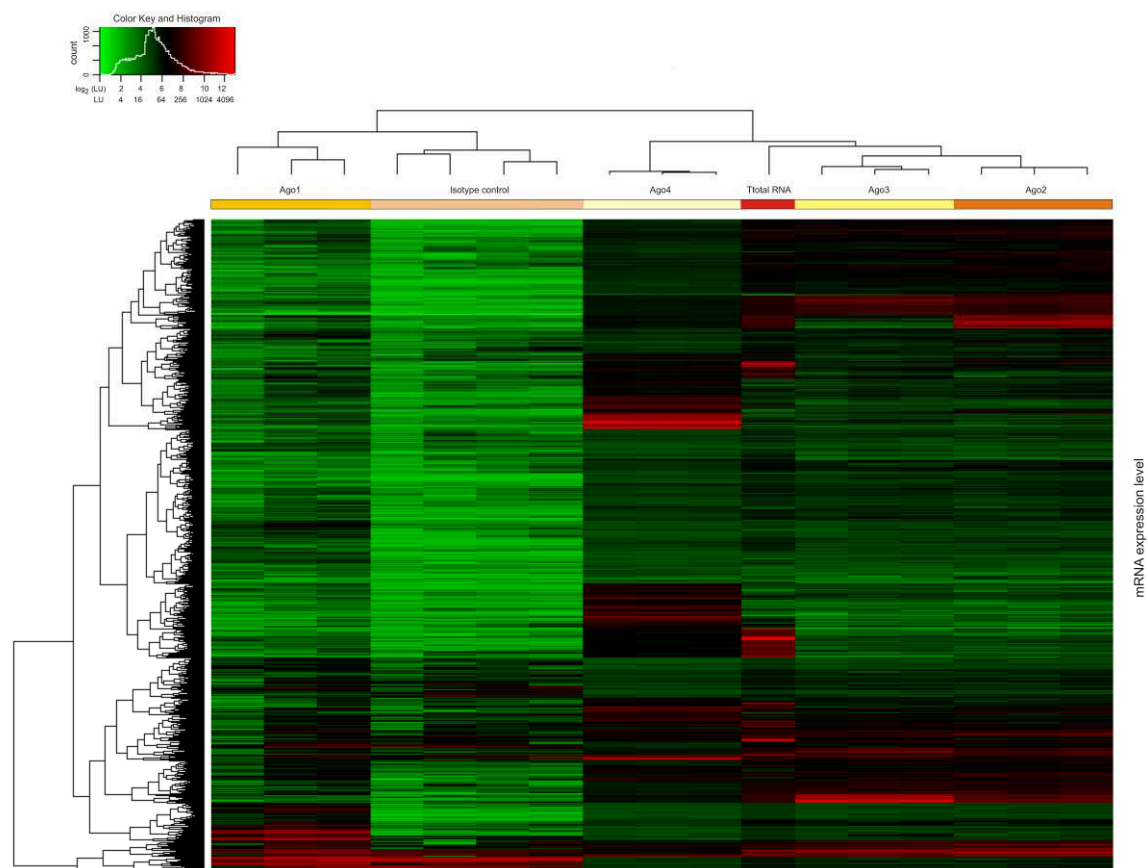
Figure 4.7.II Detection of Argonaute protein-associated mRNAs of NB4 cells. Hierarchical cluster analysis was computed, using the complete mRNA expression data of the triplicates of each Argonaute protein in comparison to the isotype controls (shown at the top). The heatmap was drawn for all significant mRNAs, identified on the basis of hierarchical clustering of all mRNAs. Significant mRNAs offer a fold change > 1.8 and a p-value < 0.05 in all replicates of the Argonaute experiments in comparison to the isotype controls.

4.8 Identification of common and Ago-specific mRNAs

In this chapter, intersection analysis was performed, to get more information about the numbers of identified Ago-associated mRNAs. The amount of common and Argonaute protein-specific mRNAs will be depicted in more detail in Figure 4.8.I.
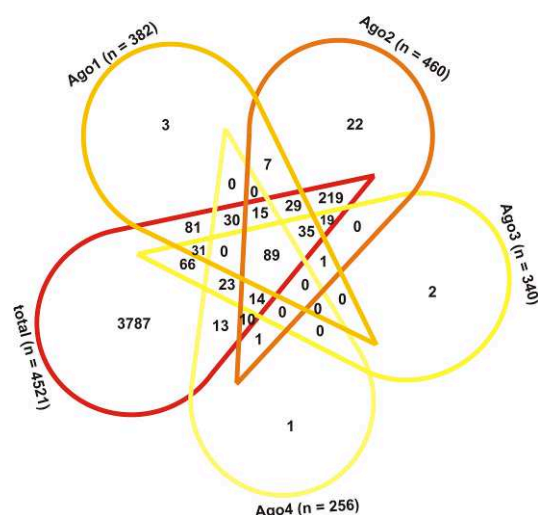
a) Ago-associated mRNAs of KASUMI-1   **b) Ago-associated mRNAs of NB4**
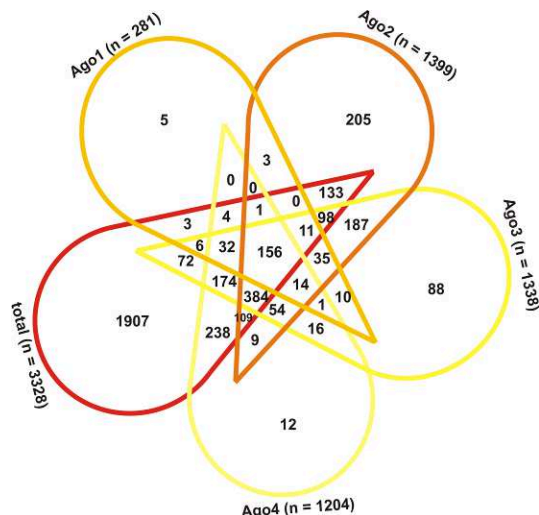
Figure 4.8.I Intersection analysis showing the relationship between significant Ago-associated mRNAs and the total RNA isolated directly from **a)** KASUMI-1 and **b)** NB4 cells. Displayed are common and Ago-specific mRNAs. The total number of RNAs is given at the outer border of each set.

With regard to the mRNAs shown in Figure 4.8.I a), only between 19% and 34.7% of 89 identified mRNAs were detected in all four human Argonaute proteins of KASUMI-1 cells, whereas up to 52.4% (Ago2) of all detected mRNAs seem to be specific for the different Argonaute proteins. In addition, the intersection analysis indicates that 16.2% (734 mRNAs) of all detected mRNAs of the total RNA were regulated by at least one Argonaute protein complex. For NB4 cells, on average 24.7% of 170 significant mRNAs were identified in all four Argonaute protein complexes, whereas up to 24.2% (338 mRNAs of Ago2) of significant mRNAs are Argonaute protein-specific (Figure 4.8.I b). Additionally, over 42.7% (1421 mRNAs) of mRNAs identified in the total RNA seem to be regulated by at least one Argonaute protein. By comparison of Ago-associated mRNAs identified in both cell lines, only 2.3% of Ago1-, 7.5% of Ago2-, 5.9% of Ago3- and 9.1% of Ago4-associated mRNAs match between KASUMI-1 and NB4 cells, whereas 65.5% of identified mRNAs of the total RNA overlap between KASUMI-1 and NB4.

Thus seen altogether, a high amount of identified mRNAs showed preferences for distinct Argonaute proteins, and therefore seem to be specific for distinct Argonaute proteins extremely changing between both cell types.

4.9 Validation of individual mRNAs provides deeper insights into microarray results

In order to validate mRNA microarrays results, a handful of mRNAs with different expression levels on the microarray were chosen for qrt-RT-PCR. The gene specific primers were located in the 3'-UTR of the mRNAs, as in the majority of cases miRNA binding occurs in the 3' region.

4.9.1 qrt-RT-PCR validation of selected Ago-associated mRNAs in KASUMI-1

Two mRNAs: *ATP6V0E1* and *PRTN3*, offering very high signal intensities between 425 and 2400 LU (by microarray hybridization), three mRNAs: *ATOX1*, *HMGA2* and *PDCD4*, possessing lower signal intensities between 45 and 1170 LU, and one mRNA: *FoxG1* holding signal intensity of approximately 5.5 LU (practically background signal intensity), were chosen for qrt-RT-PCR analysis. The corresponding expression values are summarized in Table 4.9.1.I.

Table 4.9.1.I Listing of median signal intensities (SI) of six selected mRNAs detected via microarray hybridization

Microarray SI (median of 3 replicates)	ATP6V0E1	PRTN3	ATOX1	FoxG1	HMGA2	PDCD4
Ago1	859	2122	718	6.12	282	320
isotype control	1501	5.24	160	10.6	67	337
FC: Ago1/control	0.57	404	4.5	0.58	4.2	0.95
Ago2	994	2398	302	5.72	972	1170
isotype control	1033	5.24	113	12.8	54	323
FC: Ago2/control	0.96	457	2.68	0.45	17.99	3.62
Ago3	748	1480	465	6.7	213	637
isotype control	79	144	54	108	103	103
FC: Ago3/control	9.4	10.29	8.65	0.06	2.07	6.17
Ago4	446	425	232	5.63	45.2	394
isotype control	137	140	13.8	3.35	5.96	138
FC: Ago4/control	3.25	3.03	16.76	1.68	7.59	2.86

For validation of selected mRNAs, it is more difficult to reach purity as shown for miRNAs, since mRNAs are not as strongly joined to the Argonaute protein complexes as miRNAs. Therefore, it is logical to detect more false-positive mRNAs, which have to be filtered out using the isotype controls and the empty beads.

Figure 4.9.1.I displays the expression levels of *ATP6V0E1, PRTN3, ATOX1, FoxG1, HMGA2* and *PDCD4,* and Table 4.9.1.II shows the fold changes of RNA expression between Argonaute, isotype controls and empty beads as result of qrt-RT-PCR. The highest amount of all tested mRNAs could be associated with Ago2 as previously shown for the miRNAs in Figure 4.6.1.I. A reason could be the predominant appearance of Ago2 in the AML cells, because of its important slicing function. The mRNAs *ATP6V0E1* and *PRTN3* represent the highest expression of all tested mRNAs, supporting the microarray results by use of qrt-RT-PCR. The mRNAs *ATOX1* and *PDCD4* were detected with low expression values, but with a fold change between 1.5 and 83 by comparison of Argonaute and

isotype control detected mRNAs. The expression of *FoxG1* is 34 fold higher in Ago3, and the expression of *HMGA2* is 6.8 and 20.8 fold higher in Ago2 and Ago4, respectively, in comparison to the isotype control. Probably, *FoxG1* offers an increased association with Ago3, whereas *HMGA2* possesses a stronger connection to Ago2 and Ago4. These issues will be supported by microarray results for *HMGA2,* but unfortunately not for *FoxG1*.
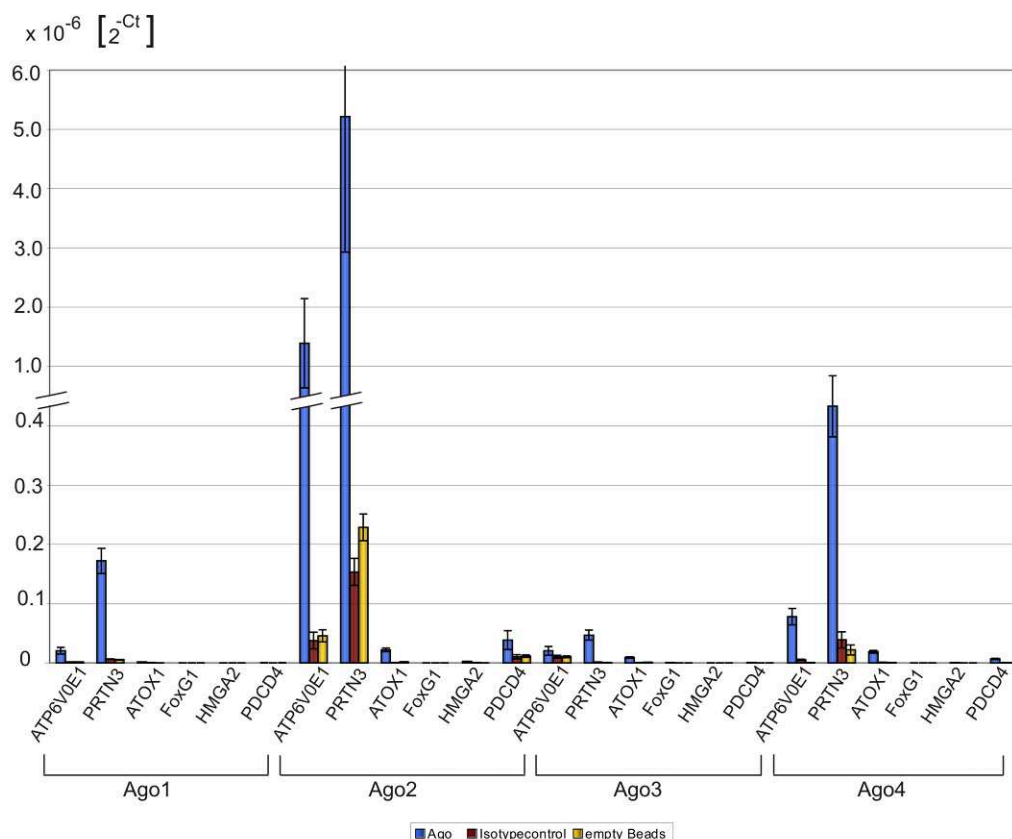
Figure 4.9.1.I Displayed are expression levels of six selected mRNAs associated with the four human Argonaute protein complexes. According to microarray data, the mRNAs *ATP6V0E1, PRTN3, ATOX1, FoxG1, HMGA2* and *PDCD4* were chosen, covering the whole range from low to high expression according to microarray hybridization.

Table 4.9.1.II Listing of median fold change (FC) of six selected mRNAs
detected via qrt-RT-PCR in KASUMI-1, n.a. = not available

RT-PCR FC (median of 3 replicates)	ATP6V0E1	PRTN3	ATOX1	FoxG1	HMGA2	PDCD4
Ago1/isotype control	15.4	28.4	4.5	0.6	n.a.	1.5
Ago1/empty beads	14.7	34.2	8.3	1.3	0.8	1
Ago2/isotype control	37	33.9	83	0.4	6.8	3.7
Ago2/empty beads	30.5	22.8	15.1	0.8	29.8	3.4
Ago3/isotype control	1.9	37.5	16.2	34	0.9	9
Ago3/empty beads	1.9	85.6	10.5	44.6	1.9	2.3
Ago4/isotype control	14.9	11.2	24.2	2.6	20.8	12
Ago4/empty beads	170.6	19.8	68.8	0.7	26.8	32.2

Altogether, microarray results could be validated with higher sensitivity by using qrt-RT-PCR. It is difficult to compare analyzed mRNAs among each other, because of the different binding efficiencies of gene-specific primers. Therefore, validation of mRNAs using qrt-RT-PCR could be used rather for verification of microarray results with regard to expression size and purity of individual RNAs.

4.9.2 qrt-RT-PCR validation of selected Ago-associated mRNAs in NB4

Table 4.9.2.I lists signal intensities and FCs of six mRNAs, which were chosen based on their expression level. Two mRNAs, *ATP6V0E1* and *ATOX1,* possessing high signal intensities between 81 and 1057 LU and four mRNAs, *ARL2, PRTN3, HMGA2* and *PDCD4*, offering low to moderate signal intensities between 4 and 186 LU on the microarray, were selected for qrt-RT-PCR validation.

Table 4.9.2.I Listing of median signal intensities (SI) of six selected mRNAs detected
via microarray hybridization

Microarray SI (median of 3 replicates)	ARL2	PRTN3	ATP6V0E1	ATOX1	HMGA2	PDCD4
Ago1	27	5.38	276	81.5	21	8.33
isotype control	4.9	109	145	5.5	6	3
FC: Ago1/control	5.49	0.049	1.9	14.9	3.5	2.77
Ago2	186	32.95	1057	294	85.9	11.04
isotype control	3.6	36	45.7	7	23.3	62.4
FC: Ago2/control	43	0.9	21.3	41.8	4.57	0.25
Ago3	67	7.08	417	133	27.9	8.4
isotype control	4	2.77	360	49.3	3	3.6
FC: Ago3/control	16.5	2.56	1.16	2.7	9.4	2.34
Ago4	53.6	4.14	310	138	19.7	12.42
isotype control	4.2	49.6	184	20.6	10.8	23
FC: Ago4/control	3.25	3.03	16.76	1.68	7.59	2.86

Figure 4.9.2.I illustrates the expression sizes of *ARL2, PRTN3, ATP6V0E1, ATOX1, HMGA2* and *PDCD4*. Among Ago1-3 isolated RNAs, the mRNA *ATP6V0E1* shows the highest expression expected of the microarray results, whereas *ATOX1* associates mostly with Ago4. *PRTN3* shows highest expression in association with Ago2, which concurs with the microarray result, just as the predominant association of *ARL2* with Ago2, 3 and 4. Moreover, the mRNAs *HMGA2* and *PDCD4,* whose signal intensities detected on the microarray predominantly disappear in the background (SI < 30), were also measured with very low expression values by qrt-RT-PCR.
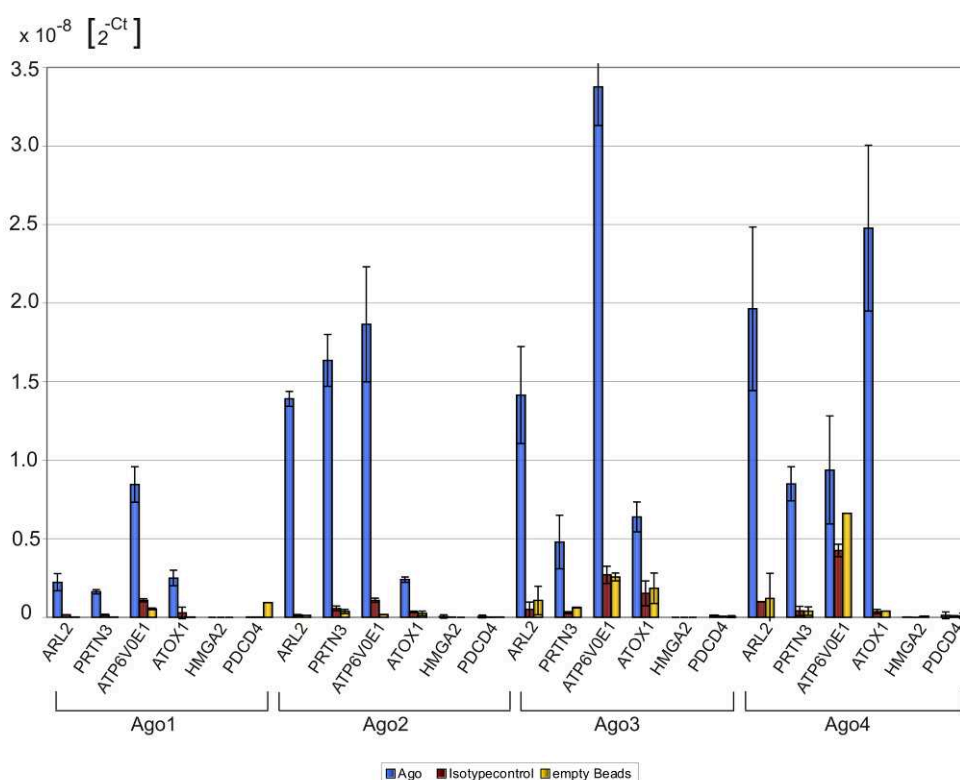
Figure 4.9.2.I Displayed are expression levels of six selected mRNAs associated with the four human Argonaute protein complexes. According to microarray data, the mRNAs, *ARL2, PRTN3, ATP6V9E1, ATOX1, HMGA2* and *PDCD4,* were chosen, covering the whole range from low to high expression.

Table 4.9.2.II Listing of median fold change (FC) of six selected mRNAs
detected via qrt-RT-PCR in NB4, n.a. = not available

RT-PCR FC (median of 3 replicates)	ARL2	PRTN3	ATP6V0E1	ATOX1	HMGA2	PDCD4
Ago1/isotype control	13.4	10.2	7.7	8.9	1	1.2
Ago1/empty beads	132.2	102.8	15.5	239.9	1	1.2
Ago2/isotype control	97.4	29	17.2	6.9	5.5	3.4
Ago2/empty beads	114.2	43.9	104.7	9.6	6.1	2.6
Ago3/isotype control	28.3	16.5	12.4	4.2	1	2.6
Ago3/empty beads	13.2	7.7	13.1	3.4	1	2.4
Ago4/isotype control	19.7	21	2.2	67.3	n.a.	n.a.
Ago4/empty beads	16.4	21.5	1.4	61.8	n.a.	n.a.

Overall, by comparison of microarray and qrt-RT-PCR results, it becomes apparent that the validation of some microarray data is very important, because of higher accuracy of the PCR. Most of the microarray results accord with the output of the PCR by trend. Therefore, the microarray results could be emphasized by qrt-RT-PCR, and the purity of immunoprecipitation, using isotype controls and empty beads could be proved with more sensitivity.

4.10 Target predictions reveal binding sites between Ago-associated miRNAs and mRNAs

It is assumed that about 20-30% of human genes are under miRNA control, and it was shown that the expression or repression of specific miRNAs can benefit different cancer types (Shi *et al.*, 2008). In comparison, 16.2% and 42.7% of detected mRNAs of the total RNA of KASUMI-1 and NB4 cells, respectively, seem to be regulated by at least one Argonaute protein.

As the molecular biology of the whole miRNA network, and how miRNAs suppress gene expression, is not fully understood, more and more prediction algorithms were developed for miRNA prediction of binding sites for mRNAs. Putative miRNA binding sites with mRNAs, associated with human Argonaute proteins, were identified using different target prediction algorithms, implemented in TargetScan, PicTar and miRanda.

In total RNA of KASUMI-1 cells, 105 miRNAs and 4521 mRNAs were identified. Using three target prediction tools (TargetScan, PicTar and miRanda), tens of thousands of target predictions could be made for the given miRNAs with only 14.7-35% overlap between any two prediction outputs. A similar result could be observed by using only the given mRNAs for prediction because the overlap between any two prediction-outputs accounts for only 4-21.2%. Therefore, it is necessary to incorporate both the identified miRNAs and mRNAs into the same target prediction. Thereby, 86.7% of expressed miRNAs were predicted to offer binding sites for 85.5% expressed mRNAs, with 31.6-47.5% overlap between any two of the three target prediction results. The same prediction analysis was performed for miRNAs and mRNAs identified within the total RNA of NB4 cells. For this cell line, 105 miRNAs and 3328 mRNAs were identified as significant. According to the target prediction, 85.7% and 84.9% of expressed miRNAs and mRNAs, respectively, possess connections to each other with an overlap of 29-46.5% between at least two prediction algorithms.

In comparison to the prediction analysis of total RNA, the target prediction of Argonaute-associated miRNAs and mRNAs is most interesting. In KASUMI-1 cells, for even 96.7% -100% of Ago1-4-associated miRNAs, binding sites for 49% to 82.6% of Ago1-4-associated mRNAs were predicted with an overlap between 20.8% and 57% of at least two target prediction algorithms (Supplement Table V.7). In NB4 cells, the prediction outcome looks a bit different. With an overlap between 26.6% and 53.6% of the results of any two prediction algorithms, 86.9% - 96% of Ago1-4-associated miRNAs could be predicted to offer binding sites for 69% - 85.6% of Ago1-4-associated mRNAs (Supplement Table V.8). Hence, it is possible that some target-mRNAs were predicted by mistake, and mRNAs, for which no miRNA binding site could be predicted will maybe regulated by miRNA binding in the 5'-UTR or in the coding sequence (CDS).

4.11 GO term classification of detected targets provides insights into molecular function and biological process regulation in AML

The target prediction analyses afford an overview of miRNA functionality by finding target-mRNAs, but up to now, the very long ID lists of Ago-associated miRNAs and mRNAs were only analyzed globally. Therefore, the Gene Ontology (GO) was used to arrange the Ago-associated mRNAs (genes) into functional groups. The GO database is divided into three different ontologies, called "Molecular Function", "Cellular Component" and "Biological Process". The structure of the database is a directed acyclic graph (DAG). A set of genes is annotated for each node (GO term), whereby the root is the most unspecific GO term. Its set of genes consists of every gene in the database and the leaves are the most specific GO terms. In order to figure out, which GO terms are most abundant within the given gene or mRNA lists, GO term enrichment was calculated using the hypergeometric distribution, implemented in GOEAST (Gene Ontology Enrichment Analysis Software Toolkit).

Figure 4.11.I and Figure 4.11.II represent enriched GO terms of the superior categories "Molecular Function" and "Biological Process" of KASUMI-1 and NB4 cells (Supplement Table V.9 and Table V.10). Most of these GO terms were identified among Argonaute-associated mRNAs in comparison to the total RNA of both cell lines. GO terms with higher enrichment in the total RNA or a p-value > 0.05 were discarded, as these GO terms are not predominantly regulated by miRNAs. For KASUMI-1, GO terms of the categories Binding, Transporter -, Catalytic -, Structural Molecule -, Translation Regulator - and Antioxidant activity has been identified as overrepresented in at least one Argonaute protein. Amongst others, the MAPK phosphatase activity seems to be regulated by Ago2 only, in the category "Molecular Function". Mitogen-activated protein kinases (MAPK) are very important, because they present a family of protein kinases that perform a crucial step in relaying signals from the plasma membrane to the nucleus. They are activated by a wide range of proliferation- or differentiation-inducing signals. With regard to the "Biological Process", only Ago2 appears to be involved in the negative regulation of different kinases, including the MAPK kinase activity. Another important GO term, called "Induction of apoptosis by p53" was enriched in Ago1 only. A process that directly activates any of the steps required for cell death by apoptosis. This is also intuitive since miRNAs act as negative regulators and p53 mediated apoptosis might be damped by miRNAs.
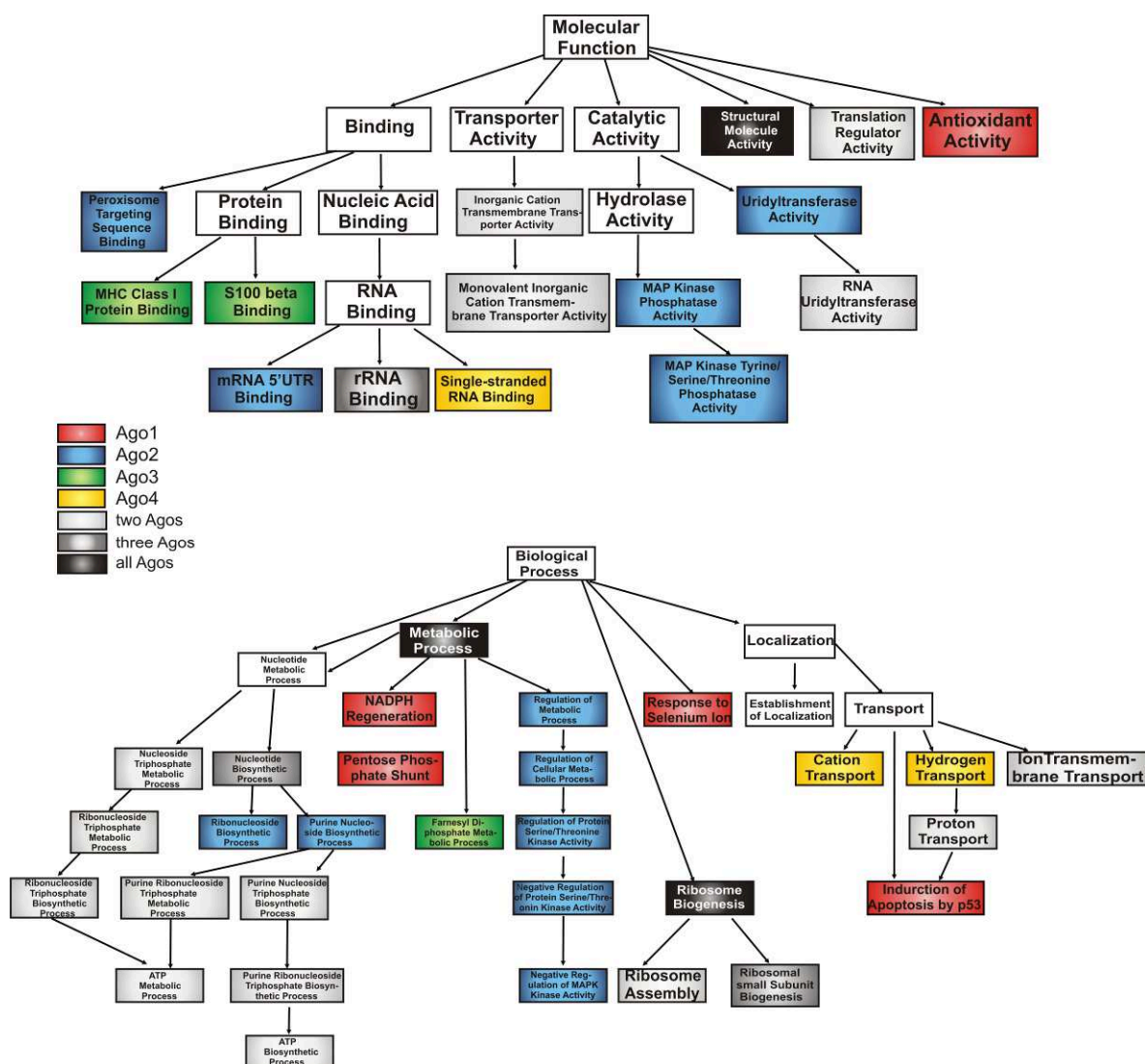
Figure 4.11.I GO (Gene Ontology) term enrichment calculations of the categories "Molecular Function" and "Biological Process", showing overrepresented (p-value < 0.05), Ago-associated GO terms in comparison to the total RNA of KASUMI-1 cells. GO terms marked in red are overrepresented in Ago1, GO terms marked in blue, green and yellow are overrepresented in Ago2, Ago3 and Ago4, respectively. GO terms overrepresented in at least two, in at least three and in all four Argonaute proteins were labeled in light grey, dark grey and black, respectively. White labeled GO terms, which were not identified as enriched in the Argonaute proteins or only enriched in the total RNA, are depicted to clarify the connections between the GO terms, because not all GO terms are represented.

With regard to the superior category "Molecular Function" in NB4 cells, GO terms of the categories Binding, Transporter -, Catalytic -and Transferase activity were identified as enriched in at least one Argonaute protein, in contrast to the total RNA. Among these GO terms, the MAPK binding seems to be regulated only by Ago1, showing that there is an interaction between Ago1 and the MAP kinase. Furthermore, the GO term Transcription factor binding has been identified as enriched in Ago4. With respect to the superior category "Biological Process" parts of the GO terms Biological regulation, Cellular -and Metabolic process, Transport and Localization are enriched in at least one Argonaute protein. Among these GO terms, the transcription appears to be regulated by at least two Argonaute proteins. More precisely, the negative regulation of gene expression and the gene silencing seem to be regulated by Ago2 and Ago4, respectively, which include any process that decreases the frequency rate or extent of gene expression.
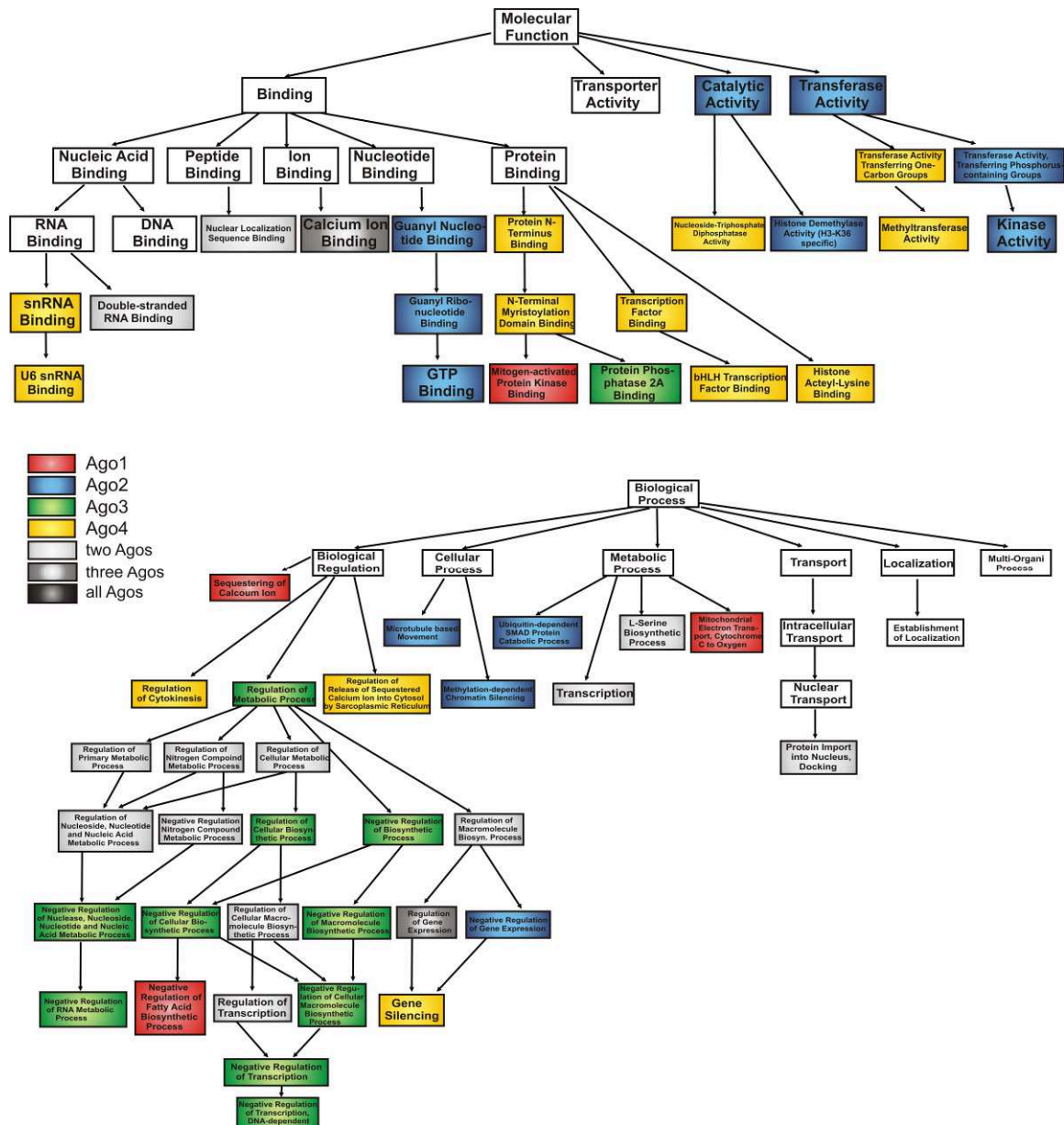
Figure 4.11.II GO (Gene Ontology) term enrichment calculations of the categories "Molecular Function" and "Biological Process", showing overrepresented (p-value < 0.05), Ago-associated GO terms in comparison to the total RNA of NB4 cells. Terms marked in red are overrepresented in Ago1, GO terms marked in blue, green and yellow are overrepresented in Ago2, Ago3 and Ago4, respectively. GO terms overrepresented in at least two, in at least three and in all four Argonaute proteins were labeled in light grey, dark grey and black, respectively. White labeled GO terms, which were not identified as enriched in the Argonaute proteins or only enriched in the total RNA are depicted to clarify the connections between the GO terms, because not all GO terms are represented.

4.12 Pathway classification of detected targets indicates concerted action of human Argonaute proteins in AML

4.12.1 Most identified KEGG pathways were detected in all human Argonaute proteins

The GO term enrichment analysis represents a first overview, showing the functions and processes, in which the Ago-associated mRNAs (genes) are involved. To get more information about the organization of these mRNAs and the pathways regulated by miRNAs, KEGG (Kyoto Encyclopedia of Genes and Genomes) pathway analyses were performed. For this purpose, Ago-associated mRNAs were classified into pathways, using the KEGG database, which provides a sorting of genes into over 380 different biological pathways. Each gene and each pathway offer KEGG identifiers. To get a first overview, all identified KEGG pathways were depicted as hierarchical clustering, together with the corresponding heatmap. Figure 4.12.1.I and Figure 4.12.1.II represent the analyses for Ago-associated mRNAs detected in KASUMI-1 and NB4 cells, respectively (Supplement Table V.11 and Table V.12).

Figure 4.12.1.I Hierarchical cluster analysis of Ago-associated mRNAs of KASUMI-1 cells classified into KEGG pathways. According to the color key top left, KEGG pathways with high expression are depicted in red, and KEGG pathways with low expression levels are illustrated in green. Undetected KEGG pathways are shown in dark grey. The Ago-associated mRNAs could be classified into 104 different pathways. Additionally, the identified pathways were classified into superior pathway categories like metabolism or transduction (see right).

After classification of Ago-associated mRNAs into 104 different KEGG pathways, the signal intensities of transcripts belonging to one pathway, were mean centered and depicted as hierarchical clustering. This analysis of Figure 4.12.1.I illustrates that the four human Argonaute proteins can still be

distinguished from each other, as it could be shown for the single mRNAs. With regard to the corresponding heatmap, it is striking that most pathways could be detected for almost all Argonaute proteins. For example, 12 pathways with the highest signal intensities up to 4,200 LU (average of the involved mRNAs) could be detected in all Argonaute protein complexes. Among these pathways, 4 can be classified into metabolic pathways, 2 into signaling pathways, and 5 pathways are important for homeostasis and cell survival like oxidative phosphorylation, glycolysis/gluconeogenesis, ribosome and phagosome. The remaining two pathways with highest expression are hematopoietic cell lineage and acute myeloid leukemia. For Ago2, additionally 12 other pathways like the mTOR -, p53 -, Jak-STAT - and TGF-β signaling pathways, possessing high signal intensities, could be identified as well. The identified mRNAs out of the total RNA were also analyzed using KEGG pathway classification. These pathways offer lower expression levels in contrast to the pathways identified among the Ago-associated transcripts, suggesting an enrichment of pathways derived from Ago-associated mRNAs.

Figure 4.12.1.II Hierarchical cluster analysis of Ago-associated mRNAs of NB4 cells classified into KEGG pathways. According to the color key top left, KEGG pathways with high expression are depicted in red and KEGG pathways with low expression levels are illustrated in green. Undetected KEGG pathways are shown in dark grey. The Ago-associated mRNAs could be classified into 150 different pathways. Additionally, the identified pathways were classified into superior pathway categories like metabolism or transduction (see right).

Ago-associated mRNAs of NB4 cells were also classified into KEGG pathways (Figure 4.12.1.II). For NB4, more Ago-associated mRNAs were identified, and these mRNAs could be classified into much more (up to 150 different) KEGG pathways. Although, a high amount of KEGG pathways with similar expression values can be identified in all human Argonaute proteins, these proteins could be separated from each other as depicted by the hierarchical cluster analysis above. Overall, the

expression level of NB4 detected KEGG pathways is not as high as the expression values of KEGG pathways found among Ago-associated mRNAs of KASUMI-1 cells. Here, the most abundant KEGG pathways containing mRNAs with very high expression values are mTOR -, VEGF – and Wnt signaling pathways.

a) Ago-associated pathways of KASUMI-1   **b) Ago-associated pathways of NB4**
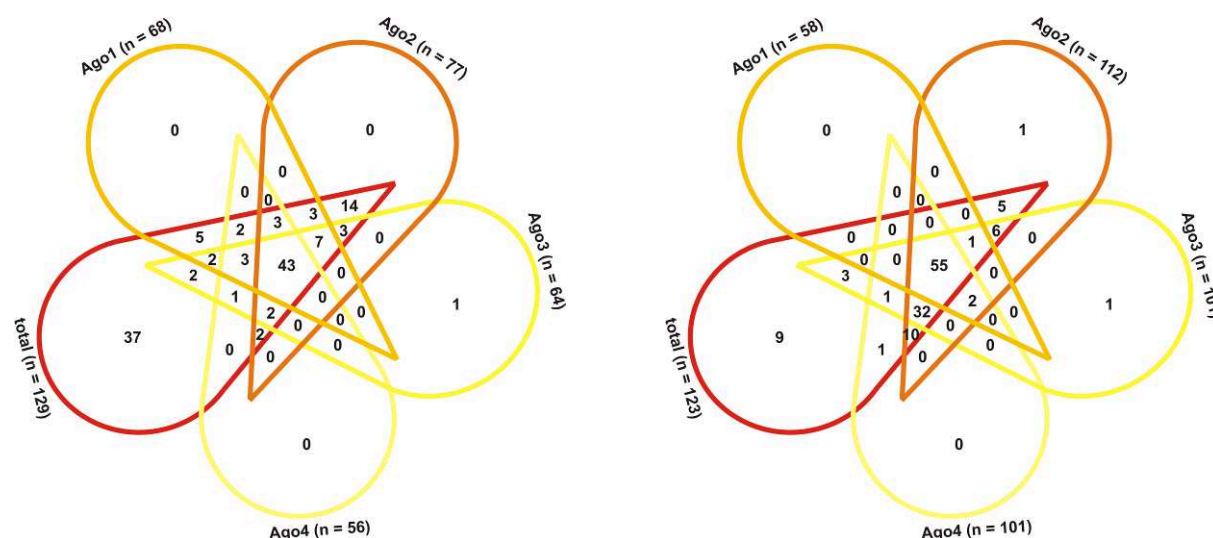
Figure 4.12.1.III Intersection analysis of KEGG pathways identified by pathway classification of Argonaute-associated mRNAs detected in **a)** KASUMI-1 and **b)** NB4 cells.

To better investigate the overlap and distinctness of detected Ago-associated KEGG pathways of KASUMI-1 and NB4 cells, an intersection analysis was performed for all human Argonaute proteins and the total RNA (Figure 4.12.1.III). An overlap of 55.8% - 76.8% (43 of KASUMI-1) and 49.1% - 94.8% (55 of NB4) of KEGG pathways can be linked to all human Argonaute proteins, whereas only 25.9% and 24.7% of Ago-associated mRNAs in KASUMI-1 and NB4 cells, respectively, could be identified in all four proteins.

4.12.2 Finding most enriched KEGG pathways with highest signal intensity

Besides the knowledge about pathways with highest signal intensity, it is also important to identify the most enriched pathways. Overrepresented KEGG pathways, enriched within the Ago-associated mRNAs were detected by hypergeometric distribution calculations. Thereby, the enrichment calculation is based on the whole set of over 42,500 human genes probed on the mRNA microarray, and the computed p-value denotes the reliability of the pathway enrichment calculations. The smaller the p-value, the higher is the probability that the resulted pathways are enriched in fact. To get an impression of the complexity of the KEGG pathway network, the most enriched pathways, associated with the four human Argonaute proteins, were visualized in Figure 4.12.2.I for KASUMI-1 and Figure 4.12.2.II for NB4 together with the identified Ago-associated miRNAs.
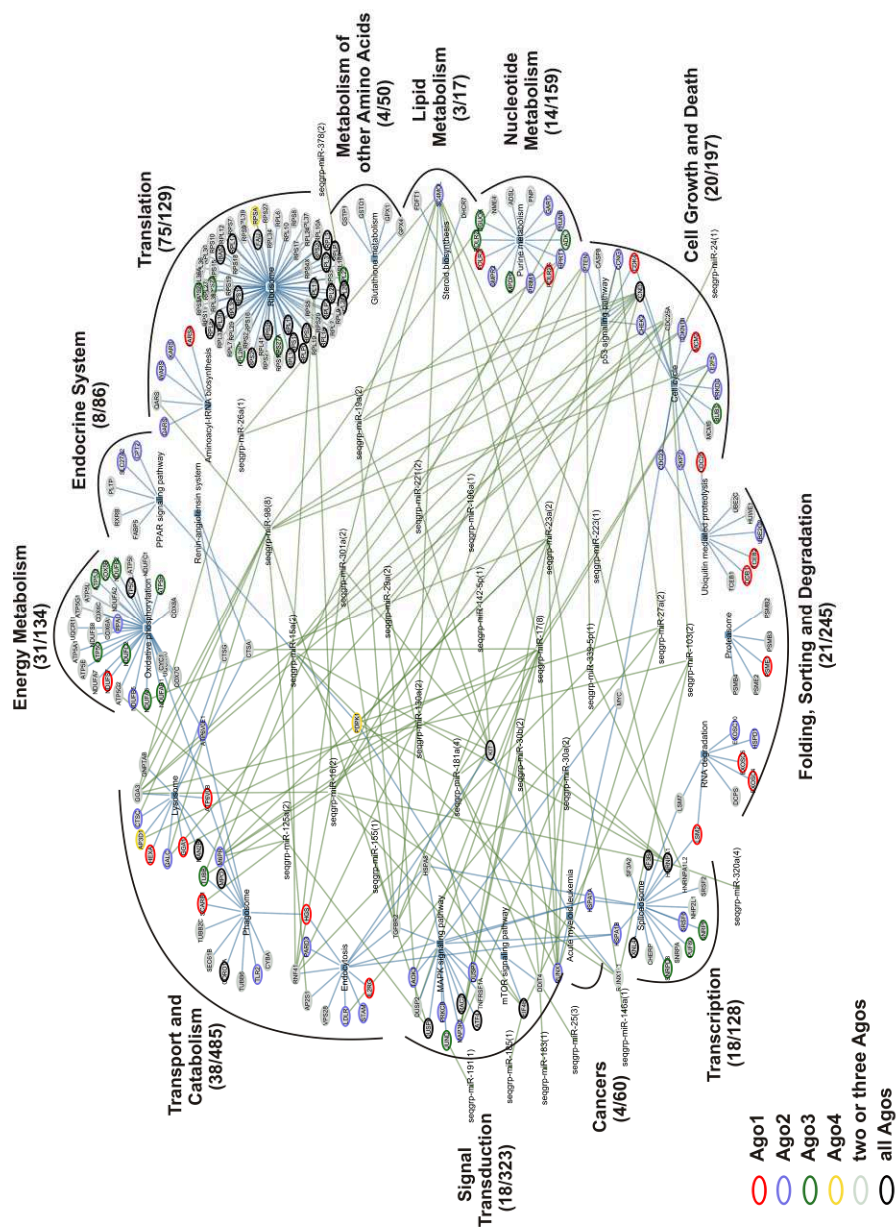
Figure 4.12.2.I KASUMI-1 network visualization of most enriched KEGG pathways. Blue edges indicate connections between KEGG pathways and Ago-associated transcripts. Green edges demonstrate connections between Ago-associated miRNAs and their regulatory target mRNAs. The target prediction is based on at least two different prediction algorithms. miRNAs possessing the same seed sequence (and therefore could bind to the same mRNAs) were classified into sequence groups (seqgrp) to reduce the complexity of the network graph. The individual genes (mRNAs) were color-coded according to their Argonaute protein association. Transcripts identified only in Ago1 were colored in red, only in Ago2 in blue, only in Ago3 in green and only in Ago4 in yellow. Transcripts which could be detected in two or three Argonaute proteins were colored in grey and transcripts found in all four Argonaute proteins were marked in black. In addition, the single pathways were classified into superior metabolic pathway categories. The numbers below the superior categories denote the number of identified genes (mRNAs) x of all genes (mRNAs) y belonging to the category (x/y).
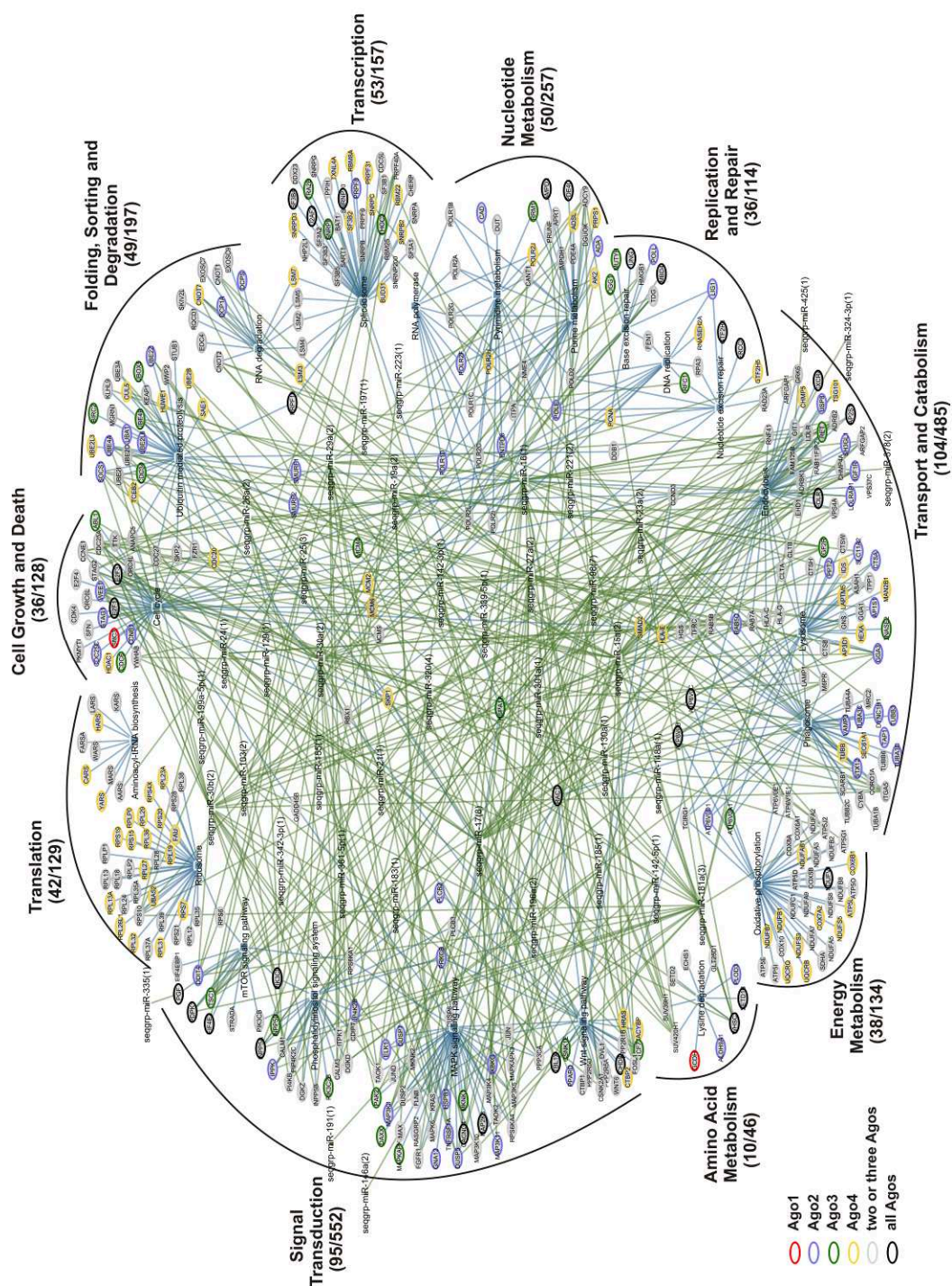
Figure 4.12.2.II NB4 network visualization of most enriched KEGG pathways. Blue edges indicate connections between KEGG pathways and Ago-associated transcripts. Green edges demonstrate connections between Ago-associated miRNAs and their regulatory target mRNAs. The individual genes (mRNAs) were color-coded according to their Argonaute protein association. For complete legend please refer to Figure 4.12.2.I.

The KEGG pathway networks, shown in Figure 4.12.2.I and Figure 4.12.2.II, were visualized, using the EGAN (Exploratory Gene Association Networks) software. By the use of EGAN, it was possible to combine significant mRNAs, identified in the four Argonaute proteins into one network. The top ten only of most enriched KEGG pathways of Ago1-4 were depicted, because of the high complexity. Furthermore, the detected miRNAs in association with the four Argonaute proteins were visualized, to clarify the interactions between the Argonaute proteins, their associated miRNAs and their target-mRNAs. Overall, 338 (42.1%) out of 802 different mRNAs identified in at least one Argonaute protein of KASUMI-1 cells and 701 (35.8%) out of 1960 Ago-associated genes of NB4, could be classified into KEGG pathways. In the corresponding network, each of these genes is color-coded according to their association with the Argonaute proteins (see legend). In the KASUMI-1 KEGG pathway network, Ago1, Ago2 and Ago3 seem to be predominant regulators, because a high amount of transcripts were associated with one of these Argonaute proteins, whereas Ago4 could be associated with only a few genes. Figure 4.12.2.II shows that in NB4 cells mainly Ago2 and Ago4, respectively, seem to regulate most transcripts, whereas Ago1 and Ago3 seem to play a secondary role.

Altogether, both networks clarify that even the presentation of only the most enriched KEGG pathways leads to a very complex and complicated graph, where it is hard to follow all edges of the pathways. Therefore, the KEGG pathways, which are overrepresented and offer the highest signal intensity, due to the high expression of genes, involved in these pathways, were filtered out.

To get more detailed information about significant KEGG pathways, discovered within the large amount of Ago-associated mRNAs in KASUMI-1 cells, the top 20 pathways, offering the highest signal intensity, were listed in Table 4.12.2.I for each Argonaute protein. Genes encoding the ribosome, phagosome, lysosome, spliceosome, cell cycle and a lot of metabolic pathways show very high signal intensities in the four Argonaute proteins. Moreover, different signaling pathways like mTOR, MAPK, Wnt and VEGF were detected under the top 20 pathways with highest signal intensity in at least two Argonaute proteins. Interestingly, the AML pathway belongs to the top 20 pathways as well and can be identified for each Argonaute protein. Besides the analysis of pathways with highest signal intensity, it is also important to determine the number of genes involved in the KEGG pathways. For further analysis, an enrichment calculation was performed, to identify overrepresented pathways within the Ago-associated mRNAs. Metabolic pathways, pathways for translation (ribosome), transport and catabolism (phagosome, lysosome, endocytosis and so on), do not show high signal intensities only, they also belong to the top 20 of most enriched pathways, listed in Table 4.12.2.II. In addition, the AML together with the mTOR and MAPK signaling pathways also appear under the top 20 of most enriched KEGG pathways in at least two Argonaute proteins. Only for Ago1, none of these signaling pathways reveal such a high enrichment, but nevertheless they are the most promising pathways to learn more about regulatory mechanisms in AML. The same calculations were performed for Ago-associated mRNAs in NB4 cells. Among the pathways important for cell growth, cell survival and genetic information processing, the signaling pathways mTOR and VEGF appear under the top 20 pathways with highest signal intensity, detected in at least three Argonaute proteins (Table 4.12.2.III). Additionally, in Ago4, the signaling pathways Wnt and MAPK only, were identified with highest signal intensity as well. As seen for KASUMI-1, the NB4 pathways, which are important for cell growth and

genetic information processing including transcription and translation offering the highest signal intensity and enrichment within the top 20 pathways (Table 4.12.2.IV). It is noticeable that a lot of signaling pathways like mTOR, VEGF, Wnt, MAPK, p53 and the phosphatidylinositol signaling system are mostly under the top 20 pathways, whereby the mTOR signaling pathway is enriched in Ago1 and Ago3, and the VEGF signaling pathway shows no enrichment. On the other hand, the Wnt and MAPK signaling pathways, offering high signal intensities in association with Ago4 only, belong to the most enriched pathways of Ago1, Ago2 and Ago3. Therefore, the signaling pathways mTOR, Wnt and MAPK, possessing a close relation to AML and to each other, are the most auspicious pathways for studying associations between APL and the pathway regulation by Argonaute proteins.

Table 4.12.2.I The top 20 KEGG pathways offering the highest **signal intensity** (SI) shown for KASUMI-1. Abbreviations: Amino. tRNA bio. - Aminoacyl-tRNA biosynthesis; AML - Acute myeloid leukemia; Arach. acid m. - Arachidonic acid metabolism; Base ex. rep. - Base excision repair; Calcium s.p. - Calcium signaling pathway; Chemokine s.p. - Chemokine signaling pathway; Cys. met. m. - Cysteine and methionine metabolism; Cyto.cyto.rec. inter. - Cytokinx10-cytokine receptor interaction; Glutathione m. - Glutathione metabolism; Gly./Gluc. - Glycolysis/ Gluconeogenesis; Glyoxy. dicarboxy. m. - Glyoxylate and dicarboxylate metabolism; GnRH s.p. - GnRH signaling pathway; Hemato. cell I. - Hematopoietic cell lineage; Jak-STAT s.p. - Jak-STAT signaling pathway; Leuko.trans.mig. - Leukocyte transendothelial migration; MAPK s.p. - MAPK signaling pathway; mTOR s. p. - mTOR signaling pathway; Nitrogen m. - Nitrogen metabolism; One carbon pbf - One carbon pool by folate; Oxi. phos. - Oxidative phosphorylation; Propa. m. - Propanoate metabolism; Protein pro. in ER - Protein processing in endoplasmic reticulum; Pyru. m. - Pyruvate metabolism; Reg. act. cyto. - Regulation of actin cytoskeleton; RNA deg. - RNA degradation; Selen. acid m. - Selenoamino acid metabolism; SNARE inter.ivt - SNARE interactions in vesicular transport; Tyrosine m. - Tyrosine metabolism; Ubi. med. prot. - Ubiquitin mediated proteolysis; VEGF s.p. - VEGF signaling pathway; Wnt s.p. - Wnt signaling pathway

Total	SI	Aqo1	SI	SI	SI	Aqo2	SI	SI	SI	Aqo3	SI	SI	SI	Aqo4	SI	SI	SI
Ribosome	3609	Ribosome	4681	4942	5157	Ribosome	4340	4446	4393	Ribosome	4732	4589	4832	Ubi. med. prot.	5983	6588	6953
Arach. acid m.	516	GnRH s p.	1460	1435	1445	Gly. / Gluc.	2525	2905	2715	Ubi. med. prot.	2646	2193	2437	Ribosome	3556	4755	4779
Gly. / Gluc.	505	Pyru. m.	1374	2200	2268	Propa. m.	2525	2905	2715	Gly. / Gluc.	1760	2309	1567	Gly. / Gluc.	1523	1683	1425
Oxi. phos.	457	Gly. / Gluc.	1374	2200	2268	Glyoxy. dicarboxy. m.	2221	1863	2042	Propa. m.	1760	2309	1567	Propa. m.	1523	1683	1425
Cys. and meth. m.	417	Propanoate m.	1374	2200	2268	Base ex. rep.	2168	2523	2346	Pyru. m.	1760	2309	1567	Pyru. m.	1523	1683	1425
Pyru. m.	398	Phagosome	1305	1243	1277	AML	1747	1562	1654	Cys. meth. m.	1531	1460	1495	Cys. meth. m.	1523	1683	1425
Propa. m.	362	SNARE inter. ivt	1298	1203	1197	Oxi. phos.	1339	1338	1339	GnRH s. p.	1265	1324	1436	Phagosome	1411	1650	1524
Phagosome	347	Adherens junction	1172	849	924	Pyru. m.	1301	1505	1403	Phagosome	944	998	968	GnRH s. p.	992	1347	1438
One carbon pbf	346	VEGF s. p.	1172	849	924	Amino.-tRNA bio.	1245	1233	1239	Gap junction	933	1031	977	Oxi. phos.	914	984	1012
Gap junction	345	Axon guidance	117	849	924	Phagosome	1242	1326	1284	Oxi. phos.	845	793	746	Endocytosis	836	1077	958
mTOR s. p.	336	AML	1074	1087	1125	One carbon pbf	1198	1032	1115	AML	825	748	588	Axon guidance	778	809	880
Protein export	306	Protein pro. in ER	903	947	1018	Selen. acid m.	1177	1207	1192	Tight junction	807	819	830	VEGF s. p.	778	809	880
Nitrogen m.	303	Oxi. phos.	863	946	976	Jak-STAT s. p.	1140	1086	1113	Spliceosome	751	761	758	Leuko trans mig	778	809	880
Glyoxy. dicarboxy. m.	286	Cys. meth. m.	835	1352	1407	mTOR s. p.	1012	1103	1058	Prot. pro. in ER	704	812	693	Adherens junction	689	905	917
Adherens junction	283	Glutathione m.	771	954	1021	Cyto-cyto rec inter	985	913	949	Calcium s. p.	647	682	634	SNARE inter ivt	666	771	845
Glutathione m.	264	Reg. act. cyto.	733	683	682	Cys meth m.	910	1042	976	Endocytosis	645	658	761	MAPK s. p.	627	926	886
Tight junction	260	Gap junction	691	880	872	GnRH s. p.	864	1046	955	Lysosome	640	541	699	Prot. pro. in ER	581	719	720
Reg. act. cyto.	248	Hemato. cell I.	653	616	643	Cell cycle	779	728	754	SNARE inter ivt	626	862	899	Reg. act. cyto.	565	713	674
Tyrosine m.	246	MAPK s. p.	647	628	650	RNA deg.	757	752	754	Axon guidance	626	862	899	AML	532	564	616
Amino.-tRNA bio.	241	Chemokine s. p.	616	473	505	Protein pro in ER	729	872	800	VEGF s. p.	626	862	899	Wnt s. p.			

Table 4.12.2.II The top 20 KEGG pathways offering the highest **enrichment** shown for KASUMI-1. Abbreviations: Amino.-tRNA bio. - Aminoacyl-tRNA biosynthesis; AML - Acute myeloid leukemia; Arach. acid m. - Arachidonic acid metabolism; Cyano. acid m. - Cyanoamino acid metabolism; Cys. meth. m. - Cysteine and methionine metabolism; DNA rep. - DNA replication; Fatty acid e.i.m. - Fatty acid elongation in mitochondria; Guta. m. - Glutathione metabolism; MAPK s.p. - MAPK signaling pathway; mTOR s.p. - mTOR signaling pathway; N-Glycan m. - N-Glycan biosynthesis; Nucleo. ex.rep. - Nucleotide excision repair; O-Glycan bio. - O-Glycan biosynthesis; One carbon pbf - One carbon pool by folate; Other gly. deg. - Other glycan degradation; Oxi. phos. - Oxidative phosphorylation; p53 s.p. - p53 signaling pathway; Pent. gluco. intercon. - Pentose and glucuronate interconversions; Pentose phos. p. - Pentose phosphate pathway; Phenyl. m. - Phenylalanine metabolism; Phos.ino.ss. - Phosphatidylinositol signaling system; PPAR s.p. - PPAR signaling pathway; Purine m. - Purine metabolism; Pyri. m. - Pyrimidine metabolism; RAS - Renin-angiotensin system; Reg. act. cyto. - Regulation of actin cytoskeleton; RNA deg. - RNA degradation; SNARE inter. ivt - SNARE interactions in vesicular transport; Steroid bio. - Steroid biosynthesis; Ubi. med. prot. - Ubiquitin mediated proteolysis; Val., leu., iso. deg. - Valine, leucine and isoleucine degradation; Wnt s. p. - Wnt signaling pathway

Total	Enrichment	Ago1	Enrichment	Ago2	Enrichment	Ago3	Enrichment	Ago4	Enrichment
Ribosome	3.37×10^{-74}	Ribosome	9.44×10^{-93}	Ribosome	8.74×10^{-40}	Ribosome	7.71×10^{-128}	Ribosome	1.50×10^{-92}
Spliceosome	1.66×10^{-54}	Oxi. phos.	8.85×10^{-12}	Spliceosome	2.45×10^{-07}	Oxi. phos.	1.98×10^{-23}	Oxi phos.	4.06×10^{-12}
Oxi. phos.	5.24×10^{-52}	Spliceosome	1.45×10^{-06}	Cell cycle	2.07×10^{-06}	Spliceosome	8.12×10^{-11}	Spliceosome	1.89×10^{-05}
Cell cycle	1.47×10^{-49}	Phagosome	8.60×10^{-06}	MAPK s. p.	2.96×10^{-06}	Phagosome	4.36×10^{-04}	mTOR s. p.	0.004442
Ubi. med. prot.	2.69×10^{-37}	Proteasome	5.09×10^{-05}	Endocytosis	2.38×10^{-05}	Proteasome	7.32×10^{-04}	PPAR s. p.	0.009733
Proteasome	2.99×10^{-29}	Lysosome	7.56×10^{-05}	Lysosome	7.22×10^{-05}	Purine m.	0.002432	Protein export	0.010103
DNA rep.	2.82×10^{-26}	RNA deg.	1.38×10^{-04}	Oxi. phos.	1.47×10^{-04}	MAPK s. p.	0.008674	Phagosome	0.018931
Purine m.	6.07×10^{-26}	Gluta. m.	8.20×10^{-04}	p53 s. p.	0.001102	Gluta. m.	0.00878	Proteasome	0.037388
Pyrimidine m.	2.29×10^{-24}	Cell cycle	0.00456	PPAR s. p.	0.001102	RAS	0.00893	Gluta. m.	0.040271
Nucleotide ex. rep.	3.12×10^{-24}	Ubi. med. prot.	0.00625	Amino.-tRNA bio.	0.001156	Steroid bio.	0.00893	Lysosome	0.042153
Phagosome	1.56×10^{-23}	N-Glycan bio.	0.00760	Wnt s. p.	0.001688	Cell cycle	0.02373	Cyano. acid m.	0.043595
Endocytosis	1.92×10^{-21}	Other glycan deg.	0.00775	Peroxisome	0.001906	SNARE inter. ivt	0.03724	AML	0.055854
RNA deg.	2.34×10^{-20}	Endocytosis	0.00786	Phagosome	0.002261	Gap junction	0.04117	Other glycan deg.	0.096874
Lysosome	4.14×10^{-20}	RAS	0.00874	Purine m.	0.002261	Val., leu., iso. deg.	0.05352	One carbon pbf	0.102608
Reg. act. cyto.	2.48×10^{-19}	Steroid bio.	0.00874	AML	0.004708	Cyano. acid m.	0.05775	Steroid bio.	0.102608
Citrate cycle	1.56×10^{-18}	Pyri. m.	0.00940	Cys. meth. m.	0.006552	Fatty acid e.i.m.	0.06573	Pheny. m.	0.102608
Wnt s. p.	1.13×10^{-16}	Arach. acid m.	0.01277	Phos. ino. ss.	0.011765	mTOR s. p.	0.07182	Focal adhesion	0.136418
Val., leu., iso. deg.	2.49×10^{-14}	Protein export	0.01707	One carbon pbf	0.015387	Lysosome	0.08371	Pentose phos. p.	0.157993
Amino.-tRNA bio.	3.27×10^{-14}	PPAR s. p.	0.02027	RAS	0.015387	Arach. acid m.	0.08667	Pent. gluco. intercon.	0.163341
p53 s. p.	1.02×10^{-13}	Pentose phos. p.	0.02135	Steroid bio.	0.015387	AML	0.09181	O-Glycan bio.	0.173934

Table 4.12.2.III The top 20 KEGG pathways offering the highest **signal intensity** (SI) shown for NB4. Abbreviations: Amino.-, nucleo. sugar m. - Amino sugar and nucleotide sugar metabolism; Amino-tRNA bio. - Aminoacyl-tRNA biosynthesis; Asco. alda. m. - Ascorbate and aldarate metabolism; Base ex. repa. - Base excision repair; Cyano. acid m. - Cyanoamino acid metabolism; Fruct. manno. m. - Fructose and mannose metabolism; Gly./Gluc. - Glycolysis / Gluconeogenesis; Hemato. cell l. - Hematopoietic cell lineage; Leuko. trans. mig. - Leukocyte transendothelial migration; mTOR s.p. - mTOR signaling pathway; N-Glycan bio. - N-Glycan biosynthesis; Non-homo. end-joi. - Non-homologous end-joining; Notch s.p. - Notch signaling pathway; Olfactory trans. - Olfactory transduction; One Carbon pbf - One carbon pool by folate; Oxi. phos. - Oxidative phosphorylation; Pent. phos. p. - Pentose phosphate pathway; Phenyl. m. - Phenylalanine metabolism; Prot. pro.in ER - Protein processing in endoplasmic reticulum; Purine m. - Purine metabolism; RAS - Renin-angiotensin system; Reg. act. cyto. - Regulation of actin cytoskeleton; Trypto. m. - Tryptophan metabolism; Tyro. m. - Tyrosine metabolism; Val.,leu.,iso. deg. - Valine, leucine and isoleucine degradation; VEGF s.p. - VEGF signaling pathway; Wnt s.p. - Wnt signaling pathway

Total	SI	Aqo1	SI	SI	SI	Aqo2	SI	SI	SI	Aqo3	SI	SI	SI	Aqo4	SI	SI	SI
Ribosome	2972	Ribosome	3843	4284	3378	Ribosome	2521	226	2264	Ribosome	1727	1774	2099	Ribosome	2481	2386	2402
mTOR s. p.	657	mTOR s. p.	761	822	669	Adherens junction	636	541	568	Base ex. rep.	568	591	506	mTOR s. p.	754	720	728
Cyano. acid m.	655	Base ex. rep.	754	809	743	Proteasome	631	582	591	mTOR s. p.	492	505	542	Adherens junction	613	514	505
Cys. meth. m.	566	Val., leu., iso. deg.	684	454	449	Gly. / Gluc.	577	487	514	Olfactory trans.	466	581	547	Phagosome	449	392	383
Propa. m.	549	N-Glycan bio.	678	526	471	Amino.-tRNA bio.	517	385	480	Val., leu., iso. deg.	394	530	565	Tight junction	421	352	345
Gly. / Gluco.	523	Phagosome	625	498	356	Reg. act. cyto.	469	419	421	Axon guidance	343	371	336	Reg. act. cyto.	409	366	358
Pyru. m.	467	Adherens junction	612	423	382	Axon guidance	466	415	410	Non-homo. end-joi.	340	359	338	Hemato. cell l.	398	369	340
Taste trans.	464	Prot proc in ER	599	530	462	Leuko. trans. mig.	446	379	389	Reg. act. cyto.	279	301	290	Fruct. manno. m.	391	357	392
Phenyl. m.	359	VEGF s. p.	570	438	387	N-Glycan bio.	428	325	326	Amino.-tRNA bio.	232	233	274	Gly. / Gluco.	342	311	343
Phagosome	354	Cyano. acid m.	487	363	150	Tight junction	390	331	345	Protein pro. in ER	228	271	268	Pentose phos. p.	335	302	327
Gap junction	320	One carbon pbf	487	363	150	Phagosome	383	331	335	N-Glycan bio.	217	282	266	Focal adhesion	334	289	282
Porphyr. m.	302	Hemato. cell l.	481	443	213	Focal adhesion	345	300	316	Leuko. trans. mig.	209	273	259	Axon guidance	329	309	326
Oxi. phos.	296	Axon guidance	468	346	254	Gap junction	285	233	263	RAS	203	244	185	Phenyl. m.	287	239	237
Adherens junction	296	Reg. act cyto.	403	305	265	VEGF s. p.	279	225	263	Phagosome	192	204	192	Gap junction	287	252	242
One carbon pbf	295	Focal adhesion	390	307	297	Amino.-, nucleo. s. m.	260	179	220	VEGF s. p.	175	217	197	Olfactory trans.	282	285	288
Reg. act. cyto.	273	Lysosome	350	269	209	Oxi. phos.	257	238	258	Adherens junction	172	212	202	Oxi. phos.	276	282	286
Amino.-tRNA bio.	270	Endocytosis	345	319	124	mTOR s. p.	249	216	251	Focal adhesion	155	184	181	Proteasome	273	262	279
Spliceosome	247	Wnt s. p.	341	253	203	Asco. alda. m.	245	190	214	Spliceosome	154	177	159	Base ex. rep.	251	251	264
Non-homo. end-joi.	246	Notch s. p.	285	276	262	Pentose phos p.	211	158	164	Notch s. p.	143	181	171	Amino.-tRNA bio.	228	194	200
Tight junction	245	Purine m.	276	230	249	Trypto. m.	198	152	168	Wnt s. p.	140	168	155	Tyro. m.	195	171	173

Table 4.12.2.IV The top 20 KEGG pathways offering the highest **enrichment** shown for NB4. Abbreviations: Aldo. reg. reab. - Aldosterone-regulated sodium reabsorption; Amino.-tRNA bio. - Aminoacyl-tRNA biosynthesis; Base ex. rep. - Base excision repair; Cyto.cyto. rec.inter. - Cytokine-cytokine receptor interaction; Gly., ser., threo. m. - Glycine, serine and threonine metabolism; Ino.phos.m. - Inositol phosphate metabolism; Lysine deg. - Lysine degradation; MAPK s.p. - MAPK signaling pathway; mTOR s.p. - mTOR signaling pathway; N-Glycan bio. - N-Glycan biosynthesis; Notch s.p. - Notch signaling pathway; Nulcleo. ex. rep. - Nucleotide excision repair; Oxi. phos. - Oxidative phosphorylation; p53 s.p. - p53 signaling pathway; Phos.ino. s.p. - Phosphatidylinositol signaling system; Pyri. m. - Pyrimidine metabolism; Pyru. m. - Pyruvate metabolism; Reg. act. cyto. - Regulation of actin cytoskeleton; RNA deg. - RNA degradation; RNA pol. - RNA polymerase; Trypto. m. - Tryptophan metabolism; Ubi. med. prot. - Ubiquitin mediated proteolysis; Wnt s.p. - Wnt signaling pathway

Total	Enrichment	Ago1	Enrichment	Ago2	Enrichment	Ago3	Enrichment	Ago4	Enrichment
Ribosome	$3.19 \times 10{-}85$	mTOR s. p.	$8.46 \times 10{-}07$	Phagosome	$2.01 \times 10{-}14$	Spliceosome	$1.03 \times 10{-}16$	Ribosome	$6.38 \times 10{-}28$
Spliceosome	$9.06 \times 10{-}55$	Cell cycle	$1.59 \times 10{-}05$	Oxi. phos.	$5.24 \times 10{-}12$	Cell cycle	$3.17 \times 10{-}11$	Spliceosome	$1.40 \times 10{-}25$
Oxi. phos.	$7.11 \times 10{-}54$	Base ex. rep.	0.001213	Cell cycle	$9.22 \times 10{-}11$	Endocytosis	$1.30 \times 10{-}08$	Cell cycle	$4.74 \times 10{-}13$
Cell cycle	$1.75 \times 10{-}42$	Aldo.-reg. reab.	0.002244	Puri. m.	$2.16 \times 10{-}10$	Oxi. phos.	$1.87 \times 10{-}08$	Ubi. med. prot.	$8.51 \times 10{-}10$
Proteasome	$5.23 \times 10{-}31$	Wnt s. p.	0.002557	Endocytosis	$3.91 \times 10{-}10$	Ubi. med. prot.	$1.62 \times 10{-}07$	Lysosome	$2.49 \times 10{-}08$
Ubi. med. prot.	$2.18 \times 10{-}30$	Lysine deg.	0.002914	MAPK s. p.	$7.20 \times 10{-}10$	Ribosome	$3.23 \times 10{-}07$	RNA deg.	$4.25 \times 10{-}08$
DNA rep.	$3.58 \times 10{-}25$	Phagosome	0.003192	Phos.ino. ss	$2.28 \times 10{-}09$	Phos. ino. ss	$4.87 \times 10{-}07$	Phagosome	$5.59 \times 10{-}08$
Purine m.	$4.84 \times 10{-}23$	Lysosome	0.006896	Pyri. m.	$1.07 \times 10{-}08$	Phagosome	$1.35 \times 10{-}06$	Amino.-tRNA bio.	$1.06 \times 10{-}06$
Nucleo. ex. rep.	$5.69 \times 10{-}20$	MAPK s. p.	0.007058	Ubi. med. prot.	$1.38 \times 10{-}08$	MAPK s. p.	$2.33 \times 10{-}06$	Nucleo. ex. rep.	$2.00 \times 10{-}06$
Pyri. m.	$1.97 \times 10{-}17$	Spliceosome	0.008375	RNA poly.	$1.65 \times 10{-}07$	Lysosome	$3.26 \times 10{-}06$	DNA rep.	$3.85 \times 10{-}06$
Phagosome	$8.45 \times 10{-}17$	Endocytosis	0.009191	Ino. phos. m.	$1.69 \times 10{-}07$	Wnt s. p.	$1.20 \times 10{-}05$	Reg. act. cyto.	$6.16 \times 10{-}06$
RNA deg.	$1.20 \times 10{-}16$	Oxi. phos.	0.009797	Lysosome	$2.62 \times 10{-}07$	mTOR s. p.	$2.04 \times 10{-}05$	RNA poly.	$8.72 \times 10{-}06$
Lysosome	$2.23 \times 10{-}16$	Gly., ser., threo. m.	0.015735	Spliceosome	$5.93 \times 10{-}07$	p53 s. p.	$3.58 \times 10{-}05$	Endocytosis	$1.10 \times 10{-}05$
Citrate cycle	$9.29 \times 10{-}16$	Trypto. m.	0.025454	Gap junction	$8.36 \times 10{-}07$	Ino. phos. m.	$4.38 \times 10{-}05$	Wnt s. p.	$1.36 \times 10{-}05$
Amino.-tRNA bio.	$1.13 \times 10{-}13$	Cyto.-cyto. rec. inter.	0.028703	Wnt s. p.	$1.40 \times 10{-}06$	Base ex. rep.	$5.36 \times 10{-}05$	Base ex. rep.	$2.68 \times 10{-}05$
Protein export	$3.40 \times 10{-}13$	Nucleo. ex. rep.	0.030379	Reg. act. cyto.	$1.50 \times 10{-}06$	Adherens junction	$7.44 \times 10{-}05$	Proteasome	$3.62 \times 10{-}05$
Mismatch repair	$3.07 \times 10{-}12$	Notch s. p.	0.034299	Aldo.-reg. reab.	$5.10 \times 10{-}06$	Purine metabolism	$8.61 \times 10{-}05$	Phos. ino. ss	$4.21 \times 10{-}05$
Pyru. m.	$9.47 \times 10{-}12$	N-Glycan bio.	0.035647	Focal adhesion	$6.29 \times 10{-}06$	Reg. act. cyto.	$9.04 \times 10{-}05$	Pyri. m.	$6.17 \times 10{-}05$
Wnt s. p.	$1.69 \times 10{-}11$	Vitamin B6 m.	0.036528	Nucleo. ex. rep.	$7.66 \times 10{-}06$	RNA deg.	$3.44 \times 10{-}04$	Adherens junction	$1.70 \times 10{-}04$
Focal adhesion	$6.80 \times 10{-}11$	Focal adhesion	0.036704	Chemokine s. p.	$9.17 \times 10{-}06$	Axon guidance	$4.84 \times 10{-}04$	Focal adhesion	$3.49 \times 10{-}04$

4.12.3 Identification of AML-relevant pathways

Due to the high amount of enriched pathways, possessing a p-value < 0.05, seven pathways were depicted separately. These pathways, the phosphatidylinositol signaling system, the mTOR -, p53-, Wnt-, VEGF- and MAPK signaling and the AML pathway have been identified in at least one Argonaute protein among the top 20 enriched KEGG pathways. Except of the VEGF signaling pathway, the six remaining pathways also belong to the top 20 pathways with highest signal intensity (based on Ago-associated mRNAs). Furthermore, these pathways have been described as dysregulated and important for survival of AML cells (Recher *et al.,* 2005, Martelli *et al.,* 2006, Shikami *et al.,* 2006).

Figure 4.12.3.I Network visualization of distinct AML-relevant signaling pathways of KASUMI-1 cells, which belong to the top 20 of highest enriched KEGG pathways. Blue edges show the connection between Ago-associated mRNAs and the pathways they belong to. Green edges represent connections between these mRNAs and their potential miRNA regulators. The connection between Ago-associated miRNAs and their target-mRNAs rely on the target prediction of at least two prediction algorithms. miRNAs offering the same seed sequence were combined into sequence groups (seqgrp). The number in bracket denotes the number of miRNAs identified in the corresponding sequence group. Additionally, the mRNAs are colored according to their Argonaute protein association with the cyclesize corresponding to their level of abundance.

Figure 4.12.3.I visualizes the network of AML-relevant pathways, belonging to the most enriched ones and/or holding the highest signal intensity. In comparison to the pathway enrichment calculations of the total RNA of KASUMI-1 cells, all Argonaute protein-associated pathways presented here, own approximately 3 fold higher signal intensities than the corresponding pathways identified in the total RNA. Moreover, in the ranking of enriched pathways, most of these Ago-associated pathways could

not be identified among the top 20 of enriched pathways of the total RNA, except of Wnt- and p53 signaling pathways, indicating that these pathways are specifically enriched in Argonaute proteins. 13 mRNAs of the presented pathways were identified in Ago2 only, whereas two transcripts, *CDK4* and *PPP2R1A*, were identified to be associated with Ago1 only, *JUND* with Ago3 and *PDPK1* with Ago4 only. In addition, 13 mRNAs appear to be regulated by two or three Argonaute proteins in common, whereas the six gene transcripts, *EIF4B*, *KIT*, *CCND2, DUSP6, RAC2* and *ATF4*, associate with all four human Argonaute proteins. Furthermore, the miR-146a, which is one of the most up-regulated miRNA in t(8;21)-positive pediatric AML patients appears to be responsible for the repression of *RUNX1T1 (ETO)*. The use of miRanda alone additionally reveals binding sites for miR-335, which is also down-regulated in pediatric AML patients carrying translocation t(8;21). Interestingly, the transcripts of the genes *KIT* and *CCND2,* which are potentially under control of down-regulated miRNAs, miR-335 and let-7b and let-7c (according to miRanda), own association with all four Argonaute proteins with signal intensity up to 4,400 LU, indicating that these miRNAs are not the main regulators of *KIT* and *CCND2*.

In NB4 cells, the most enriched pathways among the top 20 with highest signal intensity were also represented as separate pathway network. The pathways phosphatidylinositol signaling system, mTOR-, MAPK- and Wnt signaling pathways, together with the AML pathway were depicted in Figure 4.12.3.II. The AML pathway could not be detected under the top 20 enriched pathways, but for comparison reasons with the KASUMI-1 pathway regulatory network, this pathway was added to the network as well. Moreover, the miRNAs offering binding sites for at least one Ago-associated transcript were added to their potential target-mRNAs as well. As denoted in the pathway network of NB4 cells, 17 transcripts associate with Ago2 only, 10 transcripts with Ago3 and 5 transcripts with Ago4 only, whereas 48 transcripts seem to be under control of at least two Argonaute proteins, and 10 transcripts of these selected pathways appear to be regulated by all four Argonaute proteins. miR-181a, which is up-regulated in t(15;17)-positive pediatric AML patients in comparison to all other AML subtypes, seems to play an important role in the network of enriched KEGG pathways, because of its association with 12 mRNAs involved in four different pathways. Six of these protein products are protein kinases, which catalyze phosphorylation or activate distinct pathways. Furthermore, the miR-223, which is down-regulated in t(15;17)-positive AML patients, exhibit binding sites for the mRNA *INPP5B*. *INPP5B* is an inositol polyphosphate-5-phosphatase, inactivating inositol phosphate molecules, which control cellular calcium signaling.
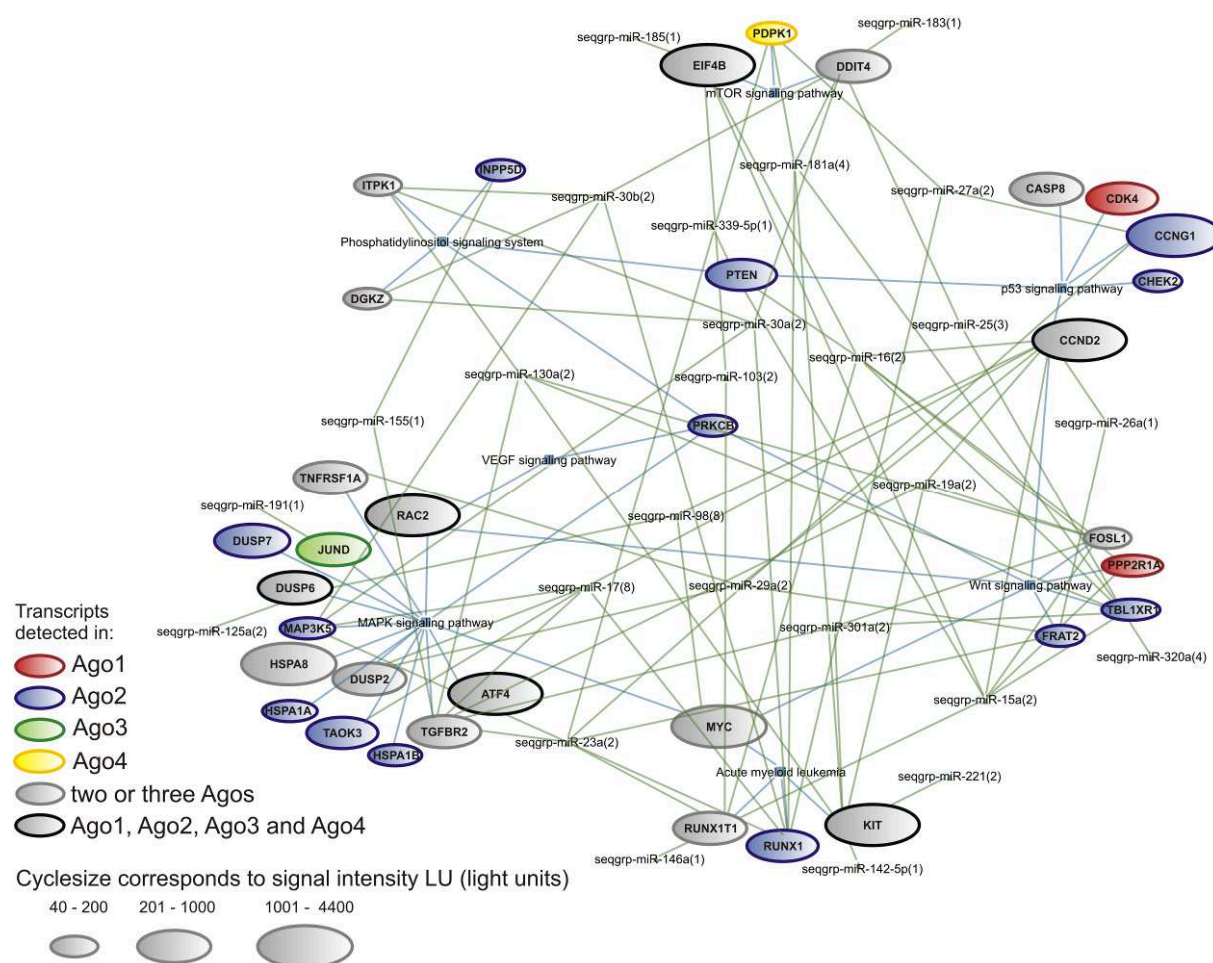
Figure 4.12.3.II Network visualization of distinct AML-relevant signaling pathways of NB4 cells, which belong to the top 20 of highest enriched KEGG pathways. Blue edges show the connection between Ago-associated mRNAs and the pathways they belong to. Green edges represent connections between these mRNAs and their potential miRNA regulators. The connection between Ago-associated miRNAs and their target-mRNAs rely on the target prediction of at least two prediction algorithms. miRNAs offering the same seed sequence were combined into sequence groups (seqgrp). Additionally, the mRNAs are colored according to their Argonaute protein association with the cyclesize corresponding to their level of abundance.

Figure 4.12.3.III displays potential interferences of AML-relevant pathways by miRNA mediated regulation in more detail. Parts of the AML, MAPK and mTOR signaling pathways were extracted from the whole pathway networks, in order to model regulatory mechanisms, which activate different signaling cascades in AML and APL cell lines. The AML pathway serves as starting point, whereby the oncogene *KIT*, by which it is known to be involved in leukemogenesis, is regulated by the four human Argonaute proteins, in cooperation with six different miRNA sequence-groups, offering binding sites for *KIT*. Due to the repression of *KIT* in KASUMI-1 cells, the activation of PIK3CD (phosphoinositide-3-kinase) could be reduced as well as the expression of PDPK1 (3-phosphoinositide dependent protein kinase-1), which is secondaryly repressed by three different miRNA sequence-groups. Consequently, the activity of AKT is reduced, leading to decreased mTOR activity in KASUMI-1 cells. In NB4 cells, PIK3CD as well as PDPK1 are under control of Argonaute-miRNA complexes, similar to the KASUMI-1 cell line model, and thus reducing the activity of AKT. However, the indirect inhibition of AKT is counteracted by direct repression of TSC1 (tuberous sclerosis 1) by seven different miRNA sequence-groups. Thus, RHEB (Ras homolog enriched in brain) could be activated, which subsequently intense

the activity of mTOR (mechanistic target of rapamycin (serine/threonine kinase)) leading to higher translation rate and increased cell growth of NB4 cells by S6K1/2 (ribosomal protein S6 kinase, 70 kDa, polypeptide 1/2) and S6 (ribosomal protein S6). However, this hypothesis cannot be confirmed directly from cell growth in cell culture and is subject for further investigations. Moreover, in KASUMI-1 cells, the MAPK signaling pathway seems to be regularly activated, with regard to the first part of the MAPK pathway in Figure 4.12.3.III, beginning at FLT3 (fms-related tyrosine kinase 3) until ERK (mitogen-activated protein kinase). ERK is normally inhibited by DUSP (dual specificity phosphatase), but due to the repression of DUSP by four different miRNA sequence-groups, the *ERK* gene could be highly activated and is able to stimulate proliferative genes by activation of SAPLA (ETS-domain protein), SRF (serum response factor (c-fos serum response element-binding transcription factor) and c-FOS (FBJ murine osteosarcoma viral oncogene homolog). In NB4 cells, it is also possible that the MAPK signaling pathway is activated by activation of ERK, because DUSP is also repressed by several miRNAs. The repression of RAS and K-RAS (v-Ki-ras2 Kirsten rat sarcoma viral oncogene homolog) by six different miRNA sequence-groups seems to be counter-intuitive at first sight. However, only a small part of KRAS is actually bound to Argonaute proteins (depicted as bars beside the gene products in Figure 4.12.3.III).

Besides these main routs, described above, which potentially lead to increased cell survival, cell growth and proliferation, a lot of genes like *eIF4B* (eukaryotic translation initiation factor 4B), *eIF4E2* (eukaryotic translation initiation factor 4E family member 2), *MKNK1* (MAP kinase interacting serine/threonine kinase 1) or *ELK-1* (ELK1, member of ETS oncogene family) seem to be also under control of Argonaute-miRNA complexes, indicating that Figure 4.12.3.III displays only a small part of the complex regulatory network of AML and APL.
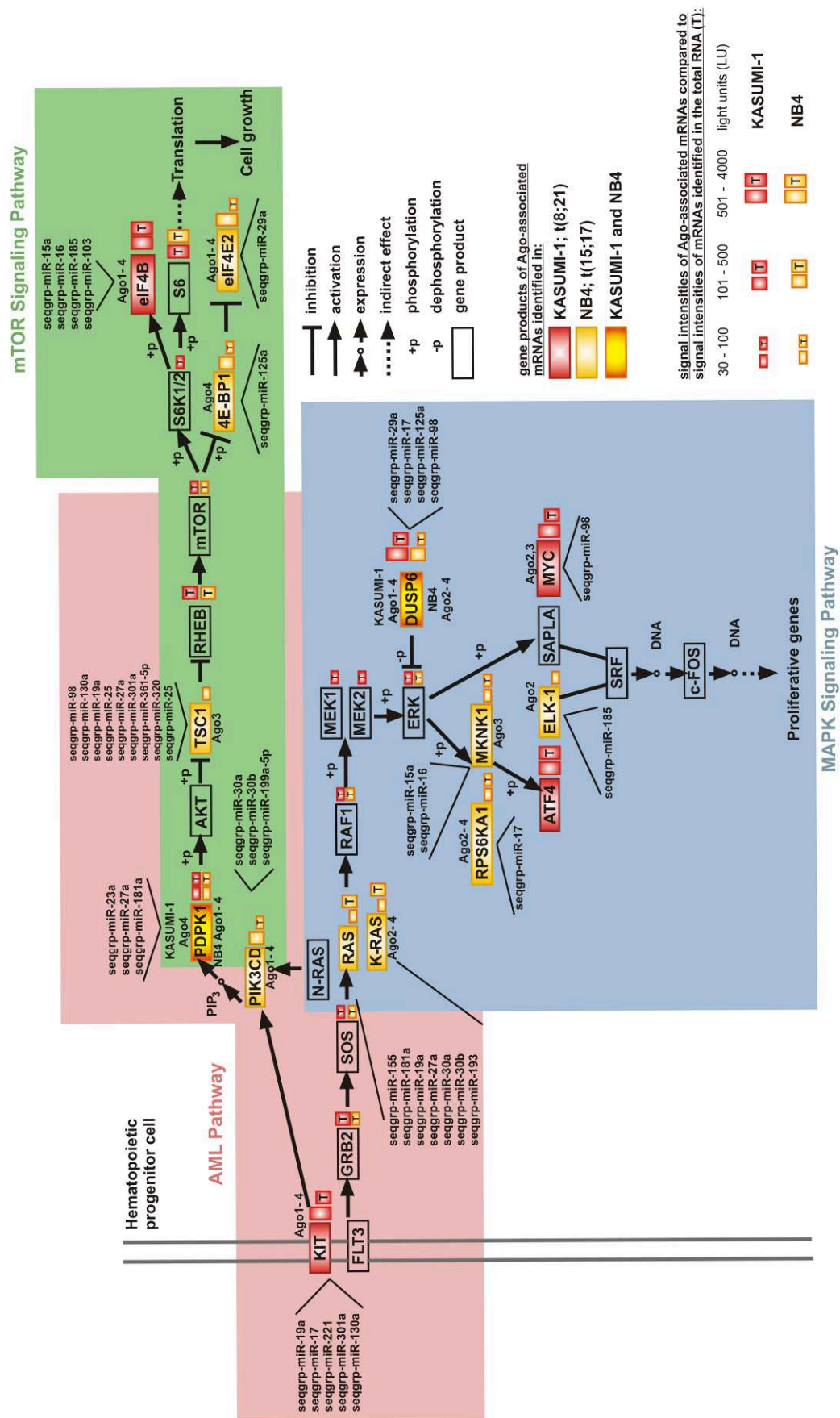
Figure 4.12.3.III Schematic overview of potential regulatory interferences into three selected AML-relevant pathways by Ago-associated miRNAs. The draft for these pathways originates from the KEGG database. Only extracts of each pathway are shown. Thereby, the AML pathway serves as starting point. The boxes describe the gene products of the pathways. The transcripts of gene products in red boxes have been identified in association with Argonaute proteins in KASUMI-1 cells, transcripts of gene products in yellow boxes have been found in Argonaute proteins of NB4 cells and transcripts of gene products in red/yellow boxes were identified in both. The amount of Ago-associated mRNAs and mRNAs identified in the total RNA are depicted as red bars for KAUMI-1 and yellow bars for NB4 right beside the gene products. The connections between the gene products are explained in the figure legend on the right.

5 Discussion

5.1 Altered miRNA expressions in AML subtypes emphasize their function as biomarker

miRNAs were initially discovered as regulators of normal homeostasis, and have recently shown to be a new class of genes that are altered in their expression in several human malignancies, and play an active role in malignant transformations (Ambros, 2004; Bartel, 2004; Gregory and Shiekhattar, 2005). Distinguishable abnormalities in miRNA expression patterns are being identified continuously in almost all types of cancer, thus providing a tool for the application of miRNAs as diagnostic or prognostic biomarker (Li *et al.*, 2010). Three independent miRNA expression profiling studies indicate that adult AML patients with t(8;21)/*AML1*(*RUNX1*)-*ETO*(*RUNX1T1*), inv(16)/*CBFB-MYH11* and t(15;17)/*PML-RARα* have unique miRNA expression signatures, capable of setting them apart from other subtypes of AML (Dixon-McIver *et al.*, 2008; Jongen-Lavrencic *et al.*, 2008; Li *et al.*, 2008). The comparison of adult and pediatric AML patient samples with regard to their miRNA expression signatures of different AML subtypes reveals a lot of agreements between both, but also a few differences. In this study, miRNA expression profiles of over 100 pediatric AML patient samples were analyzed in order to find specific signatures for distinct chromosomal abnormalities.

Pediatric patient samples carrying translocations t(8;21) and t(15;17) could be completely separated from each other, and most of these samples grouped together into two smaller, definite clusters on the basis of their miRNA expression patterns. This was expected, because both AML subtypes differ morphologically and clinically. The formation of the *PML/RARα* transcript causes maturation arrest in the promyelocytic stage (Martinez-Climent, 1997), whereas the *AML1-ETO* transcript, which alone is not responsible for a full-blown leukemia, was predicted to act as transcriptional repressor for *AML1* target genes (Elagib and Goldfarb, 2007). The inv(16) could not be separated clearly from the other translocations, as this aberration is interspersed in parts with t(8;21) and other chromosomal abnormalities. Patients with t(8;21), inv(16) and t(15;17) have a relatively favorable outcome, and are classified into a favorable cytogenetic risk-group. Genome-wide analyses revealed that miRNA expression has an influence on the outcome of adult AML patients. Li *et al.* showed that miR-126 is overexpressed in both t(8;21) and inv(16) samples of adult AML patients, and functions as oncomir by inhibition of apoptosis and induction of the viability of AML cells (Li *et al.*, 2008). For pediatric AML patients, the miR-126 could also be indicated as statistically significant and overexpressed in t(8;21) samples, suggesting that the aberrant overexpression of this miRNA may contribute to the development of AML as a secondary hit in cooperation with the primary oncogenic events, such as *AML1-ETO* formation. Moreover, miR-146a was identified as overexpressed in t(8;21)-positive pediatric AML samples, and was found down-regulated in adult AML patients (Garzon *et al.*, 2008b). Due to its high expression, this miRNA is associated with poor survival of AML patients, because of its potential function as oncomir negatively regulating genes involved in inhibition of cell growth and promotion of apoptosis (Wang *et al.*, 2010b). Furthermore, Fazi *et al.* observed a down-regulation of miR-223 in t(8;21) adult AML samples, and showed that there was an epigenetic silencing of this miRNA by the AML1-ETO oncoprotein (Fazi *et al.*, 2007). In recent studies, it was shown that the suppression of miR-223 could be associated with various types of myeloid leukemias, because this miRNA is crucial for the initiation of myeloid differentitation of progenitor cells (Fazi *et al.*, 2005). In pediatric AML patient samples, miR-223 was also found to be expressed in the majority of t(8;21) samples at lower level than in other chromosomal alterations, indicating a differentiation arrest of t(8;21)-positive AML cells, due to the *mir-223* gene suppression by AML1-ETO. The miRNAs, miR-100, miR-125b, miR-181a and miR-181b, were not reported to be overexpressed in adult AML patient samples, harboring translocation t(15;17), but could be detected as statistically significantly up-regulated in t(15;17)-positive pediatric AML patient samples in this thesis, indicating a difference of characteristics and progress of this AML subtype between adults and children. Recently, it was demonstrated that miR-100 and miR-125b significantly decrease cell proliferation (Henson *et al.*, 2009), and that miR-125b overexpression promotes malignant transformation of different hematopoietic lineages in mice (Bousquet *et al.,* 2010). Furthermore, miR-125b has already been shown to arrest myeloid differentiation of human cell lines (Bousquet *et al.*, 2008). Therefore, it might be possible that the maturation arrest in the promyelocytic stage, caused by the PML-RARα oncoprotein (encoded by t(15;17)), will be intensified by overexpression of miR-100 and miR-125b, inducing differentiation arrest combined with cell proliferation decrease, contributing to the clinical entitiy of pediatric APL. Furthermore, in a study of Marcucci *et al.*, miR-181a and miR-181b showed increase expression in CN-AML (cytogenetically normal-AML), which correlates with decreased risk of

an adverse event like failure to achieve complete remission, relapse or death (Marcucci *et al.*, 2009). In addition, both miRNAs were reported to function as tumor suppressor (Shi *et al.,* 2008b) by targeting the oncogene *KRAS* (Shin *et al.,* 2011). Thus, it is possible to classify children with t(15;17)-positive AML into a favorable cytogenetic risk-group by the high expression of the tumor suppressors miR-181a and miR-181b. Actually, the PML-RARα carrying subtype of AML is renowned to have an excellent prognosis in children further strengthening the usability of miRNAs as prognostic biomarkers in the future.

Summing up, in pediatric AML patients only a handful miRNAs could be identified as significantly differentially expressed between AML subtypes, because of the great heterogeneity of eleven different chromosomal abnormalities, compared to each other at a genome-wide level. Nevertheless, these differentially expressed miRNAs indicate that adult AML is not always compatible to AML in the pediatric age groups and that pediatric-specific miRNA signatures exist. Thus, the spectrum of hematopoietic malignancies between pediatric and adult patients is different, and for pediatric AML patients, different miRNAs seem to be involved in leukemogenesis. Due to the definite differences in outcome and survival between adult and pediatric AML patients (Lange *et al.,* 2008), this study suggests that miRNAs, identified differentially expressed in pediatric AML, are suitable novel biomarkers and potential new drug targets for the development of targeted treatment in childhood AML.

5.2 Experimental and computational identification of miRNA targets: progress and limitations

5.2.1 Experimental identification of miRNA targets using the improved PAR-CLIP-Array method

A further challenge of this thesis is the elucidation of mechanisms, underlying regulation of miRNA expression in order to get deeper insights into AML pathogenesis. For the identification of miRNAs and their target-mRNAs, associated to RNA-binding proteins (RBP), especially Argonaute proteins, different combinations of genetic, biochemical and computational approaches were developed. One of the first methods generated so far, was the immunoprecipitation (IP) of RBPs with subsequent microarray profiling, called RIP-Chip (Keene *et al.*, 2006; Tenenbaum *et al.*, 2000). The RIP-Chip method allows a global identification of multiple miRNA targets at the same time (Keene *et al.*, 2006). However, its application is limited to the characterization of kinetically stable interactions. The PAR-CLIP-Array method established in this thesis also uses miRNA microarray- and mRNA Affymetrix chip-hybridizations for a rapid detection of about hundred of miRNAs and several hundreds of mRNAs, respectively, within three days only. A second method, combining in vivo crosslinking using ultraviolet light and immunoprecipitation, was called CLIP (Ule *et al.,* 2003). Due to the UV-crosslinking, more RBP target site information could be obtained. Therefore, the PAR-CLIP-Array method uses UV irradiation of living cells as well, in order to identify a high fraction of bound miRNAs and their targets. However, the CLIP method is limited by the low efficiency of UV 254 nm RNA-protein crosslinking, whereby crosslinked target-RNA could be separated hardly from background non-crosslinked RNAs, also present in the sample (Hafner *et al.*, 2010a). On this account, the PAR-CLIP-Array method was

performed using UV 356 nm crosslinking, leading to higher yields of crosslinked RNAs. In order to further facilitate crosslinking, the PAR-CLIP-Array method uses 4-thiouridine which incorporates into RNA molecules and increases the efficiency of Argonaute-RNA binding. The use of photoactivatable nucleosides was established by Hafner and colleagues (Hafner *et al.*, 2010a). The great advantage of their PAR-CLIP method is the high-throughput sequencing of RBP associated RNAs and the precise identification of RBP binding sites, by scoring for thymidine (T) to cytidine (C) transitions in the sequenced cDNA (Hafner *et al.*, 2010a). The identification of RBP recognition elements (RRE) within the long target RNAs is not possible using the PAR-CLIP-Array method. However, if someone wants only to identify protein bound RNA molecules, the PAR-CLIP-Array method is fully sufficient, less material and resources consuming. This is of extreme importance, when dealing with patient material or cell systems that cannot be grown to high density suspension cultrues. Moreover, this method minimizes unspecific binding by stringent washing steps and controls the occurring of unspecific binding by using isotype antibody (rat IgG) and empty beads. Up to now, this is the only study applying such stringent controls in the whole co-immunoprecipitation procedure, since both negative controls of the PAR-CLIP-Array method were used for immunoprecipitation, Western Blot analysis and RNA detection, and were performed simultaneously to the Argonaute protein approach. For individual miRNAs and mRNAs, quantitative RT-PCR (qRT-PCR) amplifications revealed that small amounts of unspecific bound RNA could be isolated from both negative controls as well, although no Argonaute protein could be detected. This also demonstrates that a Western Blot on its own is not enough to monitor unspecific binding as used previously by severeal groups. Therefore, unspecifically bound RNAs identified, using isotype control and empty beads, were removed from the set of RNAs, identified in the Argonaute protein, to increase the number of true-positive RNAs. Thus, the PAR-CLIP-Array method provides high-confidential results, because of such extensive controlling, which makes this method a valid tool for rapid miRNA target identification. In summary, the PAR-CLIP-Array method combines the advantages (like 4-thiouridine and UV irradiation) of methods established so far, and due to the improvement of each single step, this method represents a material and time saving tool for rapid identification of Ago-associated miRNAs and target-mRNAs of various cell types.

5.2.2 Computational identification of miRNA target sites on complexed mRNAs using target prediction algorithms

For prediction algorithm, it is difficult to separate the noise of non-functional seed matches from functional miRNA target sites. Therefore, methods to identify miRNA targets in an unbiased manner and more experimental target validation are needed. Using the improved PAR-CLIP-Array method, a vast amount of miRNAs and mRNAs associating with the four human Argonaute proteins could be identified. For the correlation of miRNAs and their putative mRNA-targets, the prediction algorithms TargetScan, PicTar and miRanda were used to find binding sites on mRNAs, because these tools seem to be the best methods with sensitivity values ranging between 65% and 68%, in which miRanda seems to be slightly less efficient in term of specificity (Maziere and Enright, 2007).

For 49% - 82.6% (KASUMI-1) and 68% - 85.6% (NB4) of significant Ago-associated mRNAs, a putative binding site of at least one miRNA could be predicted, with regard to the results of at least one prediction algorithm, indicating that it was not possible to find miRNA binding sites for all detected

mRNAs. One reason could be the identification of unspecific bound mRNAs. In this case, these mRNAs have to be highly abundant and enriched in the Argonaute protein complexes, because otherwise they could not be detected with high significance in comparison to the negative controls. In addition, due to the stringent washing steps after immunoprecipitation, it is rather possible that a subset of mRNA-targets have more transient interaction that do not survive the washing steps, in spite of 4-thiouridine incubation and UV irradiation. Therefore, a more likely cause for lacking some miRNA binding site predictions are the different ways of how miRNAs bind their targets. If a miRNA binding site is located in the CDS or the 5'-UTR of the mRNA, computational algorithms will not predict these bindings (Maziere and Enright, 2007). The findings of Hafner and colleagues applying PAR-CLIP showed that nearly 50% of the identified binding sites are located in the CDS, because CDS and 3'-UTR sites appear to have similar sequence and structure features (Hafner *et al.*, 2010a). In addition, not all predictions are in fact binding sites between miRNAs and target-mRNAs. Moreover, the scoring and ranking strategies of these algorithms are different, and so the output differs, despite identical input datasets. The overlap between any two of these three databases lies between only 20.8% and 57.0% for target-mRNAs, identified in the four Argonaute protein complexes of KASUMI-1 cells. The predictions of Argonaute protein-associated mRNAs of NB4 cells represent an overlap between 26.6% and 53.6%, using at least two prediction algorithms. In spite of the low accordance of the different prediction methods, the use of at least two algorithms is recommended to get reliable target predictions. This is important for the trustworthiness of subsequent analyses and validations of miRNAs and their putative target-mRNAs.

Nevertheless, computational predictions are, and will remain, an important tool for miRNA investigations. However, in order to help refine and strengthen these algorithms, more experimental studies are required.

5.3 Argonaute proteins own different functions, but act in concert

The four human Argonaute proteins are ubiquitously expressed in all cell types and share extensive sequence and structure homology. Hence, all Argonaute proteins are able to perform inhibitory effects by base pairing of Ago-associated miRNAs with their target-mRNAs. For instance, Ago2 and Ago3 share the same conserved motif in the catalytic center for cleavage (Martinez *et al.*, 2002). However, Ago2 only is capable of catalyzing the cleavage of the target-mRNA by the incorporated miRNA, with perfect complementarity to the target (Liu *et al.*, 2004; Rivas *et al.*, 2005). Therefore, Ago2 is unique and has an essential role in mammalian miRNA pathway. Partially, all human Argonaute proteins have overlapping functions in the miRNA pathway, but individual proteins appear also functionally specialized in recruiting structurally distinct miRNAs for the silencing effect (Su *et al.*, 2009).

5.3.1 Argonaute proteins are specialized in their function

The specialized functions of the four human Argonaute protein complexes will be clarified by the analysis of identified, Ago-associated miRNAs and mRNAs performed in this thesis. In KASUMI-1 cells, 36.8% of all detected miRNAs were associated to each of the four Argonaute proteins, whereas the greatest part, of even 48.4%, was exclusively found in association with Ago2, suggesting a high translational repression and cleavage rate of target-mRNAs in the AML cell line by Ago2. In NB4 cells,

27.7% of all identified miRNAs could be associated with all human Argonaute proteins, in which 8.5% and 12.8% of all miRNAs associate solely with Ago2 and Ago3, respectively. With regard to the putative miRNA targets, 12.5% of all identified target-mRNAs of KASUMI-1 cells were identified in all four Argonaute protein complexes, and the largest quantity of 33.9% of all mRNAs associate exclusively with Ago2. A similar composition could be represented for NB4 cells, because 7.3% of all significant mRNAs associate with the four human Argonaute proteins, whereas the greatest part of even 15.6% of these mRNAs could be exclusively identified in the Ago2 complex. In fact, it could be shown that Ago2 appears to be most specialized in the choice of miRNA binding and recruiting for the silencing effect.

Furthermore, the comparison of Ago-associated miRNAs and mRNAs, identified in AML and APL cell lines among each other, reveals more protein- and species-specific informations of both cell lines. The identified miRNAs of the total RNA even accord with 72.1% between KASUMI-1 and NB4. By comparing Ago-associated miRNAs of KASUMI-1 and NB4 cells, an overlap of 50.8% of Ago1-, 60% of Ago2-, 43.2% of Ago3- and 59.1% of Ago4-associated miRNAs, respectively, could be observed. As expected for different cell types, there are differences in Argonaute-miRNA binding, because the overlap does not accord by 100% between both cell lines, indicating that miRNAs are able to act in cooperation with different Argonaute proteins in different cell types. On the basis of different studies, it became known that some aspects of miRNA biochemistry are in fact species-specific (Berezikov *et al.*, 2006; Landthaler *et al.*, 2008; Mourelatos *et al.,* 2002; Zhang *et al.*, 2008), and specific mammalian tissues, and cell types have their own subtypes of regulatory miRNAs (Landgraf *et al.*, 2007; Aravin *et al.*, 2006). This evidence could be confirmed by the investigations of miRNAs of the total RNA for the AML and APL cell line models, and moreover, it was considering that miRNAs possess Argonaute specificity, which changes in different cell types. Therefore, the molecular machinery of miRNAs is very flexible and has potential for complex gene expression regulation in different cell types, including transcriptional and translational control.

Due to the different Argonaute-miRNA interactions in different cell species, the comparison result of Ago-associated mRNAs of KASUMI-1 and NB4 cells is not surprising, because miRNAs have the potential to regulate hundreds of different mRNAs. 2.3% of Ago1-, 7.5% of Ago2-, 5.9% of Ago3- and 9.1% of Ago4-associated mRNAs only match between KASUMI-1 and NB4 cells, whereas 65.5% of identified mRNAs of the total RNA overlap between KASUMI-1 and NB4. Due to the different AML cell lines, a different mRNA composition was expected, whereas in total RNA an overlap of about 65% of mRNAs indicates a close relationship between the AML (KASUMI-1) and the APL (NB4) cell lines. The low accordance of Argonaute-associated mRNAs of both cell lines suggests that miRNAs inherit different regulatory functions in different cell types. From previous studies, it is known that in each cell type there are some mechanisms that differ, based on specific parameters related to species, cell types, developmental stages or environmental stimuli (Nelson *et al.,* 2010).

In summary, this thesis impressively indicates the complex regulation of post-transcriptional gene silencing of both cell lines tested. Additionally, it could be shown that each Argonaute protein works together with distinct subsets of miRNAs, which differ between AML and APL. Furthermore, each Argonaute protein also binds different subsets of mRNAs in AML and APL, due to their varying miRNA association, whereby the complexity of the regulatory machinery increases continuously.

5.3.2 Different Argonaute proteins regulate different molecular functions and biological processes

The gene ontology (GO) project has developed three structured controlled vocabularies (ontologies) that describe gene products in terms of their associated biological processes, cellular components and molecular functions in a species-independent manner. To discover and explore the main molecular functions and biological processes regulated by the four human Argonaute proteins in AML and APL, the Ago-associated mRNAs were classified into GO terms. Due to the high number of Argonaute-specific target-mRNAs, a lot of GO terms were expected to be Argonaute-specific as well. For KASUMI-1 cells, GO terms of the categories Binding, Transporter -, Catalytic -, Structural Molecule -, Translation Regulator - and Antioxidant activity are overrepresented within the mRNAs of at least one Argonaute protein. Moreover, the MAPK (mitogen-activated protein kinase) phosphatase activity seems to be regulated by Ago2 only. With regard to the "Biological Process", the function of Ago2 was characterized more precisely, because Ago2 appears to be involved exclusively in the negative regulation of different kinases including the MAP kinase activity, which is very important for signal transduction. MAP kinases present a family of protein kinases that perform a crucial step in relaying signals from the plasma membrane to the nucleus. They are activated by a wide range of proliferation- or differentiation-inducing signals and their signaling cascade is constitutively activated in a high proportion of adult AML cases (Haferlach, 2008). Hence, it seems that Ago2 tries to reduce the extent of MAP kinase activity in the AML cells to counteract further abnormal regulation.

5.3.3 Argonaute proteins reveal concerted action in pathway regulation

The GO term analysis reveals a few functions only, which were executed by the genes, post-transcriptionally regulated by different Argonaute proteins. Therefore, more functional characterization, using KEGG database, was performed by classification of Ago-associated mRNAs into different pathways. The signal intensities of mRNAs belonging to the same pathway were mean centered and visualized, using hierarchical cluster analysis and heatmap calculations. In addition, mRNA enrichment was computed, using hypergeometric distribution, to find overrepresented pathways within the mRNA lists. Subsequently, Ago-miRNA-mRNA pathway network-maps were generated to identify functionally relevant pathways, miRNA binding sites and AML-relevant processes. By analyzing the KEGG results, 55.8% - 76.8% (43 of KASUMI-1) and 49.1% - 94.8% (55 of NB4) of identified KEGG pathways could be observed for all human Argonaute proteins, indicating that about half of identified KEGG pathways are under stringent regulatory control of all human Argonaute proteins. Interestingly, a high amount of KEGG pathways are regulated by the four Argonautes, whereas on average only 25.9% and 24.7% of Ago-associated mRNAs could be identified in all four proteins of KASUMI-1 and NB4 cells, respectively. This implies that a high number of Ago-specific mRNAs and mRNAs, associated with several Argonaute proteins, are involved in around 50% of the same KEGG pathways identified in the four human Argonaute proteins. On this account, the hypothesis arises that a concerted action between the Argonaute proteins exists, whereby different Argonaute proteins regulate different parts of a distinct pathway, by binding specific mRNA-targets. This effect increases with regard to Ago-associated mRNAs of NB4 cells, because nearly the three fold amount of significant Ago-associated mRNAs could be identified for this cell line.

5.4 Argonaute-miRNA complexes are involved in the regulation of AML-relevant pathways

Among the KEGG pathways, identified to be regulated by all Argonaute proteins and responsible for cell growth, transport, metabolism and catabolism, the phosphatidylinositol signaling system, the mTOR -, MAPK -, p53 - and Wnt signaling pathways are highly enriched with mostly high signal intensities, due to Ago-associated mRNAs identified in at least one Argonaute protein of KASUMI-1 and NB4 cells. It is known that, among these pathways, extensive cross-talk and cross-activation exists, so that the activation of one pathway often leads to the activation of others. Thereby, external signals received from chemokines and cytokines, and by interactions with the local microenvironment partially regulate proliferation, differentiation and apoptosis of normal and leukemic hematopoietic stem cells (Kornblau *et al.*, 2006). A vast amount of signal transduction pathways including PI3K/Akt (part of mTOR pathway) and RAS/Raf/MEK/ERK (part of the MAPK signaling pathway) transmit the response to these signals from the cell surface to the nucleus (Steelman *et al.*, 2004). A result of either mutation or altered regulation of pathway components, or alterations in the internal and external signals, leads to the disruption of normal signaling. It is thought that these effects contribute to leukemogenesis by perturbing the rates of proliferation, differentiation and apoptosis (Steelman *et al.*, 2004; Reuter *et al.*, 2000; Gilliland and Tallman, 2002). In this thesis, it could be shown that miRNAs are also important regulators of genes involved in these pathways, potentially leading to increased cell survival, cell growth and proliferation of AML cells.

First of all, signaling through mTOR is crucial for cell physiology, because mTOR regulates numerous components involved in protein synthesis including initiation and elongation factors and the biogenesis of ribosomes themselves (Wang and Proud, 2006). Thereby, mTOR plays a central role in signaling, caused by nutrients and mitogens, such as growth factors, to regulate translation. The mTOR pathway is also aberrantly activated in hematological malignancies including AML (Recher *et al.,* 2005). In KASUMI-1 and NB4 cells, the mTOR signaling pathway appears to be regulated by all four human Argonaute proteins (Figure 4.12.3.I and Figure 4.12.3.II). The detected transcripts, involved in the mTOR signaling pathway, offer overall high signal intensities in comparison to all other pathways. The highest expression of these pathways was found in association with Ago2 (KASUMI-1) and Ago1 (NB4), indicating a strong regulation of this pathway in both cell lines. However, for pathway repression or activation, it is not only deciding how much transcripts show high incidence in the Argonaute complexes, but also which transcripts are affected by post-transcriptional gene-silencing. Thus, Figure 4.12.3.III demonstrates potential regulatory interferences of AML-relevant pathways by Ago-associated miRNAs. Thereby, in NB4 cells, the mTOR signaling pathway is potentially activated by inhibition of TSC1 by seven miRNA sequence-groups, whereby RHEB and mTOR will be activated, subsequently leading to an increase of translation and cell growth. In KASUMI-1 cells, PDPK1 is repressed by putative binding of multiple miRNAs, whereby AKT activity will be reduced and TSC1 activity increased, subsequently blocking RHEB and mTOR, indicating a negative regulation of the mTOR signaling pathway in this cell line. Additionally, the activation of the mTOR signaling by insulin is believed to be mediated by the PI3-kinase (phosphoinositide-3-kinase) pathway (Wang and Proud, 2006). Increase of PI3 kinase activity leads to oncogenic transformation that can be blocked by inhibition of mTOR by rapamycin. The PI3K/Akt signaling network is crucial to divergent processes like

cell cycle progression, differentiation, transcription, translation and apoptosis (Brazil *et al.*, 2004; Hanada *et al.*, 2004). Several recent papers have highlighted that the PI3K/Akt signaling is frequently activated in AML (Martelli *et al.*, 2006). For KASUMI-1 and NB4 cells, the PI3K signaling pathway is enriched in respect to the number of detected transcripts involved, but these transcripts reveal permanently low expression levels for each Argonaute protein. Therefore, this pathway seems not to be repressed by Argonaute-miRNA complexes, and accordingly, activation in both cell lines is possible.

The RAS/Raf/MERK/ERK pathway is a key signal transduction pathway that has been demonstrated to result in increased cell proliferation and survival along with angiogenesis and metastasis (Steelman *et al.*, 2004; Sebolt-Leopold, 2004). The signaling from this classical MAP kinase pathway also activates mTOR signaling (Wang and Proud, 2006). The MAPK pathway also transduces a large variety of external signals, leading to a wide range of cellular responses, including growth, differentiation, inflammation and apoptosis (Pearson *et al.*, 2001). MAPK itself is overexpressed or constitutively activated in hematopoietic malignancies including AML (Bowen *et al.*, 2005). The MAPK signaling pathway also reveals high expressions in KASUMI-1 cells, due to the expression of involved transcripts, whereas the Ago-associated mRNAs of NB4, involved in this pathway, offer very low expression levels in comparison to all other pathways. Thus, it can be assumed that parts of the MAPK signaling pathway will be activated in AML and repressed in APL, as depicted in Figure 4.12.3.III in more detail. This figure shows that inhibiton of DUSP by four different miRNA sequence-groups could lead to activation of the MAP kinase ERK, promoting the activation of proliferative genes in both AML cell lines. The regulation of KRAS by several miRNAs in NB4 cells could prevent this effect, but only a small part of KRAS associates with Argonaute-miRNA complexes and alternate poly(A)-tailing even avoid miRNA regulation (Jan *et al.*, 2011).

There are several more pathways regulated by Argonaute-miRNA complex interferences, which were not depicted in Figure 4.12.3.III. For instance, the p53 tumor suppressor protein is a multifunctional transcription factor that regulates cellular processes affecting proliferation, DNA repair, cell cycle checkpoints and apoptosis (Fridman and Lowe, 2003). Several studies showed that p53 protein expression was reduced in t(8;21)-positive AML cells. Low p53 protein expression and insufficient induction of p53 by DNA damage might increase the opportunity to obtain additional oncogenic events (Shikami *et al.*, 2006). Tumor cells, which are able to activate p53, may be of therapeutic benefit (Saha *et al.*, 2010). The main function of p53 is to coordinate a highly conserved intracellular pathway, known as the p53 pathway, in respond to different kinds of cellular stress (Harris and Levine, 2005; Oren, 2003). In NB4 cells, the p53 pathway shows very low abundance with regard to the identified transcripts of all four Argonaute proteins, indicating that this pathway is not repressed by miRNAs in APL. Among these mRNAs, p53 itself could not be observed, whereas TRIAP1 (TP53 regulated inhibitor of apoptosis 1), which does not belong to the p53 pathway, but regulates inhibition of apoptosis by p53, was found with moderate abundance in association with Ago2, Ago3 and Ago4, which supports the assumption of apoptosis activation in these leukemia cells, due to repression of TRIAP1 by several Argonaute proteins. In KASUMI-1 cells, mRNAs involved in p53 signaling and associated with Ago1 and Ago2 show higher abundance than the corresponding transcripts associated with Ago3 and Ago4, indicating a partially inhibition of this pathway and of apoptosis,

although, the transcript for p53 could not be verified. GO term analyses revealed that the induction of apoptosis by p53 is exclusively carried out by Ago1. Thus, it might be possible that Ago1 is responsible for tumor progression by regulating genes, which are involved in apoptosis induction by p53. Apparently, there are some mechanisms still available, which counteract AML pathogenesis and possibly make t(8;21)- and t(15;17)-positive AML thus favorable.

Furthermore, the Wnt signaling pathway participates in multiple developmental events during embryogenesis, on stem cell level and is active in certain human leukemias like AML (Wang *et al.*, 2010) as a result of the expression of transcription factor fusion proteins, such as AML1-ETO (Muller-Tidow *et al.*, 2004; Simon *et al.*, 2005). Several molecules downstream of Wnt act as either tumor suppressor or proto-oncogenes in the pathogenesis of epithelial cancers (Polakis, 2000). The Wnt pathway is not repressed by miRNAs in KASUMI-1 cells, because the transcripts, identified to be involved in this pathway, reveal low abundance in comparison to all other transcripts (Figure 4.12.1.I). In NB4 cells, the Wnt pathway appears to be activated, because the abundance of the transcripts involved, are very low as well. Only Ago1 seems to be involved in the regulation of parts of the Wnt pathway, because Ago1-associated mRNAs show moderate abundance, in contrast to all other transcripts (Figure 4.12.1.II). Several studies demonstrated that the Wnt signaling has been implicated in self-renewal and proliferation of hematopoietic progenitor cells (Murdoch *et al.*, 2003; Reya *et al.*, 2003; Austin *et al.*, 1997), but it could not be shown that this pathway is involved in human leukemia development (Muller-Tidow *et al.*, 2004; Simon *et al.*, 2005).

Taken together, a lot of signal transduction pathways are potentially interfered in their activation by Argonaute-miRNA complexes in AML and APL patients, as well as in the corresponding cell lines. These few examples alone clarify the complexity of regulation and interaction between Argonaute proteins, miRNAs and target-mRNAs, and most of them are not yet validated experimentally. Due to the high accordance in gene and miRNA occurence of patient samples and cell lines, KASUMI-1 and NB4 represent useful AML models, to reflect possible regulatory interactions between Argonaute-miRNA complexes and their target-mRNAs of both, AML and APL.

5.5 More potential candidates for further experimental validations

The Argonaute-complex-pathway networks display putative, regulatory Argonaute-miRNA-mRNA interactions in AML cell lines, which could be used for subsequent experimentally validation of miRNAs and their target-mRNAs, in order to confirm potential regulatory mechanisms, characterisyzed in section 5.4. Thereby, the putative regulation of single mutated gene products in AML-relevant pathways, described above, represents a small part of possible regulatory interactions. Frequent, receptor tyrosine kinase (RTK) signaling pathways play a central role in the pathogenesis of AML. Therefore, the focus often lies on targeting RTKs like KIT, PI3K or MAPK. The MAPK signaling cascade is constitutively activated in a high proportion of AML cases mediated by *RAS* mutations like *NRAS, KRAS* or *HRAS* (Bowen *et al.*, 2005). In NB4 cells, *KRAS* and *HRAS* were expressed at lower level, thereby *KRAS* seems to be regulated by Ago2 and Ago3 and *HRAS* by Ago4 only, suggesting that these oncogenes could be delimited reduced in their expression to prevent further leukemogenesis (Figure 4.12.3.III).

Further interesting candidates for experimental verification are KIT, MYC or PTEN. It is known that the fusion oncogene *AML1-ETO* alone is not sufficient to induce AML (Wang *et al.*, 2011). Abnormalities in genes encoding transcription factors and tyrosine kinases represent two additional classes of most frequent events in human leukemias (Wang *et al.*, 2005). For instance, studies in patients have demonstrated that the frequency of *KIT* (receptor tyrosine kinase) mutations can be as high as 48% of AML patients with t(8;21) (Wang *et al.*, 2011). A gain-of-function point mutation has been reported also for the KASUMI-1 cell line (Martelli *et al.,* 2006). In KASUMI-1 cells, the *KIT* transcript possesses a very high association and is bound to all four Argonaute proteins, in cooperation with up to six sequence-groups of Ago-associated miRNAs. Due to the important role of *KIT* in the development of leukemogenesis, this gene appears to be under stringent inhibitory control, and is a predestinated candidate for subsequent experimental validations.

In addition, the oncoprotein MYC was clearly induced by the fusion protein AML1-ETO (Muller-Tidow *et al.*, 2004) and was only found with high expression in KASUMI-1 cells to be regulated by Ago2 and Ago3. This gene plays a role in cell cycle progression, apoptosis and cellular transformation. It functions as important transcription factor and was associated with a variety of hematopoietic tumors or leukemias, and therefore, it is a promising candidate for further regulatory and pathogenic investigations.

In addition, PTEN is a tumor suppressor, which is mutated in a large number of cancers at high frequency. A recent study highlighted that PTEN phosphorylation was present in approximately 75% of AML patients, and associated with shorter overall survival (Cheong *et al.*, 2003). The *PTEN* transcript was identified in association with Ago2 in KASUMI-1 cells, and offers binding sites for several miRNAs of the sequence-groups, seqgrp-miR-15a, -16 and -339-5p. Thus, PTEN seems to be another potential candidate for further experimental validations.

Moreover, in t(8;21) the AML1-ETO fusion transcript represses wild-type *AML1* (*RUNX1*), which is a crucial transcription factor for hematopoiesis (Wang *et al.*, 2005). Thus, AML1-ETO behaves like a classical transcriptional repressor. This fusion transcript itself could not be analyzed using the standard microarray technology, but in the network model (Figure 4.12.3.I and Figure 4.12.3.II) of the AML and APL cell lines, more informations about the regulation of the tumor suppressor *AML1* are available. In both cell lines, this gene is complexed by Ago2 in cooperation with several miRNA sequence-groups, for example seqgrp-miR-23a, -27a, -30a, -30b and -17, indicating that a great fraction of wild-type *AML1* will be repressed in their translation in both, AML and APL. Recently, it was shown that the transfection with miRNA miR-17-5p, in fact, suppresses AML1 protein expression (Fontana *et al.*, 2007). This multilateral repression of *AML1* presents a further hint for AML pathogenesis, and the network model of Figure 4.12.3.I provides an overview of these, already known and still unknown, regulatory interactions. For instance, not much is known about the regulation of the ETO (RUNX1T1) repressor protein by miRNAs. As shown in the network model of KASUMI-1, the corresponding transcript is regulated by Ago2 and Ago4 in cooperation with several miRNAs, including miR-146a, which was identified as up-regulated in t(8;21)-positive, pediatric AML patients. This provides an indication for a putative down-regulation of the transcription regulator gene *ETO,* due to the abnormally high expression of miR-146a in AML. This probably leads to abnormal regulation of several downstream transcription factors involved in transcriptional repression. In contrast, the *ETO*

transcript could not be identified in the APL cell line, but instead, the *RARα* gene, representing the second part of the fusion oncogene *PML-RARα* of t(15;17)-positive AML cells. This gene was identified in association with Ago2 and Ago3 in cooperation with miR-27a. *RARα* represents a nuclear retinoic acid receptor and the encoded protein, retinoic acid receptor alpha, regulates transcription, regulation of development, differentiation and apoptosis (Entrez Gene summary), and the misregulation of this gene probably contributes to AML leukemogenesis as well. The transcription factor and tumor suppressor *PML* could not be identified in the KASUMI-1 and NB4 cell lines and therefore, it is not regulated by Argonaute proteins in APL.

5.6 Conclusions

In general, the level of activation of each of these pathways has been studied on only a small number of patients and has not determined the activation state of the other signal transduction pathways. The frequency of activation of multiple pathways and the prognostic relevance of this activation in AML is largely unkown (Kornblau *et al.*, 2006). As many as 50% of AML cases show that activating kinase mutations confer a proliferative and survival advantage to hematopoietic progenitors (Tallman *et al.,* 2005). This was also shown in this thesis, due to the negative regulation of distinct genes in AML-relevant pathways by miRNAs. This indicates that simultaneous activation of multiple signal pathways is triggered by various mechanisms like mutations in phosphatases, which commonly control activation of several signaling pathways, or even aberrant expression of miRNAs, leading to gene-silencing. This can also influence activation of these pathways, as miRNAs have diverse roles in development and pathogenesis of AML. However, there are a few studies only, demonstrating the relationship between AML subtypes, their oncogenes like *AML1-ETO* and *PML-RARα*, distinct miRNAs (overexpressed in AML or possibly repressed by these oncogenes), and genes which are up-regulated or down-regulated, due to miRNA binding leading to leukemogenesis. Additionally, it is known that each miRNA is able to regulate hundreds of targets, and it still remains a major challenge to identify and characterize all of these miRNA targets and their potential biological roles in AML, in order to understand the entire development of this disease. Therefore, this thesis describes a novel method for the global identification of miRNAs and mRNAs associated with the four human Argonaute protein complexes, and reveals a useful tool for the description of potential regulatory mechanisms in AML pathways, and the directed selection of miRNAs and their putative target-mRNAs for subsequent experimental validations. In addition, the vast majority of AML patients can be individually characterized based on distinct chromosomal aberrations and molecular markers such as miRNAs, which function as biomarkers in adult and pediatric patients (shown in this work), but treatment is still based on unspecific therapy. For a long time, directed therapy was available for APL only (Haferlach, 2008), and classical chemotherapy often remains the most used anti-cancer therapy for many different types of cancer. On this account, an increasing potential of known genetic markers and increased knowledge about altered signaling pathways in AML are needed. The network models, generated in this work, describe the function of miRNAs as biomarkers and regulatory influences of miRNAs in signaling pathways, activated in AML, providing the background and starting point for novel targeted concepts and various strategies for more specific therapies.

5.7 Outlook

Frequently activated pathways in AML are influenced by miRNA triggered gene-silencing, in which Ago-associated mRNAs could be silenced by any miRNA that is associated in the same Argonaute complex. Thus, it remains a great challenge to confirm all interactions between miRNAs and their target-mRNAs in activated signaling pathways in AML, in order to get more insights into leukemogenesis. Up to now, several approaches exist for elucidation of individual miRNA-mRNA interactions. One possibility is the overexpression or inhibition of a particular miRNA and the identification of the transcripts joining or disappearing from the pool of Argonaute-associated mRNAs upon overexpression or inhibition. For further analysis of single transcripts that altered in their expression, dual-luciferase reporter assays could be performed to prove the connection between the overexpressed or inhibited miRNA and the selected target-mRNA. Thus, distinct regulatory mechanisms potentially involved in AML pathogenesis could be validated.

A slightly different approach could be the directed down-regulation of known "oncogenic" miRNAs or the direct up-regulation of known "tumor suppressor" miRNAs in AML. Two approaches have been tested for inhibition of the levels of miRNAs using short oligonucleotides complementary to miRNAs, called antagomir (Krutzfeldt *et al.*, 2005) or using long hairpin RNAs, termed miRNA sponges (Ebert and Sharp, 2010). To achieve efficient blocking of a single miRNA, antagomirs, offering complementary sequence to the miRNA, could be transferred into cells, in order to bind and block the miRNA by base pairing (Krutzfeldt *et al.*, 2005). Sponge-RNAs are synthetic RNAs containing multiple binding sites for a miRNA of interest, and are produced from transfected plasmids within cells. As with most miRNA target genes, sponge binding sites are specific to the miRNA seed region, which allows them to block a whole family of related miRNAs (Ebert and Sharp, 2010). In contrast, elevating the level of endogenous miRNAs could be achieved by transfection of exogenous, synthetic miRNAs into the cell, or with DNA constructs that code for synthetic miRNAs (Li *et al.*, 2010). Thus, inhibitory effects performed by miRNAs, which activate or repress AML-relevant pathways, will be compensated and possibly counteract leukemogenesis.

6 References

Aguda, B.D., Kim, Y., Piper-Hunter, M.G., Friedman, A., and Marsh, C.B. (2008). MicroRNA regulation of a cancer network: consequences of the feedback loops involving miR-17-92, E2F, and Myc. Proc Natl Acad Sci U S A *105*, 19678-19683.

Ambros, V. (2004). The functions of animal microRNAs. Nature *431*, 350-355.

Aravin, A., Gaidatzis, D., Pfeffer, S., Lagos-Quintana, M., Landgraf, P., Iovino, N., Morris, P., Brownstein, M.J., Kuramochi-Miyagawa, S., Nakano, T.*, et al.* (2006). A novel class of small RNAs bind to MILI protein in mouse testes. Nature *442*, 203-207.

Asou, H., Tashiro, S., Hamamoto, K., Otsuji, A., Kita, K., and Kamada, N. (1991). Establishment of a human acute myeloid leukemia cell line (Kasumi-1) with 8;21 chromosome translocation. Blood *77*, 2031-2036.

Austin, T.W., Solar, G.P., Ziegler, F.C., Liem, L., and Matthews, W. (1997). A role for the Wnt gene family in hematopoiesis: expansion of multilineage progenitor cells. Blood *89*, 3624-3635.

Azuma-Mukai, A., Oguri, H., Mituyama, T., Qian, Z.R., Asai, K., Siomi, H., and Siomi, M.C. (2008). Characterization of endogenous human Argonautes and their miRNA partners in RNA silencing. Proc Natl Acad Sci U S A *105*, 7964-7969.

Baek, D., Villen, J., Shin, C., Camargo, F.D., Gygi, S.P., and Bartel, D.P. (2008). The impact of microRNAs on protein output. Nature *455*, 64-71.

Baltimore, D., Boldin, M.P., O'Connell, R.M., Rao, D.S., and Taganov, K.D. (2008). MicroRNAs: new regulators of immune cell development and function. Nat Immunol *9*, 839-845.

Bartel, D.P. (2004). MicroRNAs: genomics, biogenesis, mechanism, and function. Cell *116*, 281-297.

Bartel, D.P., and Chen, C.Z. (2004). Micromanagers of gene expression: the potentially widespread influence of metazoan microRNAs. Nat Rev Genet *5*, 396-400.

Basyuk, E., Suavet, F., Doglio, A., Bordonne, R., and Bertrand, E. (2003). Human let-7 stem-loop precursors harbor features of RNase III cleavage products. Nucleic Acids Res *31*, 6593-6597.

Becker, H., Marcucci, G., Maharry, K., Radmacher, M.D., Mrozek, K., Margeson, D., Whitman, S.P., Wu, Y.Z., Schwind, S., Paschka, P.*, et al.* (2010). Favorable prognostic impact of NPM1 mutations in older patients with cytogenetically normal de novo acute myeloid leukemia and associated gene- an microRNA-expression signatures: a Cancer and Leukemia Group B study. J Clin Oncol *28*, 596-604.

Behm-Ansmant, I., Rehwinkel, J., Doerks, T., Stark, A., Bork, P., and Izaurralde, E. (2006). mRNA degradation by miRNAs and GW182 requires both CCR4:NOT deadenylase and DCP1:DCP2 decapping complexes. Genes Dev *20*, 1885-1898.

Beitzinger, M., Peters, L., Zhu, J.Y., Kremmer, E., and Meister, G. (2007). Identification of human microRNA targets from isolated argonaute protein complexes. RNA Biol *4*, 76-84.

Bentwich, I., Avniel, A., Karov, Y., Aharonov, R., Gilad, S., Barad, O., Barzilai, A., Einat, P., Einav, U., Meiri, E.*, et al.* (2005). Identification of hundreds of conserved and nonconserved human microRNAs. Nat Genet *37*, 766-770.

Berezikov, E., Guryev, V., van de Belt, J., Wienholds, E., Plasterk, R.H., and Cuppen, E. (2005). Phylogenetic shadowing and computational identification of human microRNA genes. Cell *120*, 21-24.

Berezikov, E., Thuemmler, F., van Laake, L.W., Kondova, I., Bontrop, R., Cuppen, E., and Plasterk, R.H. (2006). Diversity of microRNAs in human and chimpanzee brain. Nat Genet *38*, 1375-1377.

Betel, D., Koppal, A., Agius, P., Sander, C., and Leslie, C. (2010). Comprehensive modeling of microRNA targets predicts functional non-conserved and non-canonical sites. Genome Biol *11*, R90.

Betel, D., Wilson, M., Gabow, A., Marks, D.S., and Sander, C. (2008). The microRNA.org resource: targets and expression. Nucleic Acids Res *36*, D149-153.

Bissels, U., Wild, S., Tomiuk, S., Holste, A., Hafner, M., Tuschl, T., and Bosio, A. (2009). Absolute quantification of microRNAs by using a universal reference. RNA *15*, 2375-2384.

Blaszczyk, J., Tropea, J.E., Bubunenko, M., Routzahn, K.M., Waugh, D.S., Court, D.L., and Ji, X. (2001). Crystallographic and modeling studies of RNase III suggest a mechanism for double-stranded RNA cleavage. Structure *9*, 1225-1236.

Blum, H., Beier, H., and Gross, H.J. (1987). Imporved Silver Staining of Plant Proteins, RNA and DNA in Polyacrylamide gels. Electrophoresis *8*, 93-99.

Bolstad, B.M., Irizarry, R.A., Astrand, M., and Speed, T.P. (2003). A comparison of normalization methods for high density oligonucleotide array data based on variance and bias. Bioinformatics *19*, 185-193.

Bousquet, M., Quelen, C., Rosati, R., Mansat-De Mas, V., La Starza, R., Bastard, C., Lippert, E., Talmant, P., Lafage-Pochitaloff, M., Leroux, D.*, et al.* (2008). Myeloid cell differentiation arrest by miR-125b-1 in myelodysplastic syndrome and acute myeloid leukemia with the t(2;11)(p21;q23) translocation. J Exp Med *205*, 2499-2506.

Bousquet, M., Harris, M.H., Zhou, B., and Lodish, H.F. (2010). MicroRNA miR-125b causes leukemia. Proc Natl Acad Sci U S A *107*, 21558-21563.

Bowen, D.T., Frew, M.E., Hills, R., Gale, R.E., Wheatley, K., Groves, M.J., Langabeer, S.E., Kottaridis, P.D., Moorman, A.V., Burnett, A.K.*, et al.* (2005). RAS mutation in acute myeloid leukemia is associated with distinct cytogenetic subgroups but does not influence outcome in patients younger than 60 years. Blood *106*, 2113-2119.

Brannon, M., Gomperts, M., Sumoy, L., Moon, R.T., and Kimelman, D. (1997). A beta-catenin/XTcf-3 complex binds to the siamois promoter to regulate dorsal axis specification in Xenopus. Genes Dev *11*, 2359-2370.

Brazil, D.P., Yang, Z.Z., and Hemmings, B.A. (2004). Advances in protein kinase B signalling: AKTion on multiple fronts. Trends Biochem Sci *29*, 233-242.

Brennecke, J., Stark, A., Russell, R.B., and Cohen, S.M. (2005). Principles of microRNA-target recognition. PLoS Biol *3*, e85.

Brueckner, B., Stresemann, C., Kuner, R., Mund, C., Musch, T., Meister, M., Sultmann, H., and Lyko, F. (2007). The human let-7a-3 locus contains an epigenetically regulated microRNA gene with oncogenic function. Cancer Res *67*, 1419-1423.

Burgler, C., and Macdonald, P.M. (2005). Prediction and verification of microRNA targets by MovingTargets, a highly adaptable prediction method. BMC Genomics *6*, 88.

Caldas, C., and Brenton, J.D. (2005). Sizing up miRNAs as cancer genes. Nat Med *11*, 712-714.

Calin, G.A., Dumitru, C.D., Shimizu, M., Bichi, R., Zupo, S., Noch, E., Aldler, H., Rattan, S., Keating, M., Rai, K.*, et al.* (2002). Frequent deletions and down-regulation of micro-RNA genes miR15 and miR16 at 13q14 in chronic lymphocytic leukemia. Proc Natl Acad Sci U S A *99*, 15524-15529.

Calin, G.A., Sevignani, C., Dumitru, C.D., Hyslop, T., Noch, E., Yendamuri, S., Shimizu, M., Rattan, S., Bullrich, F., Negrini, M.*, et al.* (2004). Human microRNA genes are frequently located at fragile sites and genomic regions involved in cancers. Proc Natl Acad Sci U S A *101*, 2999-3004.

Cao, X., Yeo, G., Muotri, A.R., Kuwabara, T., and Gage, F.H. (2006). Noncoding RNAs in the mammalian central nervous system. Annu Rev Neurosci *29*, 77-103.

Cerutti, L., Mian, N., and Bateman, A. (2000). Domains in gene silencing and cell differentiation proteins: the novel PAZ domain and redefinition of the Piwi domain. Trends Biochem Sci *25*, 481-482.

Chan, J.A., Krichevsky, A.M., and Kosik, K.S. (2005). MicroRNA-21 is an antiapoptotic factor in human glioblastoma cells. Cancer Res *65*, 6029-6033.

Cheloufi, S., Dos Santos, C.O., Chong, M.M., and Hannon, G.J. (2010). A dicer-independent miRNA biogenesis pathway that requires Ago catalysis. Nature *465*, 584-589.

Chen, K., and Rajewsky, N. (2006). Natural selection on human microRNA binding sites inferred from SNP data. Nat Genet *38*, 1452-1456.

Chendrimada, T.P., Finn, K.J., Ji, X., Baillat, D., Gregory, R.I., Liebhaber, S.A., Pasquinelli, A.E., and Shiekhattar, R. (2007). MicroRNA silencing through RISC recruitment of eIF6. Nature *447*, 823-828.

Cheong, J.W., Eom, J.I., Maeng, H.Y., Lee, S.T., Hahn, J.S., Ko, Y.W., and Min, Y.H. (2003). Phosphatase and tensin homologue phosphorylation in the C-terminal regulatory domain is frequently observed in acute myeloid leukaemia and associated with poor clinical outcome. Br J Haematol *122*, 454-456.

Chi, S.W., Zang, J.B., Mele, A., and Darnell, R.B. (2009). Argonaute HITS-CLIP decodes microRNA-mRNA interaction maps. Nature *460*, 479-486.

Coller, J., and Parker, R. (2004). Eukaryotic mRNA decapping. Annu Rev Biochem *73*, 861-890.

Creutzig, U., and Reinhardt, D. (2006). Akute myeloische Leukämien. In Pädiatrische Hämatologie und Onkologie Berlin, Heidelberg, New York, H. Gadner, Gaedicke G, Niemeyer C, Ritter J, ed. (Springer Verlag), pp. 690-714.

Creutzig, U., Zimmermann, M., Ritter, J., Reinhardt, D., Hermann, J., Henze, G., Jurgens, H., Kabisch, H., Reiter, A., Riehm, H.*, et al.* (2005). Treatment strategies and long-term results in paediatric patients treated in four consecutive AML-BFM trials. Leukemia *19*, 2030-2042.

Dews, M., Homayouni, A., Yu, D., Murphy, D., Sevignani, C., Wentzel, E., Furth, E.E., Lee, W.M., Enders, G.H., Mendell, J.T.*, et al.* (2006). Augmentation of tumor angiogenesis by a Myc-activated microRNA cluster. Nat Genet *38*, 1060-1065.

Didiano, D., and Hobert, O. (2006). Perfect seed pairing is not a generally reliable predictor for miRNA-target interactions. Nat Struct Mol Biol *13*, 849-851.

Dixon-McIver, A., East, P., Mein, C.A., Cazier, J.B., Molloy, G., Chaplin, T., Andrew Lister, T., Young, B.D., and Debernardi, S. (2008). Distinctive patterns of microRNA expression associated with karyotype in acute myeloid leukaemia. PLoS One *3*, e2141.

Doench, J.G., and Sharp, P.A. (2004). Specificity of microRNA target selection in translational repression. Genes Dev *18*, 504-511.

Doepfner, K.T., Boller, D., and Arcaro, A. (2007). Targeting receptor tyrosine kinase signaling in acute myeloid leukemia. Crit Rev Oncol Hematol *63*, 215-230.

Drexler, H.G., MacLeod, R.A., Borkhardt, A., and Janssen, J.W. (1995a). Recurrent chromosomal translocations and fusion genes in leukemia-lymphoma cell lines. Leukemia *9*, 480-500.

Drexler, H.G., Quentmeier, H., MacLeod, R.A., Uphoff, C.C., and Hu, Z.B. (1995b). Leukemia cell lines: in vitro models for the study of acute promyelocytic leukemia. Leuk Res *19*, 681-691.

Dreyfuss, G., Choi, Y.D., and Adam, S.A. (1984). Characterization of heterogeneous nuclear RNA-protein complexes in vivo with monoclonal antibodies. Mol Cell Biol *4*, 1104-1114.

Duprez, E., Ruchaud, S., Houge, G., Martin-Thouvenin, V., Valensi, F., Kastner, P., Berger, R., and Lanotte, M. (1992). A retinoid acid 'resistant' t(15;17) acute promyelocytic leukemia cell line: isolation, morphological, immunological, and molecular features. Leukemia *6*, 1281-1287.

Ebert, M.S., and Sharp, P.A. (2010). MicroRNA sponges: progress and possibilities. RNA *16*, 2043-2050.

Elagib, K.E., and Goldfarb, A.N. (2007). Oncogenic pathways of AML1-ETO in acute myeloid leukemia: multifaceted manipulation of marrow maturation. Cancer Lett *251*, 179-186.

Enright, A.J., John, B., Gaul, U., Tuschl, T., Sander, C., and Marks, D.S. (2003). MicroRNA targets in Drosophila. Genome Biol *5*, R1.

Entz-Werle, N., Suciu, S., van der Werff ten Bosch, J., Vilmer, E., Bertrand, Y., Benoit, Y., Margueritte, G., Plouvier, E., Boutard, P., Vandecruys, E.*, et al.* (2005). Results of 58872 and 58921 trials in acute myeloblastic leukemia and relative value of chemotherapy vs allogeneic bone marrow transplantation in first complete remission: the EORTC Children Leukemia Group report. Leukemia *19*, 2072-2081.

Eulalio, A., Behm-Ansmant, I., and Izaurralde, E. (2007). P bodies: at the crossroads of post-transcriptional pathways. Nat Rev Mol Cell Biol *8*, 9-22.

Eulalio, A., Huntzinger, E., and Izaurralde, E. (2008). GW182 interaction with Argonaute is essential for miRNA-mediated translational repression and mRNA decay. Nat Struct Mol Biol *15*, 346-353.

Fabian, M.R., Sonenberg, N., and Filipowicz, W. (2010). Regulation of mRNA translation and stability by microRNAs. Annu Rev Biochem *79*, 351-379.

Fazi, F., Rosa, A., Fatica, A., Gelmetti, V., De Marchis, M.L., Nervi, C., and Bozzoni, I. (2005). A minicircuitry comprised of microRNA-223 and transcription factors NFI-A and C/EBPalpha regulates human granulopoiesis. Cell *123*, 819-831.

Fazi, F., Racanicchi, S., Zardo, G., Starnes, L.M., Mancini, M., Travaglini, L., Diverio, D., Ammatuna, E., Cimino, G., Lo-Coco, F.*, et al.* (2007). Epigenetic silencing of the myelopoiesis regulator microRNA-223 by the AML1/ETO oncoprotein. Cancer Cell *12*, 457-466.

Fielden, M.R., Halgren, R.G., Dere, E., and Zacharewski, T.R. (2002). GP3: GenePix post-processing program for automated analysis of raw microarray data. Bioinformatics *18*, 771-773.

Filipowicz, W., Bhattacharyya, S.N., and Sonenberg, N. (2008). Mechanisms of post-transcriptional regulation by microRNAs: are the answers in sight? Nat Rev Genet *9*, 102-114.

Filippov, V., Solovyev, V., Filippova, M., and Gill, S.S. (2000). A novel type of RNase III family proteins in eukaryotes. Gene *245*, 213-221.

Fire, A., Xu, S., Montgomery, M.K., Kostas, S.A., Driver, S.E., and Mello, C.C. (1998). Potent and specific genetic interference by double-stranded RNA in Caenorhabditis elegans. Nature *391*, 806-811.

Fontana, L., Pelosi, E., Greco, P., Racanicchi, S., Testa, U., Liuzzi, F., Croce, C.M., Brunetti, E., Grignani, F., and Peschle, C. (2007). MicroRNAs 17-5p-20a-106a control monocytopoiesis through AML1 targeting and M-CSF receptor upregulation. Nat Cell Biol *9*, 775-787.

Fridman, J.S., and Lowe, S.W. (2003). Control of apoptosis by p53. Oncogene *22*, 9030-9040.

Friedman, R.C., Farh, K.K., Burge, C.B., and Bartel, D.P. (2009). Most mammalian mRNAs are conserved targets of microRNAs. Genome Res *19*, 92-105.

Frohling, S., and Dohner, H. (2008). Chromosomal abnormalities in cancer. N Engl J Med *359*, 722-734.

Gaidatzis, D., van Nimwegen, E., Hausser, J., and Zavolan, M. (2007). Inference of miRNA targets using evolutionary conservation and pathway analysis. BMC Bioinformatics *8*, 69.

Garzon, R., and Croce, C.M. (2008). MicroRNAs in normal and malignant hematopoiesis. Curr Opin Hematol *15*, 352-358.

Garzon, R., Volinia, S., Liu, C.G., Fernandez-Cymering, C., Palumbo, T., Pichiorri, F., Fabbri, M., Coombes, K., Alder, H., Nakamura, T.*, et al.* (2008b). MicroRNA signatures associated with cytogenetics and prognosis in acute myeloid leukemia. Blood *111*, 3183-3189.

Gibson, B.E., Wheatley, K., Hann, I.M., Stevens, R.F., Webb, D., Hills, R.K., De Graaf, S.S., and Harrison, C.J. (2005). Treatment strategy and long-term results in paediatric patients treated in consecutive UK AML trials. Leukemia *19*, 2130-2138.

Gilliland, D.G., and Tallman, M.S. (2002). Focus on acute leukemias. Cancer Cell *1*, 417-420.

Gilliesand JK, L.I. (2007). Regulation of p27Kip1 by miRNA 221/222 in glioblastoma. Cell Cycle *6*.

Golub, T.R., Slonim, D.K., Tamayo, P., Huard, C., Gaasenbeek, M., Mesirov, J.P., Coller, H., Loh, M.L., Downing, J.R., Caligiuri, M.A.*, et al.* (1999). Molecular classification of cancer: class discovery and class prediction by gene expression monitoring. Science *286*, 531-537.

Gonzalez-Gonzalez, E., Lopez-Casas, P.P., and del Mazo, J. (2008). The expression patterns of genes involved in the RNAi pathways are tissue-dependent and differ in the germ and somatic cells of mouse testis. Biochim Biophys Acta *1779*, 306-311.

Greenberg, J.R. (1979). Ultraviolet light-induced crosslinking of mRNA to proteins. Nucleic Acids Res *6*, 715-732.

Gregory, R.I., and Shiekhattar, R. (2005). MicroRNA biogenesis and cancer. Cancer Res *65*, 3509-3512.

Griffiths-Jones, S. (2004). The microRNA Registry. Nucleic Acids Res *32*, D109-111.

Griffiths-Jones, S. (2006). miRBase: the microRNA sequence database. Methods Mol Biol *342*, 129-138.

Griffiths-Jones, S., Saini, H.K., van Dongen, S., and Enright, A.J. (2008). miRBase: tools for microRNA genomics. Nucleic Acids Res *36*, D154-158.

Grimm, D., Wang, L., Lee, J.S., Schurmann, N., Gu, S., Borner, K., Storm, T.A., and Kay, M.A. (2010). Argonaute proteins are key determinants of RNAi efficacy, toxicity, and persistence in the adult mouse liver. J Clin Invest *120*, 3106-3119.

Grimson, A., Farh, K.K., Johnston, W.K., Garrett-Engele, P., Lim, L.P., and Bartel, D.P. (2007). MicroRNA targeting specificity in mammals: determinants beyond seed pairing. Mol Cell *27*, 91-105.

Gross, J.L., Behrens, D.L., Mullins, D.E., Kornblith, P.L., and Dexter, D.L. (1988). Plasminogen activator and inhibitor activity in human glioma cells and modulation by sodium butyrate. Cancer Res *48*, 291-296.

Grun, D., Wang, Y.L., Langenberger, D., Gunsalus, K.C., and Rajewsky, N. (2005). microRNA target predictions across seven Drosophila species and comparison to mammalian targets. PLoS Comput Biol *1*, e13.

Haferlach, T. (2008). Molecular genetic pathways as therapeutic targets in acute myeloid leukemia. Hematology Am Soc Hematol Educ Program, 400-411.

Hafner, M., Landthaler, M., Burger, L., Khorshid, M., Hausser, J., Berninger, P., Rothballer, A., Ascano, M., Jr., Jungkamp, A.C., Munschauer, M.*, et al.* (2010a). Transcriptome-wide identification of RNA-binding protein and microRNA target sites by PAR-CLIP. Cell *141*, 129-141.

Hafner, M., Landthaler, M., Burger, L., Khorshid, M., Hausser, J., Berninger, P., Rothballer, A., Ascano, M., Jungkamp, A.C., Munschauer, M.*, et al.* (2010b). PAR-CliP--a method to identify transcriptome-wide the binding sites of RNA binding proteins. J Vis Exp.

Hall, G.W. (2001). Childhood myeloid leukaemias. Best Pract Res Clin Haematol *14*, 573-591.

Hanada, M., Feng, J., and Hemmings, B.A. (2004). Structure, regulation and function of PKB/AKT--a major therapeutic target. Biochim Biophys Acta *1697*, 3-16.

Harris, S.L., and Levine, A.J. (2005). The p53 pathway: positive and negative feedback loops. Oncogene *24*, 2899-2908.

He, L., He, X., Lim, L.P., de Stanchina, E., Xuan, Z., Liang, Y., Xue, W., Zender, L., Magnus, J., Ridzon, D.*, et al.* (2007). A microRNA component of the p53 tumour suppressor network. Nature *447*, 1130-1134.

Henke, J.I., Goergen, D., Zheng, J., Song, Y., Schuttler, C.G., Fehr, C., Junemann, C., and Niepmann, M. (2008). microRNA-122 stimulates translation of hepatitis C virus RNA. EMBO J *27*, 3300-3310.

Henson, B.J., Bhattacharjee, S., O'Dee, D.M., Feingold, E., and Gollin, S.M. (2009). Decreased expression of miR-125b and miR-100 in oral cancer cells contributes to malignancy. Genes Chromosomes Cancer *48*, 569-582.

Hock, J., and Meister, G. (2008). The Argonaute protein family. Genome Biol *9*, 210.

Humphreys, D.T., Westman, B.J., Martin, D.I., and Preiss, T. (2005). MicroRNAs control translation initiation by inhibiting eukaryotic initiation factor 4E/cap and poly(A) tail function. Proc Natl Acad Sci U S A *102*, 16961-16966.

Ibanez-Ventoso, C., Vora, M., and Driscoll, M. (2008). Sequence relationships among C. elegans, D. melanogaster and human microRNAs highlight the extensive conservation of microRNAs in biology. PLoS One *3*, e2818.

Ihaka, R., and Gentleman, R. (1996). R: A Language for Data Analysis and Graphics. Journal of Computational and Graphical Statistics *5*, 299-314.

Iorio, M.V., Casalini, P., Tagliabue, E., Menard, S., and Croce, C.M. (2008). MicroRNA profiling as a tool to understand prognosis, therapy response and resistance in breast cancer. Eur J Cancer *44*, 2753-2759.

Jan, C.H., Friedman, R.C., Ruby, J.G., and Bartel, D.P. (2011). Formation, regulation and evolution of Caenorhabditis elegans 3'UTRs. Nature *469*, 97-101.

Jensen, K.B., and Darnell, R.B. (2008). CLIP: crosslinking and immunoprecipitation of in vivo RNA targets of RNA-binding proteins. Methods Mol Biol *488*, 85-98.

Jinek, M., and Doudna, J.A. (2009). A three-dimensional view of the molecular machinery of RNA interference. Nature *457*, 405-412.

John B, E.A., Aravin A, Tushl T, Sander C, Marks DS (2005). miRanda application: Human MicroRNA targets. Plos Biol *3*.

John, B., Enright, A.J., Aravin, A., Tuschl, T., Sander, C., and Marks, D.S. (2004). Human MicroRNA targets. PLoS Biol *2*, e363.

Jongen-Lavrencic, M., Sun, S.M., Dijkstra, M.K., Valk, P.J., and Lowenberg, B. (2008). MicroRNA expression profiling in relation to the genetic heterogeneity of acute myeloid leukemia. Blood *111*, 5078-5085.

Kaneda, M., Tang, F., O'Carroll, D., Lao, K., and Surani, M.A. (2009). Essential role for Argonaute2 protein in mouse oogenesis. Epigenetics Chromatin *2*, 9.

Kanehisa, M. (1996). Toward Pathway Engineering: A New Database of Genetic and Molecular Pathways. Science & Technology Japan *59*, 34-38.

Kaspers, G.J., and Zwaan, C.M. (2007). Pediatric acute myeloid leukemia: towards high-quality cure of all patients. Haematologica *92*, 1519-1532.

Kedde, M., Strasser, M.J., Boldajipour, B., Oude Vrielink, J.A., Slanchev, K., le Sage, C., Nagel, R., Voorhoeve, P.M., van Duijse, J., Orom, U.A.*, et al.* (2007). RNA-binding protein Dnd1 inhibits microRNA access to target mRNA. Cell *131*, 1273-1286.

Keene, J.D., Komisarow, J.M., and Friedersdorf, M.B. (2006). RIP-Chip: the isolation and identification of mRNAs, microRNAs and protein components of ribonucleoprotein complexes from cell extracts. Nat Protoc *1*, 302-307.

Kertesz, M., Iovino, N., Unnerstall, U., Gaul, U., and Segal, E. (2007). The role of site accessibility in microRNA target recognition. Nat Genet *39*, 1278-1284.

Khvorova, A., Reynolds, A., and Jayasena, S.D. (2003). Functional siRNAs and miRNAs exhibit strand bias. Cell *115*, 209-216.

Kiriakidou, M., Tan, G.S., Lamprinaki, S., De Planell-Saguer, M., Nelson, P.T., and Mourelatos, Z. (2007). An mRNA m7G cap binding-like motif within human Ago2 represses translation. Cell *129*, 1141-1151.

Kloosterman, W.P., Wienholds, E., Ketting, R.F., and Plasterk, R.H. (2004). Substrate requirements for let-7 function in the developing zebrafish embryo. Nucleic Acids Res *32*, 6284-6291.

Klusmann, J.H., Li, Z., Bohmer, K., Maroz, A., Koch, M.L., Emmrich, S., Godinho, F.J., Orkin, S.H., and Reinhardt, D. (2010). miR-125b-2 is a potential oncomiR on human chromosome 21 in megakaryoblastic leukemia. Genes Dev *24*, 478-490.

Kornblau, S.M., Womble, M., Qiu, Y.H., Jackson, C.E., Chen, W., Konopleva, M., Estey, E.H., and Andreeff, M. (2006). Simultaneous activation of multiple signal transduction pathways confers poor prognosis in acute myelogenous leukemia. Blood *108*, 2358-2365.

Krek, A., Grun, D., Poy, M.N., Wolf, R., Rosenberg, L., Epstein, E.J., MacMenamin, P., da Piedade, I., Gunsalus, K.C., Stoffel, M*., et al.* (2005). Combinatorial microRNA target predictions. Nat Genet *37*, 495-500.

Krutzfeldt, J., Rajewsky, N., Braich, R., Rajeev, K.G., Tuschl, T., Manoharan, M., and Stoffel, M. (2005). Silencing of microRNAs in vivo with 'antagomirs'. Nature *438*, 685-689.

Kurreck, J. (2009). RNA interference: from basic research to therapeutic applications. Angew Chem Int Ed Engl *48*, 1378-1398.

Kula-Eversole, E., Nagoshi, E., Shang, Y., Rodriguez, J., Allada, R., and Rosbash, M. (2010). Surprising gene expression patterns within and between PDF-containing circadian neurons in Drosophila. Proc Natl Acad Sci U S A *107*, 13497-13502.

Laemmli, U.K. (1970). Cleavage of structural proteins during the assembly of the head of bacteriophage T4. Nature *227*, 680-685.

Lai, E.C. (2004). Predicting and validating microRNA targets. Genome Biol *5*, 115.

Lall, S., Grun, D., Krek, A., Chen, K., Wang, Y.L., Dewey, C.N., Sood, P., Colombo, T., Bray, N., Macmenamin, P*., et al.* (2006). A genome-wide map of conserved microRNA targets in C. elegans. Curr Biol *16*, 460-471.

Landgraf, P., Rusu, M., Sheridan, R., Sewer, A., Iovino, N., Aravin, A., Pfeffer, S., Rice, A., Kamphorst, A.O., Landthaler, M*., et al.* (2007). A mammalian microRNA expression atlas based on small RNA library sequencing. Cell *129*, 1401-1414.

Landthaler, M., Gaidatzis, D., Rothballer, A., Chen, P.Y., Soll, S.J., Dinic, L., Ojo, T., Hafner, M., Zavolan, M., and Tuschl, T. (2008). Molecular characterization of human Argonaute-containing ribonucleoprotein complexes and their bound target mRNAs. RNA *14*, 2580-2596.

Lange, B.J., Smith, F.O., Feusner, J., Barnard, D.R., Dinndorf, P., Feig, S., Heerema, N.A., Arndt, C., Arceci, R.J., Seibel, N*., et al.* (2008). Outcomes in CCG-2961, a children's oncology group phase 3 trial for untreated pediatric acute myeloid leukemia: a report from the children's oncology group. Blood *111*, 1044-1053.

Langer, C., Marcucci, G., Holland, K.B., Radmacher, M.D., Maharry, K., Paschka, P., Whitman, S.P., Mrozek, K., Baldus, C.D., Vij, R*., et al.* (2009). Prognostic importance of MN1 transcript levels, and biologic insights from MN1-associated gene and microRNA expression signatures in cytogenetically normal acute myeloid leukemia: a cancer and leukemia group B study. J Clin Oncol *27*, 3198-3204.

Lanotte, M., Martin-Thouvenin, V., Najman, S., Balerini, P., Valensi, F., and Berger, R. (1991). NB4, a maturation inducible cell line with t(15;17) marker isolated from a human acute promyelocytic leukemia (M3). Blood *77*, 1080-1086.

Lee, R.C., Feinbaum, R.L., and Ambros, V. (1993). The C. elegans heterochronic gene lin-4 encodes small RNAs with antisense complementarity to lin-14. Cell *75*, 843-854.

Lee, Y., Ahn, C., Han, J., Choi, H., Kim, J., Yim, J., Lee, J., Provost, P., Radmark, O., Kim, S*., et al.* (2003). The nuclear RNase III Drosha initiates microRNA processing. Nature *425*, 415-419.

Lee, Y., Hur, I., Park, S.Y., Kim, Y.K., Suh, M.R., and Kim, V.N. (2006). The role of PACT in the RNA silencing pathway. EMBO J *25*, 522-532.

Lee, Y., Jeon, K., Lee, J.T., Kim, S., and Kim, V.N. (2002). MicroRNA maturation: stepwise processing and subcellular localization. EMBO J *21*, 4663-4670.

Lee, Y.S., Nakahara, K., Pham, J.W., Kim, K., He, Z., Sontheimer, E.J., and Carthew, R.W. (2004). Distinct roles for Drosophila Dicer-1 and Dicer-2 in the siRNA/miRNA silencing pathways. Cell *117*, 69-81.

Lewis, B.P., Burge, C.B., and Bartel, D.P. (2005). Conserved seed pairing, often flanked by adenosines, indicates that thousands of human genes are microRNA targets. Cell *120*, 15-20.

Lewis, B.P., Shih, I.H., Jones-Rhoades, M.W., Bartel, D.P., and Burge, C.B. (2003). Prediction of mammalian microRNA targets. Cell *115*, 787-798.

Li, M., Li, J., Ding, X., He, M., and Cheng, S.Y. (2010). microRNA and cancer. AAPS J *12*, 309-317.

Li, Z., Lu, J., Sun, M., Mi, S., Zhang, H., Luo, R.T., Chen, P., Wang, Y., Yan, M., Qian, Z.*, et al.* (2008). Distinct microRNA expression profiles in acute myeloid leukemia with common translocations. Proc Natl Acad Sci U S A *105*, 15535-15540.

Licatalosi, D.D., Mele, A., Fak, J.J., Ule, J., Kayikci, M., Chi, S.W., Clark, T.A., Schweitzer, A.C., Blume, J.E., Wang, X.*, et al.* (2008). HITS-CLIP yields genome-wide insights into brain alternative RNA processing. Nature *456*, 464-469.

Lim, L.P., Lau, N.C., Garrett-Engele, P., Grimson, A., Schelter, J.M., Castle, J., Bartel, D.P., Linsley, P.S., and Johnson, J.M. (2005). Microarray analysis shows that some microRNAs downregulate large numbers of target mRNAs. Nature *433*, 769-773.

Lim, L.P., Lau, N.C., Weinstein, E.G., Abdelhakim, A., Yekta, S., Rhoades, M.W., Burge, C.B., and Bartel, D.P. (2003). The microRNAs of Caenorhabditis elegans. Genes Dev *17*, 991-1008.

Lingel, A., Simon, B., Izaurralde, E., and Sattler, M. (2003). Structure and nucleic-acid binding of the Drosophila Argonaute 2 PAZ domain. Nature *426*, 465-469.

Liu, J., Carmell, M.A., Rivas, F.V., Marsden, C.G., Thomson, J.M., Song, J.J., Hammond, S.M., Joshua-Tor, L., and Hannon, G.J. (2004). Argonaute2 is the catalytic engine of mammalian RNAi. Science *305*, 1437-1441.

Liu, J., Valencia-Sanchez, M.A., Hannon, G.J., and Parker, R. (2005). MicroRNA-dependent localization of targeted mRNAs to mammalian P-bodies. Nat Cell Biol *7*, 719-723.

Lund, E., Guttinger, S., Calado, A., Dahlberg, J.E., and Kutay, U. (2004). Nuclear export of microRNA precursors. Science *303*, 95-98.

MacRae, I.J., Ma, E., Zhou, M., Robinson, C.V., and Doudna, J.A. (2008). In vitro reconstitution of the human RISC-loading complex. Proc Natl Acad Sci U S A *105*, 512-517.

Maniataki, E., and Mourelatos, Z. (2005). Human mitochondrial tRNAMet is exported to the cytoplasm and associates with the Argonaute 2 protein. RNA *11*, 849-852.

Manola, K.N. (2009). Cytogenetics of pediatric acute myeloid leukemia. Eur J Haematol *83*, 391-405.

Marcucci, G., Maharry, K., Radmacher, M.D., Mrozek, K., Vukosavljevic, T., Paschka, P., Whitman, S.P., Langer, C., Baldus, C.D., Liu, C.G.*, et al.* (2008). Prognostic significance of, and gene and microRNA expression signatures associated with, CEBPA mutations in cytogenetically normal acute myeloid leukemia with high-risk molecular features: a Cancer and Leukemia Group B Study. J Clin Oncol *26*, 5078-5087.

Marcucci, G., Radmacher, M.D., Mrozek, K., and Bloomfield, C.D. (2009). MicroRNA expression in acute myeloid leukemia. Curr Hematol Malig Rep *4*, 83-88.

Martelli, A.M., Nyakern, M., Tabellini, G., Bortul, R., Tazzari, P.L., Evangelisti, C., and Cocco, L. (2006). Phosphoinositide 3-kinase/Akt signaling pathway and its therapeutical implications for human acute myeloid leukemia. Leukemia *20*, 911-928.

Martinez-Climent, J.A. (1997). Molecular cytogenetics of childhood hematological malignancies. Leukemia *11*, 1999-2021.

Martinez, J., Patkaniowska, A., Urlaub, H., Luhrmann, R., and Tuschl, T. (2002). Single-stranded antisense siRNAs guide target RNA cleavage in RNAi. Cell *110*, 563-574.

Mathonnet, G., Fabian, M.R., Svitkin, Y.V., Parsyan, A., Huck, L., Murata, T., Biffo, S., Merrick, W.C., Darzynkiewicz, E., Pillai, R.S.*, et al.* (2007). MicroRNA inhibition of translation initiation in vitro by targeting the cap-binding complex eIF4F. Science *317*, 1764-1767.

Mayrand, S., Setyono, B., Greenberg, J.R., and Pederson, T. (1981). Structure of nuclear ribonucleoprotein: identification of proteins in contact with poly(A)+ heterogeneous nuclear RNA in living HeLa cells. J Cell Biol *90*, 380-384.

Maziere, P., and Enright, A.J. (2007). Prediction of microRNA targets. Drug Discov Today *12*, 452-458.

Meshinchi, S., and Arceci, R.J. (2007). Prognostic factors and risk-based therapy in pediatric acute myeloid leukemia. Oncologist *12*, 341-355.

Meshinchi, S., Smith, F.O., and Arceci, R.J. (2003). Prognostic factors and risk-based therapy in pediatric acute myeloid leukemia. Curr Oncol Rep *5*, 489-497.

Mi, S., Lu, J., Sun, M., Li, Z., Zhang, H., Neilly, M.B., Wang, Y., Qian, Z., Jin, J., Zhang, Y.*, et al.* (2007). MicroRNA expression signatures accurately discriminate acute lymphoblastic leukemia from acute myeloid leukemia. Proc Natl Acad Sci U S A *104*, 19971-19976.

Mili, S., and Steitz, J.A. (2004). Evidence for reassociation of RNA-binding proteins after cell lysis: implications for the interpretation of immunoprecipitation analyses. RNA *10*, 1692-1694.

Moss, E.G., Lee, R.C., and Ambros, V. (1997). The cold shock domain protein LIN-28 controls developmental timing in C. elegans and is regulated by the lin-4 RNA. Cell *88*, 637-646.

Motoyama, K., Inoue, H., Nakamura, Y., Uetake, H., Sugihara, K., and Mori, M. (2008). Clinical significance of high mobility group A2 in human gastric cancer and its relationship to let-7 microRNA family. Clin Cancer Res *14*, 2334-2340.

Mourelatos, Z., Dostie, J., Paushkin, S., Sharma, A., Charroux, B., Abel, L., Rappsilber, J., Mann, M., and Dreyfuss, G. (2002). miRNPs: a novel class of ribonucleoproteins containing numerous microRNAs. Genes Dev *16*, 720-728.

Mrozek, K., and Bloomfield, C.D. (2006). Chromosome aberrations, gene mutations and expression changes, and prognosis in adult acute myeloid leukemia. Hematology Am Soc Hematol Educ Program, 169-177.

Mrozek, K., Heerema, N.A., and Bloomfield, C.D. (2004). Cytogenetics in acute leukemia. Blood Rev *18*, 115-136.

Muller-Tidow, C., Steffen, B., Cauvet, T., Tickenbrock, L., Ji, P., Diederichs, S., Sargin, B., Kohler, G., Stelljes, M., Puccetti, E.*, et al.* (2004). Translocation products in acute myeloid leukemia activate the Wnt signaling pathway in hematopoietic cells. Mol Cell Biol *24*, 2890-2904.

Murdoch, B., Chadwick, K., Martin, M., Shojaei, F., Shah, K.V., Gallacher, L., Moon, R.T., and Bhatia, M. (2003). Wnt-5A augments repopulating capacity and primitive hematopoietic development of human blood stem cells in vivo. Proc Natl Acad Sci U S A *100*, 3422-3427.

Nelson, P.T., Kiriakidou, M., Mourelatos, Z., Tan, G.S., Jennings, M.H., Xie, K., and Wang, W.X. (2010). High-throughput experimental studies to identify miRNA targets directly, with special focus on the mammalian brain. Brain Res *1338*, 122-130.

Nottrott, S., Simard, M.J., and Richter, J.D. (2006). Human let-7a miRNA blocks protein production on actively translating polyribosomes. Nat Struct Mol Biol *13*, 1108-1114.

O'Connell, R.M., Rao, D.S., Chaudhuri, A.A., Boldin, M.P., Taganov, K.D., Nicoll, J., Paquette, R.L., and Baltimore, D. (2008). Sustained expression of microRNA-155 in hematopoietic stem cells causes a myeloproliferative disorder. J Exp Med *205*, 585-594.

Oren, M. (2003). Decision making by p53: life, death and cancer. Cell Death Differ *10*, 431-442.

Orom, U.A., Nielsen, F.C., and Lund, A.H. (2008). MicroRNA-10a binds the 5'-UTR of ribosomal protein mRNAs and enhances their translation. Mol Cell *30*, 460-471.

Paquette, J., and Tokuyasu, T. (2010). EGAN: exploratory gene association networks.Bioinformatics *26*, 285-286.

Parker, R., and Sheth, U. (2007). P bodies and the control of mRNA translation and degradation. Mol Cell *25*, 635-646.

Pearson, G., Robinson, F., Beers Gibson, T., Xu, B.E., Karandikar, M., Berman, K., and Cobb, M.H. (2001). Mitogen-activated protein (MAP) kinase pathways: regulation and physiological functions. Endocr Rev *22*, 153-183.

Penalva, L.O., Tenenbaum, S.A., and Keene, J.D. (2004). Gene expression analysis of messenger RNP complexes. Methods Mol Biol *257*, 125-134.

Perel, Y., Auvrignon, A., Leblanc, T., Michel, G., Reguerre, Y., Vannier, J.P., Dalle, J.H., Gandemer, V., Schmitt, C., Mechinaud, F.*, et al.* (2005). Treatment of childhood acute myeloblastic leukemia: dose intensification improves outcome and maintenance therapy is of no benefit--multicenter studies of the French LAME (Leucemie Aigue Myeloblastique Enfant) Cooperative Group. Leukemia *19*, 2082-2089.

Peters, L., and Meister, G. (2007). Argonaute proteins: mediators of RNA silencing. Mol Cell *26*, 611-623.

Petersen, C.P., Bordeleau, M.E., Pelletier, J., and Sharp, P.A. (2006). Short RNAs repress translation after initiation in mammalian cells. Mol Cell *21*, 533-542.

Pillai, R.S., Bhattacharyya, S.N., Artus, C.G., Zoller, T., Cougot, N., Basyuk, E., Bertrand, E., and Filipowicz, W. (2005). Inhibition of translational initiation by Let-7 MicroRNA in human cells. Science *309*, 1573-1576.

Plasterk, R.H. (2006). Micro RNAs in animal development. Cell *124*, 877-881.

Polakis, P. (2000). Wnt signaling and cancer. Genes Dev *14*, 1837-1851.

Recher, C., Dos Santos, C., Demur, C., and Payrastre, B. (2005). mTOR, a new therapeutic target in acute myeloid leukemia. Cell Cycle *4*, 1540-1549.

Reuter, C.W., Morgan, M.A., and Bergmann, L. (2000). Targeting the Ras signaling pathway: a rational, mechanism-based treatment for hematologic malignancies? Blood *96*, 1655-1669.

Reya, T., Duncan, A.W., Ailles, L., Domen, J., Scherer, D.C., Willert, K., Hintz, L., Nusse, R., and Weissman, I.L. (2003). A role for Wnt signalling in self-renewal of haematopoietic stem cells. Nature *423*, 409-414.

Rivas, F.V., Tolia, N.H., Song, J.J., Aragon, J.P., Liu, J., Hannon, G.J., and Joshua-Tor, L. (2005). Purified Argonaute2 and an siRNA form recombinant human RISC. Nat Struct Mol Biol *12*, 340-349.

Rubnitz, J.E., Lensing, S., Zhou, Y., Sandlund, J.T., Razzouk, B.I., Ribeiro, R.C., and Pui, C.H. (2004). Death during induction therapy and first remission of acute leukemia in childhood: the St. Jude experience. Cancer *101*, 1677-1684.

Rubnitz, J.E., Raimondi, S.C., Halbert, A.R., Tong, X., Srivastava, D.K., Razzouk, B.I., Pui, C.H., Downing, J.R., Ribeiro, R.C., and Behm, F.G. (2002). Characteristics and outcome of t(8;21)-positive childhood acute myeloid leukemia: a single institution's experience. Leukemia *16*, 2072-2077.

Saha, M.N., Micallef, J., Qiu, L., and Chang, H. (2010). Pharmacological activation of the p53 pathway in haematological malignancies. J Clin Pathol *63*, 204-209.

Sasaki, T., Shiohama, A., Minoshima, S., and Shimizu, N. (2003). Identification of eight members of the Argonaute family in the human genome small star, filled. Genomics *82*, 323-330.

Scherer, W.F., Syverton, J.T., and Gey, G.O. (1953). Studies on the propagation in vitro of poliomyelitis viruses. IV. Viral multiplication in a stable strain of human malignant epithelial cells (strain HeLa) derived from an epidermoid carcinoma of the cervix. J Exp Med *97*, 695-710.

Schmitter, D., Filkowski, J., Sewer, A., Pillai, R.S., Oakeley, E.J., Zavolan, M., Svoboda, P., and Filipowicz, W. (2006). Effects of Dicer and Argonaute down-regulation on mRNA levels in human HEK293 cells. Nucleic Acids Res *34*, 4801-4815.

Schwarz, D.S., Hutvagner, G., Du, T., Xu, Z., Aronin, N., and Zamore, P.D. (2003). Asymmetry in the assembly of the RNAi enzyme complex. Cell *115*, 199-208.

Sebolt-Leopold, J.S. (2004). MEK inhibitors: a therapeutic approach to targeting the Ras-MAP kinase pathway in tumors. Curr Pharm Des *10*, 1907-1914.

Seca, H., Almeida, G.M., Guimaraes, J.E., and Vasconcelos, M.H. (2010). miR signatures and the role of miRs in acute myeloid leukaemia. Eur J Cancer *46*, 1520-1527.

Selbach, M., Schwanhausser, B., Thierfelder, N., Fang, Z., Khanin, R., and Rajewsky, N. (2008). Widespread changes in protein synthesis induced by microRNAs. Nature *455*, 58-63.

Shi, X.B., Tepper, C.G., and deVere White, R.W. (2008). Cancerous miRNAs and their regulation. Cell Cycle *7*, 1529-1538.

Shi, L., Cheng, Z., Zhang, J., Li, R., Zhao, P., Fu, Z., and You, Y. (2008b). hsa-mir-181a and hsa-mir-181b function as tumor suppressors in human glioma cells. Brain Res *1236*, 185-193.

Shibata, M., Kurokawa, D., Nakao, H., Ohmura, T., and Aizawa, S. (2008). MicroRNA-9 modulates Cajal-Retzius cell differentiation by suppressing Foxg1 expression in mouse medial pallium. J Neurosci *28*, 10415-10421.

Shikami, M., Miwa, H., Nishii, K., Kyo, T., Tanaka, I., Shiku, H., Kita, K., and Nitta, M. (2006). Low p53 expression of acute myelocytic leukemia cells with t(8;21) chromosome abnormality: association with low p14(ARF) expression. Leuk Res *30*, 379-383.

Shimada, A., Taki, T., Tabuchi, K., Tawa, A., Horibe, K., Tsuchida, M., Hanada, R., Tsukimoto, I., and Hayashi, Y. (2006). KIT mutations, and not FLT3 internal tandem duplication, are strongly associated with a poor prognosis in pediatric acute myeloid leukemia with t(8;21): a study of the Japanese Childhood AML Cooperative Study Group. Blood *107*, 1806-1809.

Shin, K.H., Bae, S.D., Hong, H.S., Kim, R.H., Kang, M.K., and Park, N.H. (2011). miR-181a shows tumor suppressive effect against oral squamous cell carcinoma cells by downregulating K-ras. Biochem Biophys Res Commun *404*, 896-902.

Shivdasani, R.A. (2006). MicroRNAs: regulators of gene expression and cell differentiation. Blood *108*, 3646-3653.

Shtutman, M., Zhurinsky, J., Oren, M., Levina, E., and Ben-Ze'ev, A. (2002). PML is a target gene of beta-catenin and plakoglobin, and coactivates beta-catenin-mediated transcription. Cancer Res *62*, 5947-5954.

Simon, M., Grandage, V.L., Linch, D.C., and Khwaja, A. (2005). Constitutive activation of the Wnt/beta-catenin signalling pathway in acute myeloid leukaemia. Oncogene *24*, 2410-2420.

Slovak, M.L., Kopecky, K.J., Cassileth, P.A., Harrington, D.H., Theil, K.S., Mohamed, A., Paietta, E., Willman, C.L., Head, D.R., Rowe, J.M.*, et al.* (2000). Karyotypic analysis predicts outcome of preremission and postremission therapy in adult acute myeloid leukemia: a Southwest Oncology Group/Eastern Cooperative Oncology Group Study. Blood *96*, 4075-4083.

Song, J.J., and Joshua-Tor, L. (2006). Argonaute and RNA--getting into the groove. Curr Opin Struct Biol *16*, 5-11.

Song, J.J., Liu, J., Tolia, N.H., Schneiderman, J., Smith, S.K., Martienssen, R.A., Hannon, G.J., and Joshua-Tor, L. (2003). The crystal structure of the Argonaute2 PAZ domain reveals an RNA binding motif in RNAi effector complexes. Nat Struct Biol *10*, 1026-1032.

Song, J.J., Smith, S.K., Hannon, G.J., and Joshua-Tor, L. (2004). Crystal structure of Argonaute and its implications for RISC slicer activity. Science *305*, 1434-1437.

Starczynowski, D.T., Morin, R., McPherson, A., Lam, J., Chari, R., Wegrzyn, J., Kuchenbauer, F., Hirst, M., Tohyama, K., Humphries, R.K., *et al.* (2011). Genome-wide identification of human microRNAs located in leukemia-associated genomic alterations. Blood *117*, 595-607.

Stark, A., Brennecke, J., Bushati, N., Russell, R.B., and Cohen, S.M. (2005). Animal MicroRNAs confer robustness to gene expression and have a significant impact on 3'-UTR evolution. Cell *123*, 1133-1146.

Stark, A., Brennecke, J., Russell, R.B., and Cohen, S.M. (2003). Identification of Drosophila MicroRNA targets. PLoS Biol *1*, E60.

Steelman, L.S., Pohnert, S.C., Shelton, J.G., Franklin, R.A., Bertrand, F.E., and McCubrey, J.A. (2004). JAK/STAT, Raf/MEK/ERK, PI3K/Akt and BCR-ABL in cell cycle progression and leukemogenesis. Leukemia *18*, 189-218.

Su, H., Trombly, M.I., Chen, J., and Wang, X. (2009). Essential and overlapping functions for mammalian Argonautes in microRNA silencing. Genes Dev *23*, 304-317.

Takamizawa, J., Konishi, H., Yanagisawa, K., Tomida, S., Osada, H., Endoh, H., Harano, T., Yatabe, Y., Nagino, M., Nimura, Y., *et al.* (2004). Reduced expression of the let-7 microRNAs in human lung cancers in association with shortened postoperative survival. Cancer Res *64*, 3753-3756.

Tallman, M.S., Gilliland, D.G., and Rowe, J.M. (2005). Drug therapy for acute myeloid leukemia. Blood *106*, 1154-1163.

Tenenbaum, S.A., Carson, C.C., Atasoy, U., and Keene, J.D. (2003). Genome-wide regulatory analysis using en masse nuclear run-ons and ribonomic profiling with autoimmune sera. Gene *317*, 79-87.

Tenenbaum, S.A., Carson, C.C., Lager, P.J., and Keene, J.D. (2000). Identifying mRNA subsets in messenger ribonucleoprotein complexes by using cDNA arrays. Proc Natl Acad Sci U S A *97*, 14085-14090.

Tusher, V.G., Tibshirani, R., and Chu, G. (2001). Significance analysis of microarrays applied to the ionizing radiation response. Proc Natl Acad Sci U S A *98*, 5116-5121.

Ule, J., Jensen, K.B., Ruggiu, M., Mele, A., Ule, A., and Darnell, R.B. (2003). CLIP identifies Nova-regulated RNA networks in the brain. Science *302*, 1212-1215.

Vasilatou, D., Papageorgiou, S., Pappa, V., Papageorgiou, E., and Dervenoulas, J. (2010). The role of microRNAs in normal and malignant hematopoiesis. Eur J Haematol *84*, 1-16.

Vasudevan, S., Tong, Y., and Steitz, J.A. (2007). Switching from repression to activation: microRNAs can up-regulate translation. Science *318*, 1931-1934.

Wagenmakers, A.J., Reinders, R.J., and van Venrooij, W.J. (1980). Cross-linking of mRNA to proteins by irradiation of intact cells with ultraviolet light. Eur J Biochem *112*, 323-330.

Wakiyama, M., Takimoto, K., Ohara, O., and Yokoyama, S. (2007). Let-7 microRNA-mediated mRNA deadenylation and translational repression in a mammalian cell-free system. Genes Dev *21*, 1857-1862.

Wang, Y.Y., Zhou, G.B., Yin, T., Chen, B., Shi, J.Y., Liang, W.X., Jin, X.L., You, J.H., Yang, G., Shen, Z.X., *et al.* (2005). AML1-ETO and C-KIT mutation/overexpression in t(8;21) leukemia: implication in stepwise leukemogenesis and response to Gleevec. Proc Natl Acad Sci USA *102*, 1104 1109.

Wang, X., and Proud, C.G. (2006). The mTOR pathway in the control of protein synthesis. Physiology (Bethesda) *21*, 362-369.

Wang, Y., Sheng, G., Juranek, S., Tuschl, T., and Patel, D.J. (2008). Structure of the guide-strand-containing argonaute silencing complex. Nature *456*, 209-213.

Wang, Y., Krivtsov, A.V., Sinha, A.U., North, T.E., Goessling, W., Feng, Z., Zon, L.I., and Armstrong, S.A. (2010). The Wnt/beta-catenin pathway is required for the development of leukemia stem cells in AML. Science *327*, 1650-1653.

Wang, Y., Li, Z., He, C., Wang, D., Yuan, X., Chen, J., and Jin, J. (2010b). MicroRNAs expression signatures are associated with lineage and survival in acute leukemias. Blood Cells Mol Dis *44*, 191-197.

Wang, Y.Y., Zhao, L.J., Wu, C.F., Liu, P., Shi, L., Liang, Y., Xiong, S.M., Mi, J.Q., Chen, Z., Ren, R.*, et al.* (2011). C-KIT mutation cooperates with full-length AML1-ETO to induce acute myeloid leukemia in mice. Proc Natl Acad Sci U S A *108*, 2450-2455.

Webster, R.J., Giles, K.M., Price, K.J., Zhang, P.M., Mattick, J.S., and Leedman, P.J. (2009). Regulation of epidermal growth factor receptor signaling in human cancer cells by microRNA-7. J Biol Chem *284*, 5731-5741.

Wightman, B., Burglin, T.R., Gatto, J., Arasu, P., and Ruvkun, G. (1991). Negative regulatory sequences in the lin-14 3'-untranslated region are necessary to generate a temporal switch during Caenorhabditis elegans development. Genes Dev *5*, 1813-1824.

Wightman, B., Ha, I., and Ruvkun, G. (1993). Posttranscriptional regulation of the heterochronic gene lin-14 by lin-4 mediates temporal pattern formation in C. elegans. Cell *75*, 855-862.

Winter, J., Jung, S., Keller, S., Gregory, R.I., and Diederichs, S. (2009). Many roads to maturity: microRNA biogenesis pathways and their regulation. Nat Cell Biol *11*, 228-234.

Wu, L., and Belasco, J.G. (2008). Let me count the ways: mechanisms of gene regulation by miRNAs and siRNAs. Mol Cell *29*, 1-7.

Wuchty, S., Fontana, W., Hofacker, I.L., and Schuster, P. (1999). Complete suboptimal folding of RNA and the stability of secondary structures. Biopolymers *49*, 145-165.

Xie, X., Lu, J., Kulbokas, E.J., Golub, T.R., Mootha, V., Lindblad-Toh, K., Lander, E.S., and Kellis, M. (2005). Systematic discovery of regulatory motifs in human promoters and 3'-UTRs by comparison of several mammals. Nature *434*, 338-345.

Yan, K.S., Yan, S., Farooq, A., Han, A., Zeng, L., and Zhou, M.M. (2003). Structure and conserved RNA binding of the PAZ domain. Nature *426*, 468-474.

Yang, W., and Steitz, T.A. (1995). Recombining the structures of HIV integrase, RuvC and RNase H. Structure *3*, 131-134.

Yang, Z., Edenberg, H.J., and Davis, R.L. (2005). Isolation of mRNA from specific tissues of Drosophila by mRNA tagging. Nucleic Acids Res *33*, e148.

Yi, R., Qin, Y., Macara, I.G., and Cullen, B.R. (2003). Exportin-5 mediates the nuclear export of pre-microRNAs and short hairpin RNAs. Genes Dev *17*, 3011-3016.

Zamore, P.D., Tuschl, T., Sharp, P.A., and Bartel, D.P. (2000). RNAi: double-stranded RNA directs the ATP-dependent cleavage of mRNA at 21 to 23 nucleotide intervals. Cell *101*, 25-33.

Zhang, R., Wang, Y.Q., and Su, B. (2008). Molecular evolution of a primate-specific microRNA family. Mol Biol Evol *25*, 1493-1502.

7 Abbreviations

4SU	4'-thiouridine
Ago	Argonaute protein
ALL	acute lymphoid leukemia
AML	acute myeloid leukemia
APL	acute promyelocytic leukemia
BM	bone marrow
BMFZ	Biologisch Medizinisches Forschungszentrum
bp	base pair
BSA	bovine serum albumin
CEBPA	CCAAT/enhancer-binding protein alpha
C. elegans	*Caenorhabditis elegans*
CLIP	crosslinking immunoprecipitation
CLL	chronic lymphocytic leukemia
Ct	cycle threshold
DNA	deoxyribonucleic acid
dNTP	deoxyribonucleotide triphosphate
D. melanogaster	*Drosophila melanogaster*
dsRBD	double-stranded RNA-binding domain
FAB	French-American-British
FDR	false discovery rate
FBS	fetal bovine serum
FC	fold change
FXR1	fragile X-related protein 1
GO	gene ontology
GOEAST	Gene Ontology Enrichment Analysis Software Toolkit
EGAN	Exploratory Gene Association Network
HITS	high-throughput sequencing
IP	immunoprecipitation
KEGG	Kyoto Encyclopedia of Genes and Genomes
kDa	kilodalton
LU	light units
miRNA/miR	microRNA
miRNA*	microRNA star
MLL	mixed lineage leukemia
mRNA	messenger ribonucleic acid
NP40	nonidet P-40
NPM1	nucleophosmin
nt	nucleotide
orf	open reading frame
PACT	protein activator of PKR

PAGE	polyacrylamide gel electrophoresis
PAR	photoactivatable ribonucleotide
PAZ	piwi-argonaute-zwille
P-bodies	processing bodies
PB	peripheral blood
PCR	polymerase chain reaction
PIWI	P-element induced wimpy testis
PKR	protein kinase RNA-activated
PNK	polynucleotide kinase
Pol II	polymerase II
RBP	RNA binding protein
RIP	RBP immunoprecipitation
RISC	RNA-induced silencing complex
RLC	RISC-loading complex
RNA	ribonucleic acid
RNAi	RNA interference
RNP	ribonucleo protein
RRE	RBP recognition element
SDS	sodium dodecyl sulfate
SI	signal intensity
siRNA	small-interfering RNA
SNP	single nucleotide polymorphism
TRBP	tar RNA-binding protein
UTR	untranslated region
UV	ultraviolet
WB	Western Blot
WBC	white blood cell count

8 Supplement

(see printed version, CD back of the book)

Table V.1 AML Patient-characteristics

Description of pediatric AML patients analyzed for miRNA expression profiling. Listed are the patient IDs and characteristics like patient ID, gender, age, date of birth, date of diagnosis, AML subtype, karyotype, blast count and cell amount.

Table V.2 AML miRNA microarray-data

Measured signal intensities of all detected miRNAs of 102 pediatric AML patients used for heatmap generation. The columns list the miRNA expression profiles of each patient and the rows list the signal intensities of each miRNA. Additionally, statistical testing, to finde differentially expressed miRNAs between AML subtypes are listed in the third sheet of Table V.2.

Table V.3 KASUMI-1 Ago-miRNA microarray-data

Signal intensities of all miRNAs identified in the four human Argonaute protein complexes, the isotype controls and total RNA of KASUMI-1. In addition, the FC and p-value (Welch-test) of signal intensities of Ago identified miRNAs in comparison to the corresponding signal intensities of miRNAs identified in the isotype controls, were calculated. The significance of each miRNA is denoted as "high" and "no" with regard to the FC and p-value. miRNAs marked as high and middle were used for subsequent analyses.

Table V.4 NB4 Ago-miRNA microarray-data

Signal intensities of all miRNAs identified in the four human Argonaute protein complexes, the isotype controls and the total RNA of NB4. In addition, the FC and p-value (Welch-test) of signal intensities of Ago identified miRNAs in comparison to the corresponding signal intensities of miRNAs, identified in the isotype controls, were calculated. The significance of each miRNA is denoted as "high" and "no" with regard to the FC and p-value. miRNAs marked as high and middle were used for subsequent analyses.

Table V.5 KASUMI-1 Ago-mRNA Microarray-data

Signal intensities of all mRNAs identified in the four human Argonaute protein complexes, the isotype controls and the total RNA of KASUMI-1. In addition, the FC and p-value (Welch-test) of signal intensities of Ago identified mRNAs in comparison to the corresponding signal intensities of mRNAs, identified in the isotype controls, were calculated. In addition, for each Argonaute protein the filtered data (FC ≥ 1.8 and p-value ≤ 0.05 miRNA signal intensity Ago/iso) were listed separately.

Table V.6 NB4 Ago-mRNA microarray-data

Signal intensities of all mRNAs identified in the four human Argonaute protein complexes, the isotype controls and the total RNA of NB4. In addition, the FC and p-value (Welch-test) of signal intensities of Ago identified mRNAs in comparison to the corresponding signal intensities of mRNAs identified in the isotype controls, were calculated. In addition, for each Argonaute protein the filtered data (FC > 1.8 and p-value < 0.05 miRNA signal intensity Ago/iso) were listed separately.

Table V.7 KASUMI-1 Seqgrp and Target-predictions

Classification of Ago-associated miRNAs into sequence-groups and their combination with Ago-associated, predicted target-mRNAs together with the listing of databases which predict binding sites between the miRNAs and their target-mRNAs.

Table V.8 NB4 Seqgrp and Target-predictions

Classification of Ago-associated miRNAs into sequence-groups and their combination with Ago-associated, predicted target-mRNAs together with the listing of databases which predict binding sites between the miRNAs and their target-mRNAs.

Table V.9 KASUMI-1 GO term classification

Classification of Ago-associated mRNAs into GO terms. The calculations of enriched GO terms within the data sets were listed in this table as well.

Table V.10 NB4 GO term classification

Classification of Ago-associated mRNAs into GO terms. The calculations of enriched GO terms within the data sets were listed in this table as well.

Table V.11 KASUMI-1 KEGG pathway classifications

Classification of Ago-associated mRNAs into KEGG pathways. Ago-associated miRNAs offering binding sites for these mRNAs according to at least two prediction algorithms were listed in this table as well.

Table V.12 NB4 KEGG pathway classifications

Classification of Ago-associated mRNAs into KEGG pathways. Ago-associated miRNAs offering binding sites for these mRNAs according to at least two prediction algorithms were listed in this table as well.

9 Publications

1st Publication submitted

Argonaute-miRNA complexes reveal concerted action in disease related pathways of a human, glioblastoma cell line

Svenja Daschkey[1], Gunter Meister[2], Arndt Borkhardt[1], Pablo Landgraf[1]

1 Department of Pediatric Oncology, Hematology and Clinical Immunology, Heinrich-Heine University Düsseldorf, Düsseldorf, Germany, 2 Max Planck Institute of Biochemistry, Martinsried

2nd Publication submitted

microRNAs distinguish cytogenetic subgroups in pediatric AML and contribute to complex regulatory networks in AML-relevant pathways

Svenja Daschkey[1], Silja Röttgers[2], Jochen Harbott[2], Gunter Meister[3], Arndt Borkhardt[1], Pablo Landgraf[1]

1 Department of Pediatric Oncology, Hematology and Clinical Immunology, Heinrich-Heine University Düsseldorf, Düsseldorf, Germany, 2 Children's University Hospital; Department of Hematology and Oncology, Giessen, Germany, 3 Max Planck Institute of Biochemistry, Martinsried

Talk

microRNA expression profiling in acute myeloid leukemia patients

Svenja Daschkey[1], Torsten Haferlach[2], Arndt Borkhardt[1], Pablo Landgraf[1]

1 Department of Pediatric Oncology, Hematology and Clinical Immunology, Heinrich-Heine University Düsseldorf, Düsseldorf, Germany, 2 Munich Leukemia Laboratory (MLL) GmbH, Munich, Germany

XXII. annual conference of Kind-Philipp foundation for leukemia research
June 10-13, 2009, Wilsede, Germany

Poster presentation

microRNA expression profiling in AML patients

Svenja Daschkey[1], Torsten Haferlach[2], Arndt Borkhardt[1], Pablo Landgraf[1]

1 Department of Pediatric Oncology, Hematology and Clinical Immunology, Heinrich-Heine University Düsseldorf, Düsseldorf, Germany, 2 Munich Leukemia Laboratory (MLL) GmbH, Munich, Germany

Keystone Symposia on Molecular and Cellular Biology – The Biology of RNA Silencing
April 25-30, 2009, Fairmont Empress Victoria, Victoria, British Columbia, Canada

10 Acknowledgements

Svenja Daschkey

Personal details

Date of Birth	15.08.1982
Place of Birth	Oelde, Nordrhein-Westfalen

Experience

Heinrich-Heine University Duesseldorf Department of Pediatric Oncology, Hematology and Clinical Immunology	Doctor of Science in Leukemia Genetics Title of PhD thesis: „miRNA expression profiling of pediatric AML patient samples and global identification of Argonaute protein-associated RNAs in respective cell line models"	04/2008 - 04/2011
Bielefeld University	Master of Science in Genome Based Systems Biology Title of master's thesis: "Identification and characterization of small non-coding RNAs in *Sinorhizobium meliloti* 2011"	10/2005 - 03/2008
Bielefeld University	Bachelor of Science in Bioinformatic and Genome Research Title of bachelor's thesis: "Mapping and bioinformatic analysis of the cytosolic proteome of *Corynebacterium jeikeium* K411"	10/2002 - 10/2005

Publications

BMC Genomics, PMID: 20398411	"A genome-wide survey of sRNAs in the symbiotic nitrogen-fixing alpha-proteobacterium *Sinorhizobium meliloti*"	04/17/2010
Proteomics, PMID: 17352426	"A comprehensive proteome map of the lipid-requiring nosocomial pathogen *Corynebacterium jeikeium* K411"	04/07/2007

Education

Augustin-Wibbelt-grammar-school Warendorf	final secondary-school examinations advanced courses: Biology and German	08/1999 - 06/2002

Düsseldorf, 04/28/2011

Affirmation

Hereby, I declare on oath that I composed this dissertation independently and self-consistent. I used only the references and resources indicated in this thesis. This PhD thesis was never submitted in presented or similar form to any other institution or examination board and I have not venture a doctoral examination without success so far.

S. Daschkey

Svenja Daschkey

Düsseldorf, 04/28/2011